Author:
Turner, J. P

Title:
Tectonic and stratigraphic evolution of the West Jaca thrust-top basin, Southwest Pyranees

TECTONIC AND STRATIGRAPHIC EVOLUTION OF THE WEST JACA THRUST-TOP BASIN, SOUTHWEST PYRENEES

by

Jonathan Paul Turner B.Sc.

A thesis submitted for the degree of Doctor of Philosophy
to the Department of Geology, University of Bristol.

January 1988

DECLARATION

The material presented in this thesis is the result of my own independent research carried out in the Department of Geology, University of Bristol, and in northern Spain, under the supervision of Drs. P.L. Hancock and B.P.J. Williams. Any previously published or unpublished work used is given full acknowledgment.

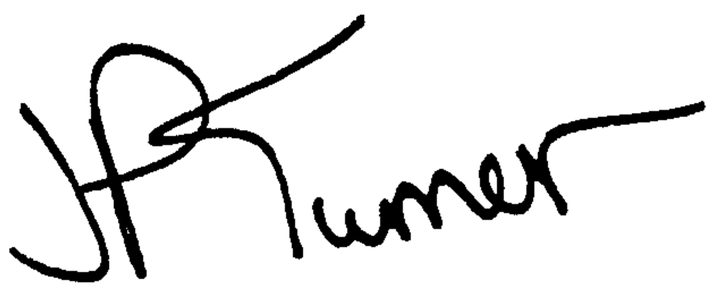

J.P. Turner

December 1987

TECTONIC AND STRATIGRAPHIC EVOLUTION OF THE WEST JACA THRUST-TOP BASIN, SOUTHWEST PYRENEES

JONATHAN PAUL TURNER

ABSTRACT

This thesis presents the results of structural mapping, sedimentological profiling and a brittle microtectonic survey within the Oligo-Miocene molasse of the West Jaca basin and contiguous parts of the Ebro basin. The study area is centred on Sanguesa, a town about forty kilometres southeast of Pamplona, Navarra. The investigated rocks are mainly contained in the western half of the Jaca basin, a tectonic unit that rode piggyback on the Gavarnie Thrust Sheet, the westernmost South Pyrenean Thrust Sheet. During the evolution of the West Jaca thrust-top basin, many of the special phenomena that result when sedimentation is contemporaneous with orogenic contraction were developed. A series of four strike-normal (N-S) sections reveal that the Pena flexure, the local expression of the thrust front, may be interpreted as a passive-roof duplex accommodating up to 45% (8 km) shortening at the southwest tip of the Gavarnie Thrust Sheet. The preservation of pre-, syn- and post-thrust front molasse across the flexure allows a particularly complete analysis of its sedimentary and tectonic history to be made. Local lateral (E-W) variations in structural style, combined with regional lateral contrasts in stratigraphic and facies relationships, demonstrate that the South Pyrenean thrust front propagated both toward the foreland and also to the west; that is, parallel to the long axis of the orogen. The interaction of the thrust front with an earlier formed, larger-scale, basement duplex accounts for many of the apparent anomalies in the timing and rates of subsidence in the South Pyrenean basins. The evolution of the thrust system in the West Jaca basin is reflected by increasing division of the main basin into sub-basins whose boundaries are defined by blind and emergent ramps. Differential rates of subsidence between sub-basins exerted the dominant control on alluvial architecture, especially fluvial sand body geometry.

ACKNOWLEDGMENTS

This research has been carried out under the inspiring supervision of Paul Hancock who I thank most sincerely for his encouraging and critical guidance throughout. Brian Williams is thanked for his sedimentological advice and enthusiasm. Both in the field and office, I have benefitted considerably from many stimulating discussions with fellow postgraduates and research workers. In particular, I wish to express my gratitude to Philip Allen, Mark Enfield, Peter Friend, David Lawrence, Larry Middleton, Colin North, Simon Todd, Joaquin del Valle, David Went, Graham Williams and Paul Wright.

Additionally, I am grateful to Michael Caswell-Daniels of Shell UK Ltd., Ebro Boys Christopher Gerrard and Casper Johnson, Pamela Waddell and many other friends for having helped to make my postgraduate stay in Bristol such an enjoyable one. Fieldwork in Spain was an exceptionally memorable experience due in no small part to the hospitality of Asuncion and Juan Echegoyen, Isabel Jimenez and the people of Sanguesa who are warmly and appreciatively recalled. The teaching of Peter Gardner of Richard Tauntons College, Southampton played the major role in encouraging me to pursue geology at university. I thank Glenise Maytham for having typed the manuscript and Simon Powell for his expert photographic work.

I am sincerely grateful for the support received from Shell International Petroleum Company Ltd. who financed this project generously.

My deepest thanks, however, are reserved for my parents whose constant support and positive advice has never wavered.

CONTENTS

LIST OF FIGURES

LIST OF PLATES

LIST OF TABLES

KEY TO LOGS AND MAPS

LOGS


planar bases


erosive bases

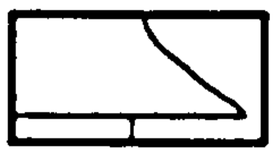
upward-fining

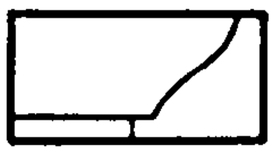
upward-coarsening

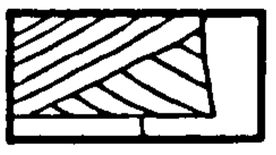
planar cross-stratification

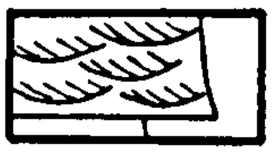
trough cross-stratification

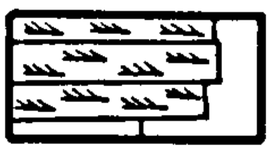
current-ripple lamination


plane-bed lamination

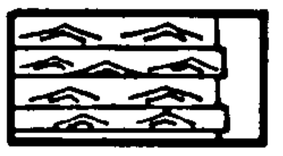
wave-ripples


reactivation surfaces


rootlets

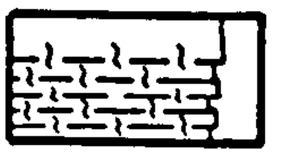
bioturbation

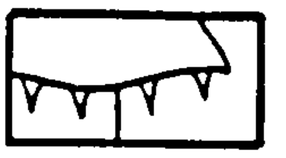
desiccation cracks


lateral accretion surfaces

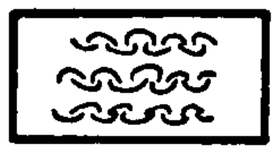
flowrolls

sand volcanoes

gypsum

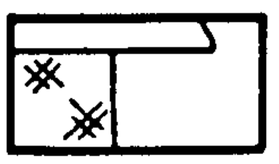
colour mottling


palaeosol


exposure gap


composite palaeocurrent


individual palaeocurrents (uni- and bidirectional)

MAPS


trace of thrust (teeth in hangingwall)


trace of normal faults (box in hangingwall)

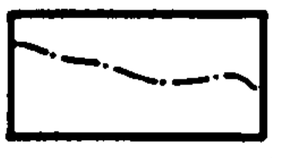
unconformable contact

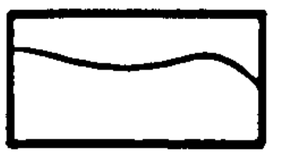
conformable contact

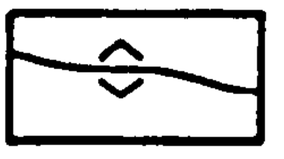
anticline axial trace

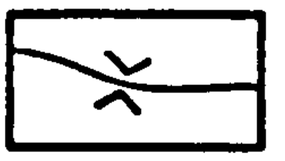
syncline axial trace

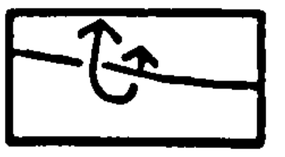
overturned anticline axial trace

CHAPTER 1

INTRODUCTION

1.1 PURPOSE AND SCOPE

During the last twenty years, the southern Pyrenees have attracted geologists seeking to establish links between thin skin fault systems and clastic sedimentation. Most work has been concentrated in the central part of the South Pyrenees, particularly in the Graus, Ainsa and Jaca thrust-top basins (Fig. 1.1). There has, however, been little investigation of the westernmost part of the southern Pyrenees and it was this lack of understanding that provided the initial stimulus for this research project.

Thrust-top basins are a category of sedimentary basin which, according to the definition of Ori & Friend (1984), formed and were filled while being carried piggyback on active thrust sheets. They are usually located on the outermost edge of an orogen as part of a suite of structurally detached foreland basins, many of whose structural and stratigraphic attributes they share. Foreland basins are basins which subside as a result of the flexural deformation of foreland lithosphere (Beaumont 1978; Beaumont 1981; Karner 1985; Kusznir & Karner 1985). Such subsidence is a mechanical response to loading of the lithosphere by thrust sheets stacked along the external margin of a mountain belt. One consequence of thrusting and sedimentation occurring synchronously is the uncommonly clear picture of structural control on sedimentation that may be gained.

A special appeal of the western part of the Jaca thrust-top basin is that it is not separated from the Ebro basin, the South Pyrenean foreland, by outcrops of older rocks in the Exterior Sierras. The transitional boundary between the basins permits investigation of the details of the sedimentary and deformation history of the southward migration, from the early Oligocene to the early Miocene, of the depocentre between the basins. The Exterior Sierras are a strike-parallel topographic range of thrusted Mesozoic and Palaeogene limestone and marl that extend along the southern margin of the South Pyrenean thrust-top basins for 150 km (Fig. 1.1). The preservation of pre-, syn- and post-orogenic molasse sediments in both the West Jaca basin and the Ebro basin allows a more complete analysis of sedimentary and tectonic relationships. By integrating a series of balanced and schematic structural sections with data on stratigraphic development, sedimentary facies and provenance, and the inferences from a brittle microtectonic survey, this thesis aims to provide a comprehensive view of the development of a composite foreland basin adjacent to an evolving mountain front.

1.2 PHYSIOGRAPHY

The study area (Plate 1.1a), in the westernmost part of the South Pyrenean basin system (Fig. 1.1) is situated southeast of Pamplona and within the land-locked provinces of Navarra and Zaragoza. It is bounded on the north roughly by the Pamplona-Jaca (N240) road, on the east by longtitude 3°45' passing through the Sierra de Santo Domingo (Fig. 1.2), on the west by the Pamplona-Tafalla autopista and on the south by an approximately E-W line coincident with latitude 47°. Within the roughly 24000 km^2 of the study area there are spectacular variations in geologically controlled geomorphology, climate, vegetation and human temperament.

Topographically, the most significant regional feature is a strike-parallel ridge that extends fifty kilometres westward from south of the Sierra de Santo Domingo. The ridge is coincident with a structure here called the Pena flexure (Fig. 1.2) and it rises to a maximum height of 1100m, that is, about 550m above the mean regional elevation of the Ebro basin. The Pena flexure ridge separates the West Jaca thrust-top basin to the north from the relatively undeformed rocks of the Ebro basin, and it forms a prominent topographic divide within a rugged, maquis-covered landscape that, in parts, is forested. The West Jaca basin is characterised by a first order relief of undulating hills underlain by sandstone-dominant sediment, and plains underlain by siltstone-dominant sediment. This hilly relief contrasts strongly to the relatively barren tablelands of the desert-like Ebro basin stretching for a hundred kilometres south of the Pena flexure. The West Jaca basin is part of the South Pyrenean thrust-fold belt and it extends northward into a terrain of limestone sierras that lie to the north of the gullied badlands of the Canal de Berdun (Fig. 1.2).

1.3 SURFACE GEOLOGY

The distribution of principal stratigraphic units and major structures in the West Jaca basin are shown in Fig. 1.3. This thesis follows the definition of molasse by Bertrand (1897) in which it is used to describe a sedimentary facies which either follow or are partly contemporaneous with flysch, and were deposited as both a late- and post-orogenic facies.

In the region of the West Jaca molasse basin, the Tertiary sequence generally becomes progressively younger from north to south, local reversals of this direction being related to the outcrops of major fold hinges or strike faults. Several compound anticlines located immediately to the north and southeast of the West Jaca basin are responsible for exposing early Palaeogene

and Cretaceous limestone. The most notable anticlines follow the Sierras de Illon and Leyre in the north, the Sierra de Alaiz bounding the northwest corner of the molasse basin, and the Sierra de Santo Domingo in the southeast (Fig. 1.2). Between the compound anticlines there are wide outcrops of middle to upper Eocene flysch that have achieved a classic status by virtue of their descriptions by clastic sedimentologists (eg. Ten Haaf 1966; Rupke 1976; Mutti 1977, 1985; Mutti & Johns 1979; Johns *et al.* 1981).

Much of the length of the northern margin of the molasse basin is defined by the trace of a thrust juxtaposing upper Eocene marls to the north, and lower and middle Oligocene molasse sandstone. However, along the western third of the northern margin of the basin, the contact is unfaulted and there is a conformable sequence of transitional marine-continental sediments of latest Eocene age (Mangin 1962; Puigdefabregas 1975). The occurrence of duck footprint casts (Plate 1.1b) in two parts of the sequence has made it a popular stop on the bill of field excursions to the area.

Within the West Jaca basin, correlating the distribution of mappable formations and the positions of emergent and blind thrust faults permits its division into several sub-areas or sub-basins (Fig. 1.2 and 1.3). In the present study, a sub-basin is defined as a distinctive area of former subsidence that was a hydrologically isolated depocentre within a larger host basin. Sub-basin fills become progressively younger toward the west of the study area with a corresponding increase in the spacing between thrust faults. For example, in the area of the Ruesta fault zone (Fig. 1.2), in the northeast part of the study area, emergent thrusts expose rocks of early Oligocene age belonging to the lower part of the molasse sequence. However, toward the west, large wavelength and high amplitude folds accommodated most of the orogenic contraction and, at the centre of the Olleta sub-basin (Fig. 1.2), lower Miocene sediments are preserved.

The absence of closely spaced thrusts and folds immediately south of the Pena flexure, along the northern margin of the Ebro basin (Fig. 1.3), emphasises the importance of this flexure as a major structural divide. The flexure is underlain by middle Oligocene to lower Miocene conglomerate and sandstone molasse whose dips become progressively gentler southward, further from the influence of Pyrenean thrusts. South of the Pena flexure, the Ebro basin margin sediments are flat lying or gently tilted, post-orogenic sandstone and siltstone.

1.4 REVIEW OF PREVIOUS RESEARCH

Much of the earliest work in the western part of the South Pyrenees was stimulated by exploration for economic potash deposits that occur within the upper Eocene rocks of central Navarra (del Valle 1929, 1932). An important early attempt to elucidate the regional structure and stratigraphy was that of Selzer (1934) who investigated a zone between the Palaeozoic Axial Zone of the Pyrenees and the Ebro basin (Fig. 1.1). He displayed paticular foresight in his N-S section across the thrust-fold belt which emphasises the importance of the diapiric rise of Triassic evaporites in the development of major structures (Fig. 1.4). Maps and sections published by the Instituto Geologico y Minero de Espana twenty years later (1950a, 1950b, 1954, 1959) depicted relationships in the molasse fill of the West Jaca and Ebro basins that may now be interpreted as progressive unconformities and growthfolds (cf. Riba 1976a).

Until the late 1960s the Pyrenees were generally considered to be a Hercynian mountain belt rejuvenated by Alpide orogenesis (eg. de Sitter 1964). However, fundamental palaeomagnetic work (van der Voo 1969) demonstrated that, between the late Triassic and late Cretaceous, the Iberian peninsula experienced a 35° anticlockwise rotation. Van der Voo's hypothesis generated considerable debate, much of which focused on the position of the pole of rotation (see Ries 1978). An early idea was that one phase of rotation, with a pole located at the western end of the Pyrenees, was sufficient to explain the entire Mesozoic to Palaeogene history of Iberian plate movement (Carey 1958; van der Voo 1969). However, a three-stage history of rotation and translation, with the initial rotational episode centring on a pole of rotation near Paris (Le Pichon *et al.* 1970, 1971; Boillot 1984), was shown to be more compatible with known Pyrenean regional geology (Choukroune *et al.* 1973) and global tectonic events. This model involved an eastward rotational shift of the Iberian microplate along a small-circle transform fault and later northward directed collision of Iberia with the remainder of western Europe during the latest Cretaceous. The three-stage evolution accords with the early history of North Atlantic seafloor spreading and accounts for the Mesozoic extension and crustal thinning which preceded collision in the Pyrenees (see Boillot 1984). Most importantly, however, it provided an explanation for the existence of the North Pyrenean Fault (Fig. 1.1), an onland extension of the postulated small-circle transform fault which behaved as a major left-lateral transcurrent fault during the Mesozoic rotation of Iberia (Pavoni 1964; Mattauer 1969; Le Pichon *et al.* 1971; Choukroune 1976; Choukroune & Mattauer 1978; Olivet *et al.* 1981, 1982).

However, the final climactic episode of Pyrenean orogeny in the early Palaeogene was dominated by roughly head-on collision of Iberia and Europe (Mattauer & Henry 1971) during which time the South Pyrenean Thrust Sheets shown in Fig. 1.1 began developing. Seguret (1972) first recognised the South Pyrenean Thrust sheets and he used them to erect a tectonostratigraphy for the entire central and western part of the South Pyrenees. The definition of a thrust sheet used here is the conventional one, that is, a discrete tectonic unit, usually kilometres wide and tens of kilometres long, which has been detached from an underlying basement on one or more thrust faults. The present study concerns the evolution of the western end of the largest of these South Pyrenean thrust sheets, the Gavarnie Thrust Sheet (Fig. 1.1).

Following the publication of Seguret's thesis, discussion focused on evaluating the roles of horizontal compressive forces and gravitational forces as driving mechanisms for the translation of the South Pyrenean Thrust Sheets. Choukroune & Seguret (1973), for example, concluded that gravitational gliding played a negligible role in the emplacement of detached units such as the Gavarnie Thrust Sheet. However, Sole-Sugranes (1979) suggested that the earlier formed thrust sheets are gravitational structures and the later ones, most notably the Garvarnie Thrust Sheet, are related to horizontal compression. He attributed the Oligo-Miocene movements of the Gavarnie Thrust Sheet on which the present study concentrates, to local gravitational instabilities and isostatic readjustment of the South Pyrenean foreland crust after the orogenic climax.

The uniqueness of thrust-top basins has only been recognised during the last twelve years and in the South Pyrenean basins, research has concentrated on describing the close relationship between structural evolution and sediment deposition in an orogenic setting (eg. Puigdefabregas & Soler 1973; Puigdefabregas 1975; Riba 1976a, 1976b; Nijman 1981; Atkinson 1983; Camara & Klimowitz 1985; Hirst & Nichols 1986; Farrell *et al.* 1987). The linking of deformation with sedimentation has been made possible largely by recent elucidation of the structure of the Pyrenees. To aid their interpretations, structural geologists have constructed balanced cross sections that span the width of the Pyrenees, on the premise of the region being dominated by thin skin linked thrust systems (eg. Deramond 1979; Deramond *et al.* 1984; Parish 1984; Williams & Fischer 1984; Labaume *et al.* 1985; Williams 1985; Seguret & Daignieres 1986; Nichols 1987). These sections demonstrate that the development of the South Pyrenean thrust system was dominated by a piggyback sequence of thrusting toward the Ebro basin foreland. Additionally, superbly

exposed lacustrine, alluvial and deep water facies clastic sequences, exposed throughout the South Pyrenees, have led to the publication of numerous detailed sedimentological case studies that have contributed to the current state of understanding of depositional proceseses (eg. Puigdefabregas 1973; Rupke 1976; Mutti 1977; Puigdefabregas & van Vliet 1978; Nijman & Puigdefabregas 1978; Mutti & Johns 1979; Friend *et al.* 1979; Farrell 1984).

The study area was in a subtropical or tropical position in the early and mid Tertiary. Oligocene floras of tropical type (eg. Plate 1.1c) were described from the Ebro basin by Fliche (1906) and Depape (1950), and Margalef (1957) proposed great seasonal differences from his studies of Miocene lacustrine deposits. Pinilla & Riba (1972) suggested that the Ebro basin in the Tertiary was hot, with rainfall concentrated in the north against the Pyrenees.

1.5 STRATIGRAPHY OF THE JACA AND EBRO BASINS

Establishing a reliable chrono- and/or biostratigraphy in continental molasse sequences is notoriously difficult and in most cases it is only possible to establish a lithostratigraphic framework. As a result of gross structrual diachronism, and hence the lateral impersistence of synorogenic lithofacies, the Jaca and Ebro basins are no exception to the general rule. Stratigraphic subdivision of the premolasse Traissic to Eocene sequence is more straightforward and there have been few changes to ideas about the succession since publication of some of the earliest maps of the area (IGME 1950a, 1950b, 1954, 1959). The ease of lithostratigraphic correlation in premolasse rocks is largely a consequence of the abundance of fossils in these dominantly marine seuqences.

Because of the relative lithological monotony of the continental molasse succession, early maps of the West Jaca basin (IGME 1950a, 1950b, 1954, 1959) do not show subdivisions in the molasse sequence which was lumped together as 'Oligocene'. Later, an integration of data on lateral facies transitions, unconformities, sandstone petrology and general palaeontology allowed Soler & Puigdefabregas (1970) to distinguish four divisions within the continental Palaeogene and early Neogene sequence. They proposed four formation names which, in ascending order, are the Campodarbe, Anzanigo, Bernues and Uncastillo Formations (Table 1.1). The present study modifies the stratigraphic succession proposed by Puigdefabregas (1975), itself a modification of that developed by Soler & Puigdefabregas (1970). Puigdefabregas (1975) divided the Anzanigo Formation into two parts and incorporated both of them in

the Campodarbe Formation within which he recognised three divisions, the Lower Middle and Upper Campodarbe Formation. Above the Campodarbe Formation, the limits of the Bernues Formation (Table 1.1) are defined by lower and upper unconformities exposed to the east of the study area at Pena Oroel and Riglos, respectively. Of the three formations recognised by Puigdefabregas (1975), the Uncastillo Formation is biostratigraphically well constrained because it has been dated as Aquitanian on the basis of vertebrates from the central part of the northern Ebro basin margin (Crusafont & Pons 1969).

However, there remains a nomenclatural problem because within the Campodarbe Formation three distinct and mappable units may be recognised. Here, the middle and upper divisions of the formation (the lower division is not present in the West Jaca basin) are accorded member status and named after type localities where they are most completely exposed (Fig. 1.2, Table 1.1). Although the redefined lithostratigraphic units have been assigned ages in Table 1.1, it is important to note that they are provisional in the absence of fossils or isotopic dates.

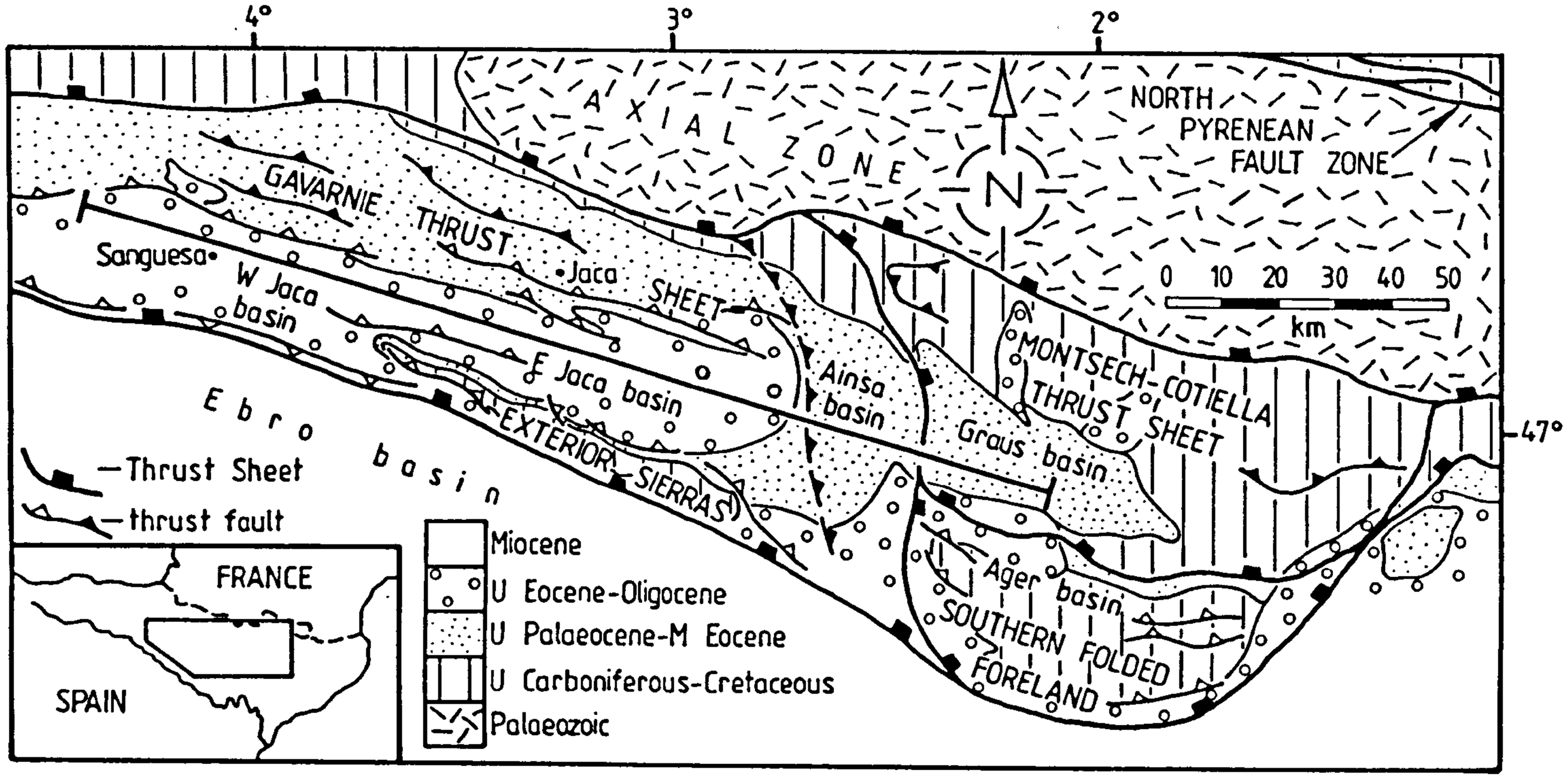

Fig. 1.1. Location of the main South Pyrenean Thrust Sheets and tectonic setting of the South Pyrenean thrust-top basins. Thrust sheet boundaries are shown with a solid box ornament irrespective of age and are taken from Seguret (1972). The traces of thrusts depicted with open barbs cut pre-Oligocene rocks; those with solid barbs cut Oligo-Miocene rocks. Also shown is the line of section in Fig. 2.10. Modified from Seguret (1972, fig. 6), Choukroune & Seguret (1973) and Deramond *et al.* (1984, fig. 4).

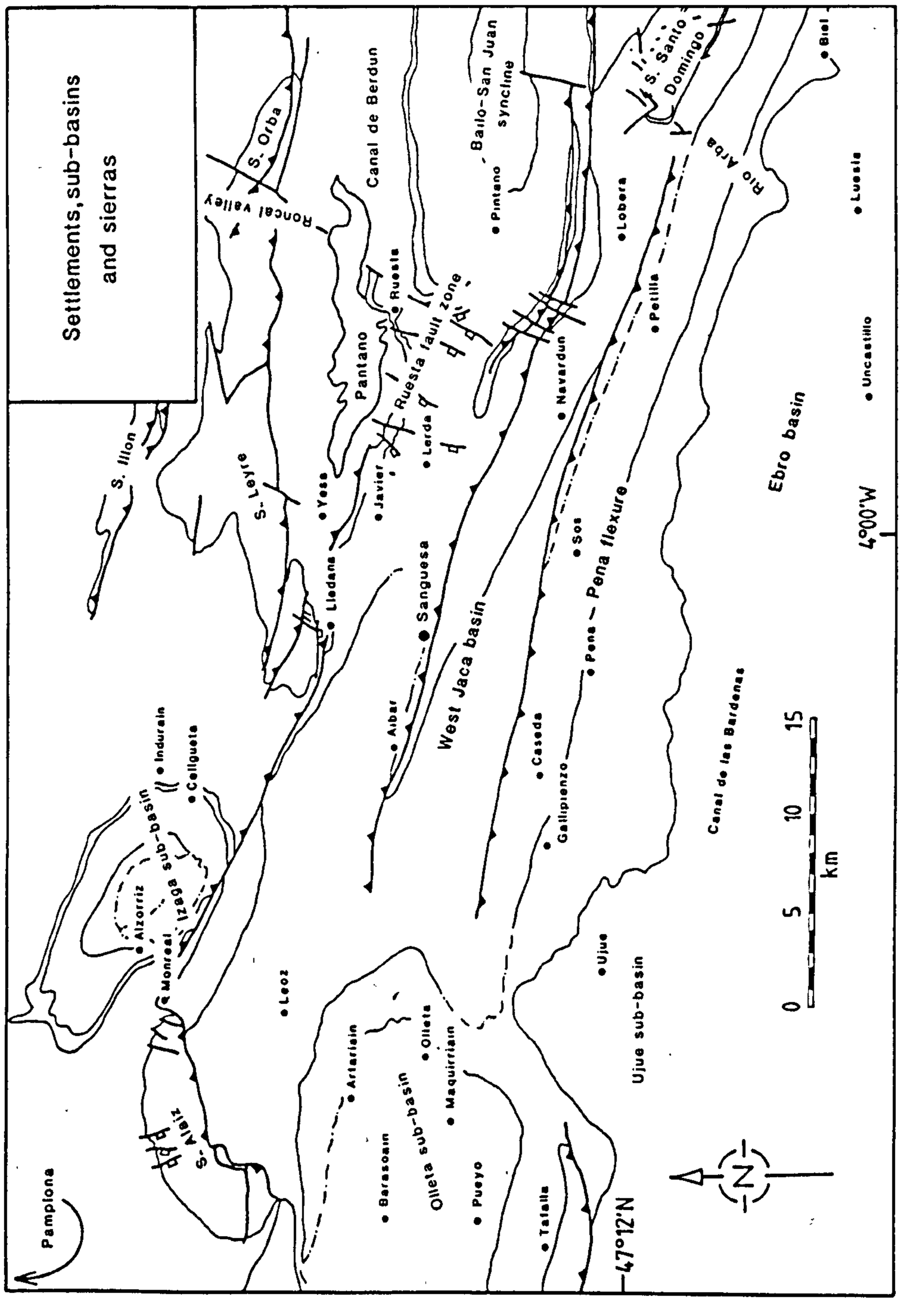

Fig. 1.2. Location of towns, villages, sierras, mountains and sub-basins in the study area.

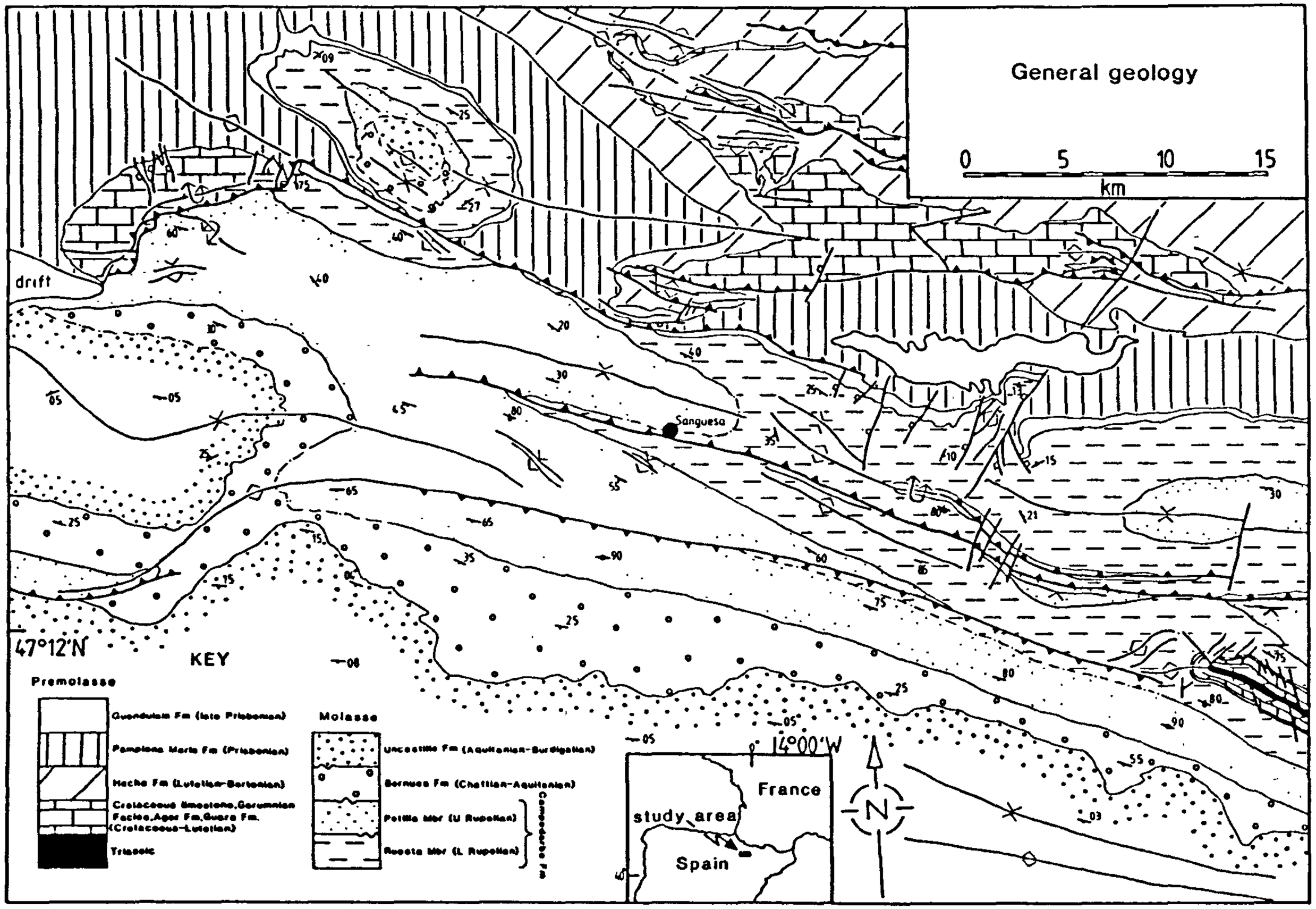

Fig. 1.3. General geological map of the study area. Compiled from the author's observations, Puigdefabregas (1975), IGME (1974, 1976, 1978a, 1978b) and Castiella *et al.* (1978).

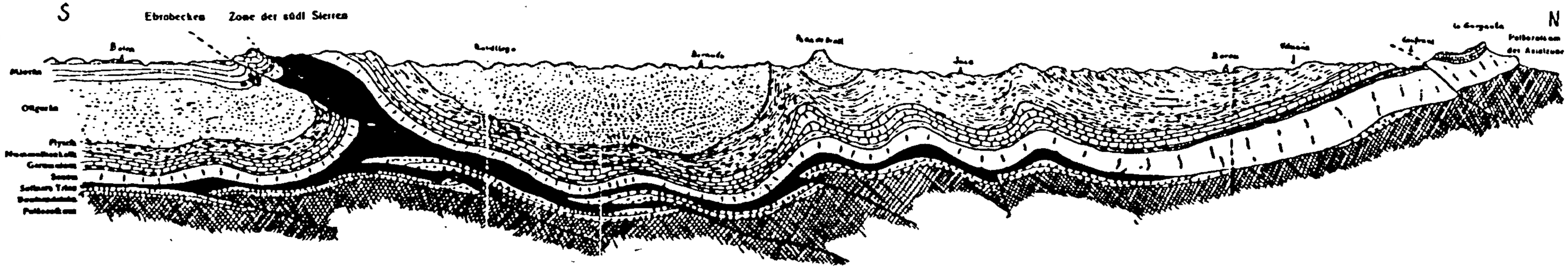

Fig. 1.4. North-south section from the Palaeozoic Axial Zone, through the central part of the Jaca basin, to the Ebro basin. From Selzer (1934, abb. 20).

Plate 1.1a. Landsat image of the Southwest Pyrenees and Ebro basin. Box shows rough boundaries of the study area. Scale bar in lower left corner is 15 km. S-Sanguesa.

Plate 1.1b. Casts of duck footprints on the base of a sandstone within the earliest Oligocene Guendulain Formation.

Plate 1.1c. Imprints of palm leaves found at the base of the early Miocene palaeochannel illustrated in Fig. 6.8.

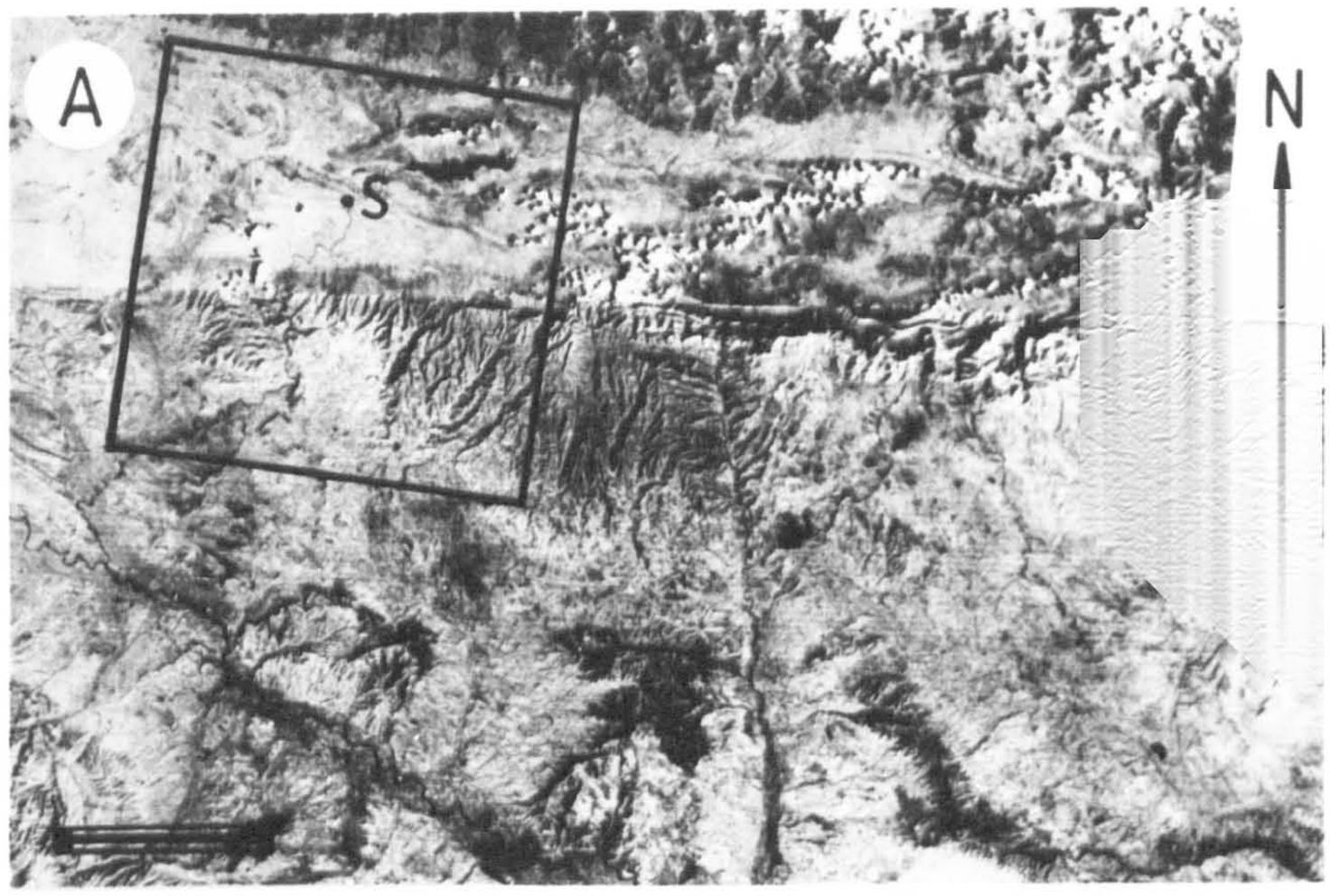
A
S
N

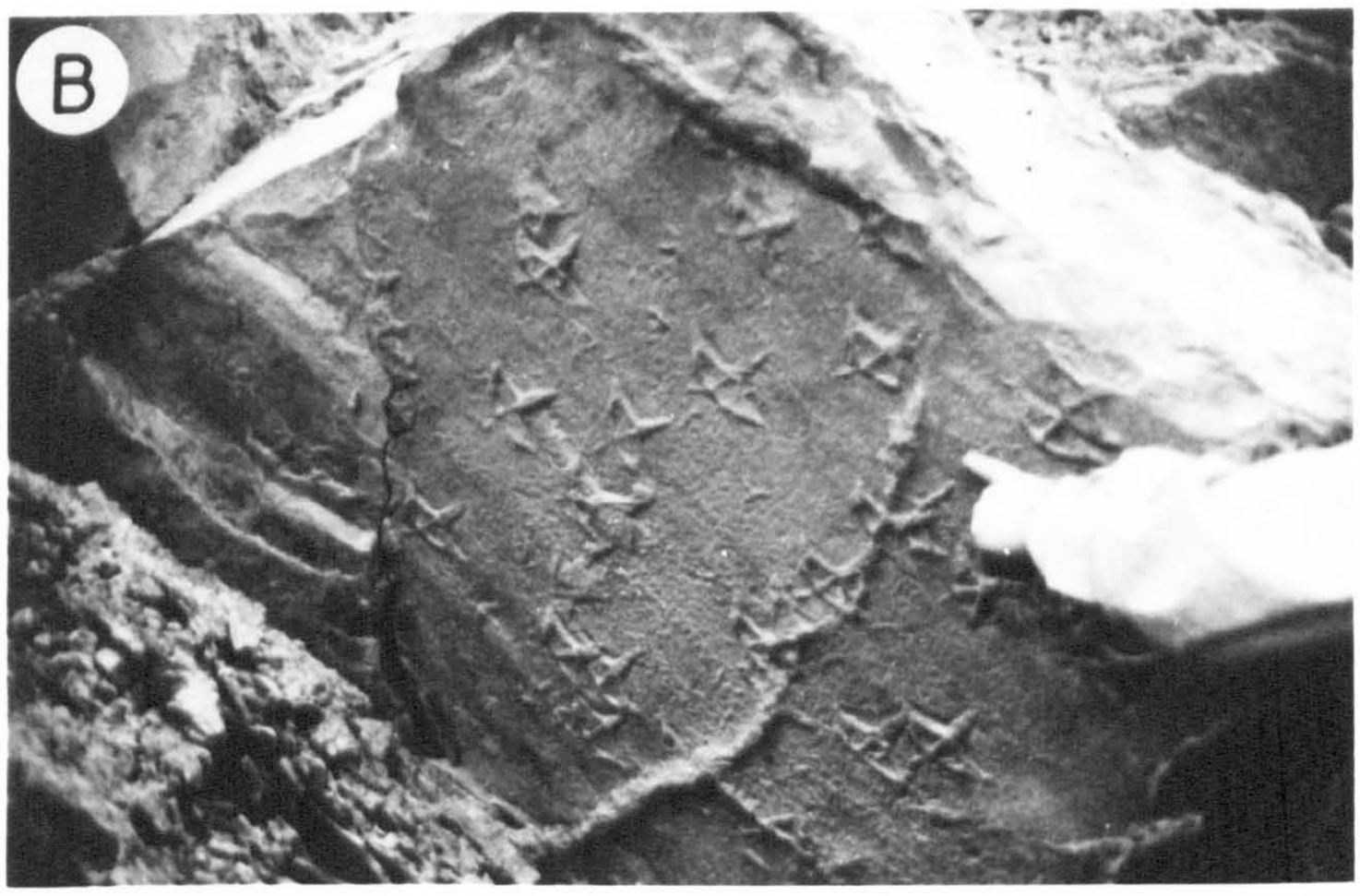
B

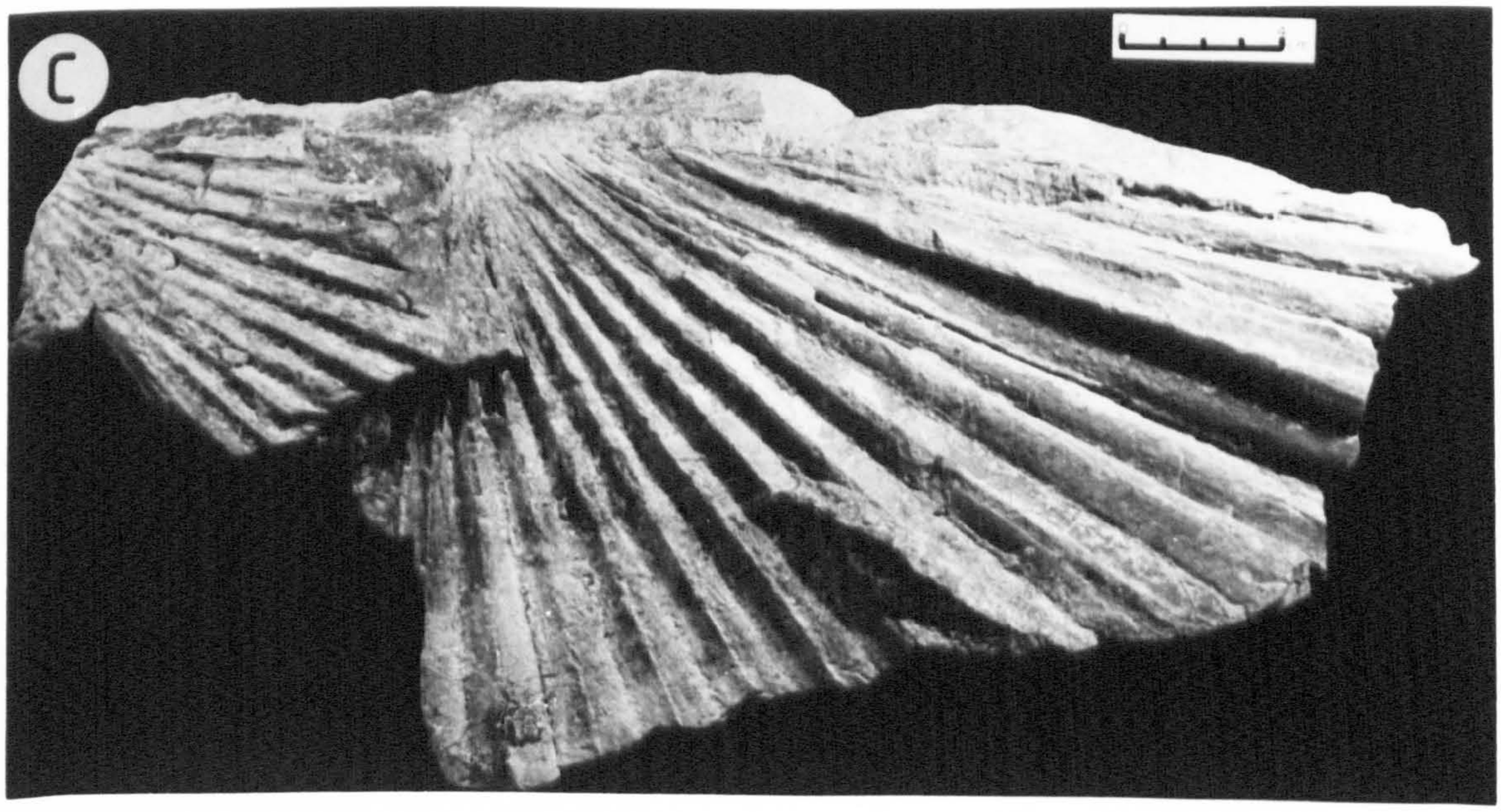
C

Table 1.1. Stratigraphic subdivision of the Jaca basin molasse sequence

Age		After Soler & Puigdefabregas (1970)	After Puigdefabregas (1975)	This study	
Burdigalian	Miocene	Uncastillo Fm	Uncastillo Fm	Uncastillo Fm	
Aquitanian					
			Bernues Fm	Bernues Fm	
Chattian		Bernues Fm			
U Rupelian	Oligocene		U Campodarbe Fm	Petilla Member	
L Rupelian		Anzanigo Fm	M Campodarbe Fm	Ruesta Member	Campodarbe Fm
Priabonian	Eocene	Campodarbe Fm (dominantly marine facies)	L Campodarbe Fm	Gaiardon Member	
Bartonian					

CHAPTER 2

STRUCTURAL EVOLUTION

2.1 CONVENTIONS AND METHODOLOGY

The Jaca thrust-top basin is the westernmost part of the detached Pyrenean margin of the Ebro basin and it rode piggyback on the Gavarnie Thrust Sheet (Fig. 1.1) during the Eocene and Oligocene (Seguret 1972). The eastern part of the Jaca basin is bounded along its southern margin by the Exterior Sierras, a prominent range of hills underlain by Mesozoic and lower Palaeogene limestones and marls. The Exterior Sierras constitute the emergent tip of the Gavarnie Thrust Sheet (Fig. 1.1) and their structure was first investigated in detail by Soler & Puigdefabregas (1970). They recognised that there had been 10 km of southward movement of the Gavarnie Thrust Sheet between the late Oligocene and early Miocene, after which time the thrust system locked.

However, the absence of exposed major structures in the thrust front zone of the West Jaca basin makes it a more problematic structure to elucidate and has led to the region being neglected by structural geologists. Indeed some tectonic maps of the South Pyrenees (eg. Choukroune & Seguret 1973) have incorrectly implied that, to the west of the Exterior Sierras, a buried Gavarnie tip line trends obliquely across the long axis of the West Jaca basin and dies out to the northwest. By presenting four N-S strike-normal sections, linked by an E-W strike-parallel section, this chapter proposes a solution to the structural evolution of the South Pyrenean thrust front in the West Jaca basin, and, it establishes a regional structural framework for the subsequent stratigraphic description and discussion.

Because the general aspects of thrust system nomenclature have received much attention in recent publications (eg. McClay & Price 1981; Boyer & Elliott 1982; Butler 1982a; Morley 1986; Platt *et al.* 1986) they are not reviewed here. It is, however, appropriate to draw attention to the main principles on which the present sections were constructed because the special features of the study area dictated a few less well known approaches. The principal axiom followed during balanced section construction is that the area of the section has not changed during deformation and hence it is retrodeformable. This in turn implies that plane strain was experienced during deformation; an assumption widely regarded as valid if the section line is drawn perpendicular to the regional strike of thrusts and thus, parallel to thrust transport direction (Fig. 2.1).

The sections illustrated in Figs. 2.2, 2.3, 2.4 and 2.5 have been line-length balanced, that is, they have been drawn so that bed lengths at different structural levels through the deformed stratigraphic succession are equal. If the area of the deformed cross section remains constant, then the sinuous bed lengths measured around folds and across faults must balance, otherwise the section cannot be correct (Dahlstrom 1969; Hossack 1979). However, a vital characteristic of thrust-top basins is that shortening and sedimentation are contemporaneous events. The Oligo-Miocene molasse was deposited on a 'basement' that had already experienced significant shortening. Therefore, the sections across the West Jaca basin only line-length balance from the base of the Palaeocene to the base of the Oligocene, above which, bed lengths systematically decrease. The existence of localised unconformities and other growth fold phenomena throughout the West Jaca basin molasse sequence testify to this syndepositional shortening. All the sections were constructed assuming that, at the time of their propagation, thrust ramps initiated at angles of up to 30° from thrust flats.

2.2 STRATIGRAPHY OF THE SECTIONS

The Triassic to Eocene stratigraphic succession, comprising the sub-Ruesta Member premolasse 'basement' shown on the sections of Figs. 2.2-2.5 is based largely on the work of Puigdefabregas (1975) and IGME (1974, 1976, 1978a, 1978b). Throughout the South Pyrenees the evaporite-rich and muddy Keuper facies of the upper Triassic is an important regional detachment horizon permitting thin skin fault systems to develop. In the study area, the only outcrop of Triassic rocks is in the core of the Sierra de Santo Domingo where the succession comprises variegated marls and deformed gypsiferous evaporites. It lacks fossils and has been attributed to the Triassic System on the basis of its general lithostratigraphic attributes, which are those of well dated Triassic sequences elsewhere in the west Alpide realm, and its position beneath rocks of late Cretaceous age (Selzer 1934).

A major hiatus followed deposition of the Triassic succession; Jurassic and lower and middle Cretaceous rocks being absent in any of the Sierras bordering the Jaca molasse basin. Extreme lateral thickness variations characterise the upper Cretaceous rocks that crop out in the Sierras de Illon, Leyre, Alaiz and Santo Domingo (Fig. 2.1) (Souquet, 1967). In general, the upper Cretaceous thins southward from 1300m in the Sierra de Alaiz, where it comprises grey marl and sandstone, to 200m in the Sierra de Santo Domingo, where it comprises buff coloured sandy limestone.

A distinctive fluviolacustrine red bed horizon up to 70m thick is sandwiched between the Cretaceous sandy limestone and the Palaeocene alveolined limestone in the Sierras de Orba, Leyre and Santo Domingo. This unit is commonly called the Garumnian facies and it forms a laterally persistent horizon straddling the Mesozoic-Cenozoic boundary (Souquet 1967).

The Garumnian facies is succeeded by Palaeocene pale grey, planktoniferous limestone of the Ager Formation (Mey *et al.* 1968) which thins southward from a maximum thickness of 240m in the Sierra de Leyre to 70m in the Ebro basin.

Up to 1100m of Eocene rocks in the study area are represented by a stratigraphically complex sequence of deep to shallow marine clastics and carbonates that are divisible into two main flysch units separated by a transgressive sandstone series. The onset of post-flysch marine regression and the establishment of terrestrial conditions is marked by an upper Eocene deltaiccomplex capped by 60m of evaporite defining the Guendulain Formation (Mangin 1960).

2.3 SEQUENTIAL DEVELOPMENT OF THRUSTS

The earliest major structure to form in the study area was the thrust culmination of the Sierra de Orba (thrust 1: Figs. 2.1 and 2.3). The age of the culmination is constrained as latest Eocene by its deformation of the upper Eocene Pamplona Marls Formation and its lack of effect on early Oligocene molasse. No evidence exists to suggest that the three closely spaced forethrusts in the culmination evolved as part of a 'leading' or 'trailing' imbricate fan (see Butler 1982a for definitions). However, it is likely that following the development of the three forethrusts, the imbricate fan experienced resistance to further thrusting which was mechanically resolved by the formation of a steep backthrust of less than one kilometre total displacement (see Plate 2.1a). The culmination may be traced for about eight kilometres west and twenty kilometres east along strike from the line of section in Fig. 2.3. Its western termination is probably represented by a lateral ramp located beneath the central part of the Sierra de Leyre (Fig. 2.1).

The next generation of thrusting was concentrated along the major frontal ramp that may be traced from the conjectured lateral ramp in the central Sierra de Leyre, westward for 44 km, to the western extent of the Sierra de Alaiz (thrust 2: Figs. 2.1, 2.4 and 2.5). This thrust episode is dated as latest Eocene, largely on the basis of slumps and flowrolls (Sorauf 1965) that are characteristic of the late Eocene Guendulain Formation and the lowest part

of the Ruesta Member molasse along the northern margin of the West Jaca basin (eg. Plate 2.1b) and in the Izaga sub-basin. These syndepositional deformation structures occur in muddy lacustrine sediments and acording to Kelling & Williams (1966), slumps and flowrolls are reliable indicators of palaeoseismicity in slowly accumulated lacustrine sequences. Figure 2.7 shows that in the Sierra de Alaiz, the Leyre-Alaiz thrust cuts rocks of the mid Oligocene Petilla Member with a relatively smooth trajectory (in the sense of Cooper & Trayner 1986). However, it will be demonstrated that it had a history of reactivation which began in the latest Eocene.

Recent workers on mountain fronts have questioned whether they are unique structures formed during a single episode in the history of a thrust system (eg. Jones 1982; Banks & Warburton 1986; Morley 1986; Vann *et al.*, 1986). They argue that with a piggyback sequence of thrust development, where the thrust front has formerly propagated through the orogen hinterland toward the foreland, why are structures characteristic of mountain fronts not more common in the internal parts of orogenic belts? It is proposed here that the imbricate fans of the Sierras de Orba and Leyre, and especially the backthrusted 'pop-up' geometry of the Sierra de Orba, are particularly characteristic of thrust fronts that have been described from elsewhere (eg. Morley 1986; Vann *et al.* 1986). Hence, the Sierra de Illon, Orba, Leyre and Alaiz culminations most likely represent 'frozen' palaeothrust fronts that developed during the latter part of the Eocene and have since been incorporated into the thin skin thrust system by further thrust propagation during the Oligocene.

The Ruesta thrust was the earliest thrust to significantly affect the palaeogeographic configuration of the molasse basin and it possesses a frontal ramp and hangingwall anticline (shown in Fig. 2.8) that extend for 15 km along strike to the south of Pintano and Ruesta (thrust 3: Figs. 2.1 and 2.3). The Ruesta thrust was active during deposition of the Ruesta Member and above its western lateral ramp there is a sub-area characterised by several map scale, transversely-striking normal faults that are interpreted here as hangingwall 'collapse' faults (see the strike-parallel section in Fig. 2.6). This sub-area shall be called the Ruesta fault zone and it reflects regional net extension in the culmination above the lateral ramp of the Ruesta thrust. A later chapter will show how the structural evolution of the Ruesta fault zone is recorded by the distribution of alluvial facies and dispersal directions in the Ruesta Member. Gentle folding of the Petilla Member in the Bailo-San Juan de la Pena syncline (Fig. 2.1), in the hangingwall of the Ruesta thrust, indicates that the thrust was active until at least the start of deposition of the Petilla Member.

Further propagation of the thrust front southward led to uplift and tilting above the Sanguesa thrust (thrust 4: Figs. 2.1, 2.3 and 2.4) from the beginning of Petilla Member deposition, as constrained by a localisd angular unconformity at the Ruesta Member/Petilla Member boundary (Plate 2.1c) at Sanguesa. The Sanguesa thrust may be traced for 60 km along strike, terminating at its western tip above the proposed Alaiz-Ujue oblique ramp (see Figs. 2.1 and 2.6).

To the west of the Sierra de Santo Domingo, in the southeast of the study area, a range of gullied hills underlain by Oligo-Miocene molasse extend along strike for fifty kilometres. These hills are here called the Pena flexure (Fig. 2.1) and they form a structural and topographic divide between the thrust belt of the West Jaca basin and the autochthonous, relatively undeformed Ebro foreland basin. The flexure is interpreted here as a syndepositional mountain front structure serving to accommodate a shortening of up to 45%, which to the east, is expressed by emergent thrusts in the Exterior Sierras (see Nichols 1987).

The sections in Figs. 2.3 and 2.4 show that the Pena flexure is a passive-roof duplex, a structural assemblage originally defined by Banks & Warburton (1986) on the basis of evidence from the frontal Himalayan ranges of Pakistan. The Pena flexure passive-roof duplex was the last and most forelandward major thrust structure to develop in the study area and its tectonic climax was during deposition of the Bernues Formation, in the late Oligocene, when it induced substantial alluvial fan development along its southern flanks (see Chapter 5). However, erosion of the Ruesta Member above the Pena flexure suggests that it was a zone of at least minor uplift and tilting from the mid Oligocene onward.

Passive-roof duplexes evolve by a process of progressive footwall collapse and accretion of horses to the hangingwall in a structural sequence initially described by Boyer & Elliott (1982). The distinctive feature of a passive-roof duplex, however, is that the roof thrust displays a backthrust sense of displacement, in contrast with the more usual forelandward displacing roof thrust characteristic of most duplexes. Passive-roof duplexes of various scales have also been described from the Canadian Rocky Mountain foothills (Jones 1982; Charlesworth & Gagnon 1985; Price 1986) and the southern Norwegian Caledonides (Morley 1987). They are thought here to form at orogen margins where, during the waning stages of thrust propagation and below a critical depth to detachment, the most economical mechanism of duplex development is to form an emergent backthrust. Along such orogen margins, the relat-

ively thin deforming cover means that the overburden represented by a crustal wedge above an incipient backthrust is small and mechanically easy to underthrust. The backthrust therefore evolves by passive underthrusting of the overlying foreland wedge by the hinterland thrust system. Evidence for the existence of a passive-roof duplex beneath the Pena flexure is based on the following observations and relationships.

(1) The Pena flexure passive-roof duplex caused a southward tilting of the Ebro basin margin sequence. This is reflected by the consistent southward dispersal directions recorded by palaeocurrent indicators in the alluvial sediments deposited during development of the structure (see Chapter 5). The presence of forelandward tilted sequences along foreland basin margins has frequently been used as a criterion for postulating the existence of a blind basin margin duplex (eg. Williams 1985).

(2) The presence of an upward-steepening, or listric, roof thrust to the duplex provides an explanation for the occurence of numerous offlap unconformities within the Petilla Member and Bernues Formation successions along the southern flank of the Pena Flexure (see Chapter 5). The listric shape of the backthrust caused the depositional surface to experience continuous southward tilting as the passive-roof sequence was underthrust.

(3) Puigdefabregas & Soler (1973) and Nichols (1987) have demonstrated that only 15 km east along strike from the eastern limit of the passive-roof duplex, there is up to 14 km of shortening across the Exterior Sierras. Despite this shortening further to the east, the transition from the West Jaca basin to the Ebro basin is marked at the present surface by only a single backthrust with less than two kilometres of displacement. Furthermore, no major lateral ramp separates the Pena flexure from the Exterior Sierras (Fig. 2.1).

At its western end, the Pena flexure terminates at a blind oblique ramp, here called the Alaiz-Ujue oblique ramp (Fig. 2.1), which separates the Olleta sub-basin to the west from the central area of Ruesta and Petilla Member rocks to the east. The location of this ramp is marked by arcuate fold axial traces and a general 45° anticlockwise rotation of regional structural trends. In addition, there is a dramatic 3 km increase in the thickness of the entire molasse sequence to the west of the ramp in the Olleta sub-basin (see Figs. 2.6 and 2.9).

Although the Pena flexure passive-roof duplex was the last major structure to develop in the piggyback sequence of thrust propagation through the West Jaca basin, there is some evidence suggesting that there was a reversion of

thrusting toward the orogen hinterland. For example, angular unconformities beneath the Bernues and Uncastillo Formations in the Izaga sub-basin, record two episodes of proximal emergent thrusting in the hangingwall of the Leyre-Alaiz thrust during the late Oligocene and early Miocene.

More spectacular than these episodes of thrusting was the reactivation of the Sierra de Alaiz culmination, a late Oligocene or early Miocene event resulting in a 45° anticlockwise rotation of the Sierra de Alaiz about a pivot point at its eastern end. This rotational reactivation was a consequence of an eastward deterioration in the gliding quality of Keuper facies beneath the Sierra de Alaiz (J. del Valle: personal communication in 1985). Flexing along the crestal culmination of the Sierra de Alaiz during reactivation led to the formation of several steep, normal cross-faults along its northwest margin (Fig. 2.1).

2.4 DIACHRONEITY OF DEFORMATION IN THE SOUTH PYRENEAN BASINS

The geometric evolution of the West Jaca basin thrust system largely conforms with the classical Canadian Rocky Mountain model that invokes a piggyback, forelandward propagating sequence of thrusting. In a South Pyrenean context, the N-S sequential development of thrusts accounts for most N-S variations in the age of thrusts and structural style as revealed by the sections in Figs. 2.2-2.5. However, the various ages of localised unconformities in the Oligo-Miocene fill of the West Jaca thrust-top basin (see Fig. 2.9) record lateral (E-W) diachroneity of deformation. Each unconformity is related to local detachment of the basin from its pre-Triassic 'basement' and consequent tilting of the synorogenic land surface. Unconformities range in age from early Oligocene in the Ruesta fault zone, through mid to late Oligocene in the central part of the molasse basin, to early Miocene in the Olleta sub-basin.

The sections shown in Figs. 2.2-2.6 reveal the following lateral variations in the West Jaca basin thrust system.

(1) The depth to detachment, and hence the thickness of the deforming sedimentary cover, increases westward from 2 to 6.8 km.
(2) There is a gradual change in the attitude of the regional sole thrust, from a forelandward tilt in the east to a hinterlandward tilt in the west.
(3) There is a westward increase in thrust ramp spacing from about 2 to about 20 km.
(4) Shortening decreases from 30% in the west to 7% in the east.

The following two processes are considered to have been the principal ones controlling lateral variations in the thrust system:

(1) the westward (ie. laterally) migrating deformation front in the South Pyrenees;
and
(2) the waning of orogenic contraction from the early Oligocene onward.

The inference that thrusting started earlier in the east follows from observations which show that the eastern part of the study area experienced the transition from subsidence and net sediment accumulation to uplift and net erosion (topographic inversion) earlier than the western part of the study area. For example, the Ruesta fault zone was a region of molasse sedimentation for less than 5 Ma (based on the Tertiary stratigraphic subdivision of Harland *et al.* 1982) before its topographic inversion at the end of Ruesta Member deposition. In contrast, the Olleta sub-basin experienced up to 14 Ma of relatively undisturbed subsidence and sedimentation before it was detached from the basement and topographically inverted during Uncastillo Formation deposition in the early Miocene. Thus, the thickest and stratigraphically most extensive molasse accumulated in the Olleta sub-basin where subsidence was most prolonged (Fig. 2.9). As a consequence, the thickest skinned deformation occurred in the western part of the West Jaca basin (Fig. 2.6) where the sole thrust detachment horizon was at its greatest depth.

The westward propagation of the deformation front also caused the locus of subsidence and deposition to migrate along the length of the West Jaca basin. Thus, between the late Oligocene and early Miocene, during the time of greatest subsidence and sediment accumulation in the Olleta sub-basin, the area of maximum deposition in the east was located further south in the Ebro basin. This variable locus of deposition is reflected in the attitude of the sole thrust which dips toward the Ebro basin in the eastern part of the West Jaca basin (Fig. 2.3) whereas, further west, it is at its maximum depth beneath the Olleta sub-basin (Fig. 2.5).

Suppe (1985) has noted that in the Front Ranges of the Canadian Rockies, reductions in stratigraphic thickness are accompanied by an increase in thrust frequency and several other workers have described similar relationships in which thickness of the deforming cover controls thrust ramp spacing (eg. Bombolakis 1986; Morley 1987). It is likely that, in the West Jaca basin, the progressive westward increase in thickness of the deforming cover accounts for the greater N-S separation between thrust ramps in the west (compare the sections in Figs. 2.3 and 2.5).

During the closing stages of Pyrenean orogenesis, westward propagation of the deformation front through the West Jaca basin was accompanied by decreasing contraction. This decline in late orogenic contraction is reflected in the reduced amount of shortening that may be calculated from the sections across the western part of the basin compared with those across the eastern part. Additionally, there is evidence that, as proposed by Morley (1987), at the limit of thrust front advance it is kinematically more favourable to reactivate pre-existing thrusts in the hinterland than to form new thrusts. For example, directly to the north of the Olleta sub-basin, there was early Miocene reactivation of the Sierra de Alaiz thrust, a structure that was initiated in the late Eocene.

The laterally migrating deformation front that played such an important role in the structural and stratigraphic evolution of the West Jaca basin may also be shown to have influenced the development of the South Pyrenean basin on a regional scale. Figure 2.10 is an E-W section showing stratigraphic and facies relationships in the South Pyrenean basins. The section demonstrates the E-W diachroneity of sedimentation in the South Pyrenees with a marine regression sequence that ranges in age from mid Eocene in the Graus basin (Fig. 1.1) to early Oligocene in the West Jaca basin. Also illustrated in Fig. 2.10 are a series of individual, but thick, alluvial fan conglomerate sequences that become progressively younger toward the west, from mid Eocene in the Graus basin to early Miocene in the West Jaca basin. These conglomerate-filled 'tectonic valleys' are interpreted here as reflecting the local emergence of thrusts. The progressively younger ages of the conglomerates toward the west suggests that the deformation front responsible for them propagated westward during a series of punctuated displacment events. It is proposed here that such a front, migrating both parallel and normal to the long axis of the Pyrenees, exerted an important influence on the tectonic evolution of the South Pyrenean thrust-top basins.

2.5 STRUCTURAL EVOLUTION OF THE WEST JACA BASIN: CONCLUSIONS

(1) In the West Jaca basin, the westernmost compartment of the South Pyrenean thrust-top basins, the Pena flexure marks the location of a thrust front that divides the thrust-fold belt from the Ebro basin, the relatively undeformed foreland basin. The Pena flexure is here interpreted as a passive-roof duplex.

(2) The southward decrease in age of the West Jaca basin thrust system, and N-S variations in structural style, as revealed by strike-normal balanced

sections through the basin, are accounted for by a piggyback sequence of thrust propagation toward the foreland. Lateral E-W variations in the amount of shortening, the depth to detachment, thrust ramp spacing and the attitude of the sole thrust are attributed to a combination of a westward migrating deformation front and a westward decrease of late orogenic contraction.

(3) Oligo-Miocene advance of the thrust front through the West Jaca basin is recorded in the stratigraphic evolution of the basin-fill. In particular, the laterally diachronous deformation front was an important factor in controlling the development and distribution of localised unconformities.

(4) During their Palaeogene to early Neogene evolution, the South Pyrenean thrust-top basins were affected by a thrust front that migrated both southward toward the foreland, and westward, parallel to the orogen axis. The latter, axially migrating deformation front is reflected in a highly diachronous marine regression sequence and a series of discrete alluvial fan conglomerate sequences that become progressively younger westward.

2.6 ORIGIN OF THE SOUTH PYRENEAN THRUST SYSTEM AND ITS CONTROL ON BASIN SUBSIDENCE

This section will address the following questions.

(1) What is the origin of the South Pyrenean contractional duplex, recently documented in the pre-Triassic 'basement' by Camara & Klimowitz (1985, fig. 7) (see Fig. 2.11), and what is its relationship with the 'cover' thrust system?

(2) What caused the South Pyrenean thrust front to migrate westward, parallel to the axis of the orogen?

(3) Is it necessary to invoke an external geodynamic influence to generate up to seven kilometres of Oligo-Miocene subsidence observed in the Olleta sub-basin and, if so, what was the nature of this influence?

The tectonic map of the South Pyrenees in Fig. 2.11 shows the spatial and geometric relationship between the blind contractional duplex and the westward migrating cover system of thrusts. Camara & Klimowitz (1985) speculated that the basement duplex is related to a syncollisional dextral motion between the Iberian and European plates. Their hypothesis is rejected here because it seems unlikely that what would have been a relatively minor component of dextral motion, compared with the dominant head-on collision of Iberia with Europe, could have generated a duplex quite the size of the one they describe.

Instead, it is proposed here that the basement duplex may have been a relatively long lived structure that initiated as an extensional duplex during the early Cretaceous, when Iberia was being displaced south-eastward by the left-lateral North Pyrenean Transform Fault (Fig. 2.11) (Le Pichon *et al.* 1971; Choukroune 1976; Choukroune & Mattauer 1978; Olivet *et al.* 1981; Boillot 1984). During this roughly 30 Ma (using the stratigraphic subdivision of Harland *et al.* 1982) episode of left-lateral motion, most of the geometrically necessary crustal extension was accommodated by an evolving constructive plate margin (Fig. 2.11). However, in the vicinity of the transform fault, locally generated extension was accommodated by imbricate arrays of en-echelon normal fault splays (Fig. 2.11).

Arrays of imbricate splay faults related to bends on large strike-slip faults generally evolve in an analogous way to ramps on dip-slip faults (Woodcock & Fischer 1986, fig. 5). However, on straight segments of strike-slip faults, such as the North Pyrenean Transform Fault during the mid Cretaceous, splays commonly initiate as non-sequential riedel fractures (Tchalenko 1970; Woodcock & Fischer 1986, fig. 8). The basement duplex first described by Camara & Klimowitz (1985) is thus interpreted here as having initiated as an array of linked normal faults, of riedel-type origin, related to the development of the North Pyrenean Transform Fault. It is reasonable to speculate that this normal faulting may have controlled the progressive northward thickening of the Cretaceous sequence shown in the N-S sections of Figs. 2.2-2.5.

During the latest Cretaceous, a kinematic change occurred and the Iberian plate began to move northward toward Europe (Fig. 2.11) (Olivet *et al.* 1981; Grimaud *et al.* 1982; Boillot 1985). However, there is substantial geophysical and sedimentological evidence to suggest that the final collisional episode between Iberia and Europe was laterally diachronous (Mattauer & Henry 1971; Ries 1978). Thus, from the earliest Palaeocene until the early Oligocene, the locus of collision migrated progressively westward and may be envisaged as a westward 'zipping-up' of the orogen. Diachronous collision had the following main consequences in the South Pyrenees.

(1) It generated the southward, and westward migrating system of thrusts that are recorded in the along-strike diachroneity of deformation and sedimentation in the South Pyrenean thrust-top basins (Section 2.4).

(2) Collision caused kinematic inversion (ie. a reversal in the sense of dip-slip fault motion) of the extensional basement duplex so that it then comprised an imbricate series of large thrust faults.

Kinematic inversion of the basement duplex caused significant loading and flexural subsidence along the length of the South Pyrenean foreland margin. The final amount of subsidence and sediment accumulation in any one part of this foreland margin therefore depended largely on the relative timing of kinematic inversion-related subsidence and the subsequent halt to this subsidence brought about by local topographic inversion by the westward-propagating 'cover' thrust system. This relationship between basement duplex-generated subsidence and cover thrust-generated topographic inversion is clearly illustrated by comparing sediment thicknesses between various parts of the Gavarnie Thrust Sheet, especially in the West Jaca basin. For example, in the eastern part of the study area, where the Oligocene sequence is 2500m thick (see section (b), Fig. 2.11), there was a gap of only 6.6 Ma between the initiation of subsidence, generated by the basement duplex, and topographic inversion. In the Olleta sub-basin, however, there was a prolonged gap of approximately 20 Ma between subsidence and topographic inversion, thus allowing the accumulation of a 7000m thick Oligo-Miocene sequence (see section (a), Fig. 2.11).

This hypothesis of roughly coeval initiation of subsidence, and diachronous topographic inversion is consistent with the work of Williams & Fischer (1984) who proposed that the thin skin thrust systems of the South and North Pyrenees postdate, and therefore truncate, earlier formed structures such as the North Pyrenean Transform Fault. In the ideas discussed here, the kinematically inverted basement duplex occurs beneath the sole thrust of the South Pyrenean thin skin thrust system and is thus not truncated by it.

The tectonic evolution discussed above is illustrated in the maps and sections of Fig. 2.11 and shall be summarised here.

(1) During the late Aptian to Santonian, the Iberian microplate moved south-eastward due to its left-lateral displacement along the North Pyrenean Transform Fault. An array of riedel-type, imbricate normal faults splayed from a straight segment of the transform fault to form a large extensional duplex.

(2) A kinematic change in the latest Cretaceous caused northward movement of Iberia and its subsequent non-orthogonal collision with Europe from the early Palaeocene onward. This diachronous collisional episode kinematically inverted the Cretaceous extensional duplex and caused a major South Pyrenean thrust front to propagate southward, toward the foreland, and westward, parallel to the direction of migration of the locus of collision.

(3) The newly formed contractional duplex imposed a significant load on the South Pyrenean foreland margin causing widespread subsidence and sedimentation in the South Pyrenean basins. The amount of subsidence and sediment accumulation in any one area was largely determined by the timing of topographic inversion of the South Pyrenean basins; itself, controlled by the westward-propagating cover thrust system. This relationship between subsidence and diachronous topographic inversion led to large variations in molasse thickness between the east and west parts of the study area.

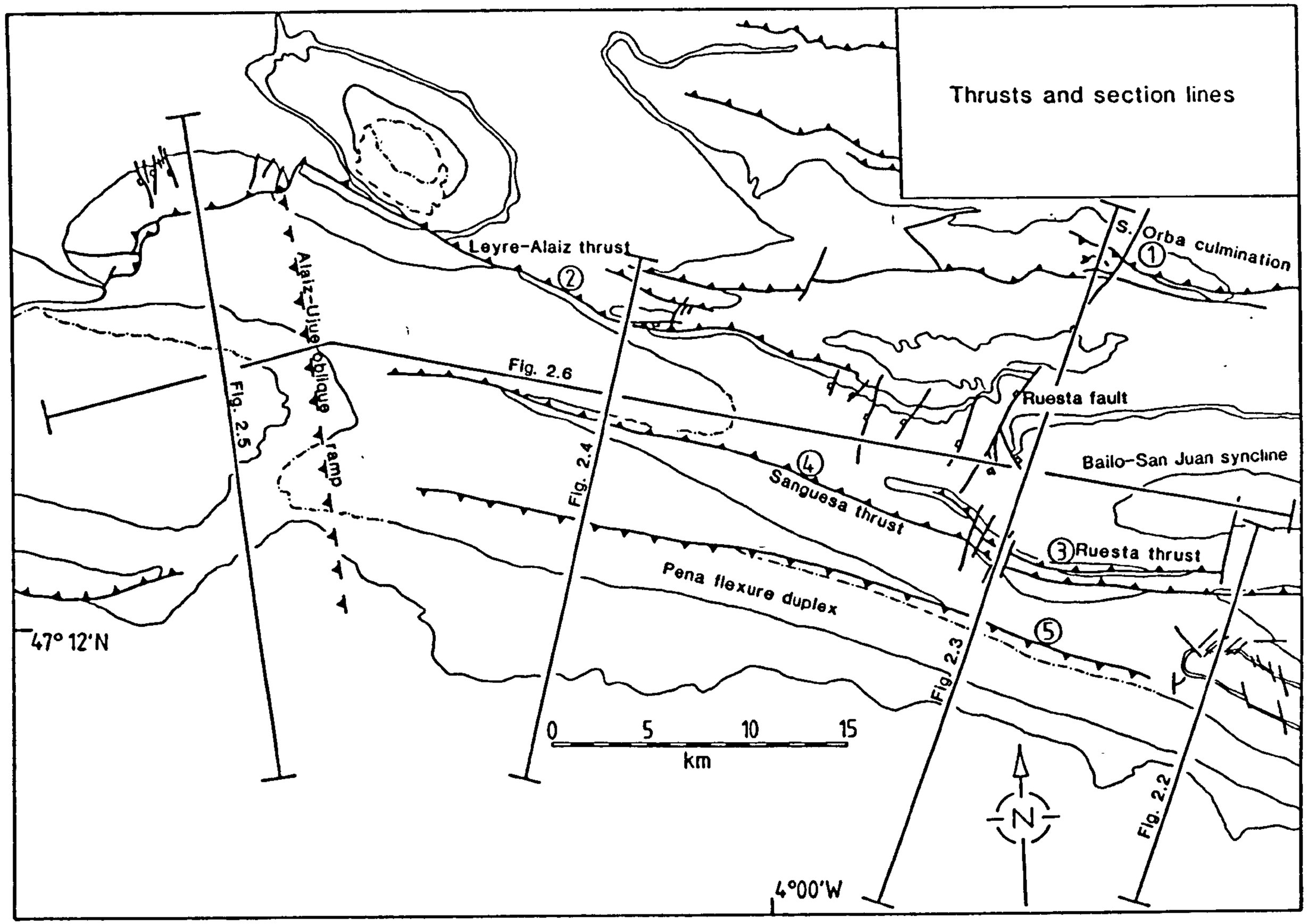

Fig. 2.1. Major structures and locations of section lines in the West Jaca thrust-top basin. Circled numbers refer to the sequence of thrust development (see text for discussion). Structural symbols and lithostratigraphic contacts as in Fig. 1.3.

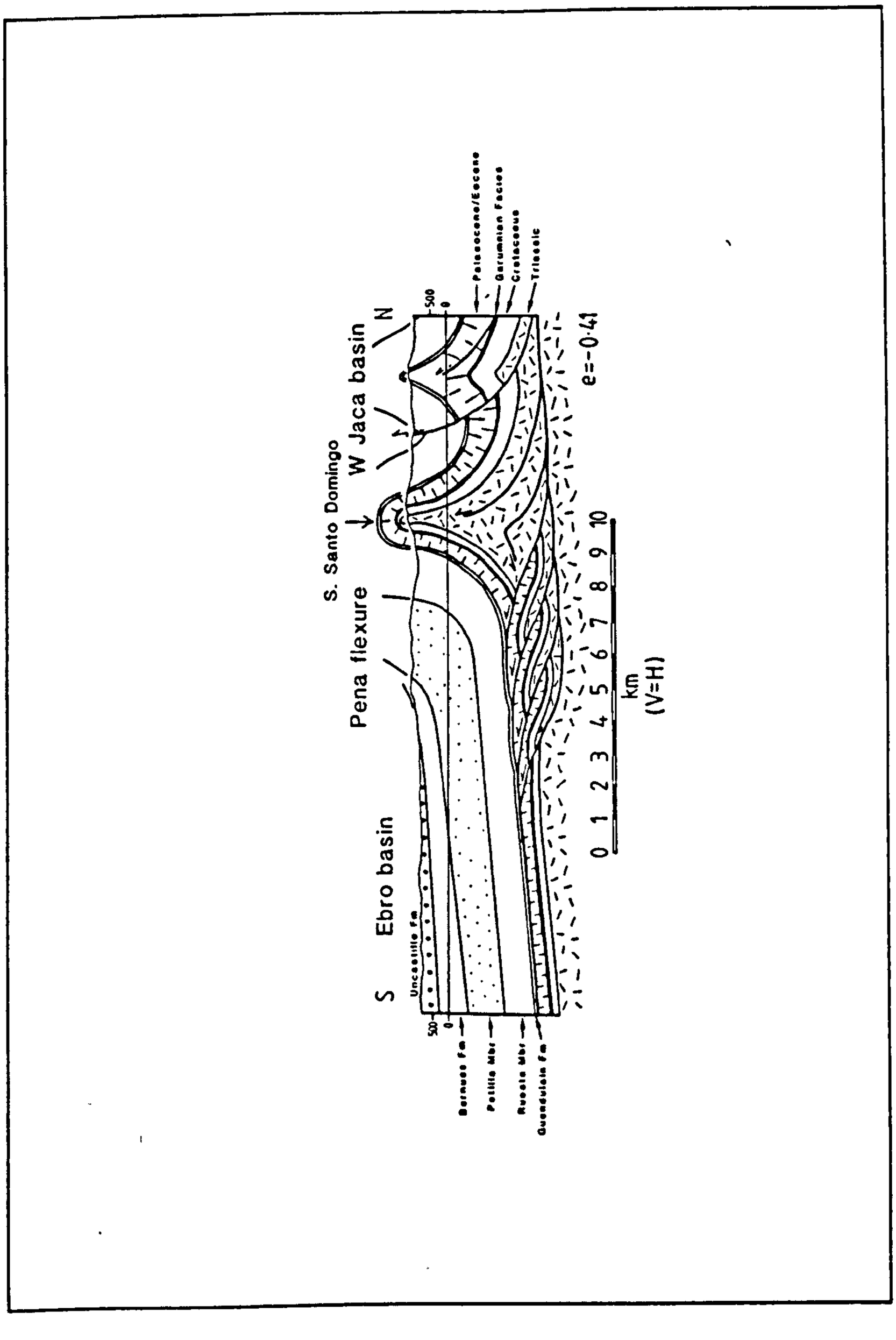

Fig. 2.2. Line-length balanced section through the Sierra de Santo Domingo. e - extension (negative extension across a strike-normal section indicates net contraction).

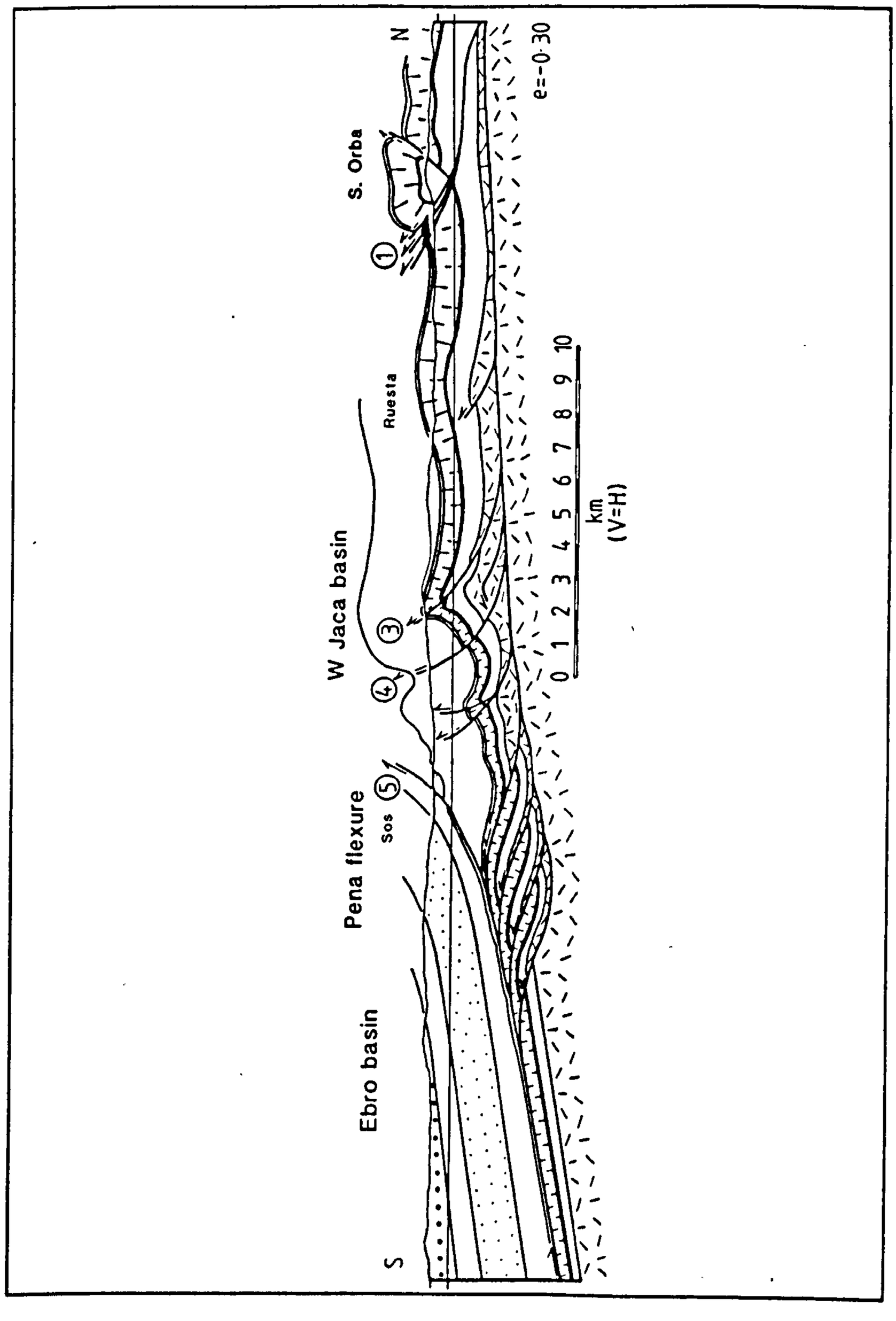

Fig. 2.3. Line-length balanced section from the Sierra de Orba to the Ebro basin. Ornament as in Fig. 2.2. e - extension.

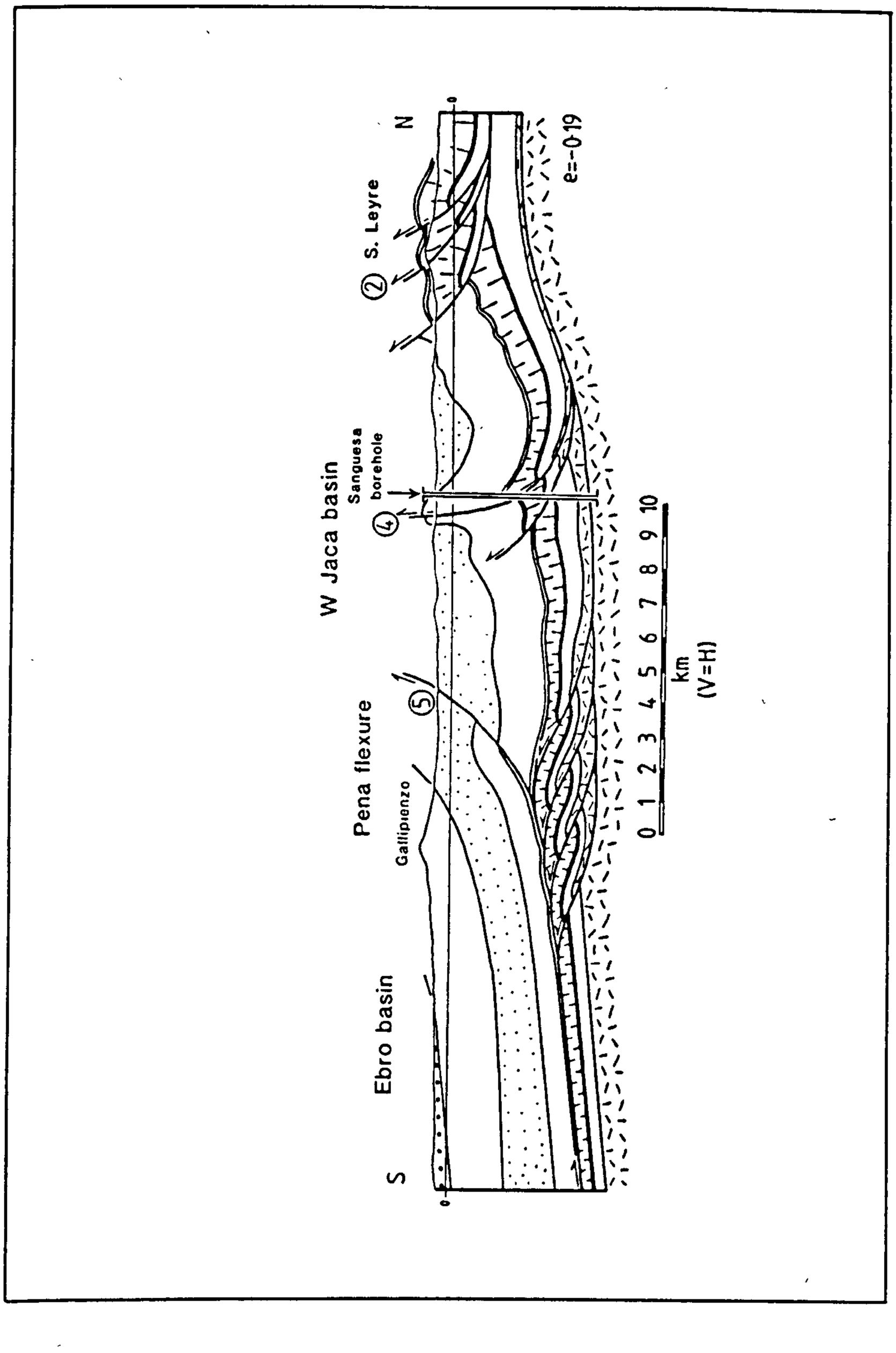

Fig. 2.4. Line-length balanced section from the Sierra de Leyre to the Ebro basin. Ornament as in Fig. 2.2. e - extension.

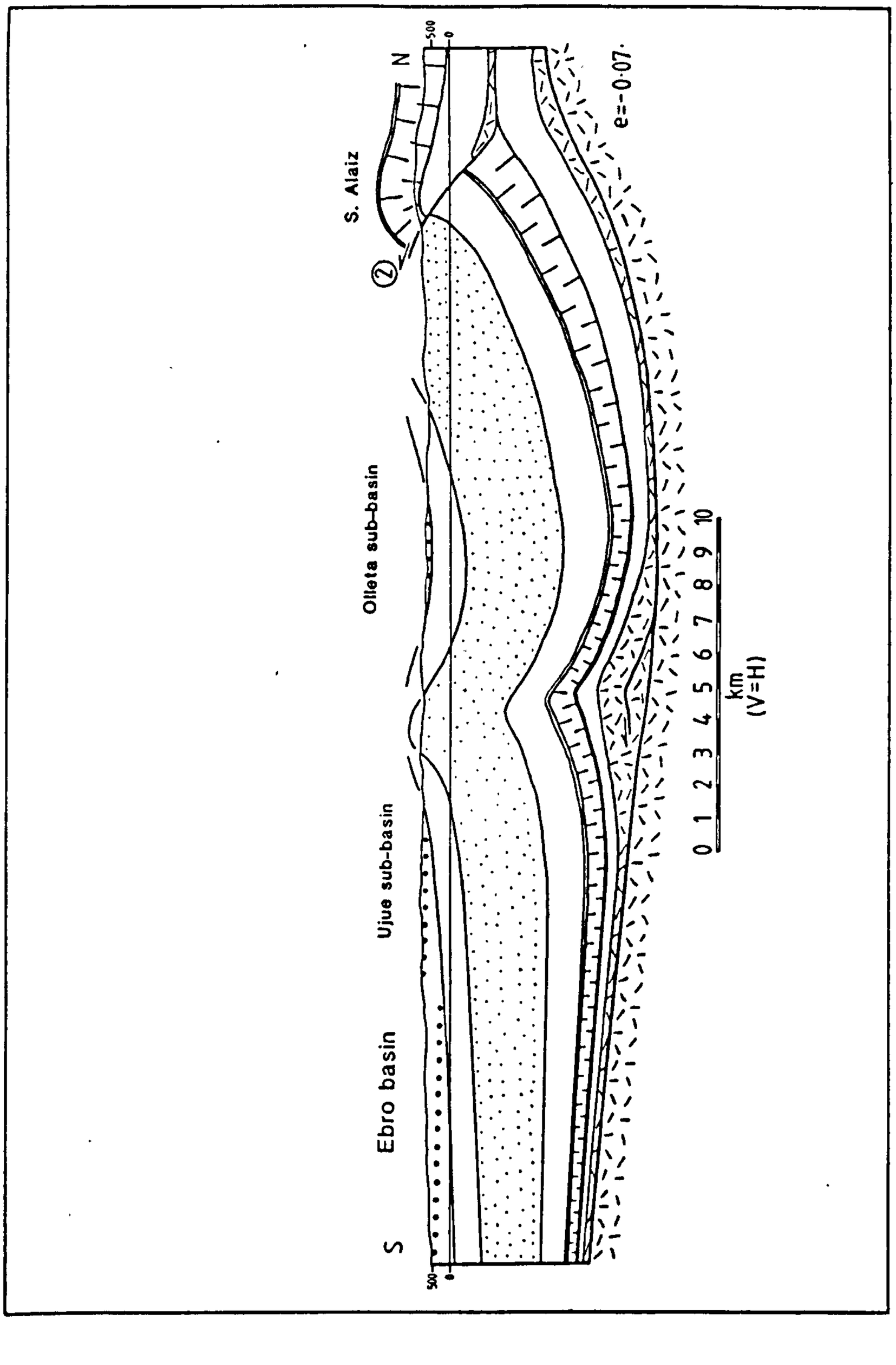

Fig. 2.5. Line-length balanced section from the Sierra de Alaiz, through the Olleta sub-basin. Ornament as in Fig. 2.2. e - extension.

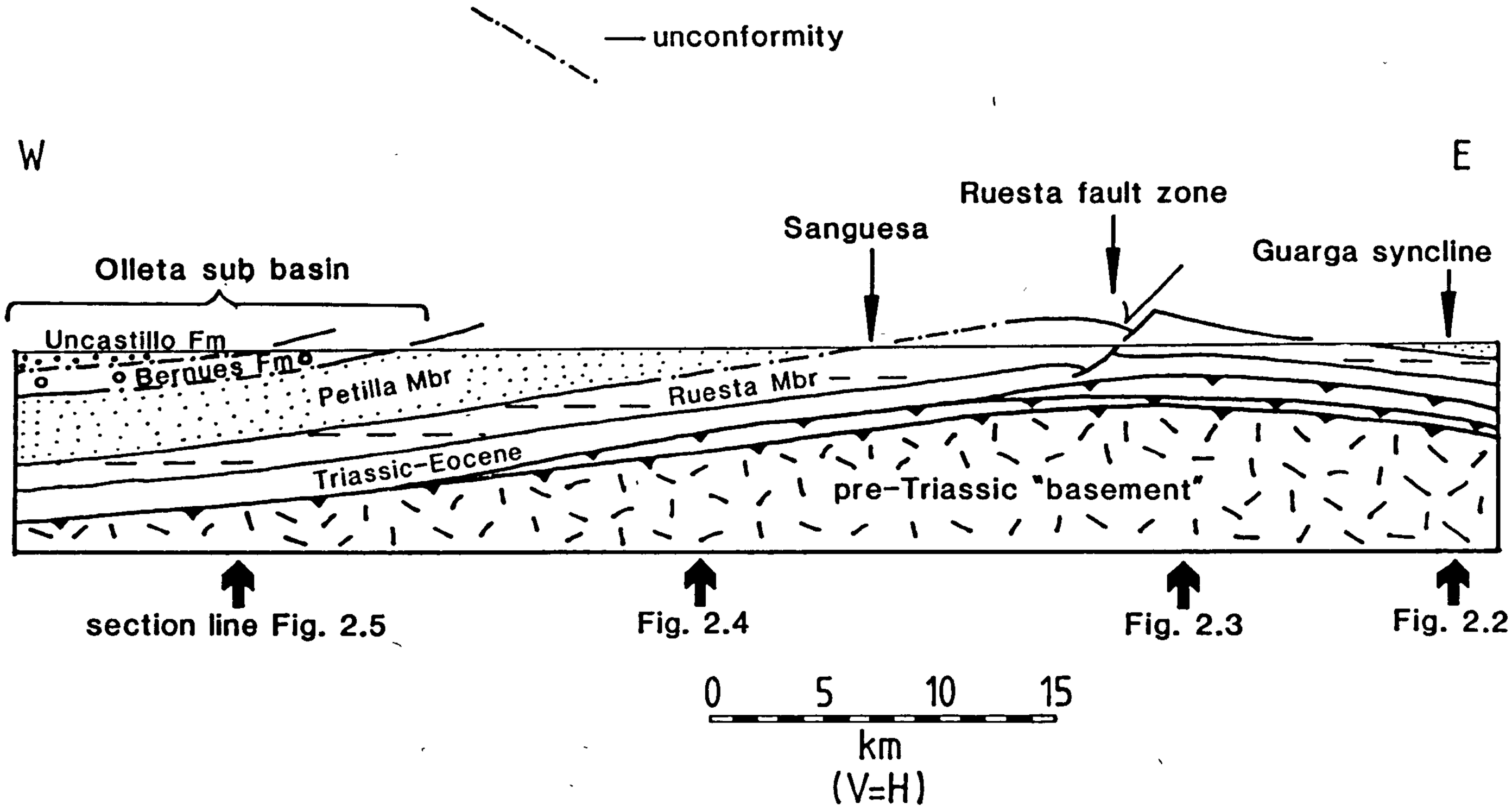

Fig. 2.6. Strike-parallel section through the West Jaca basin. Ornament as in Fig. 2.2. Solid teeth mark the footwalls of individual thrust faults.

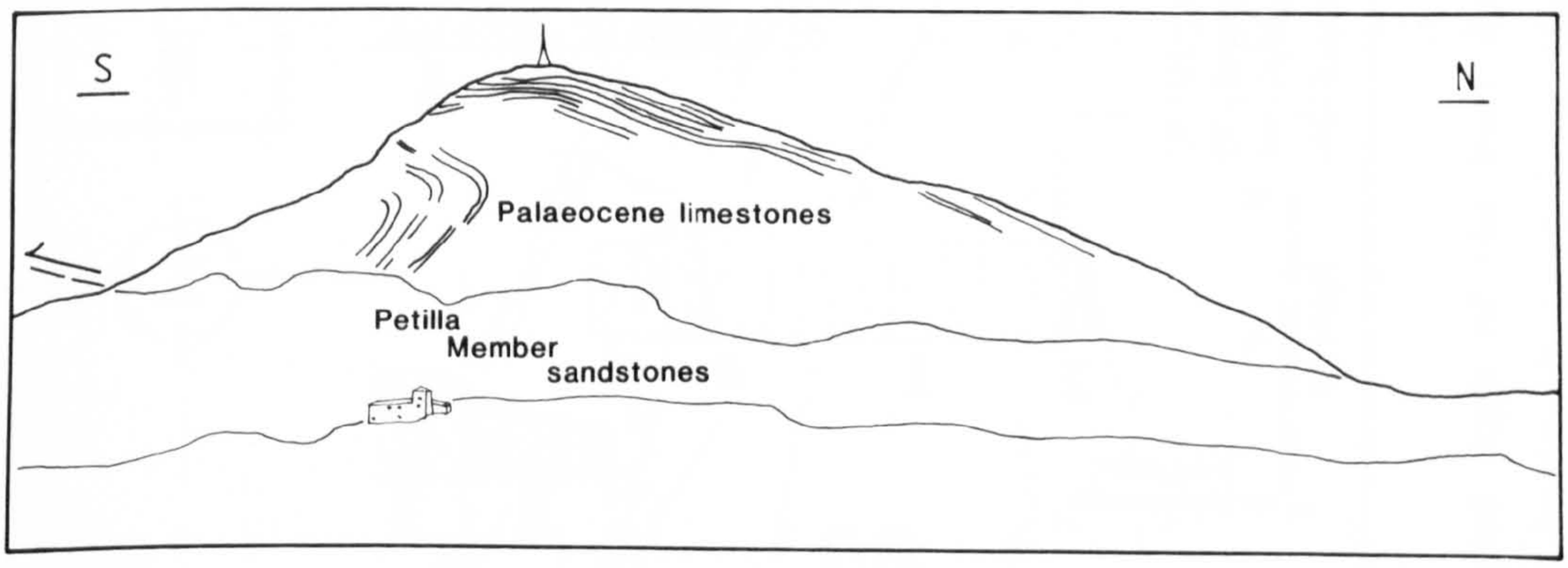
S
N
Palaeocene limestones
Petilla
Member
sandstones

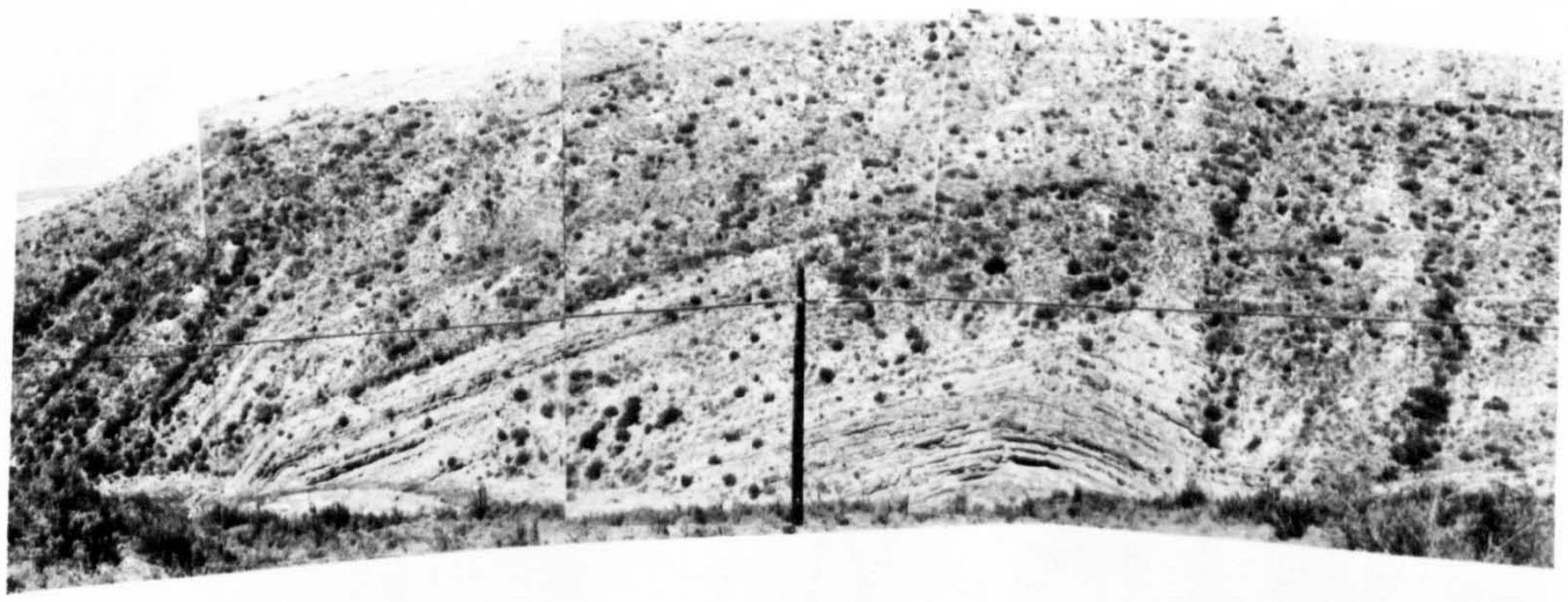

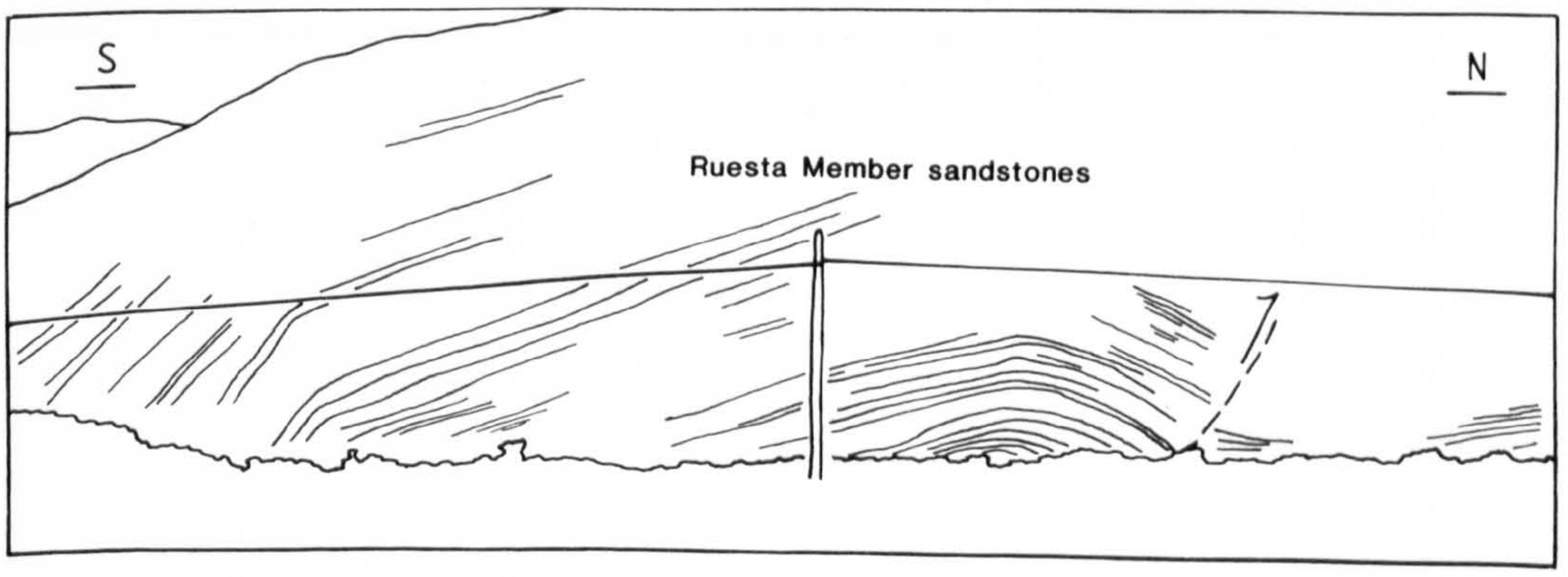
S
N
Ruesta Member sandstones

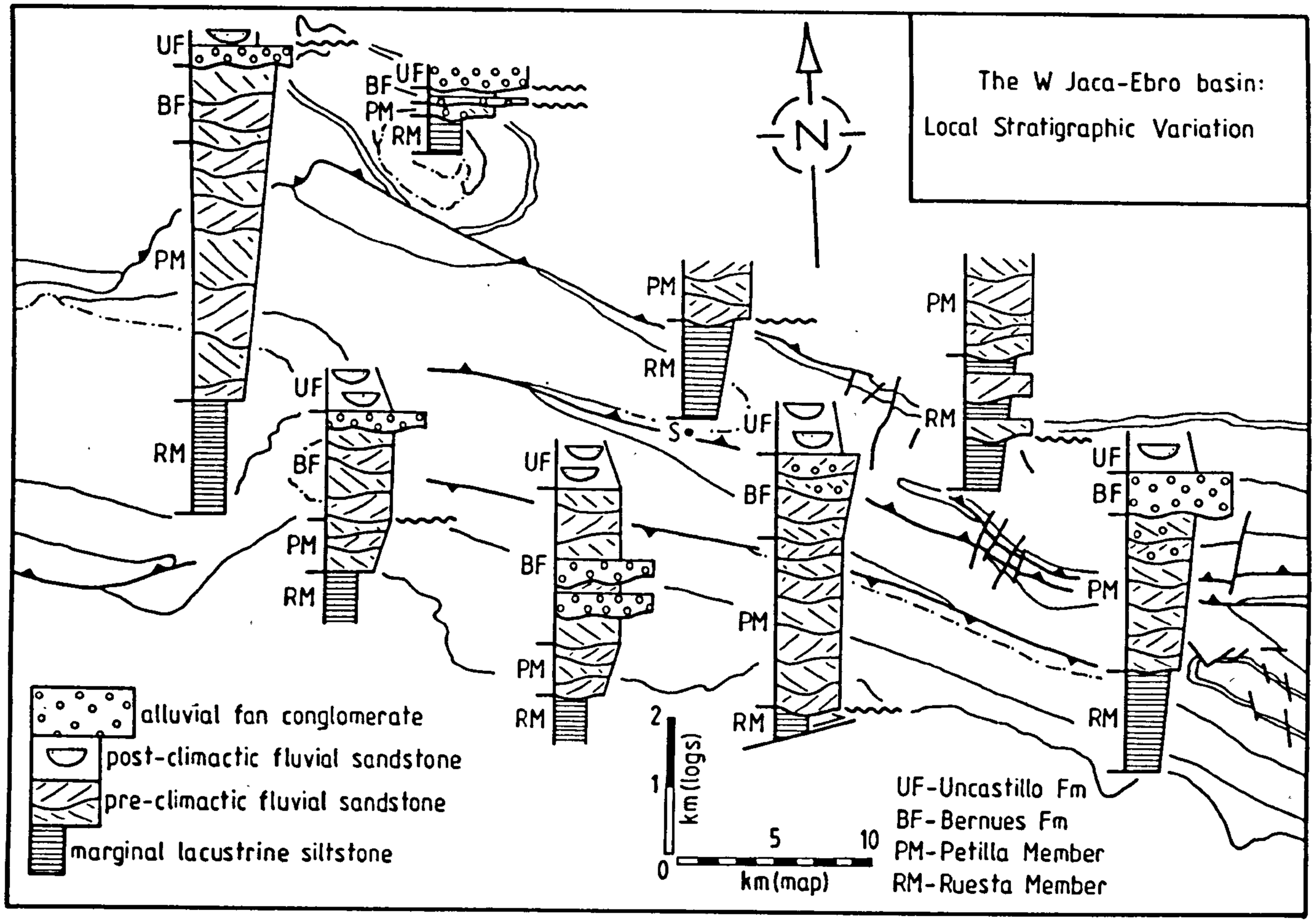

Fig. 2.9. Scaled and schematised facies logs of the West Jaca basin molasse sequence located within a map of the basin derived from that shown in Fig. 1.3. The logs depict an increase in thickness of the sequence and a decrease in the age of facies transitions and localised unconformities (shown with wavy lines) toward the western part of the study area.

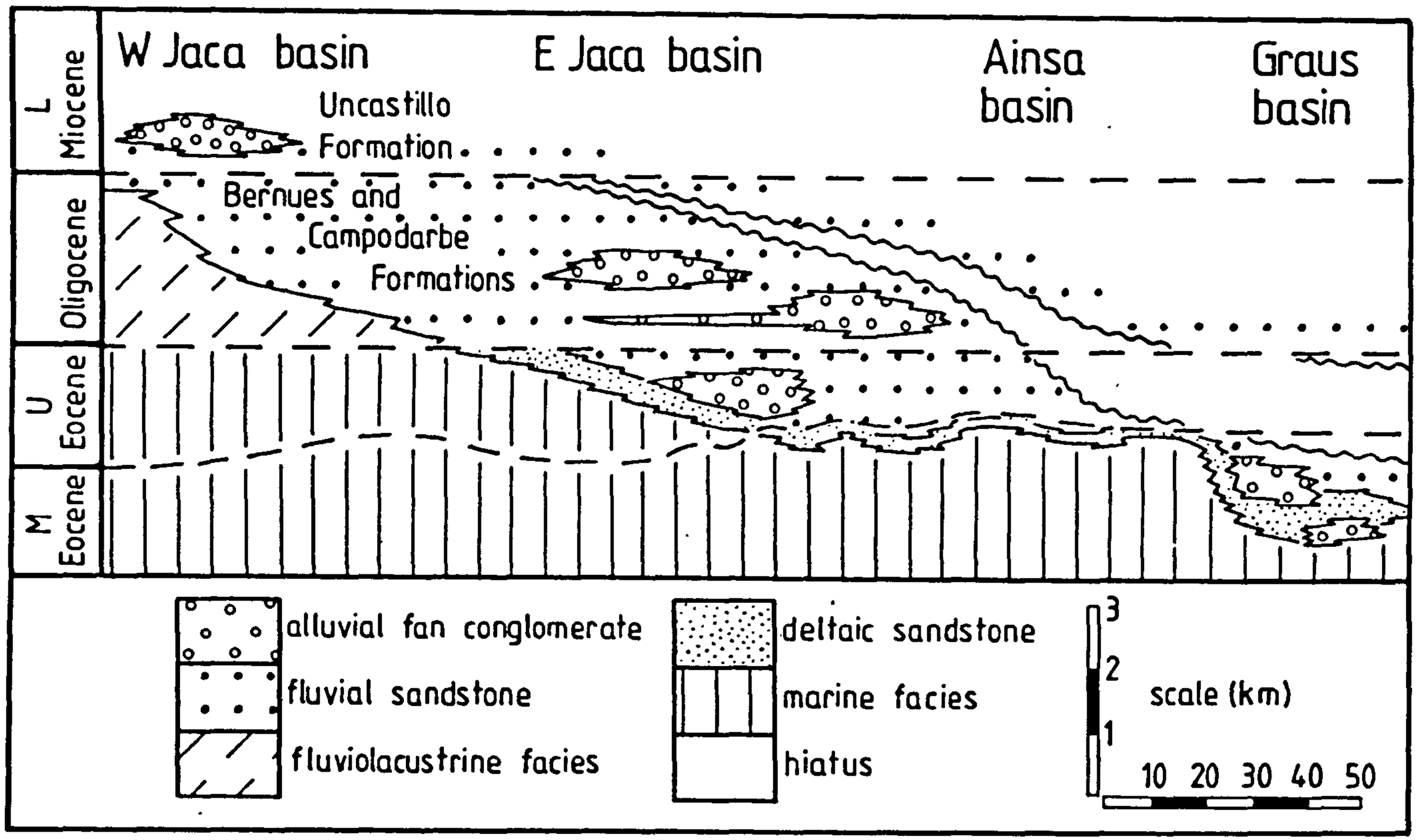

Fig. 2.10. Stratigraphic and facies relationships in the South Pyrenean basins; the line of section is shown in Fig. 1.1. The section emphasises the highly diachronous style of Eocene to Miocene sedimentation along the length of the South Pyrenees. Modified from Puigdefabregas *et al.* (1975, fig. 1).

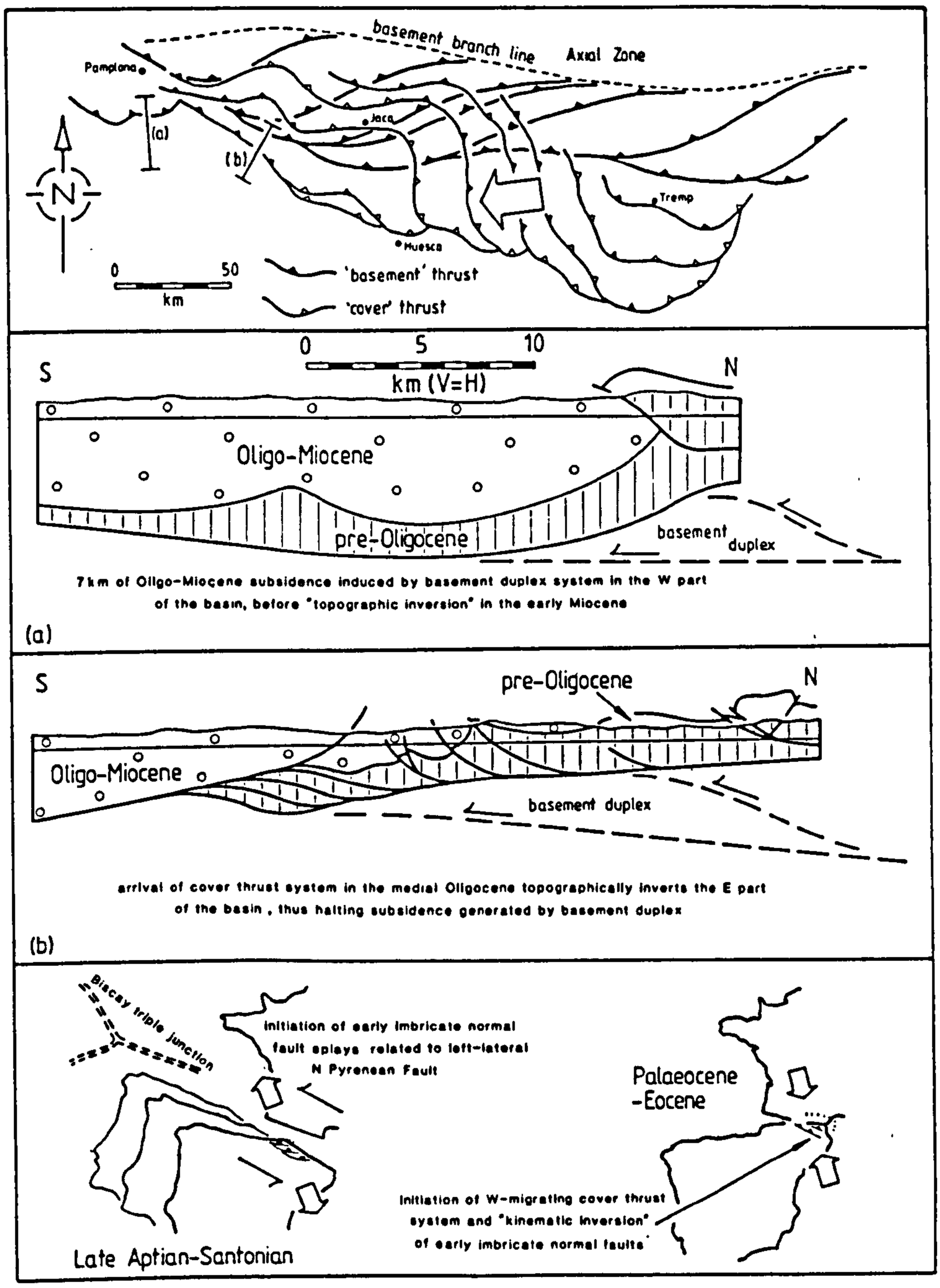

Fig. 2.11. Top map shows the 'basement' and 'cover' thrust systems of the South Pyrenees recognised by Camara & **Klimowitz** (1985, fig. 7) and lines of the simplified strike-normal sections, (a) and (b). The lower maps are modified from Boillot (1984, fig. 2) and they depict the movement of the Iberian microplate, with respect to Europe, between the early Cretaceous and Eocene. See text for discussion.

Plate 2.1a. Backthrust (marked by a dashed line) emplacing Cretaceous limestone on Palaeocene limestone. The backthrust forms part of the Sierra de Orba culmination shown on the section in Fig. 2.3 and is exposed in the Roncal valley. North is to the left.

Plate 2.1b. Slump fold in the latest Eocene Guendulain Formation exposed near Yesa, at the northern margin of the molasse basin. Compass-clinometer for scale.

Plate 2.1c. Localised, angular unconformity dividing Ruesta Member and Petilla Member rocks at Sanguesa. A4 clipboard for scale.


A

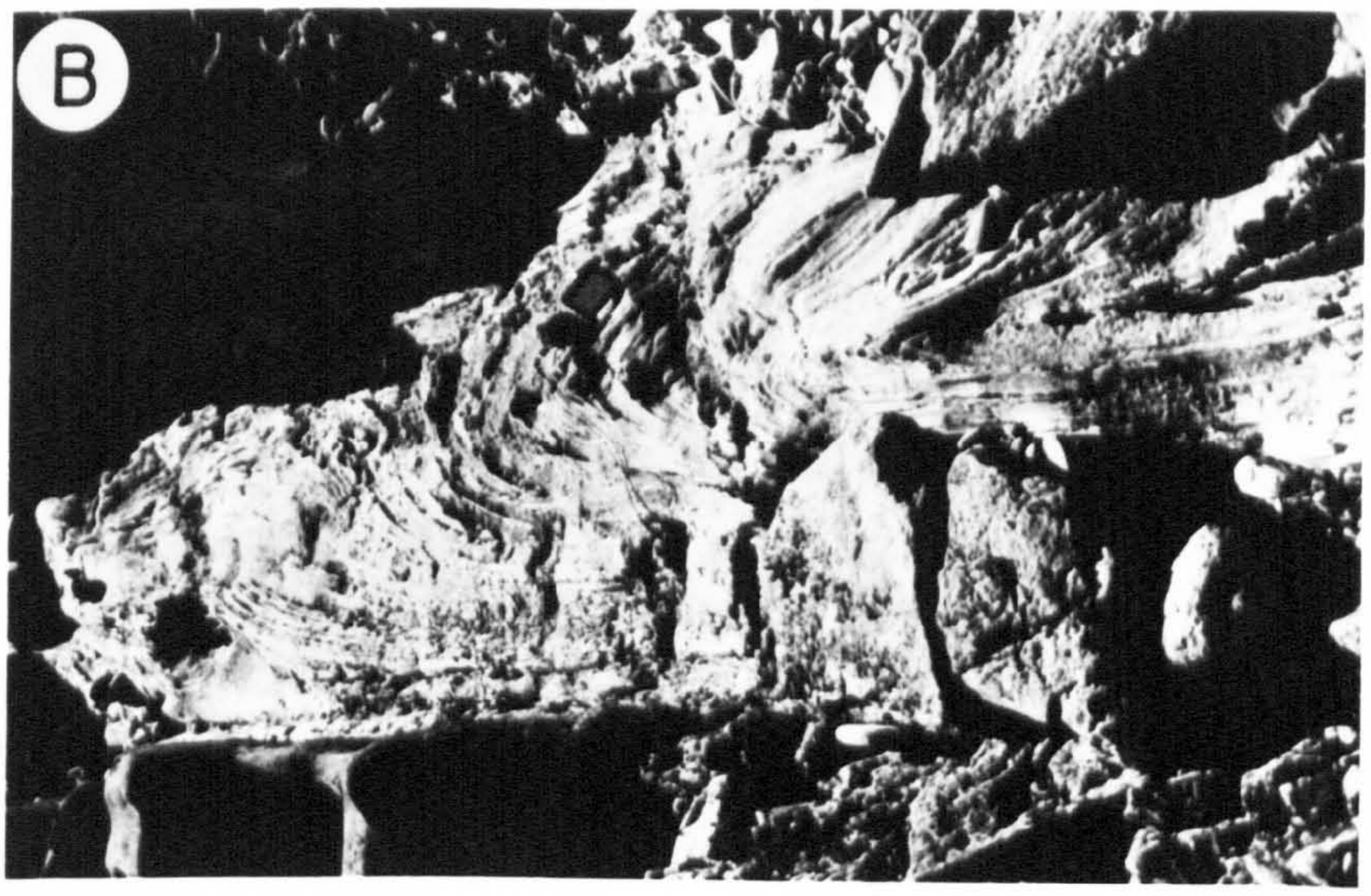
B


C

CHAPTER 3

BASIN EVOLUTION DURING DEPOSITION OF THE RUESTA MEMBER

3.1 MARINE REGRESSION IN THE SOUTH PYRENEAN BASINS

In the West Jaca basin, the base of the Campodarbe Formation rests on a 60m thick lagoonal sequence (Mangin 1962; Puigdefabregas *et al.* 1975) of marine-continental transition sediments belonging to the Guendulain Formation (Puigdefabregas 1975). These variably bedded, wave- and current-rippled sandstones and siltstones crop out in the northern part of the basin where they separate the Pamplona Marls Formation from the Campodarbe Formation. The Guendulain Formation is of great regional significance as it represents a major period of marine regression during the latest Eocene (Puigdefabregas 1975).

In the South Pyrenean thrust-top basins the timing of uplift and marine regression locally varies from earliest Eocene in the Graus basin (van Eden 1970; Nijman & Nio 1975) to mid and latest Eocene in the eastern and western parts of the Jaca basin (see Fig. 2.10). Vail *et al.* (1977) have recognised up to five global cycles of eustatic sea level change during the Eocene. They attribute them to changes in the volume of seawater and to changes in the shapes of the ocean basins. However, the demonstrable diachronism of the onset of terrestrial conditions in the South Pyrenees suggests that it is most appropriate to invoke a diastrophic or regional tectonic mechanism of relative sea level change.

The later timing of marine regression toward the west accords with the westward propagating thrust system that was noted in Chapter 2 to have affected the South Pyrenean thrust-top basins during the Eocene to early Micoene. Additionally, it has been noted that the thickness of the marine-continental transition sequence in the West Jaca basin is exceptionally restricted. This supports the likelihood of a localised tectonic mechanism having enhanced the rate of uplift, thus producing an abnormally thin transition sequence with respect to the thicknesses of the subjacent and superjacent flysch and molasse sequences. It is proposed here that the thrust front caused local emergence of the depositional surface above sea level during its westward propagation through the South Pyrenean foreland. The dominant mechanism of uplift and regression was one of crustal thickening due to thin skin thrusting.

Labaume *et al.* (1985) have also observed the rapidity of transition from marine to continental environments in the Jaca basin. They suggested that,

throughout the Eocene, the South Pyrenean basin was becoming progressively shallower. However, they proposed that final uplift was caused by the locking of Iberian upper mantle subduction and consequent thickening of the South Pyrenean foreland crust.

3.2 REGIONAL LACUSTRINE AND MARGINAL LACUSTRINE SEDIMENTATION

3.2.1 General facies description

The successions external to the Ruesta fault zone comprise two principal facies herein called the Wave-Rippled **Sandstone** Facies and Mottled Siltstone with Sandstone Facies. The Wave-Rippled Sandstone Facies is typically developed near Monreal (Fig.3.1) in the Izaga sub-basin and near Liedana (Fig. 3.1). These are sand-dominated sequences that are characterised by a heterolithic suite of thin-bedded (beds are generally between 5 and 60 cm thick), current-rippled sandstone with siltstone, punctuated by planar based, tabular, fine-grained sandstone beds with wave ripples on their upper surfaces. The thin-bedded units occur in packages of stacked, planar based, very fine-grained sandstone that are up to three metres thick in total. Tabular fine-grained sandstone beds are the coarsest component in these sequences and they commonly contain low angle, planar tabular cross-stratification above soft sediment deformation horizons at their bases (Plate 3.1a).

The soft sediment deformation horizons comprise a dominantly vertical (ie. bedding-normal) structure with a 'loaded' base of interfingering sandstone and underlying siltstone or mudstone. The tabular sandstone beds are between 5 and 30 cm thick and they display abundant wave-rippled upper surfaces with short ripple wavelengths of between 40 and 100 mm. Both between separate beds in a single sequence, and, between sequences several kilometres apart, the wave ripple crests generally exhibit a consistent orientation. Occasionally, in the troughs between individual wave ripples, ladderback ripples (Reineck & Singh 1980) with wavelengths of up to 30 mm and crests oriented normally to the trends of the larger wave ripples, were observed. Where not disturbed by soft sediment deformation, the bases of the tabular, wave-rippled sandstones are bioturbated and they commonly exhibit toolmarks, longitudinal scour marks and flute casts.

Near Javier, Navardun (Fig. 3.2), Petilla (Fig. 3.3) and at the head of the Rio Arba valley, typical sequences in the Mottled Siltstone with Sandstone Facies are exposed. The dominant component of this facies is massive, or occasionally laminated (eg. the facies log at Petilla in Fig. 3.3), siltstone to mudstone with subordinate thin-bedded, fine-grained sandstone and a few

erosively based sandstone bodies. Some finer, siltstone dominated intervals contain rootlets (eg. abundant at Javier) and are mottled and reddened by incipient calcrete development (Stage 1 of Leeder 1975). This incipient calcretisation is mainly recorded by a blue-grey mottling; however, at Javier calcrete nodules up to 25 mm diameter are common. The thin-bedded, fine-grained sandstone contains current ripple lamination, that shows an angle of climb of up to 12°, and occurs in stacked, planar based packages up to three metres thick and containing between three and twenty individual beds. Individual planar based sandstone beds have bioturbated bases and are laterally persistent for up to forty metres.

Upward fining, erosively based sandstone bodies are volumetrically the most variable component of the Mottled Siltstone with Sandstone Facies, generally comprising between 5 and 20% of a succession. They commonly possess burrowed bases with a moderate erosive relief of between 20 and 50 cm. Vertical spacing betwen these sandstone units increases south-eastward from Navardun (Fig. 3.2), where they are between one and five metres thick, and have a mean spacing of ten metres, to Petilla, where the sand bodies are up to two metres thick and spaced at a mean vertical distance of 20m. At the head of the Rio Arba valley, erosively based, sandstone bodies are exceptionally rare and the sequence is most notable for its infrequent limestone horizons. The limestone occurs as single units, between 5 and 30 cm thick, that are internally massive or 'rubbly'.

As is common in many alluvial sequences of the South Pyrenees, the sand bodies at Javier, Navardun and Petilla have suffered from a diagenetic obliteration of their internal bedforms (cf. Friend *et al.*, 1986) that is thought to be due to a high detrital carbonate content. However, where bedforms are preserved the sandstone bodies are dominated by planar and trough cross-stratification, commonly with current ripple laminated upper parts. The sand bodies are generally of single storey construction although thicker units at Navardun do contain up to three individual storeys. This thesis shall follow the terminology of Galloway (1981) to describe 'multistorey' and 'multilateral' sandstone bodies in which vertically and laterally arranged channel-fill sequences are separated by basal erosion surfaces.

3.2.2 Depositional environments

The Wave-Rippled Sandstone Facies described from Monreal (Fig. 3.1), the Izaga sub-basin and Liedana (Fig. 3.1) shows evidence of deposition in an environment affected by both wave and current processes. The abundant wave-

rippled and current-rippled tabular sandstones with non-erosive, planar bases record deposition in shallow water (Allen 1981a) by frictional sediment dispersal (see Wright 1977). Such a process involves the splitting and deceleration of flow at points where rivers enter lakes. Sediment is consequently deposited as areally extensive, blanket-like units of great lateral persistence on the shallow lake floor. Similar frictional sedimentation at shallow lake margins has been recorded from Lake Maracaibo, Venezuela by Hyne *et al.* (1979) and the Devonian Orcadian basin of southeast Shetland by Allen (1981b, fig. 8). In the Wave-Rippled Sandstone Facies, further evidence for deposition in shallow to very shallow water at the lake margin is provided by the relatively short wavelength of wave ripples (Allen 1981a) and the presence of rare ladderback ripples. These are formed by water draining from the troughs between pre-existing ripples that developed at a time of higher water level (Reineck & Singh 1980).

The presence of soft sediment deformation phenomena on the bases of wave-rippled tabular sandstone units reflects slope instability and the likelihood of there having been repeated seismicity during sedimentation (cf. Allen & Banks 1972; Steel & Aasheim 1978; Farrell 1984). However, the relative ease with which overpressuring and consequent dewatering in lacustrine sediments can occur should not be underestimated (Bennett, 1977). The characteristics of soft sediment deformation in the Wave Rippled Sandstone Facies fit most closely with the description of structures called 'flowrolls' by Sorauf (1965). He attributed them to vertical movement of sediment as a result of differences in specific gravity (ie. unstable sand and mud sequences). However, similar structures have been described from Pembrokeshire by Williams (1969) who assigned them an origin that combined vertical and lateral displacement of sediment. By virtue of their dominant vertical structure, the flowrolls at Monreal, the Izaga sub-basin and Liedana are thought to have formed primarily by vertical escape of pore water, perhaps triggered by seismicity. However, occasional fine-grained sandstone imbricate folds, with mudstone-filled cores and axial planes inclined up to 30° from bedding, do provide evidence of small downslope lateral movements.

It is difficult to know whether the Ruesta Member lake system was a single large lake or several smaller lakes. Because the Izaga sub-basin is allochthonous and was located distant from the main basin (see Chapter 2) until the late Oligocene, it is likely that the Wave-Rippled Sandstone Facies of the Izaga sub-basin represents the deposits of a lake isolated from the Monreal and Liedana lake system.

In the Mottled Siltstone with Sandstone Facies preserved at Javier, Navardun (Fig. 3.2), Petilla (Fig. 3.3) and in the Rio Arba valley, the siltstone dominated, colour mottled sequences with occasional, thicker, erosively based sandstone bodies record deposition on an alluvial plain periodically traversed by relatively small fluvial channels. The prevalence of colour mottled siltstone with packages of thin-bedded, planar based, fine-grained sandstone suggests that the alluvial plain experienced a relatively low rate of sedimentation that was dominated by sheetflood and extra-channel processes (cf. McKee *et al.* 1967; Williams 1971; Steel and Aasheim 1978; Tunbridge 1981). Bown & Kraus (1981) attributed colour mottling to alternate wetting and drying of the soil zone, but its significance in terms of sedimentation rate is that blue-grey and red mottling reflects relatively long periods of soil formation and groundwater table stability (van der Meulen 1986).

Leeder (1973) has stated that, as a rough guide, sandstone body, or coarse member, thickness equates with bankfull channel depth of the channel that deposited the sand body. Considering that individual storeys of erosively based sandstone bodies are only up to four metres thick and that, within each vertical succession, they are widely spaced, the origin of the extra-channel intervals of Mottled Siltstone with Sandstone Facies sequences is questionable. Puigdefabregas & van Vliet (1978) have used a similar argument of an exceptionally high overbanks to channel ratio in their alluvial successions from the South Pyrenean basins, to propose the existence of an external supplier of fines in addition to channels.

3.3 NORMAL FAULTING AND SEDIMENTATION IN THE RUESTA FAULT ZONE

During the late Eocene to early Miocene, a subsurface lateral ramp at Ruesta was expressed at the depositional surface by a NNE-trending normal fault zone about ten kilometres wide. An analysis of facies distribution, sediment dispersal directions and the stratigraphic development of the area permits the tectonic evolution of the fault zone to be determined.

3.3.1 General facies description

An east-west transect across the width of the Ruesta fault zone reveals a variety of facies deposited at various stages in the development of the fault zone. Successions are exposed at Lerda, in a series of outcrops across the main fault and to the east of the main fault at Pintano (Fig. 3.4). The rocks exposed in these sections are broadly divisible into four facies. They are the Massive Grey Mudstone Facies, the Wave-Rippled Sandstone Facies, the Multistorey Sand Body Facies and the Mottled Siltstone with Sandstone Facies.

Figure 3.5 illustrates a facies log through the succession exposed in the core of the ramp anticline at Lerda illustrated in Fig. 2.8. The lower 30m of the sequence comprises rocks of the Massive Grey Mudstone Facies and is characterised by a heterolithic suite (bed thicknesses average 40 cm) of dark grey, parallel-laminated mudstone and siltstone containing planar based, tabular beds of current ripple laminated and occasional planar tabular cross-stratified, very fine-grained sandstone and fine-grained sandstone. Dark grey mudstone and siltstone is the dominant component in the Massive Grey Mudstone Facies, comprising 75% of the sequence at Lerda. In addition to an internally massive or parallel-laminated structure, the finer intervals of the Lerda succession exhibit occasional evidence of vertical water escape by the presence of flowrolls (Sorauf 1965).

The subordinate thicknesses of sandstone occur as laterally persistent units that commonly grade upward from massive, fine-grained sandstone to current ripple laminated or planar tabular cross-stratified, very fine-grained sandstone. The sandstone beds are between 20 and 120 cm thick with common flute casts on their bases and rare erosive bases with very low erosive reliefs of less than 20 cm, over a lateral distance of about 10m. This facies compares with the turbidite facies of Link & Osborne (1978) illustrated in Fouch & Dean (1982, fig. 17).

The 30 to 140m section illustrated in the facies log of Fig. 3.5 comprises a sequence that displays typical features of the Mottled Siltstone with Sandstone Facies. In the 30 to 40m interval of the succession there is a transitional suite of planar and erosively based fine-grained sandstone that marks the start of upward coarsening in the sequence as a whole. The upper 100m of the sequence is dominated by colour mottled, massive siltstone and very fine-grained sandstone containing several erosively based, upward-fining sandstone bodies , constructed from between one and three storeys, that constitute 12% of the succession. The sand bodies comprise individual storeys of between 70 and 200 cm thickness with bases that display erosive reliefs of up to 50 cm. Many of the sand bodies have suffered from a diagenetic obliteration of sedimentary structures (see Friend *et al.* 1986), but where preserved, the most common bedforms are planar tabular and trough cross-stratified lower parts with current ripple laminated and upper plane-bed laminated upper parts. Between the sandstone bodies, the Mottled Siltstone with Sandstone Facies sequence at Lerda is dominated by poorly exposed sections of massive siltstone and subordinate packages of stacked, planar based, current ripple laminated, fine-grained sandstone between 20 and 200 cm thick.

A second occurrence of the Massive Grey Mudstone Facies forms part of a 50m thick succession located immediately to the east of the main fault, in the Barranco de Pintano (Fig. 3.4), and is illustrated in Plate 3.1b. The lower two thirds of this succession comprises monotonous, massive, dark grey mudstone that contains very rare, isolated beds of laterally persistent, planar based, medium-grained to very fine-grained sandstone. The sandstone beds are between 8 and 35 cm thick and display consistent upward fining from a massive, medium-grained sandstone base containing rare intraformational siltstone clasts, to an upper part of parallel laminated and current ripple laminated fine-grained and very fine-grained sandstone. Bases of the sandstones commonly exhibit flute casts and a variety of different groove marks.

At approximately 35m from the base of this succession there is a sharp facies transition from Massive Grey Mudstone Facies to Wave-Rippled Sandstone Facies that shows clearly on Plate 3.1b. Above this sharp transition, the sequence is characterised by buff coloured, tabular beds of sandstone between 25 and 130 cm thick, with thin siltstone intervals between the sandstone. Soft sediment deformation horizons dominate the basal parts of the sandstone beds that have planar to irregular, non-erosive bases and upper surfaces which commonly display straight crested, wave ripples. Occasional metre-thick sandstone units grade from a slumped and deformed massive base of medium-grained sandstone to current ripple laminated upper parts and a wave-rippled or interference-rippled upper surface.

Elsewhere, the Wave-Rippled Sandstone Facies is present about one kilometre west of the above exposure, in the Barranco de Pintano, to the west of the main fault in the Ruesta Fault zone (Fig. 3.4). In this outcrop of limited vertical extent, exceptionally laterally persistent, planar based beds of medium-grained to fine-grained sandstone comprise roughly 60% of the sequence. The sandstones are between 10 and 60 cm thick and are characterised by upper surfaces which display straight crested wave ripples of between 50 and 90 mm wavelength that show a marked consistency in their orientation both vertically through the sequence and over a wide area (see Plate 3.1c and Section 3.3.2). In detail, the sandstone beds have planar bases that exhibit burrowing and rare groove marks, and internally they are either massive or ripple-laminated. The inter-sandstone siltstone intervals that comprise approximately 40% of the succession are massive or parallel-laminated and, toward the top of the Wave-Rippled Sandstone Facies sequence in this area, there are common desiccation cracks. Also present in these upper parts of the sequence are ladderback ripples with short wavelengths of up to 30 mm and crest

orientations perpendicular to those of the larger wave ripple crests between which they occur.

The Wave-Rippled Sandstone Facies at this outcrop contains spectacular evidence of local slope instability in the form of a complexly slumped horizon, between 130 and 170 cm thick, that is now a melange of sandstone and mudstone. Recumbent slump folds, such as that illustrated in Plate 3.1d, are cut by a syndepositional, axial plane cleavage in the mudstone- and siltstone-filled cores of sandstone fold noses. The cleavage appears to be a relatively late formed structure in the sequence of development of the slump horizon by virtue of the fact that it is not contorted by later movements. The cleavage is defined by an alignment of platy minerals in the mudstone and consists of surfaces spaced between 0.5 and 3 mm apart that are 'divergent' with respect to the geometry of the enclosing slump fold (see fig. 5.2 of Hobbs *et al.* 1976). Individual folds are tight to isoclinal, recumbent to downward facing and commonly deform a sandstone bed that may be traced for up to ten metres around the hinges of different folds.

Evidence of slumping having begun after the initiation of sandstone lithification is provided by small, wrinkle marks, in the hinge zones of folds, that parallel fold axes. The bases of the slump unit has well developed load casts (cf. Collinson & Thompson 1982,fig. 9.1) with 'flames' of mudstone and siltstone that penetrate up to 30 cm from the base of the sandstone bed. The slump is draped by a 10 cm thick sandstone with a planar base and wave-rippled upper surface.

The top of the Wave-Rippled Sandstone Facies succession in the Barranco de Pintano, west of the main fault in the Ruesta fault zone, is marked by a sharply defined transition to the Multistorey Sand Body Facies illustrated in Plate 3.2a and Fig. 3.6. The Multistorey Sand Body Facies comprises multistorey and multilateral sandstone bodies that typically constitute 25 to 30% of the facies. In Plate 3.2a and Fig. 3.6, the planar, non-erosive base of a 9m thick, two storey sand body overlies Wave-Rippled Sandstone Facies rocks containing desiccation cracks. Internal stratification in this sand body is almost completely absent (although this absence does not necessarily imply that the sandstone is not constructed from bedforms; Friend *et al.* 1986) and it is constructed from a lower, planar based storey of medium-grained sandstone, and an upper, medium-grained sandstone storey with a base that displays up to 350 cm of erosive relief (see Fig. 3.6).

The single storey sand body illustrated in Fig. 3.7 erosively truncates the underlying Wave-Rippled Sandstone Facies sequence and displays well devel-

oped 'wings' (Friend *et al.* 1979) as shown by the lateral thinning of the sandbody from a maximum thickness of four metres. The sandstone bodies illustrated in Figs. 3.6 and 3.7 form the basal units of the Multistorey Sand Body Facies in the Ruesta fault zone which is approximately 280m thick. In general, it comprises sand bodies with erosive reliefs of between 5 and 350 cm, and width: depth ratios of between 15 and 50, that are constructed from between one and three storeys. Internal stratification, where present, is dominated by trough cross-stratification, up to 30 cm amplitude, in the basal parts of sand bodies (see Plate 3.2b) and upper plane-bed lamination in their upper parts. The inter-sandstone body intervals of this facies constitute 70 to 75% of the sequence and consist of massive, unmottled, pale brown siltstone with subordinate planar based, current ripple laminated beds of fine-grained sandstone up to 10 cm thick that are generally stacked in packages between 20 and 250 cm-thick.

Figure 3.8 is a facies log through the Mottled Siltstone with Sandstone Facies succession exposed at Pintano (Fig. 3.4), about four kilometres to the east of the main fault in the Ruesta fault zone. This sequence is dominated by massive, blue-grey and red, colour mottled siltstone that forms 89% of the succession. The siltstone is pervasively colour mottled and contains localised pockets of centimetre-diameter calcrete nodules and, at 15m in the facies log of Fig. 3.8, there is a mature 25 cm thick calcrete horizon. This pale grey calcrete is laterally persistent for more than 50m, with a planar base and top, and is dominated internally by a bedding-normal 'pipe' texture. Erosively based sandstone bodies are either one or two storey units with erosive reliefs on their bases of between 10 and 60 cm, and well developed, laterally thinning wings. The sand bodies are generally constructed from large scale, planar tabular cross-stratification and occasionally exhibit poorly developed lateral accretion surfaces similar to the epsilon cross-stratification of Allen (1963).

3.2.2 Palaeocurrents

In this thesis, all palaeocurrent data has been statistically processed using the PALEO program of Cooper & Marshall (1981). In Figure 3.4, which summarises Ruesta Member dispersal directions that are inferred from a variety of palaeocurrent indicators, station RD1 represents data derived from the soft sediment deformation horizon described from Wave-Rippled Sandstone Facies in the Barranco de Pintano (Section 3.3.1). Williams *et al.* (1969) recorded a similar type of axial plane cleavage to that in the Ruesta fault zone example, from sandstone soft sediment deformation horizons in eastern Australia. They thought the cleavage developed during slumping as a result of the rotation and

alignment of pre-existing platy minerals.

In Ludlow Series slump sheets in Wales, Woodcock (1976) used fold vergence and axial plane cleavage as a palaeoslope indicator. Good exposure conditions in his example allowed him to be confident that slump fold axes strike parallel to the strike of the palaeoslope and that the folds verge downslope (Woodcock, 1976). In the Ruesta fault zone soft sediment deformation horizon, mud was mobilised as a semi-fluid sediment and flowed into the sandstone fold cores from beneath. The development of the unit thus involved a combination of both vertical movement and subsequent lateral translation causing the formation of a "slump structure" (Keunen 1948; Kelling & Williams 1966; Williams 1969). A slumping direction, and hence a palaeoslope orientation, was gained from measuring the direction of vergence of the folds by means of recording the orientation of the syndepositional axial plane cleavage. The palaeocurrent pattern displayed by the rose diagram from station RD1 reveals that the Wave-Rippled Sandstone Facies slump horizon was horizontally translated eastward, toward the Ruesta fault.

Straight crested, symmetrical, vortex type (Bagnold 1946) wave ripples constitute the source of data for the construction of the rose diagrams from stations RD2 and RD3 (Fig. 3.4). Azimuths of the crests of such structures are oriented normally to the direction of movement of the waves which formed them. However, there exists some debate as to whether this direction of wave movement reflects lake palaeobathymetry, wind direction, or, a combination of the two (see Boyd 1983, p.59). A reason for the potential ambiguity of directional data derived from wave generated structures in lacustrine sediments is the complex interaction of processes such as wind, longshore drift and the disruption of bathymetry by fluvial inflows to the lake margin. Tanner (1967, p.191) found that the strikes of the crests of 69% of wave ripple marks are approximately parallel with the interpreted lake shoreline in the late Jurassic Morrison Formation of New Mexico (Pickard & High 1972). In the palaeogeographic reconstruction shown in Fig. 3.9, the orientations of wave ripple crests are taken to be roughly parallel with the shoreline of the former lake. Boyd (1983) has confirmed the validity of this axiom by demonstrating the correspondence of lake shoreline trend inferred from wave ripples with trends deduced from less equivocal palaeoslope and shoreline indicators such as planar cross-stratification. Additionally, the stratigraphic and areal consistency of Ruesta Member wave ripple orientations in the Ruesta fault zone (see Plate 3.1c) gives one confidence that the structures are reflecting a relatively long term trend, for example, a stable lake shoreline.

Although the three rose diagrams of stations RD4, 5 and 6 (Fig. 3.4) display various degrees of dispersion, this does not necessarily reflect the directional variance of the depositional systems in which they formed. Allen (1966, fig. 22) postulated a hierarchical organisation of flow vector fields and bedforms, and the dependence of current directional data on rank of bedform or derived internal structure (also see Miall 1974). This hierarchy ranges from channel forms, which exhibit the lowest directional variability, to small scale ripples, which exhibit the highest directional variability. For example, the weakly bimodal rose diagram constructed from data recorded from station RD4 is derived from measurements of the strikes of steep sided channel margins (cf. Bluck & Kelling 1963) and displays a relatively low dispersion because it is based on the least variable 'element' in Allen's (1966) hierarchy. The palaeocurrent pattern recorded by station RD4 reveals that the sandstone bodies of the Multistorey Sand Body Facies are the products of a depositional system that flowed south-westward, roughly parallel to the trend of the Ruesta fault zone.

The rose diagrams from stations RD5 and 6 are both derived from the orientations of Order Three and Order Four bedforms of Allen (1966), and hence, they exhibit a greater directional variance. They are largely based on measurements of trough cross-stratification axes and record the direction of migration of sinuous crested dunes at a low to medium stage of flow (Harms & Fahnestock 1965). From studying valley sandurs in southern Iceland, Bluck (1974, fig. 15) demonstrated a roughly inverse relationship between the variability of orientation of sedimentary structures and stage of flow. Trough cross-stratification data may thus be expected to exhibit a high to moderate directional variance. At stations RD5 and 6, the rose diagrams indicate that the Mottled Siltstone with Sandstone Facies sequences at Pintano and Navardun are the products of deposystems draining eastward, away from the main Ruesta normal fault, and axially westward, subparallel to the trace of the Ruesta thrust, respectively.

3.3.3 Depositional environments

At several outcrops in the Ruesta fault zone (eg. see the succession above the unconformity illustrated in Fig. 3.10 and Plate 3.2d), the four facies described in section 3.3.1 are demonstrably separate components of an upward coarsening sequence that, in ascending order, comprises the following facies: the Massive Grey Mudstone Facies, the Wave-Rippled Sandstone Facies, the Multistorey Sand Body Facies and the Mottled Siltstone with Sandstone Facies.

In the Massive Grey Mudstone Facies, the dominance of dark, parallel-laminated non-bioturbated mudstone and siltstone suggests that deposition was dominated by suspension of fine-grained sediment on the slopes and flat plain of a lake basin. The possible high organic content and absence of bioturbation and wave generated structures is typical of the hypolimnion zone where, beyond wave base, water circulation and oxygenation are minimal (Beadle 1974). The subordinate, current ripple laminated, weakly erosive, graded sandstone beds resemble thin Bouma Tabc units (see Bouma 1962) and record episodic deposition by turbidity currents. Thus, the Massive Grey Mudstone Facies is the product of deposition in an offshore lacustrine environment, however, the presence of turbidites places little constraint on the distance from the shoreline since Sturm & Matter (1978) have recorded turbidites 9 km from the mouths of rivers entering the 14 km long Lake Brienz in Switzerland (cf. Link & Osborne 1978).

Wave-Rippled Sandstone Facies sequences to the east and west of the main Ruesta normal fault display abundant evidence of deposition in a shallow water zone affected by both wave and current processes. In these sequences, the dominance of planar based, laterally persistent sandstone beds, that display basal soft sediment deformation horizons and wave modified upper surfaces, records blanket-like, 'frictional' sedimentation (cf. Allen 1981b) of sandy overflows probably contributed by rivers entering the lake. Ladderback ripples between the larger wave ripple crests and, toward the top of the succession, desiccation cracks suggest a fluctuating lake level that occasionally caused subaerial exposure of the shallow lake deposits. This is a similar interpretation to that made of Wave-Rippled Sandstone Facies in Section 3.2.2.

In the 280m thick sequence of Multistorey Sand Body Facies to the west of the Ruesta normal fault, the occurrence of thick single storey and multistorey sandstone bodies with erosive bases, well developed wings and internal trough cross-stratification and primary current lineation record deposition by south-westward flowing (see Section 3.3.2) fluvial channels traversing an alluvial plain. The inter-sand body sequence of buff siltstones and thin, planar based, current ripple laminated sandstone packages represent non-channelised deposition by sheetflood processes in the floodplain environment. In the succession as a whole, the relatively high ratio of channel sandstone to overbank fines and, the lack of mottling or incipient palaeosols reflect an alluvial basin experiencing a locally high subsidence rate (cf. Leeder 1978; Bridge & Leeder 1979). Consequently, the preferential accumulation of channel sandstone deposits resulted in an alluvial sequence which contrasts greatly

with the low sand body density successions of the Mottled Sandstone with Siltstone Facies.

The sandstone bodies illustrated in Figs. 3.6 and 3.7 and Plate 3.2a record the style of transition from the Wave-Rippled Sandstone Facies underlying the Multistorey Sand Body Facies sequence in the Ruesta Fault zone. The planar base of the sandbody in Fig. 3.6, its upward coarsening, with respect to underlying marginal lacustrine sandstone, and its occurrence between lacustrine and fluvial sediments suggest that this sandstone body is a mouth bar deposit (Elliott 1974; Friend *et al.* 1981). The mouth bar developed at a point of fluvial inflow to the lake margin where frictional deceleration and dispersion of the flow at the river mouth caused nearshore, suspensional deposition in a similar process to that described by Hyne *et al.* (1979). Subsequent lakeward progradation of the fluvial system is reflected by an erosively based channel storey that overlies the planar based mouth bar (see Fig. 3.6).

The erosively based fluvial sand body in Fig. 3.7, however, is notable for the absence of a transitional mouth bar sequence and there is a direct jump from a marginal lacustrine to a fluvial suite. This sandstone body is interpreted as the product of a fluvial channel contributing sediment to the lake margin represented by the underlying Wave-Rippled Sandstone Facies. A possible local base level change is reflected by the high erosive relief of 320 cm on the base of the sand body shown in Fig. 3.7. It is likely that erosive downcutting of the channel into underlying lacustrine sandstone was a response to local uplift that caused a relatively sudden end to lacustrine deposition with consequent rapid lake shoreline regression.

In the Rhine fluvial dominated delta, lower width to depth ratios were recorded from progressively more downstream sand bodies by Oomkens (1970). In comparison with the sandstone body illustrated in Fig. 3.6, the sand body in Fig. 3.7 has fewer erosive channel storeys and a greater width to depth ratio. This suggests that the sand body of Fig. 3.7 resulted from a more stable channel located relatively further upstream with respect to the sand body of Fig. 3.6. The lateral impersistence of the sandstone body in Fig. 3.6 and its multistorey and multilateral structure reflects deposition by widely spaced channels, adjacent to a lake margin, with relatively high avulsion frequencies (cf. Elliott 1974).

Comparison of the Mottled Siltstone with Sandstone Facies of the Pintano area with published descriptions of similar sequences (eg. McKee *et al.* 1967; Williams 1971, Singh 1972; Steel & Aasheim 1978) suggests that the dominance

of colour mottled siltstone containing decimetre- to metre-thick packages of stacked, planar based, fine-grained sandstone beds records deposition by discrete overbank flooding events in a floodbasin environment. The low volume of erosively based, channel sandstone bodies in the Mottled Siltstone with Sandstone Facies (11%) contrasts with descriptions of other alluvial sequences (eg. Allen 1970; Nami & Leeder 1978; Bridge & Leeder 1979; Bridge & Diemer, 1983) and possibly reflects a tectonic control on the low channel density in the Pintano area during Ruesta Member deposition.

Bown & Kraus (1981) attributed colour mottling to alternate wetting and drying of the soil zone, an interpretation that is consistent with the presence of the bedding-normal 'pipes' or tube texture in the calcrete horizon at Pintano. Steila (1976, fig. 6.4) states that such a texture is characteristic of vertisols, a sub-mature category of clayey soils that have deep, wide cracks formed during periods of moisture deficiency. The clays making up vertisols swell upon wetting and shrink when dried.

3.3.4 Melange emplacement and unconformity development

This section deals with locally developed stratigraphic features that reflect deformation processes which occurred during the evolution of the Ruesta fault zone. Immediately to the west of the village of Ruesta, a 300m long sinuous roadcut exposes the Guendulain Formation and the lowest part of the Ruesta Member containing syn- and post-depositionally deformed sandstone and mudstone (Plate 3.2c). The sequence comprises several large allochthonous blocks of Wave-Rippled Sandstone Facies sediments that were emplaced into a dark, mudstone-dominated succession. The blocks are up to fifty metres in diameter and were emplaced as internally cohesive, lithified units. Within each block, sandstone is pervasively veined and dissected by breccia zones. Evidence for early soft sediment deformation before emplacement of the blocks is provided by occasional, metre-thick slump horizons and large slump folds.

Elter & Schwab (1959) described from the northern Apennines, brecciated sediments intercalated with flysch, which they termed olistostrome deposits following the definition of 'olistostrome' given by Flores (1956). Likewise, descriptions by Elter & Trevisan (1973) interpreted the Apennine olistostromes as shedding from the front of active, blind and emergent submarine thrust tips. However, Naylor (1982) has suggested limiting use of the term 'olistostrome' to submarine debris flows; he would probably refer to the assemblage at Ruesta as a melange. Melanges are associated with numerous plate margin and foreland basin settings, including oversteepened zones and thrust tips.

At Ruesta, the melange is interpreted here as a gravitational collapse structure that moved downslope, toward the west-northwest as uplift occurred in the footwall of the Ruesta fault. Naylor (1981) lists very rapid sedimentation, erosional over-steepening of slopes or seismic triggers as the three main mechanisms by which intense slumping may be initiated. Since no evidence suggests that there was locally an exceptionally high rate of Ruesta Member sedimentation or that there were erosionally steepened slopes, seismic triggering is seen as the most likely cause of the melange.

Figure 3.10 and Plate 3.2d illustrate a cliff face exposure located approximately 100m west of the trace of the main Ruesta fault, in the Barranco de Pintano. The Barranco exposure displays an angular unconformity that divides a lower, erosively truncated succession of Massive Grey Mudstone Facies from an upward-coarsening upper succession of Massive Grey Mudstone Facies, Wave-Rippled Sandstone Facies and Multistorey Sand Body Facies. The dip of the lower unit, beneath the unconformity, progressively steepens eastward from 5 to 15° toward the fault, over a distance of 120m. The upper unit dips fairly consistently 6° WSW throughout the extent of the exposure, and it onlaps the unconformity.

The eastward steepening lower unit is interpreted here as part of a hangingwall rollover anticline of the type first described by Hamblin (1965). The generation of hangingwall rollover anticlines is a direct consequence of the displacement and rotation of a hangingwall block along a listric normal fault (eg. Bally *et al.* 1981; Gibbs 1983; Gibbs 1984; Davison 1986; Gibbs 1987). The angular unconformity that divides the lower and upper units in the Barranco exposure shown in Fig. 3.10 is a localised unconformity (Riba 1976a) that records the progressive evolution of the rollover anticline. Similar unconformities have been described in early Alpide passive margin sequences by Wiedenmayer (1963), Bernoulli (1964), Casati & Gaetani (1968) and Cadisch *et al.* (1968). These workers interpret their comparable unconformities as recording the formation of tilted fault blocks during sedimentation. Progressive displacement on simple, planar normal faults led to the creation of elevated and subsided zones of subaerial erosion and marine sedimentation, thus generating localised unconformities.

In the Barranco exposure, a mechanism of localised subsidence, rapidly followed by uplift and renewed subsidence, is required to explain the two depositional episodes, separated by a short erosional hiatus, that are implied by this outcrop. Figure 3.11 shows schematically a two stage sequence that could have given rise to the stratigraphic configuration exhibited by the

Barranco exposure. The model involves the migration of a hangingwall 'fulcrum', a concept defined by Leeder & Gawthorpe (1987, fig. 1) as the point where hangingwall displacement tends to zero. A fulcrum therefore divides a subsiding zone of net sedimentation from an uplifting zone of net erosion. As displacement on a listric normal fault proceeds, the wavelength of the rollover anticline increases (Gibbs 1984). Thus, because the position of the fulcrum is controlled by the position of the rollover anticline hinge line, it follows that the location of the fulcrum with respect to the generating normal fault is not fixed, but with time and progressive displacement, migrates away from the fault (Fig. 3.11). In such a setting, a zone of net sedimentation prior to faulting will become, after fault initiation, one of net erosion on the uplifted side of a fulcrum, before returning to being a zone of subsidence as the fulcrum migrates away from the fault.

3.3.5 Evolution of the Ruesta fault zone

Each stage in the development of the Ruesta fault zone may be identified from an integrated analysis of depositional environments, dispersal directions and stratigraphic phenomena in the Ruesta Member. Although without a sound biostratigraphy the exact timing of events is difficult to resolve, it is nevertheless possible to propose a precise sequence that is illustrated schematically in Fig. 3.12.

(1) During the latest Eocene, the area occupied by the fault zone was located immediately south of a major series of mountain front culminations that marked the southern limit of thrust propagation (see Chapter 2). According to Mangin (1962) and Puigdefabregas *et al.* (1975), the Guendulain Formation records extensive lagoonal deposition across the width of what was to become the Ruesta fault zone. The monotony of the Guendulain Formation suggests that there was no significant surface faulting during sediment accumulation.

(2) From the earliest Oligocene, southward propagation of the thrust front detached the northern part of the West Jaca basin from its pre-Triassic basement. Seismicity generated by movements on blind faults is reflected in the lowest Ruesta Member melange near Ruesta. However, the uniformity of Massive Grey Mudstone Facies rocks in the hangingwall and footwall of the Ruesta fault shows that it had not emerged at the depositional surface. Lakes occupy the topographicallly lowest and hydrologically most closed parts of basins. Deposition in the offshore, central part of a large lake reflects the low clastic influx and general tectonic inactivity that characterised the Ruesta area during the earliest Oligocene.

(3) Continued displacement on the Ruesta thrust (Fig. 2.1) caused stretching over a lateral ramp underlying the Ruesta area. Stretching generated a hangingwall 'collapse' fault to form in a comparable way to the hanging-wall drop faults described by Butler (1982a, 1982b). However, in contrast with drop faults, the collapse fault at Ruesta is probably a relatively superficial structure not connected to the regional linked fault system (N. Fry: personal communication in 1987).

The early development of a hangingwall rollover anticline created an ESE-dipping palaeoslope. The sense of this palaeoslope is recorded by a soft sediment deformation horizon within the Wave-Rippled Sandstone Facies that indicates mass movement downslope, toward the now emergent Ruesta fault. The period immediately following emergence of the Ruesta fault was also characteriserd by a greater clastic influx. The rapid upward coarsening and upward shallowing recorded by several sequences in the fault zone (eg. see Fig. 3.10 and Plates 3.1b and 3.2d) reflects this increased tectonic activity.

(4) Additional regional uplift and displacement on the Ruesta fault resulted in a more strongly defined division between its hangingwall and footwall depositional environments and dispersal directions. Increased tilting of the depositional surface in the zone influenced by the rollover anticline produced a localised unconformity. Regional elevation of the fault zone and the generation of a subaerial fault scarp led to the creation of a major new sediment source. The resulting increased clastic influx caused the shallow water lacustrine environment, characteristic of the early stages of development of the rollover anticline, to be replaced by a fluvial system. The transition from marginal lacustrine to fluvial deposition is recorded by an upward coarsening mouth bar sequence (see Fig. 3.6 and Plate 3.2a). The low to moderate sinuosity channels that comprised the fluvial environment flowed axially toward the south-southwest, that is, parallel to the fault scarp.

From computer simulated models of half grabens, Bridge & Leeder (1979) predicted that channel deposits preferentially accumulate at the lowest level in a basin. Channel sandstone to overbank fines ratios in three sequences across the Ruesta fault zone (see Fig. 3.12) demonstrate that the channel sandstone accumulated preferentially in the lowest level of the fault zone. The highest channel sandstone to overbank fines ratio occurs at the crest of the rollover anticline whilst the lowest ratios occur at Pintano, in the footwall of the Ruesta fault, and at Lerda, on the uplifted side of the

fulcrum. The variation in sedimentation rates across the fault zone is also reflected by a greater degree of palaeosol development in the sediment starved zones at Lerda and Pintano. Conversely, the fine-grained sequence near the rollover anticline is unmottled and generally suggestive of a significantly higher sedimentation rate.

3.4 BASIN CONFIGURATION

Figure 3.9 illustrates the proposed palaeoenvironment of the West Jaca basin at the end of deposition of the Ruesta Member. The basin had become elevated above sea level and marine sedimentation was succeeded by widespread continental deposition. Before forelandward propagation of the regional thrust front from the northern margin of the study area, the West Jaca basin was a low lying, tectonically inactive area dominated by deep water and marginal lacustrine environments. However, in the earliest Oligocene, propagation of the Ruesta thrust into the northeast corner of the study area generated a new sediment source and a localised zone of emergent faulting, the Ruesta fault zone (Fig. 3.13). The presence of a fault bounded structural high, represented by the Ruesta thrust, locally influenced sedimentation and complicated the simple lateral and/or axial drainage pattern that typifies most foreland basin fills.

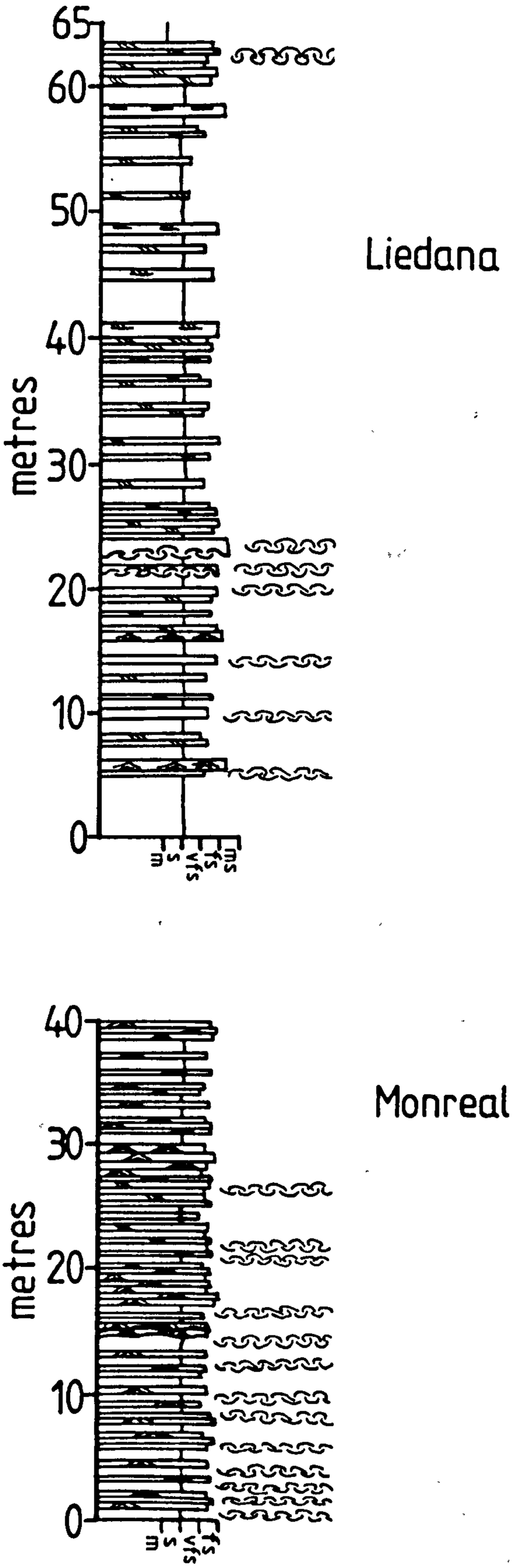

Fig. 3.1. Ruesta Member Wave-Rippled Sandstone Facies at Monreal and Liedana: graphic logs.

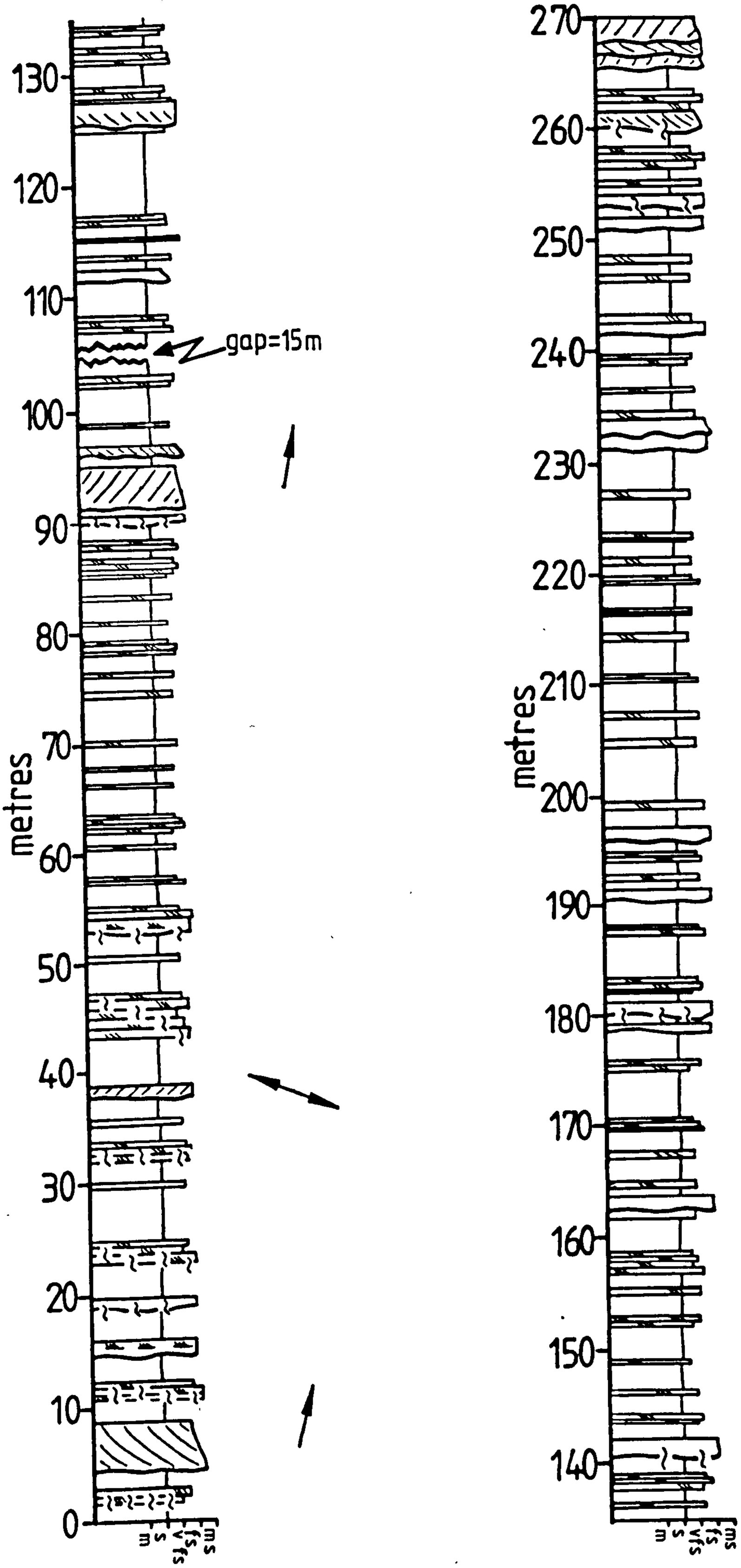

Fig. 3.2. Ruesta Member Mottled Siltstone with Sandstone Facies at Navardun: graphic log.

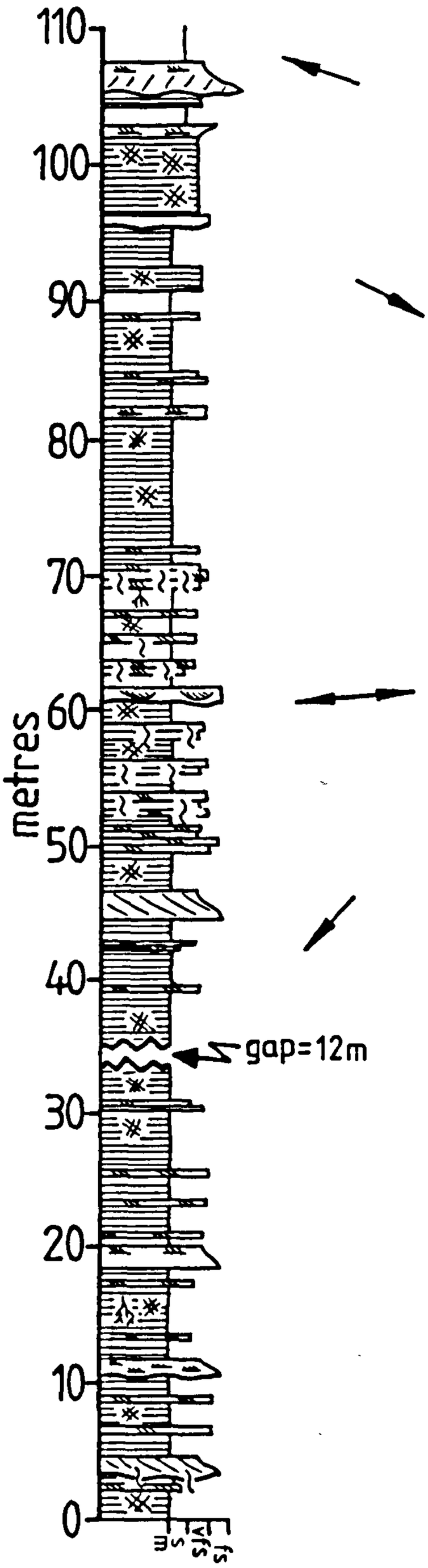

Fig. 3.3. Ruesta Member Mottled Siltstone with Sandstone Facies at Petilla: graphic log.

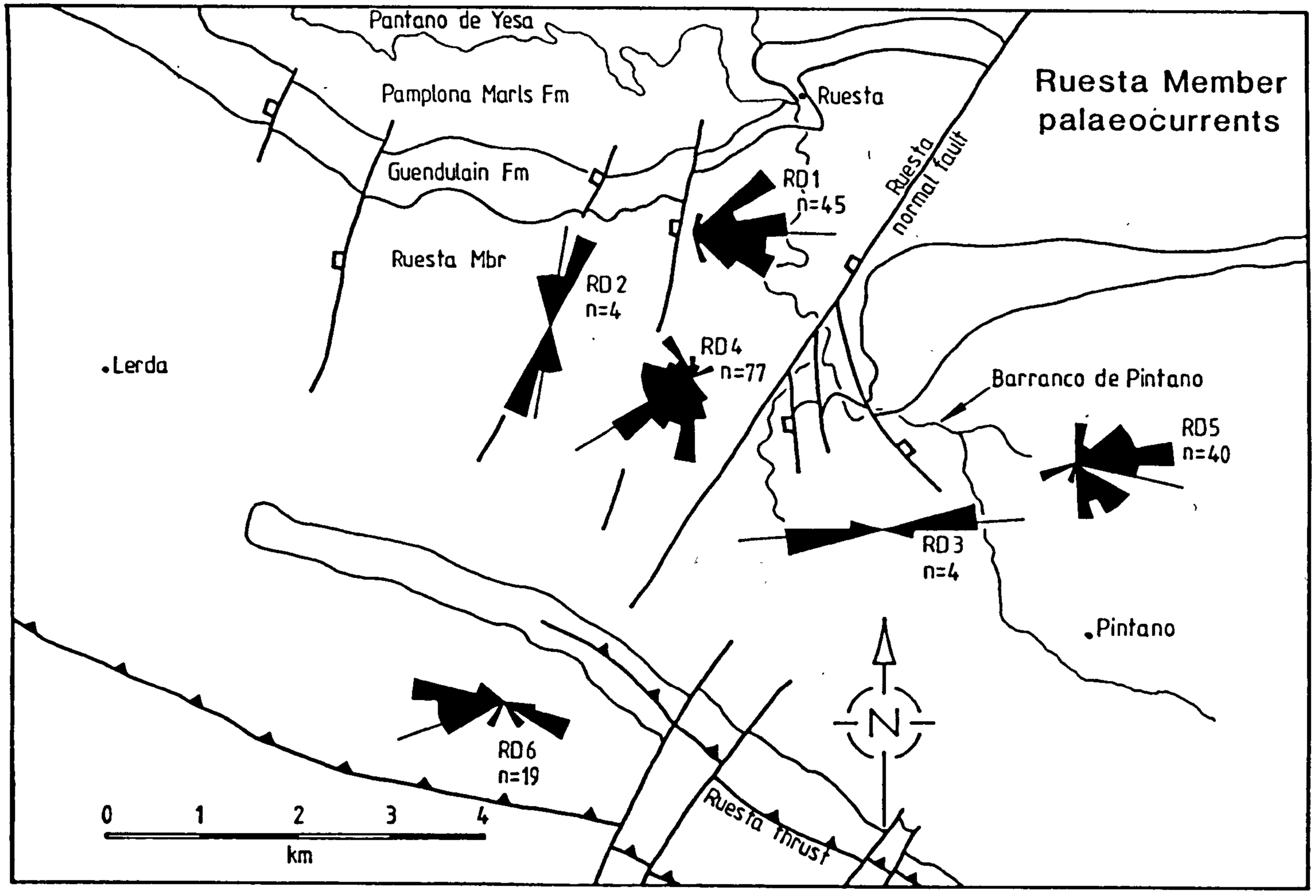

Fig. 3.4. Rose diagrams of palaeocurrent data at six stations superimposed on a structural and stratigraphic map of the Ruesta fault zone.

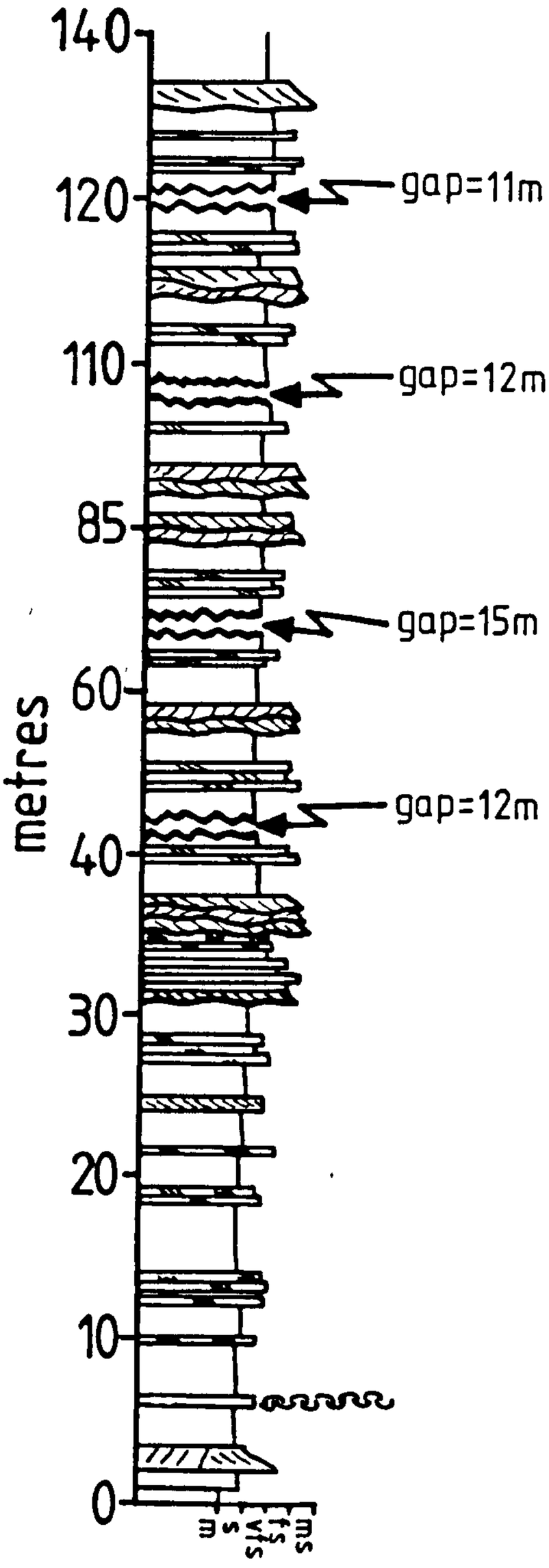

Fig. 3.5. Ruesta Member Massive Grey Mudstone Facies (0-30m) and Mottled Siltstone with Sandstone Facies (40-140m) at Lerda: graphic log.

Fig. 3.6. Photomosaic and interpretive line drawing of a 12m thick mouth bar sandstone body, approximately 1500m south of Ruesta. Note the internal, high relief, erosive base of a prograding channel sand body that overlies the mouthbar.

Fig. 3.7. Photomosaic and interpretive line drawing of a channel sandstone body, approximately 2000m south of Ruesta.

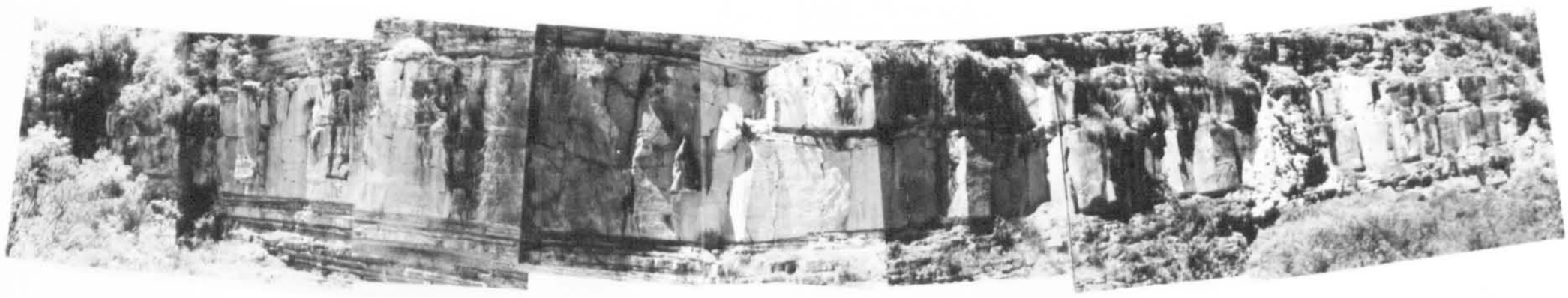

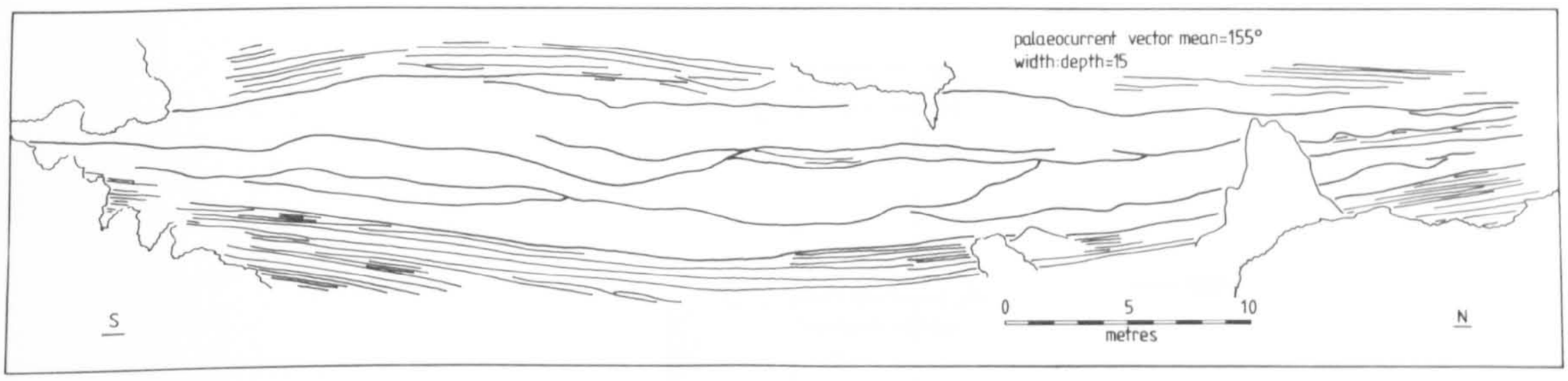
palaeocurrent vector mean=155°
width:depth=15
S
0
5
10
metres
N

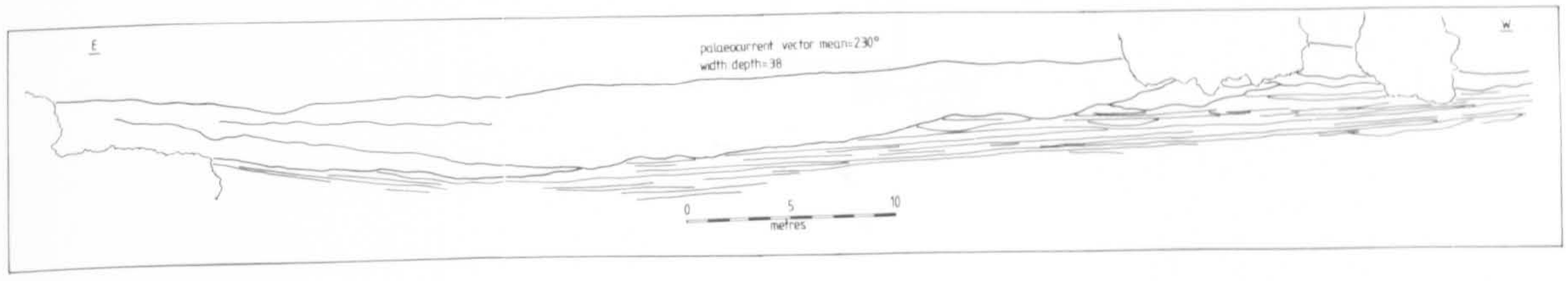
E
palaeocurrent vector mean=230°
width:depth=38
W
0
5
10
metres

Fig. 3.6. Photomosaic and interpretive line drawing of a 12m thick mouth bar sandstone body, approximately 1500m south of Ruesta. Note the internal, high relief, erosive base of a prograding channel sand body that overlies the mouthbar.

Fig. 3.7. Photomosaic and interpretive line drawing of a channel sandstone body, approximately 2000m south of Ruesta.

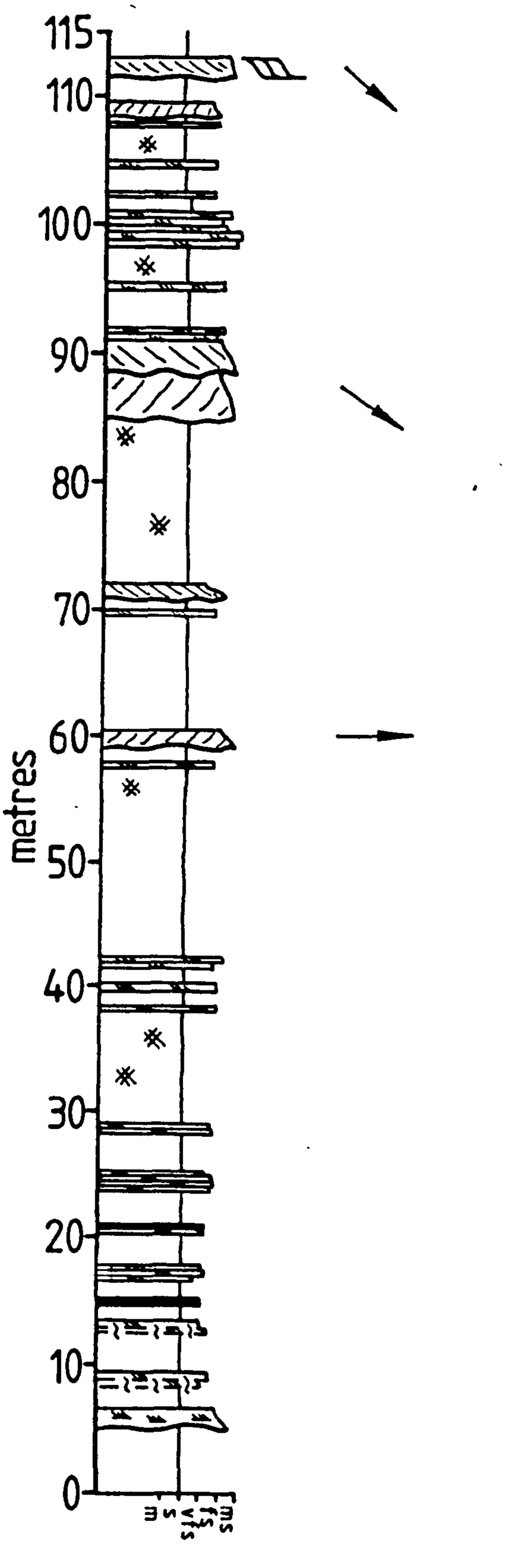

Fig. 3.8. Ruesta Member Mottled Siltstone with Sandstone Facies at Pintano: graphic log.

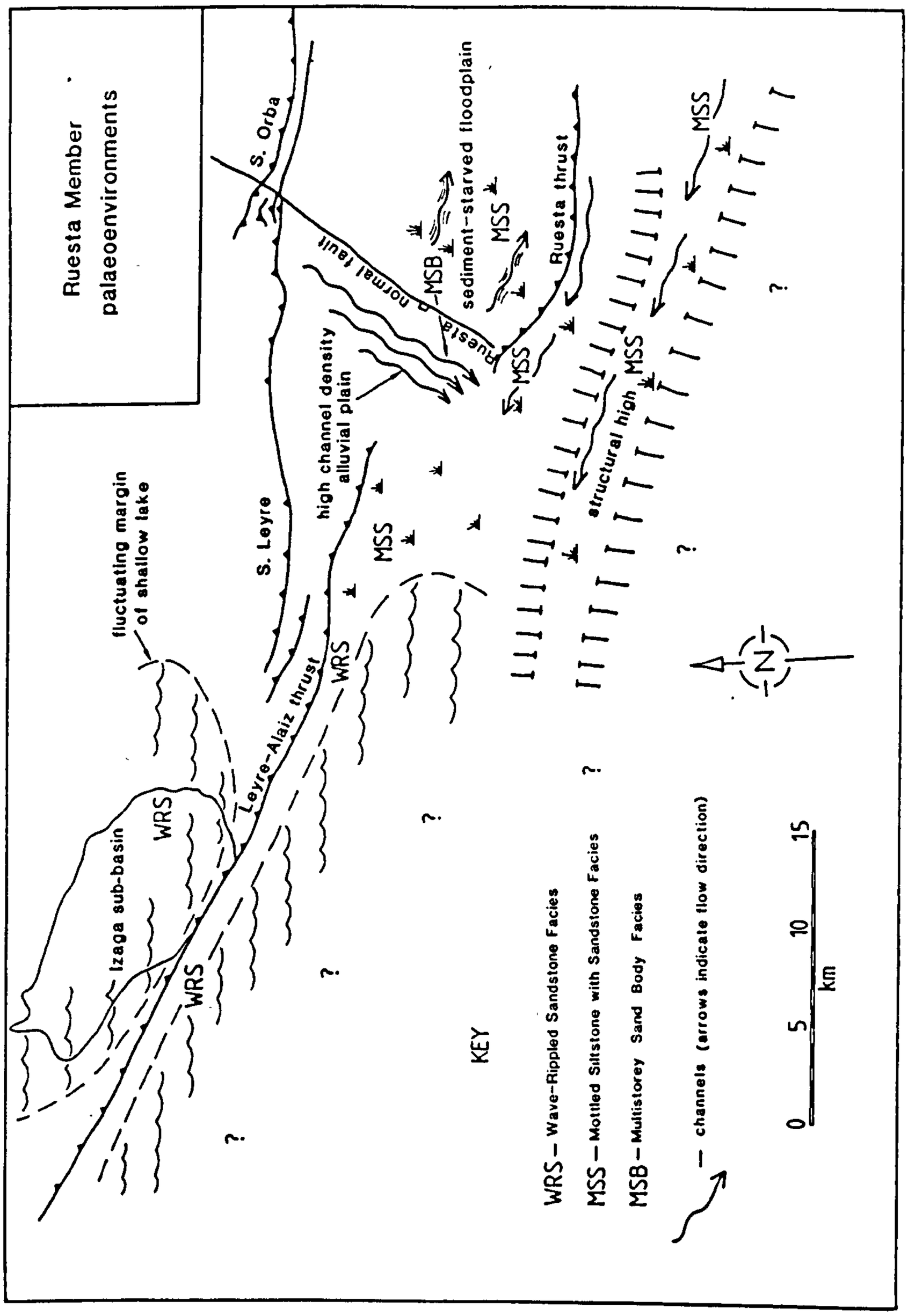

Fig. 3.9. Schematic palaeoenvironmental reconstruction of the study area during deposition of the Ruesta Member.

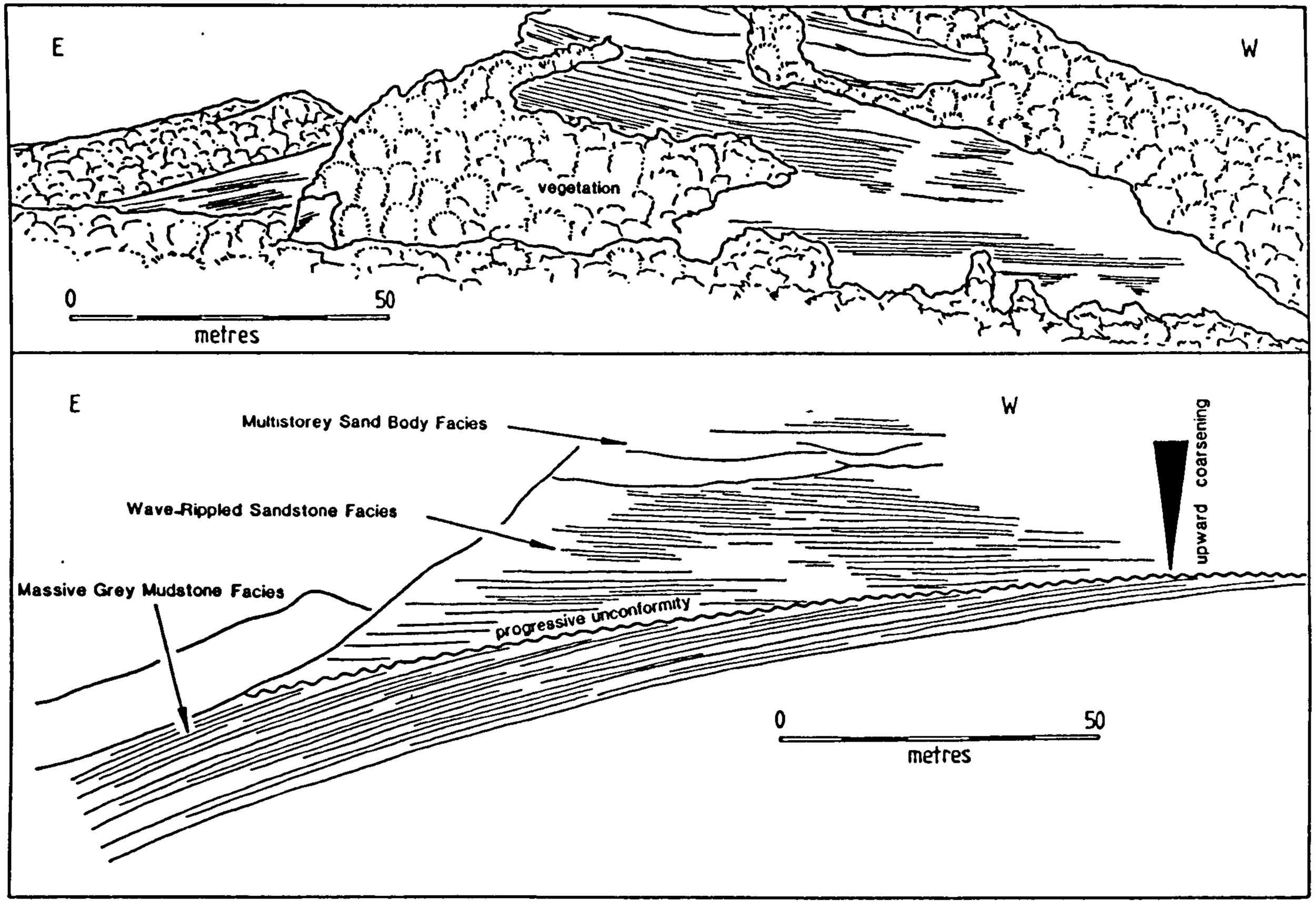

Fig. 3.10. Sketch from a photograph (a) and interpretation (b) of the localised angular unconformity exposed 200m west of the Ruesta normal fault and also depicted in Plate 3.2d. Note the erosive truncation of the lower series, beneath the unconformity, and the onlap of the upward coarsening upper series, above the unconformity.

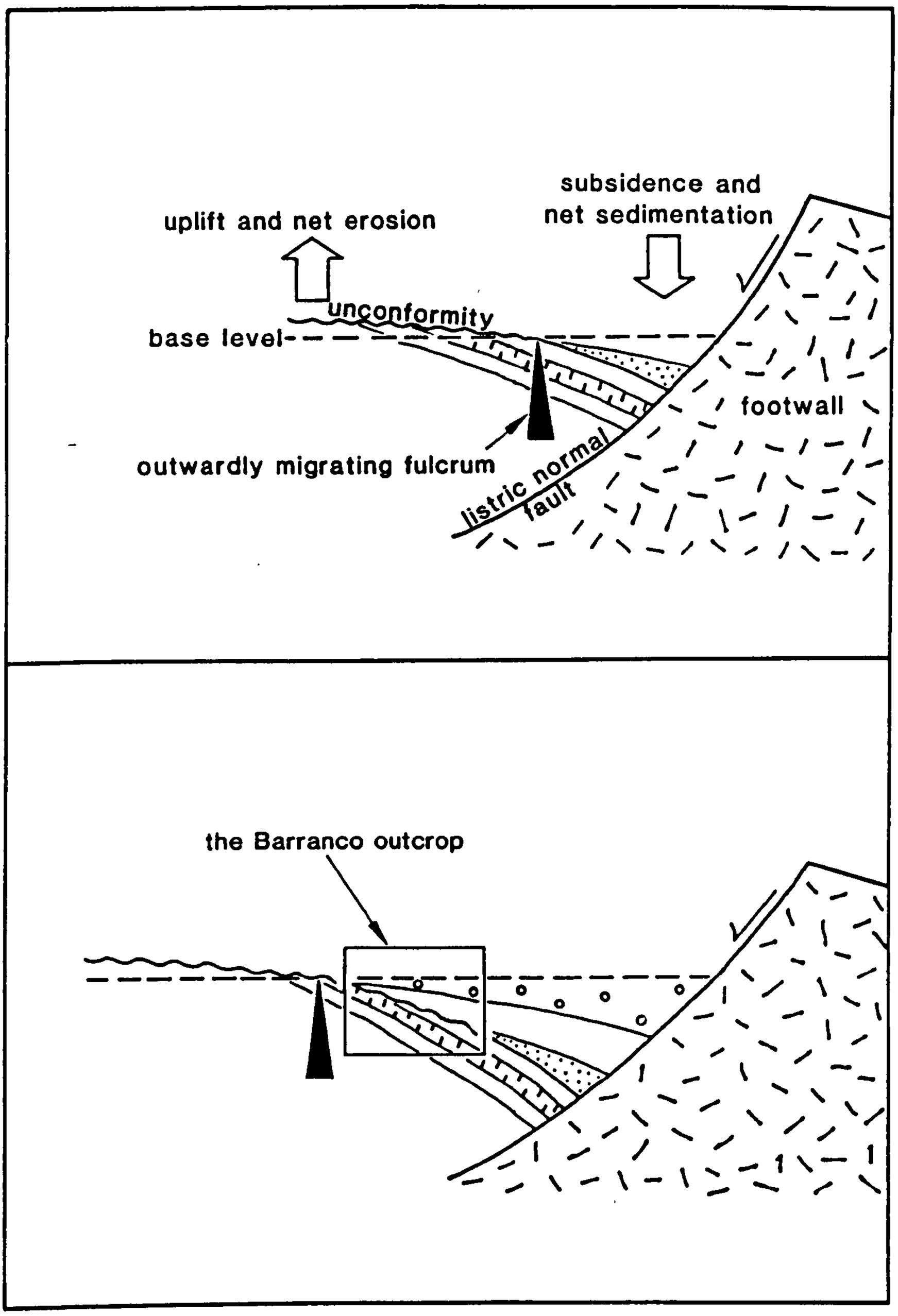

Fig. 3.11. Model to explain the evolution of the localised unconformity exposed 200m west of the Ruesta normal fault and illustrated in Fig. 3.10.

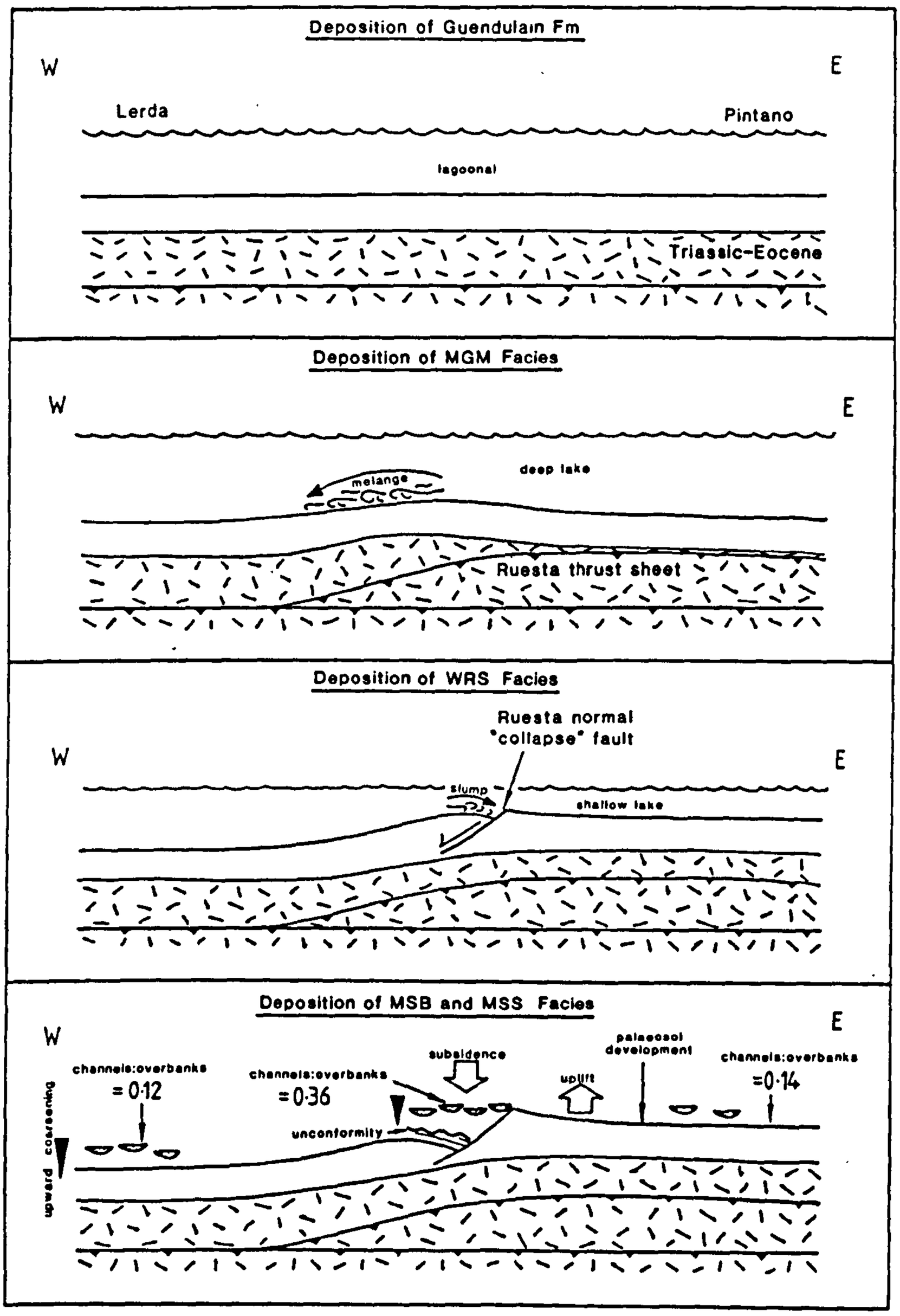

Fig. 3.12. Four stage evolution of the Ruesta fault zone depicted by schematic, strike-parallel sections through the fault zone. Sub-Ruesta Member stratigraphy is shown with stipple.

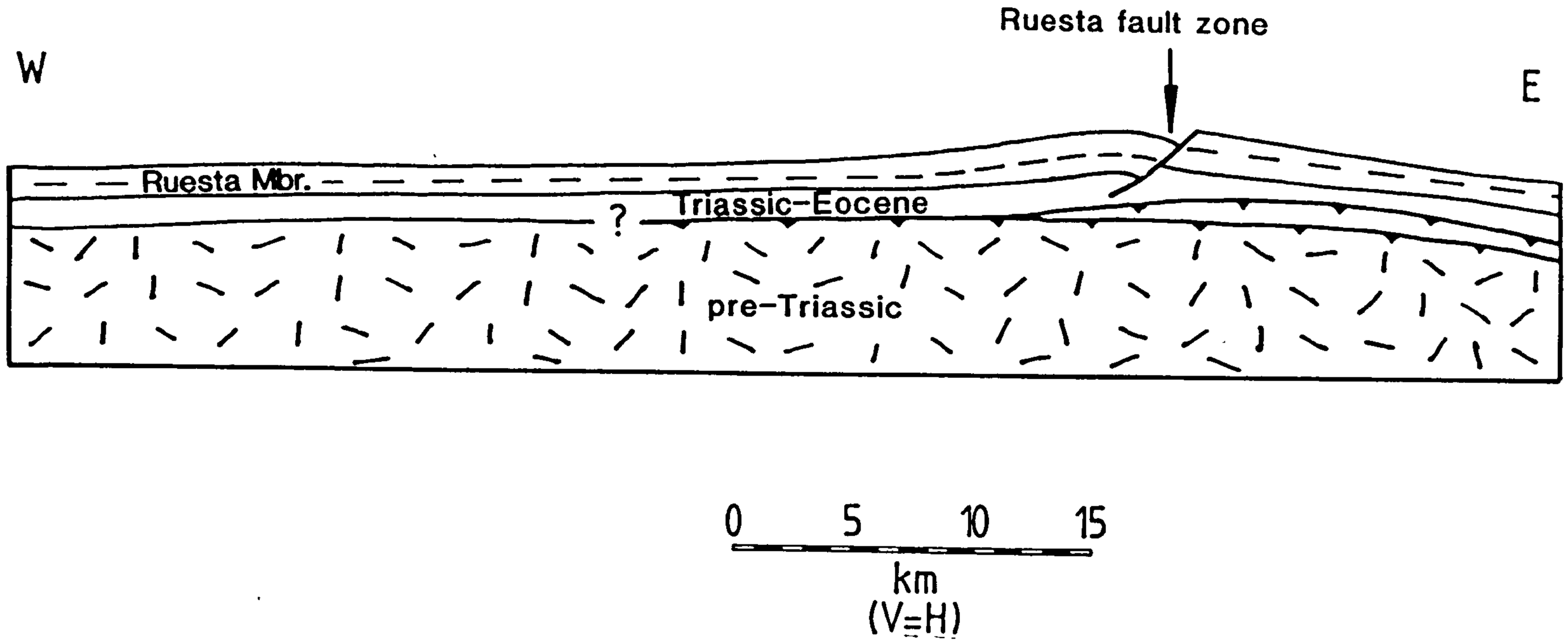

Fig. 3.13. Strike-parallel section through the study area along the line of section 2.6 shown in Fig. 2.1. The section depicts the shape in profile of the basin at the end of Ruesta Member deposition.

Plate 3.1a. Flowrolls at the base of a sandstone in a Wave-Rippled Sandstone Facies sequence in the Izaga sub-basin.

Plate 3.1c. Wave-Rippled Sandstone Facies 400m east of the Ruesta normal fault. Note the consistency of wave-ripple orientations between the eight separate beds visible in the photograph.

Plate 3.1b. Fifty metre thick succession, immediately west of the trace of the Ruesta normal fault, showing a rapid but conformable facies change from Massive Grey Mudstone Facies to Wave-Rippled Sandstone Facies about two thirds of the way up the sequence.

Plate 3.1d. Mud-cored fold nose within a Wave-Rippled Sandstone Facies slumped horizon.


C

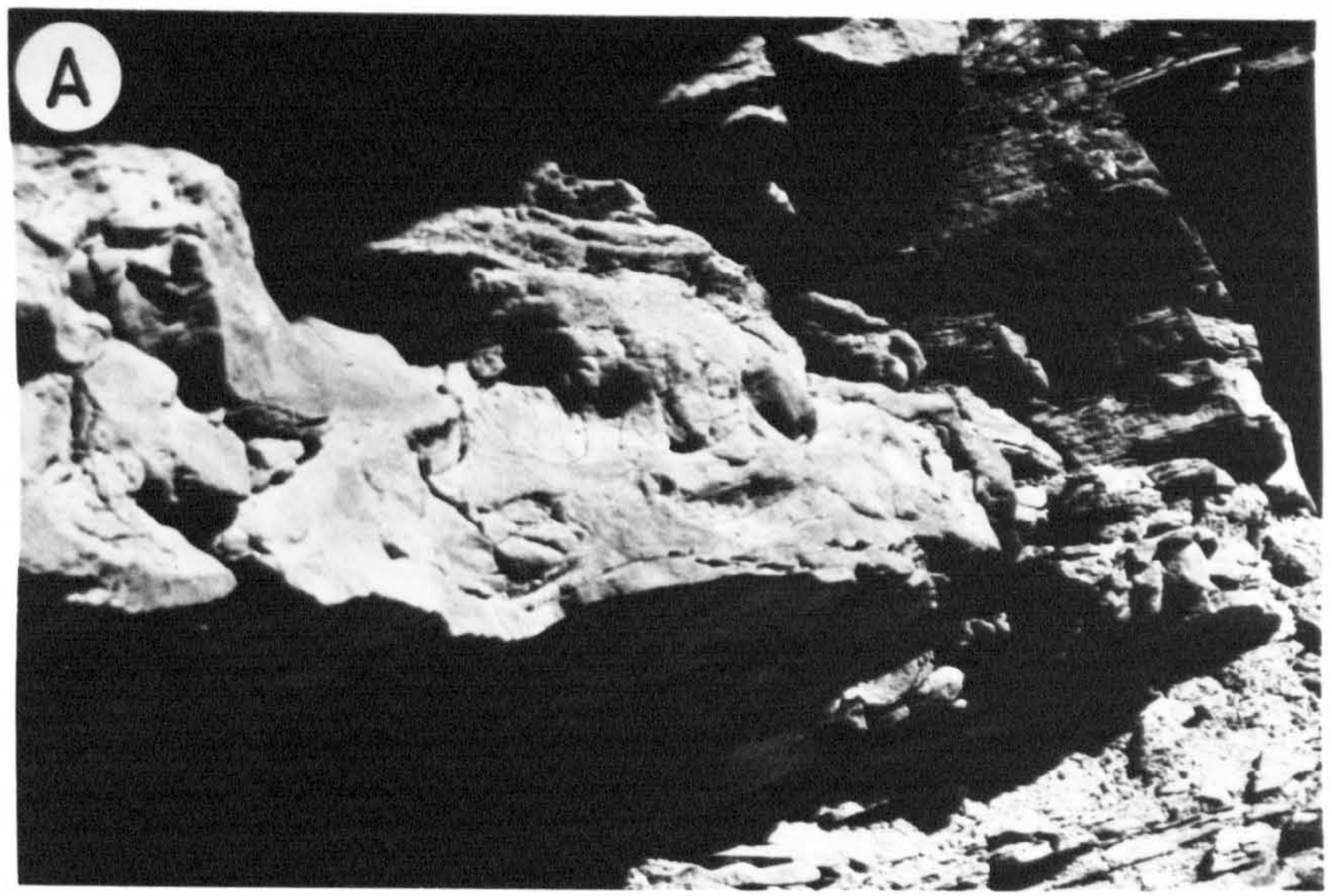
A


D

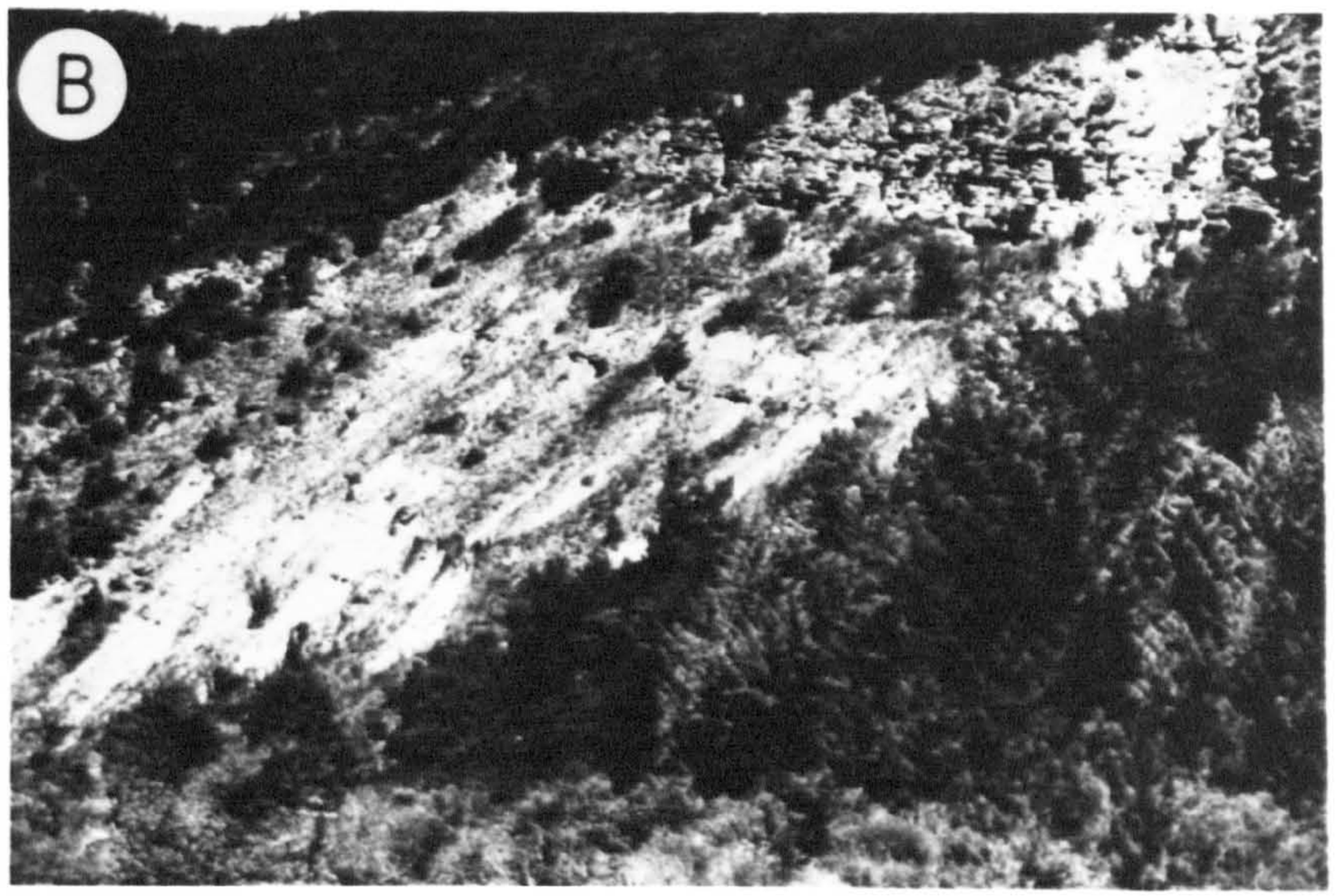
B

Plate 3.2c. Melange at Ruesta, displaying its chaotic internal organisation.

Plate 3.2a. Detail of the transition from Wave-Rippled Sandstone Facies to Multistorey Sand Body Facies at the base of the sandstone illustrated in Fig. 3.6.

Plate 3.2b. Trough cross-stratification in Multistorey Sand Body Facies near Ruesta.

Plate 3.2d. Localised, angular unconformity 200m west of the Ruesta normal fault also illustrated in Fig. 3.10. Dashed line marks the trace of the unconformity.

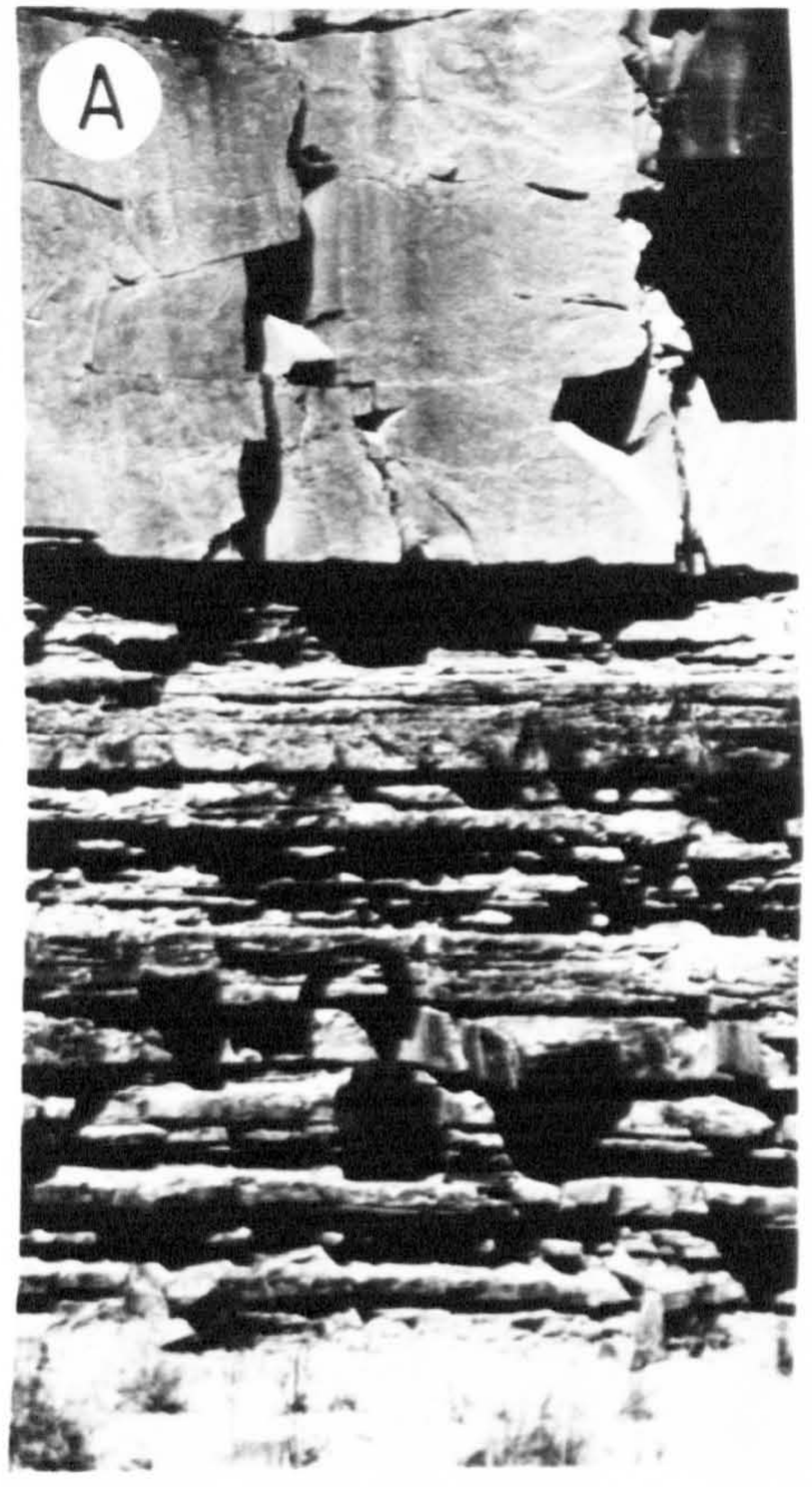
A


B


C

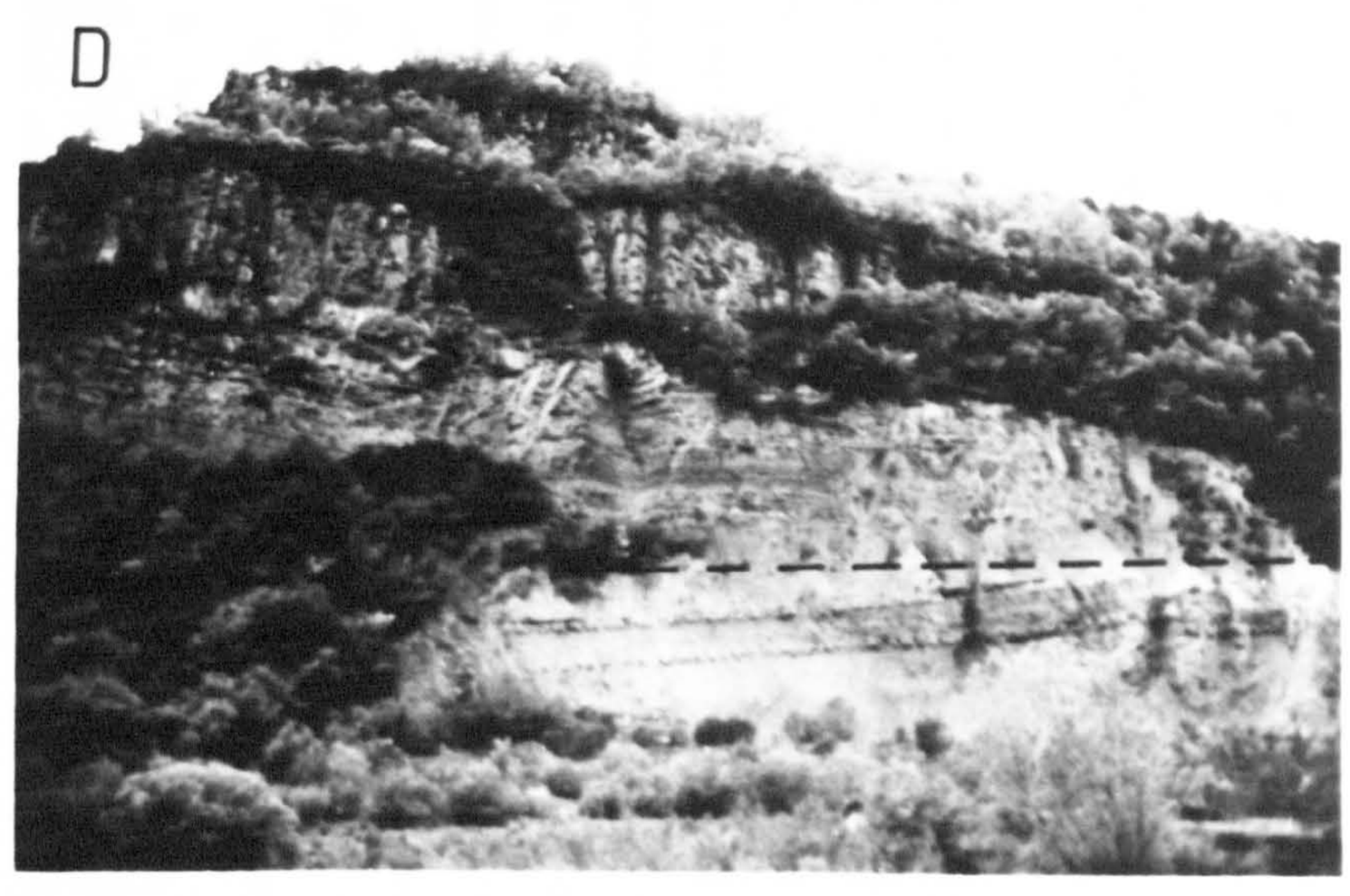
D

CHAPTER 4

BASIN EVOLUTION DURING DEPOSITION OF THE PETILLA MEMBER

4.1 ALLUVIAL SEDIMENTATION IN THE WESTERN PART OF THE BASIN

4.1.1 General facies description

In the Izaga and Olleta sub-basins, and at Aibar and Gallipienzo, four facies are identified. They are, respectively, the Gravelly Sandstone Facies, the Sheet Sandstone Facies, the Mottled Siltstone with Sandstone Facies and the Wave-Rippled Sandstone Facies. The facies logs shown in Figs. 4.1 and 4.2 represent sections through Gravelly Sandstone Facies sequences exposed near Alzoriz in the Izaga sub-basin. This facies consists of sand dominated sequences characterised by closely spaced, erosively based, upward fining sandstone bodies that commonly contain a thick gravel base comprising up to half the thickness of a sand body. Erosively based sandstone bodies constitute approximately forty percent of the total succession, each sandstone being up to eight metres thick with a width to depth ratio greater than fifteen (see the sheet like geometry of the sequence in Plate 4.1a). Thus, according to the nomenclature of Friend *et al.* (1979), they are termed'sheet' sandstone bodies. The sheets are generally simple, single storey units with gravel lags, that contain up to fifty percent intraformational siltstone clasts, which rapidly pass upward into trough and subordinate planar tabular cross-stratified, coarse-grained to fine-grained sandstone. Upper plane-bed lamination is a common sedimentary structure displayed by the sand bodies and it occurs in vertically restricted intervals at the bases, middle parts and upper parts of the sandstone bodies. The finer intervals between erosively based sheets comprise unmottled siltstone with thin-bedded, planar based, fine-grained to medium-grained sandstone beds stacked in packages up to 250 cm thick. In detail, individual planar based sandstone packages are commonly burrowed and display classic waning flow sequences of upper plane-bed lamination (shown by primary current-lineated surfaces) passing upward into cosets of trough cross-lamination and ripple cross-lamination.

A special feature of the Gravelly Sandstone Facies at Alzoriz is the abundant dewatering structures that are particularly well developed in the upper part of the logged section depicted in Fig. 4.2. Plan views of areally extensive bedding planes show that they are disturbed by irregular hummocks and sand volcanoes (see Plate 4.1b) related to fluidisation. The sand volcanoes are up to 100 cm in diameter, 30 cm high and of composite form, comprising between two and four cones. The sand volcanoes mark the points of

emergence on a bedding plane of vertical water escape vents that may be recognised in cross section by sharp anticlines separated by broad synclines.

The characater of the Petilla Member exposed between Sanguesa and Aibar is shown in the Section illustrated in Fig. 4.3. This section displays many of the typical characteristics of the Mottled Siltstone with Sandstone Facies described in Chapter 3. The present facies comprises thick intervals of reddened and mottled siltstone with packages of internally massive, stacked, thin-bedded, planar based and intensely burrowed, fine-grained sandstone up to 300 cm thick. At Aibar and Sanguesa, the siltstone contains gypsum in thin beds and rare, post-depositional, discordant veins. Siltstone constitutes approximately 75% of the Aibar succession and it separates erosively based, multistorey sandstone bodies. The sand bodies are between 2 and 12m thick and have erosive reliefs of between 20 and 200 cm amplitude, that increase in size as the sequence is ascended. The sandstones are constructed from between one and six upward fining storeys that display trough and subordinate planar tabular cross-stratification, commonly passing upward to ripple or upper plane-bed lamination. Medium-grained to fine-grained sandstone dominates the sand bodies which have width to depth ratios of between 6 and 20 and, in two examples, display relatively impersistent lateral accretion surfaces. These are similar in their shape and internal structure to the epsilon cross-stratification of Allen (1963) and, at Aibar, the lateral accretion surfaces are 250 cm wide, 55 cm high and laterally persistent for less than twelve metres.

Petilla Member rocks cropping out along the northern flank of the Olleta sub-basin, near Leoz, belong to the Sheet Sandstone Facies described more fully in Section 4.2 of this chapter. In the Olleta sub-basin, the facies is characterised by upward fining, erosively based, multistorey and multilateral sheet sandstone bodies (see Friend *et al.* 1979) with width to depth ratios of between 100 and 500. Internal bedforms in the sheets are dominated by planar tabular cross-stratification up to 80 cm high and subordinate trough cross-stratification with ripple cross-laminated upper parts to the sand bodies. Sheet sandstone bodies are separated by unmottled pale brown siltstone comprising about 65% of the total thickness of the Olleta sub-basin Sheet Sandstone Facies.

The Petilla Member north of Gallipienzo displays features typical of the Wave-Rippled Sandstone Facies described in greater detail in Chapter 3. At Gallipienzo, this facies comprises planar based beds of fine-grained sandstone with internal ripple cross-lamination and common wave ripple modified upper

surfaces. The sandstones are laterally persistent for up to 200m, up to 90 cm thick and occur either as laterally extensive packages of two to four stacked beds, or, as individual units. Sandstone makes up roughly 70% of the sequence and is separated by pale brown, laminated or massive siltstone with common desiccation cracks.

4.1.2 Palaeocurrents

Rose diagrams depicting inferred palaeocurrent directions measured from the Alzorriz, Aibar and Leoz sequences described in section 4.1.1 are presented in Fig. 4.4. In each section, the sedimentary structures from which the data are derived have similar directional properties and are of similar scale (ie. they belong to similar 'orders' of Allen's fluvial bedform hierarchy; see Allen 1966; Allen 1968; Bluck 1974). At Alzorriz, the 73 palaeocurrent indicators are dominantly planar tabular cross-stratification, interpreted here as the deposits of transverse barforms. The eleven indicators measured from Aibar are channel axes that were derived by measuring the margins of erosively based sandstone bodies (cf. Bluck & Kelling, 1962). At Leoz, in the Olleta sub-basin, palaeocurrent directions were inferred from trough cross-stratification axes and the bidirectional crests of related ripple cross-lamination.

The rose diagrams in Fig. 4.4 reveal that the dominant drainage direction in the northwest part of the study area during Petilla Member deposition was south-southwestward, toward the foreland. It is proposed here that this forelandward dipping palaeoslope was imposed upon the area by the demonstrable movement on the Leyre-Alaiz thrust at various times during the Oligocene (see Section 2.3). Activation of the Leyre-Alaiz thrust during Petilla Member deposition implies that the Alzorriz-Aibar, laterally draining alluvial system breached the trace of the thrust.

4.1.3 Depositional environments

Some of the uncertainties involved with identifying ephemeral flow and distinguishing it from more perennial conditions have been discussed by Tunbridge (1981). He states that upper plane-bed parallel laminations are often the main, or only sedimentary structure found in sands deposited by ephemeral streams and floods (also see McKee *et al.* 1967). At Alzorriz, the abundance of upper plane-bed lamination and the presence of coarse, upward-fining, erosively based, gravel-sandstone bodies, that contain no lateral accretion surfaces or clear channel margins, reflects the ephemeral origin of the Gravelly Sandstone Facies. The variability in siltstone content through the two Alzorriz sections suggests that the area was located at the extremities of some floods (that gave rise to high siltstone content, sheetflood

deposits) whilst being located in the central parts of other floods (generating gravelly and sandy streamflood deposits) (cf. Scott *et al.* 1969). The erosively based, upward fining units record streamflood deposition in exceptionally wide and shallow channels, as evidenced by their sheet-like bed geometries (see Plate 4.1a).

Collinson (1978) has questioned whether erosively based units of two metres thickness or less, in which channel margins cannot be recognised, should be attributed to channel deposition at all. However, the detailed description of modern streamflood deposits in central Australia by Williams (1971) shows that the Alzorriz erosively based units are typical of superimposed streamflood channel deposits. Their upward transition from a gravelly lag to trough cross-stratification, that commonly passes up to planar cross-stratification and upper plane-bed lamination, reflects decreasing depth of flow as streamflood channels became filled. Somewhat similar deposits have been described from the rock record by Steel & Aasheim (1978) and Tunbridge (1981), both of whom also document variable amounts of soft sediment deformation associated with the ephemeral flood facies they described.

Sand and mud volcanoes, similar to the ones at Alzorriz, have been described from, among other places, modern sediments in New Zealand, Ridd (1970) and the Carboniferous of western Ireland by Rider (1978), where they are associated with growth faults. Both these authors recognised that dewatering structures develop in beds experiencing abnormally high pore fluid pressure (also see Bennett 1977). Hubbert & Rubey (1959) suggest that rapid accumulation of interbedded mudstone and sandstone can result in permeability seals that lead to higher beds in a sequence 'floating' on lower, overpressured mudstone. Under such circumstances, seismic shocks, such as might have occurred during Leyre-Alaiz thrust motions at the same time as Petilla Member deposition, may trigger dewatering (cf. Farrell 1984).

In the Mottled Siltstone with Sandstone Facies of Aibar (Fig. 4.3), the dominance of massive, colour mottled siltstone containing rare gypsum, with occasional erosively based sand bodies and packages of stacked planar based, thin-bedded sandstone, suggests that the sequence was deposited in a distal equivalent of the environment in which the Gravelly Sandstone Facies of Alzorriz were laid down. The finer grain size of the succession at Aibar, in comparison with that at Alzorriz, and its greater degree of palaeosol related colour mottling (Bown & Kraus 1981; van der Meulen 1986) and bioturbation suggest that the Mottled Siltstone with Sandstone Facies sequence records a former floodbasin dominated by occasional small sheetfloods and infrequently

traversed by small, steady-state channels. This interpretation is consistent with the environmental analysis made from more detailed descriptions of the Mottled Siltstone with Sandstone Facies of the Ruesta Member in Sections 3.2.1 and 3.3.1. The presence of lateral accretion surfaces in two channelised sand bodies at Aibar testifies to their deposition by stable and more perennial channels up to 6m wide and 1m deep, and with average width to depth ratios of four (determined from formulae given by Allen 1965; Khan 1971; Ethridge & Schumm 1978) (see Sections 4.2.4 and 6.3.3).

In the Sheet Sandstone Facies on the northern flank of the Olleta sub-basin, the dominance of upward fining, erosively based sheet sandstone bodies displaying occasional lateral accretion surfaces, records deposition by fluvial channels, probably of moderate to high sinuosity, draining across an areally extensive floodplain. The floodplain overbank sediments are represented in the facies by the volumetrically dominant inter-sandstone intervals comprising unmottled, pale brown siltstone. The laterally extensive, upward-fining fluvial sandstone sheets were formed by either the lateral coalescence of contemporaneous meanderbelts on the floodplain, or, by the superimposition of an active meanderbelt with an underlying, abandoned meanderbelt. Large scale planar tabular cross-stratification and subordinate trough cross-stratification in the sand bodies record the development of within-channel macroform bars and the downstream migration of sinuous crested dunes (cf. Cant & Walker 1978, fig. 14) (see Section 4.2.5).

Largely by analogy with the more completely exposed, but similar, sequences in the Ruesta Member (see Section 3.2.1 and 3.3.1), the Wave-Rippled Sandstone Facies to the north of Gallipienzo was deposited at the margins of a shallow, sandy lake. The non-erosive, planar bases of the laterally persistent, thin-bedded sandstone with wave-rippled upper surfaces, records frictional sedimentation of blanket-like units on the shallow lake floor, probably near points of flow into the lake (cf. Hyne *et al.* 1979; Allen 1981b). The Wave-Rippled Sandstone Facies near Gallipienzo represents the terminal facies of a major fluvial system that drained westward, parallel to the basin long axis, during Petilla Member deposition (Section 4.2)

4.2 SHEET SANDSTONE FACIES

The Sheet Sandstone Facies is most dramatically exposed at the Navarrese hamlet of Petilla and in the upper part of the Rio Arba valley. As its name implies, the facies is dominated by fluvial sandstone bodies that, according to the nomenclature of Friend *et al.* (1979), are classified as sheet type sand

bodies on the basis of their exceptionally high width to depth ratios. The total thickness of the Sheet Sandstone Facies is 2300m, within which there are up to 140 laterally extensive sandstone bodies. In contrast with their enclosing siltstone, the sand bodies have been preferentially enhanced by weathering and tilted to a sub-vertical attitude, such that they crop out as prominent 'walls' which march spectacularly across the hillside for up to six kilometres (see Plate 4.2). Up to 1400m of logged section from the Rio Arba valley, and 770m of section from Petilla, provides complete profiles through the Sheet Sandstone Facies, thus allowing an insight into the depositional and tectonic processes responsible for the evolution of this distinctive lithofacies..

4.2.1 Sheet Sandstone Facies between Biel and the Rio Arba: general facies description

Figure 4.5 shows a 1430m, incomplete measured section through the Sheet Sandstone Facies in the Rio Arba valley. There are approximately 90 erosively based, upward fining sandstones that make up about 38% of the succession. The proportion of the section occupied by sand bodies systematically decreases upward, from 42 to 34%. Individual sandstones are between 1.5 and 13m thick and have width to thickness ratios of between 100 and 800. In vertical section, sandstone bodies consist of a single storey or, more commonly, thicker multistorey units comprising between two and four upward fining storeys separated by erosion surfaces (eg. see Plate 4.1c). In the Rio Arba section, single storey sand bodies become increasingly common toward the top of the succession. The few lateral exposures accessible for detailed observation reveal complex multistorey and multilateral arrangements of third and second order (Allen 1983) internal erosion surfaces. Wide (up to 12m) and shallow, internal scours filled with thin gravel lags overlain by ripple cross-laminated, fine-grained sandstone and siltstone are common. These internal scours have width to depth ratios of between 10 and 20, and occur at all levels within the sandstone sheets.

In detail the Rio Arba sand bodies display broad, gently curviplanar bases with erosive reliefs of up to two metres. Erosive bases are commonly burrowed and overlain by a gravel lag horizon of variable thickness (a few centimetres to 30 cm), comprising up to 50% intraformational siltstone and mudstone clasts. Individual sandstone storeys between erosion surfaces display a pronounced upward fining, from a gravelly base to fine-grained or very fine-grained sandstone at the top of a unit. As the Rio Arba succession is ascended, an increasing proportion of sandstones are dominated by massive gravel

and pebble grade sandstone clasts derived from reworking of the lower Campodarbe Formation molasse succession. This suggests that the Rio Arba sequence, as a whole, coarsens upward toward the overlying Bernues Formation.

The assemblage of sedimentary structures within each erosively based sandstone is fairly consistent. Each storey is commonly constructed from a planar tabular cross-stratified basal part of coarse-grained to medium-grained sandstone that overlies a gravel lag. Planar tabular cross-stratification passes up to trough cross-stratified and, more rarely, upper plane-bed laminated, medium-grained sandstone. Upper surfaces of some sand bodies display current ripples and occasional reactivation surfaces may be recognised at various levels in the sandstones.

In eight examples of medium- to fine-grained sandstones in the Rio Arba section, lateral accretion surfaces of similar morphology to the epsilon cross-stratification of Allen (1963), comprise a large part of the vertical extent of an individual erosively based storey. Dimensions of the lateral accretion surfaces vary from between six to fifteen metres wide (measured parallel to bedding and normally to the azimuth of dip of a lateral accretion surface) and 65 to 250 cm deep, although their upper parts are frequently truncated by the erosive base of a succeeding storey. Asymptotic ripple foresets, with amplitudes of between three and fifteen centimetres, dominate internal stratification of the lateral accretion surfaces (cf. Miall 1985 fig. 5b).

The intervals between sand bodies in the Rio Arba section comprise 62% of the total thickness of the succession and are characterised by pale brown, mottled siltstone. The siltstone displays a blue-grey to red colour mottling that commonly nucleates about vertical, dendritic rootlets up to 30cm deep. Occasional horizons of centimetre-diameter calcrete modules, similar to those described by Puigdefabregas & van Vliet (1978, fig. 7b) occur at various levels through the section. Within the siltstone dominated sequences, planar based, laterally persistent beds of fine-grained sandstone, up to 30 cm thick and with burrowed bases, are common. These laterally extensive, fine-grained sandstones are internally massive, or they display upper plane-bed lamination passing up to ripple cross-lamination, and occur as individual units or as packages of up to six stacked units.

In the NNE-SSW oriented valley of the Rio Biel, seven kilometres to the east of the Rio Arba, the Sheet Sandstone Facies display similar gross characteristics and sandstone body morphology. However, at Biel the sand bodies are generally coarser grained, thicker and more widely spaced. To the

east of Biel, the Sheet Sandstone Facies may be traced for ten kilometres along strike to Fuendecalderas, where it is truncated by a major N-S trending lateral ramp previously recognised by Puigdefabregas (1975) and recently interpreted by Nichols (1987, fig. 4).

4.2.2 Sheet Sandstone Facies between Petilla and Sos: general facies description

The Sheet Sandstone Facies exposed at Petilla is illustrated in the facies log of Fig. 4.6. Roughly thirty five sandstone bodies comprise 26% of the 700m thick logged sequence, in contrast to 38% of the Rio Arba sequence that consists of sandstone. Additionally, the proportion of sandbodies in the sequence decreases westward, toward Sos, where they constitute about five percent of the Sheet Sandstone Facies. As the Petilla sequence is ascended there is an increasing proportion ooccupied by sandstones, ranging from 20% at the base to 31% toward the top. Because of their generally single storey construction, sandstone bodies at Petilla are significantly thinner than those in the Rio Arba and they vary from 1.5 to 5m thick.

Lateral profiles reveal a multilateral arrangement of third and second order (Allen 1983) erosion surfaces that define broad, internal scours, up to 1.5m deep, 15m wide, and with width to depth ratios of between 10 and 16. These internal scours are filled with complexes of 'foreset macroforms' (Miall 1985) that comprise stacked cosets of planar tabular cross-stratification with subordinate trough cross-stratification and, in the upper parts of the scours, ripple cross-lamination. Vertical profiles through sand bodies at Petilla display a less well defined upward fining and generally finer grain size than those in the Rio Arba section. Erosive bases, with up to 150 cm of erosive relief, are overlain by a rare, thin gravel lag horizon and planar tabular cross-stratified, medium-grained sandstone, with foreset amplitudes of between 10 and 50 centimetres. Trough cross-stratified and current ripple laminated, medium- to fine-grained sandstone characterises the upper parts of sand bodies. Five examples of lateral accretion surfaces, comprising gently dipping, planar tabular cross-laminated, medium- to fine-grained sandstone, were recognised at Petilla. Where present, they dominate the vertical extent of an erosively based storey and are up to twelve metres wide and two metres deep.

Seventy four percent of the sequence consists of blue-grey and red, colour mottled siltstone containing horizons of small calcrete nodules. Within these finer-grained intervals occur common packages of stacked planar based, thin-bedded, fine-grained sandstone displaying upper plane-bed lamination and upper

surfaces with current-ripples. Toward Sos, the Sheet Sandstone Facies becomes increasingly dominated by mottled siltstone and thin-bedded, planar based, fine-grained sandstone. To the west of Sos, no major erosively based sand bodies exist in the equivalent sequence along strike from Petilla, and it is characterised by the Wave-Rippled Sandstone Facies described from Gallipienzo in section 4.1.1.

4.2.3 Palaeocurrents

Palaeocurrent data for the Rio Arba and Petilla sections presented in Fig. 4.4 show drainage directions deduced mainly from trough cross-stratification axes and, where accessible for measurement, erosive channel margins and lateral accretion surfaces. Both the rose diagrams display wide dispersions, and consequent low vector magnitudes, about the vector means of 314° and 287° for the Rio Arba and Petilla sequences, respectively. With large populations of fluvial palaeocurrent data, Bridge (1985) has suggested that a wide dispersion is a qualitative indicator of deposition by a high sinuosity channel system. Similarly divergent spreads of palaeocurroent data are reported from the ancient high-sinuosity fluvial systems studied by Nami (1976, plate 1), Stewart (1981, fig. 1) and Plint (1983, fig. 12). However, all these workers emphasise the relative consistency in palaeocurrent directions recorded from individual, upward fining sequences, a point which also applies to individual, upward fining sand bodies in the Sheet Sandstone Facies (compare the general consistency of unidirectional and bidirectional palaeocurrents inferred from individual sandstones in the facies logs of Figs. 4.5 and 4.6).

4.2.4 Fluvial palaeomorphology

Since the early 1960s, geomorphologists have been able to demonstrate an empirical relationship between fluvial channel morphology and flow characteristics (eg. Schumm 1960, 1963; Leopold & Wolman 1960). Many of the empirical equations that have been developed rely on being able to estimate accurately channel width and depth dimensions. The recognition that lateral accretion surfaces represent the deposits of ancient point bars (Allen, 1963, 1965) has provided a widely available indicator of channel bankfull width and depth.

Allen (1965) suggested that the fully preserved width of an 'epsilon' cross set (see Allen 1963) approximates to two thirds of the bankfull width of the channel that formed it. The validity of this generalisation was substantiated by later work on ancient sequences (eg. Donaldson 1969; Cotter 1971; Leeder 1973; Elliott 1976; Morton & Donaldson 1978) and it is an axiom followed here. However, in the study area it has been necessary to employ

compensatory factors to allow for channel depths in straight reaches being consistently smaller than on channel bends, and, the differential compaction of sand and mud (Donaldson 1969; Cotter 1971; Khan 1971; Ethridge & Schumm 1978). This thesis adopts the compensation method of Khan (1971) and Ethridge & Schumm (1978) in which:

$$D^* = D.0.585/0.9,$$

where D* is channel depth and D is full lateral accretion set thickness.

In the Sheet Sandstone Facies logged sections of the Rio Arba and Petilla, thirteen fully preserved examples of lateral accretion surfaces were recognised. However, because of the vertical tilting of the beds, only one of these is accessible for measurement. The dimensions of this lateral accretion set (900 cm:210 cm) were used to calculate an average width to depth ratio of 9.9 for the Sheet Sandstone Facies palaeochannels. However, channel dimensions were derived by the method of Leeder (1973) in which coarse member thickness approximates to channel bankfull depth. Average coarse member thickness (not total sand body thickness which might represent multistorey, stacked coarse members) is remarkably consistent through the sections in the Rio Arba and at Petilla where they are 340 and 320 cm, respectively. Thus, from a mean bankfull channel depth of 330 cm, channel width was determined using the width to depth ratio deduced from the lateral accretion surfaces.

Of the five palaeomorphologic parameters presented in Fig. 4.7 (width to depth ratio, sinuosity, meander wavelength, meander amplitude and meanderbelt width), only sinuosity is not derived from estimates of width or depth dimensions. Meander wavelength and meander amplitude, respectively, are calculated from the following formulae given by Leopold & Wolman (1960):

$$L_m = 10.9\ w^{1.01}, \text{ and}$$

$$A_m = 2.7\ w^{1.1}\ ,$$

where L_m is meander wavelength, w is bankfull channel width and A_m is meander amplitude. Meanderbelt width was inferred from the following equation given by Collinson (1978), that assumes a sinuosity of greater than 1.7 (Leeder 1973):

$$W_m = 64.6h^{1.54},$$

where W_m is meanderbelt width and h is bankfull channel depth.

Palaeosinuosity, however, was deduced from the following equation first developed by Langbein & Leopold (1966), and modified by Miall (1976), which relates sinuosity to the angular change in mean channel orientation:

$$\text{sinuosity} = 1/1 - (\theta/252)^2,$$

where θ is the maximum angular range of the mean channel azimuths. The

sinuosity value of 2.3 for the Sheet Sandstone Facies presented in Fig. 4.7 uses the mean value of the highest five angular changes in mean channel orientation from 29 available measurements of angular change greater than 100°. The palaeomorphology of the Sheet Sandstone Facies, as presented in Fig. 4.7, provides additional semi-quantitative information on the depositional environment of this impressive fluvial sequence. Comparison with the palaeomorphology of the Uncastillo Formation Ribbon Sandstone Facies provides an insight to some of the controls on fluvial sequence development.

4.2.5 Depositional environments and the tectonic significance of the sheet sandstone bodies

In his review of the criteria for recognising meandering fluvial sediments in the rock record, Jackson (1978) selected the following seven useful parameters: (1) exhumed meanderbelts, (2) high bank stability, (3) low gradient, (4) substantial proportion of muddy fine member, (5) asymmetrical, mud-filled channels, (6) high palaeocurrent variance and (7) a lack of very coarse-grained material. Of these, the Sheet Sandstone Facies contains substantial fine member (60-75%), a high palaeocurrent variance (eg. see Fig. 4.4) and a lack of coarse conglomerate. Additionally, one might expect to see exhumed meanderbelts if the flat bedded exposure conditions described from the Murillo point bars by Puigdefabregas (1973), for example, pertained in the Rio Arba and Petilla sections. Therefore, considering the attributes listed above, and knowing that the Sheet Sandstone Facies comprises repetitive, erosively based, upward fining units (cf. Allen 1970), it is here interpreted as a product of meandering fluvial sedimentation.

Of the published lithofacies models for meandering streams, the Sheet Sandstone Facies seem to lie somewhere between Classes 2 and 3 of Jackson (1978) which are, respectively, sand bed streams with modest thickness of fine member and, sand bed streams lacking mud and rock gravel. Thus, the Sheet Sandstone Facies was deposited by mixed load streams of moderate width to depth ratio that generated upward fining, sand dominated deposits with some preservation of lateral accretion surfaces and rare channel fill siltstone.

Galloway (1981) predicted that multilateral sheet sandstones are characterised by a low overbank component in the depositional sequence. The higher than expected percentage of fines in the Rio Arba (62%) and Petilla (74%) sections thus requires an explanation. This high mean 68% value of fines suggests that the fines aggradation rate and/or fines preservation potential was exceptionally high in the Sheet Sandstone Facies floodbasin environment. There are two possible interpretations of this inference.

(1) It was demonstrated in Chapter 2 that during Petilla Member times the area of Sheet Sandstone Facies deposition was located immediately forelandward of a developing thrust front. It is therefore reasonable to invoke a high rate of subsidence, generated by tectonic loading at the basin margin (cf. Royden & Karner 1984), that would maximise sediment preservation potential.

(2) Puigdefabregas & van Vliet (1978) speculated that the unusually high ratio of overbank to channel sediments in their Oligocene fluvial sequences requires another source of fines in addition to those channels preserved within the fines sequence. A similar problem was investigated by Allen & Matter (1982).

In Chapter 8, it will be shown that, in contrast to an accelerated rate of basin subsidence during Uncastillo Formation times, basin subsidence was not exceptionally rapid during deposition of the Sheet Sandstone Facies. Furthermore, it may be demonstrated that basin subsidence rate was decelerating during Petilla Member times. It is a contention in this thesis that an additional supplier of fines is most appropriate to account for the large proportion of overbank sediments in the Sheet Sandstone Facies.

The planar tabular cross-stratification that commonly overlies an erosional channel base and gravel lag in the Sheet Sandstone Facies is interpeted as a product of migrating transverse bars of up to 70 cm amplitude (cf. Levey 1978, fig. 6). The presence of some reactivation surfaces in these planar tabular cross beds suggests bar emergence and reworking at low flow stage (cf. Levey 1978, fig. 10; Plint 1983). Trough cross-stratification, comprising the middle and upper parts of Sheet Sandstone Facies coarse members, represents in-channel migration of sinuous crested dunes (cf. Cant & Walker 1978, fig. 14).

Perhaps the scarcity of lateral accretion surfaces, reflecting sedimentation by lateral accretion of point bars (Allen 1963) is surprising in a 1600m measured section through a meandering fluvial facies, even considering the limits of exposure in a vertical succession. However, the abundance of planar tabular and trough cross-stratification, and the presence of symmetrical sandstone- and siltstone-filled scours or 'chutes', provides evidence that Sheet Sandstone Facies point bars were complex units that have some affinities with the coarse-grained point bar model of McGowen & Garner (1970). In such a depositional system, lateral accretion surfaces commonly comprise only the upper third or quarter of the vertical extent of a point bar sequence (McGowen & Garner 1970; Nijman & Puigdefabregas 1978). Bluck (1971) has questioned whether meander migration can be so slow, relative to vertical aggradation

rate, to preserve complete point bar sequences. If not, then that part of a point bar most susceptible to erosion, and hence non-preservation, is the upper part containing lateral accretion surfaces.

Multistorey sand bodies, such as those in the Rio Arba section (eg. Plate 4.1c), are interpreted as products of rapid downstream meander migration (cf. Bluck 1971) coupled with a moderate subsidence rate. This combination generates stacked lower and middle point bar sequences, separated by erosion surfaces, whose upper accretionary bank deposits (lateral accretion surfaces) are eroded by a migrating meander loop. The lack of muddy channel fills and predominance of sandstone throughout Sheet Sandstone Facies coarse members suggests that chute cutoff was common, and hence, neck cutoff was not a significant process (Fisk 1947). McGowen & Garner (1970) suggested that the generation of chutes on the upper point bar is indicative of seasonal fluctuations in flow, with chute bars forming at times of high flow stage. The importance of chute cutoff as an abandonment mechanism in Sheet Sandstone Facies channels suggests it is a product of deposition in a seasonally fluctuating, perennial flow regime.

Lastly, it is pertinent to discuss how sandstone bodies of a few kilometres width were produced by meanderbelts only half a kilometre wide. It has been established that the Sheet Sandstone Facies was deposited on an areally extensive floodplain over which channels were relatively free to migrate, both gradually and avulsively. However, Collinson (1978) has shown that it is often necessary to invoke an external, or allocyclic, influence if there is a large discrepancy (positive or negative) between meanderbelt width (as derived from equations discussed in Section 4.2.4) and sand body width. With the Sheet Sandstone Facies, there are two other factors to consider that hint at the influence of an external process: (1) preferential preservation of structures that indicate a northward palaeocurrent direction in the Rio Arba and Petilla sections (see Fig. 4.4); and (2) development of the embryonic Pena flexure duplex, immediately to the north of the Sheet Sandstone Facies, during Petilla Member times (see Chapter 2).

The preservation potential of the deposits of high-sinuosity fluvial systems may be studied from the following two aspects.

(1) Variations in the type of bedforms that develop according to their position within a meander bend. For example, Jackson (1976) concluded that the necessary reversal in the sense of helical flow between adjacent meander bends causes the classic upward fining profile, typical of high sinuosity fluvial deposits, to develop only at the downstream end of meander bends in the Wabash River, Illinois.

(2) Preferential **preservation** of restricted meander loops according to their position with respect to the direction and rate of meander migrration. For example, Leeder & Alexander (1987) demonstrated that tectonic tilting of the depositional surface, at a high angle to the flow direction of the Madison and South Fork Rivers, Montana, caused the development of asymmetrical meanderbelts. These may be recognised by the preferred dip of successive lateral accretion units in meander loops.

From the sedimentological analysis presented here, it is difficult to see why there should have been any long term preferential preservation of certain bedforms in restricted parts of Sheet Sandstone Facies meander bends. However, could the northward bias in palaeocurrents (Fig. 4.4) reflect a southward tilt imposed on the fluvial system by the growing monoclinal form of the Pena flexure? A possible **response** of Sheet Sandstone Facies meanderbelts to this southward or forelandward dipping slope may have been enhanced lateral migration and avulsion of the entire axial system toward the south, with abandonment and preferential preservation of meander loops on the north, or upslope side of the fluvial system. Such an interpretation may help to explain how fluvial sandstone bodies with a mean thickness of 3.3m can attain widths of up to 6000m.

To summarise, the Sheet Sandstone Facies as exposed in the Rio Arba valley and at Petilla records sedimentation from a highly sinuous (~2.3), mixed load fluvial system that flowed axially westward, toward a sandy, shallow lake. Areally extensive channel sandstones were generated by vertical aggradation and tectonically enhanced lateral migration of mature meanderbelts with widths of up to 200m. Stable, long lived channels were characterised by low avulsion frequencies and rapid meander migration. A rough guide to the floodbasin fines **aggradation** rate may be gained by comparing the stage of palaeosol development reached in the fines sequence with the palaeosol maturity/sedimentation rate curves provided by Leeder (1975, fig. 2). This indicates that the coarse nodules collected from the overbank sequence are typical of an aggradation rate of less than 0.5 mm yr^{-1}.

The greater proportion of overbank fines in the Petilla section suggests an increased dominance of suspended load downstream and/or an increased rate of basin subsidence downstream. Significantly, the proportion of the section occupied by channel sand bodies systematically increases upward through the succession at Petilla, from 20 to 31%. This reflects decelerating basin subsidence as the deformational climax of the underlying Pena flexure duplex was approached. However, an opposite trend is observed in the more 'upstream'

section in the Rio Arba valley, where the percentage of channel sandstone decreases upward from 42 to 34%. The accelerating basin subsidence rate that this inference implies is compatible with a westward propagating thrust front (see Chapter 2). Such an axially migrating thrust system could account for along-strike variation in the timing of subsidence and uplift.

In terms of channel dimension, morphology and sequence development, a modern analogue for the meandering stream environment of the Sheet Sandstone Facies is provided by Cedar Creek, Nebraska (Jackson 1978). However, in terms of sediment load characteristics, the Cedar Creek analogue differs in important respects due to its unique aeolian sand source. A similar lithofacies to the Sheet Sandstone Facies has been described from the Eocene rock record of the eastern Graus basin (Fig. 1.1) by van der Meulen (1982, 1986). He interprets these sheet sand bodies as being of sheetflood dominated fluvial origin.

4.3 BASIN CONFIGURATION

The strike-parallel section (Fig. 4.8) and proposed palaeoenvironmental map (Fig. 4.9) for end Petilla Member times illustrate that continued thrust front advance during Petilla Member deposition achieved uplift across the eastern and central parts of the study area. Consequently, this enlarging region of thrusted and elevated upland provided a large sediment source that generated a greater clastic influx than Ruesta Member times. As a result of increased sediment availability and the relatively steep depositional slopes imposed on the basin, the widespread lacustrine environments that characterised Ruesta Member deposition gave way to alluvial systems. Ruesta Member lake margins thus shrank until only the southwest corner of the study area was occupied by a lake at the end of Petilla Member times.

In the West Jaca basin, two independent alluvial systems dominated Petilla Member deposition. In the northwest part of the study area, a laterally (forelandward) draining alluvial fan - ephemeral streamflood plain - fluvial channel system flowed for up to 25 km to the south-southwest, before terminating at the northern margin of the shallow sandy lake. An axially, or west-northwestward flowing mature meanderbelt system occupied the southeast part of the study area and drained a tectonically active hinterland situated approximately 100 km to the east of the West Jaca basin.

The presence of the laterally draining system is a feature to be anticipated in a thrust-top basin (Ori & Friend 1984) in which deposition occurs 'behind' or hinterlandward of an active thrust front. Axially flowing systems seem to typify those more distal parts of foreland basins where significant

forelandward dipping depositional slopes are not important. In the West Jaca basin, prior to the onset of local crustal loading by thrust emergence at the depositional surface, the dominant depositional slope was controlled by along-strike variations in the timing of uplift and subsidence. For example, in Chapter 2 it was shown that the Southwest Pyrenean **foreland** basin was characterised by an axially propagating thrust front during the Oligo-Miocene, with deformation spreading from the east toward the west. Such diachronous deformation laterally juxtaposed uplifting sediment sources and subsiding basins and, in the West Jaca basin, explains the existence of a major, axially draining, synorogenic depositional system.

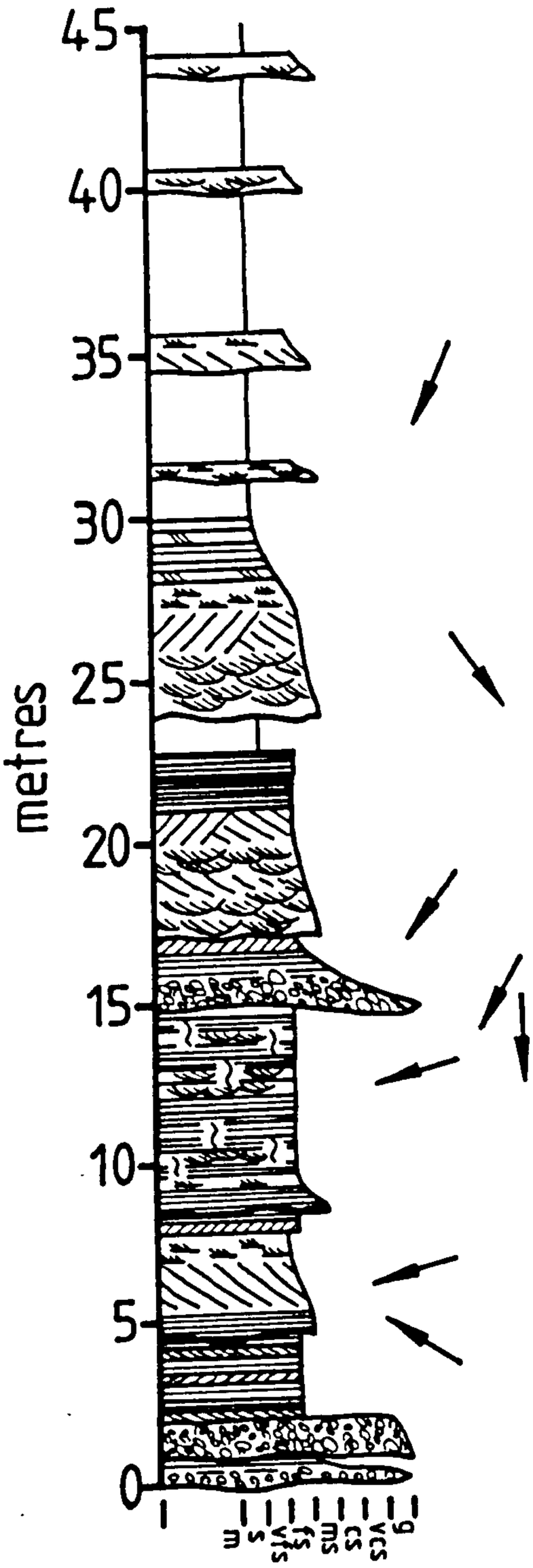

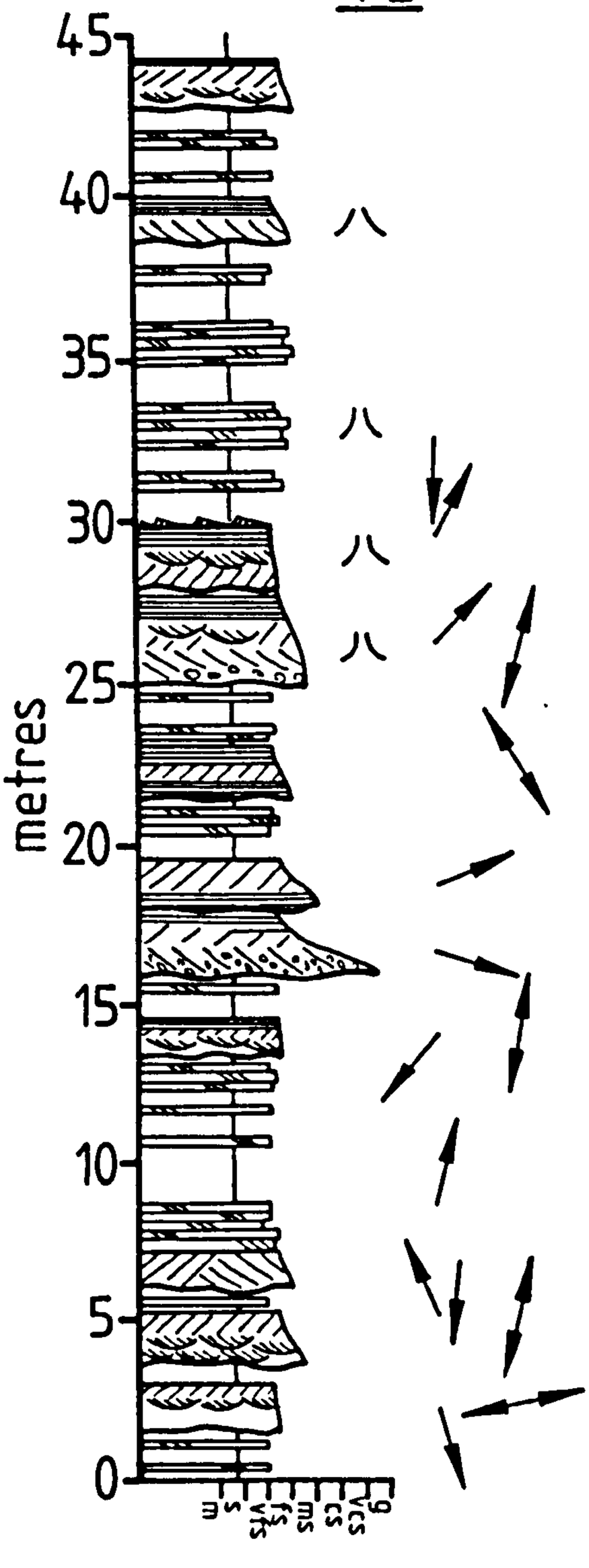

Fig. 4.1. Petilla Member Gravelly Sandstone Facies 1000m south of Alzorriz, Izaga sub-basin: graphic log.

Fig. 4.2. Petilla Member Gravelly Sandstone Facies at Alzorriz, Izaga sub-basin: graphic log.

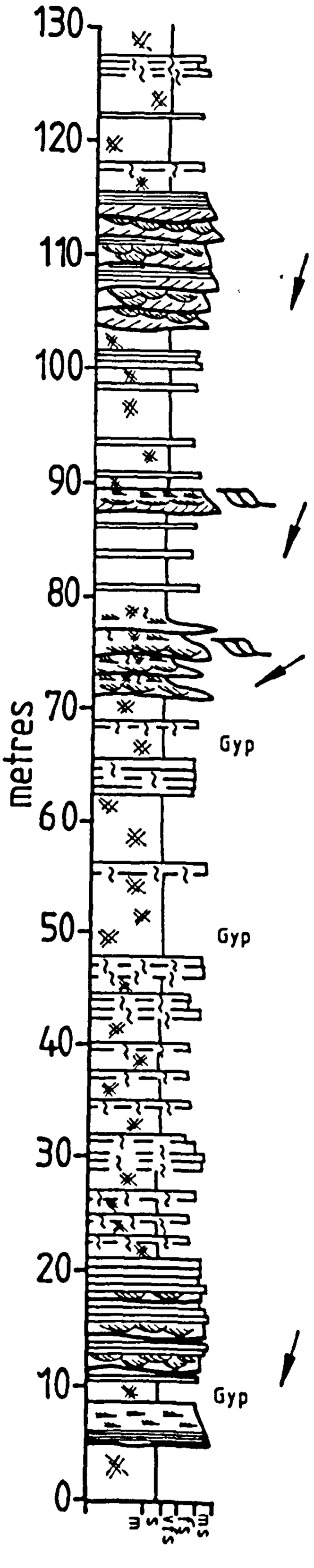

Fig. 4.3. Petilla Member Mottled Siltstone with Sandstone Facies at Aibar: graphic log.

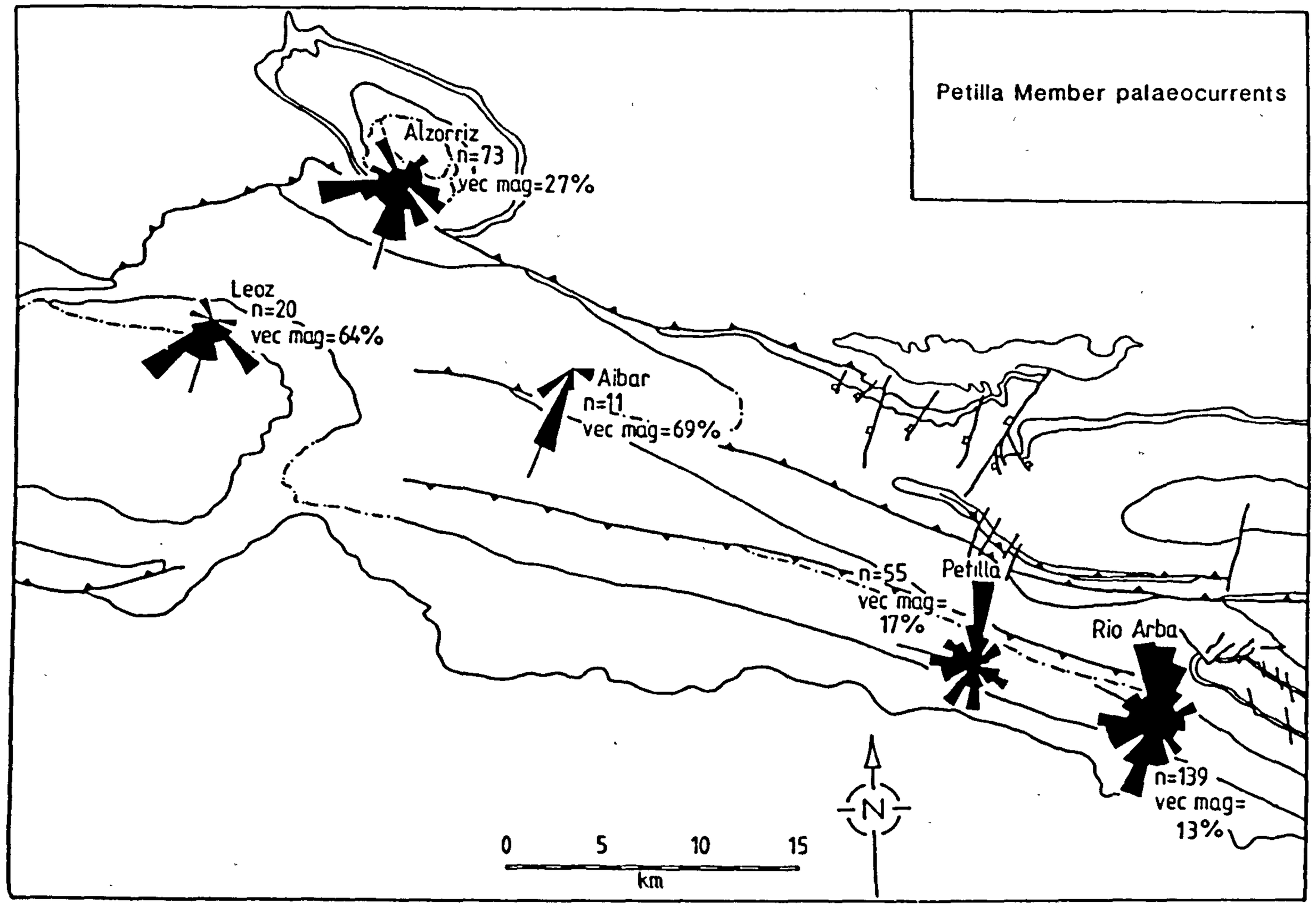

Fig. 4.4. Palaeocurrent rose diagrams depicting Petilla Member dispersion directions in the study area. Structural symbols and lithostratigraphic contacts as in Fig. 1.3.

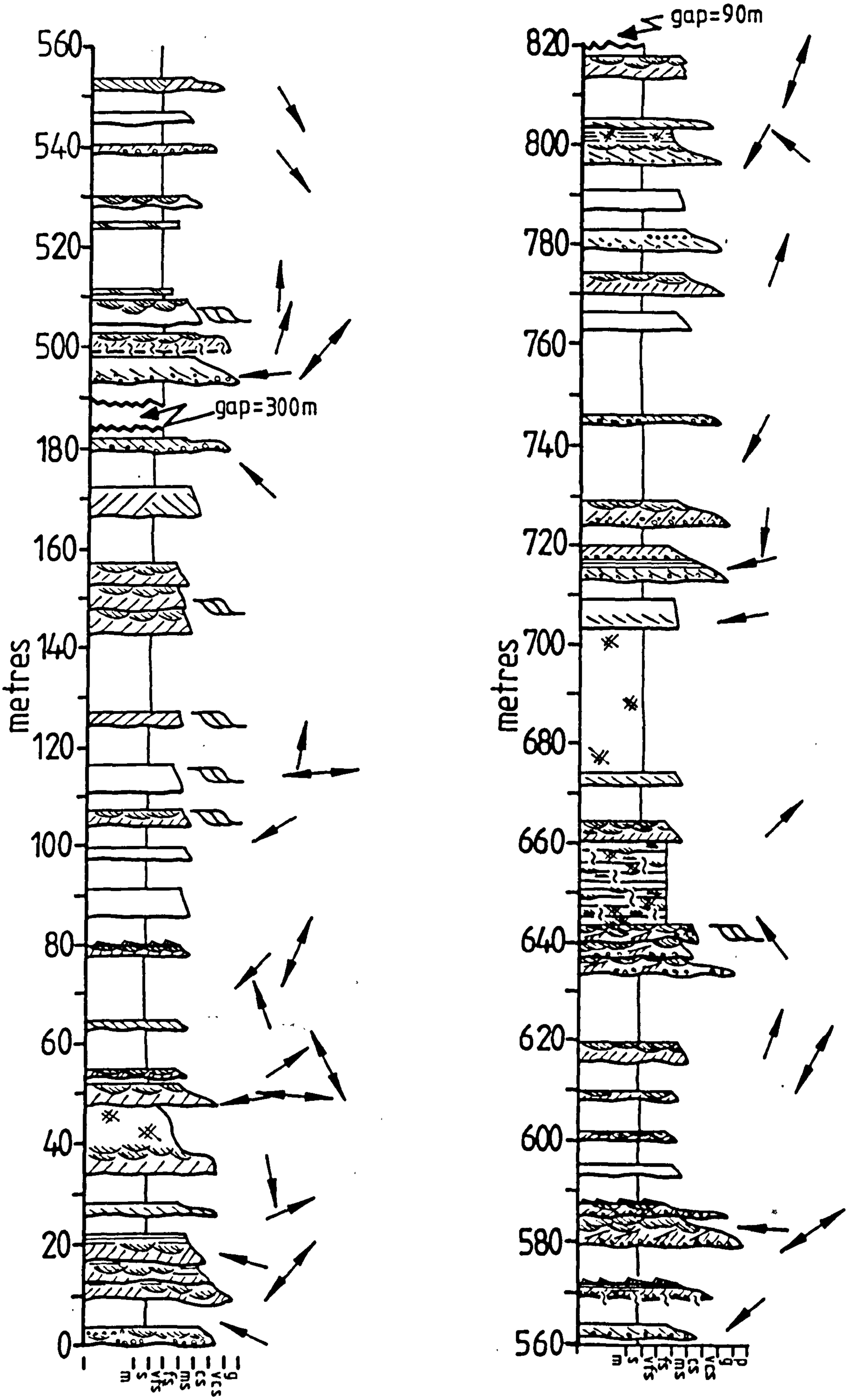

Fig. 4.5a. Petilla Member Sheet Sandstone Facies in the Rio Arba valley: graphic log.

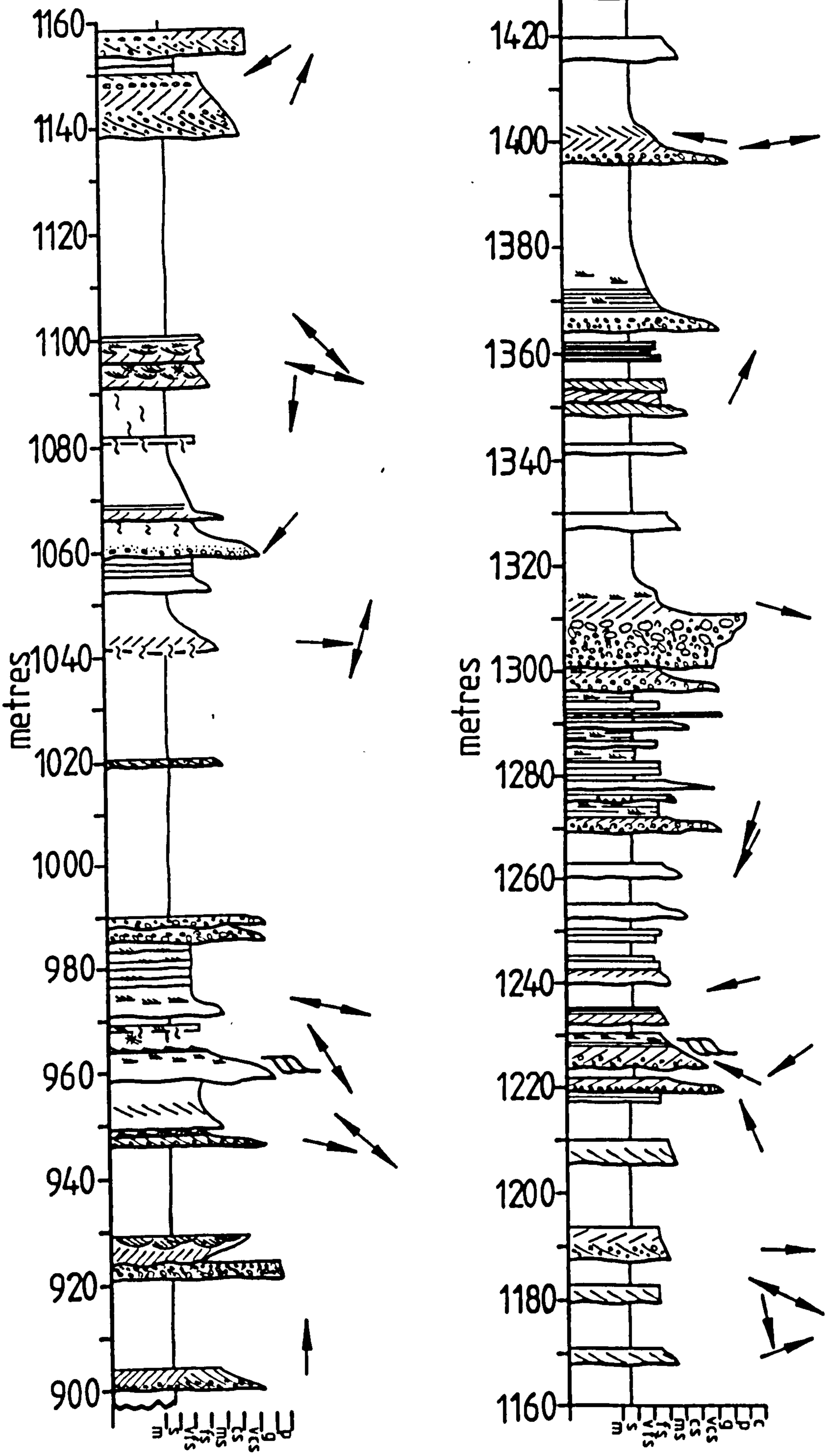

Fig. 4.5b. Petilla Member Sheet Sandstone Facies in the Rio Arba valley: graphic log.

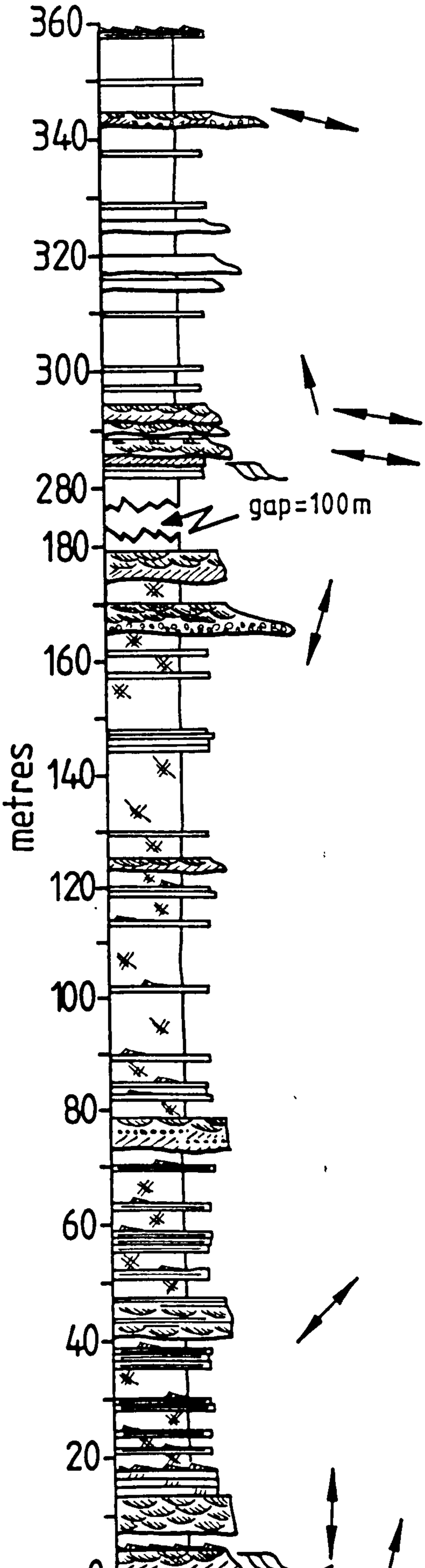

Fig. 4.6a. Petilla Member Sheet Sandstone Facies at Petilla: graphic log.

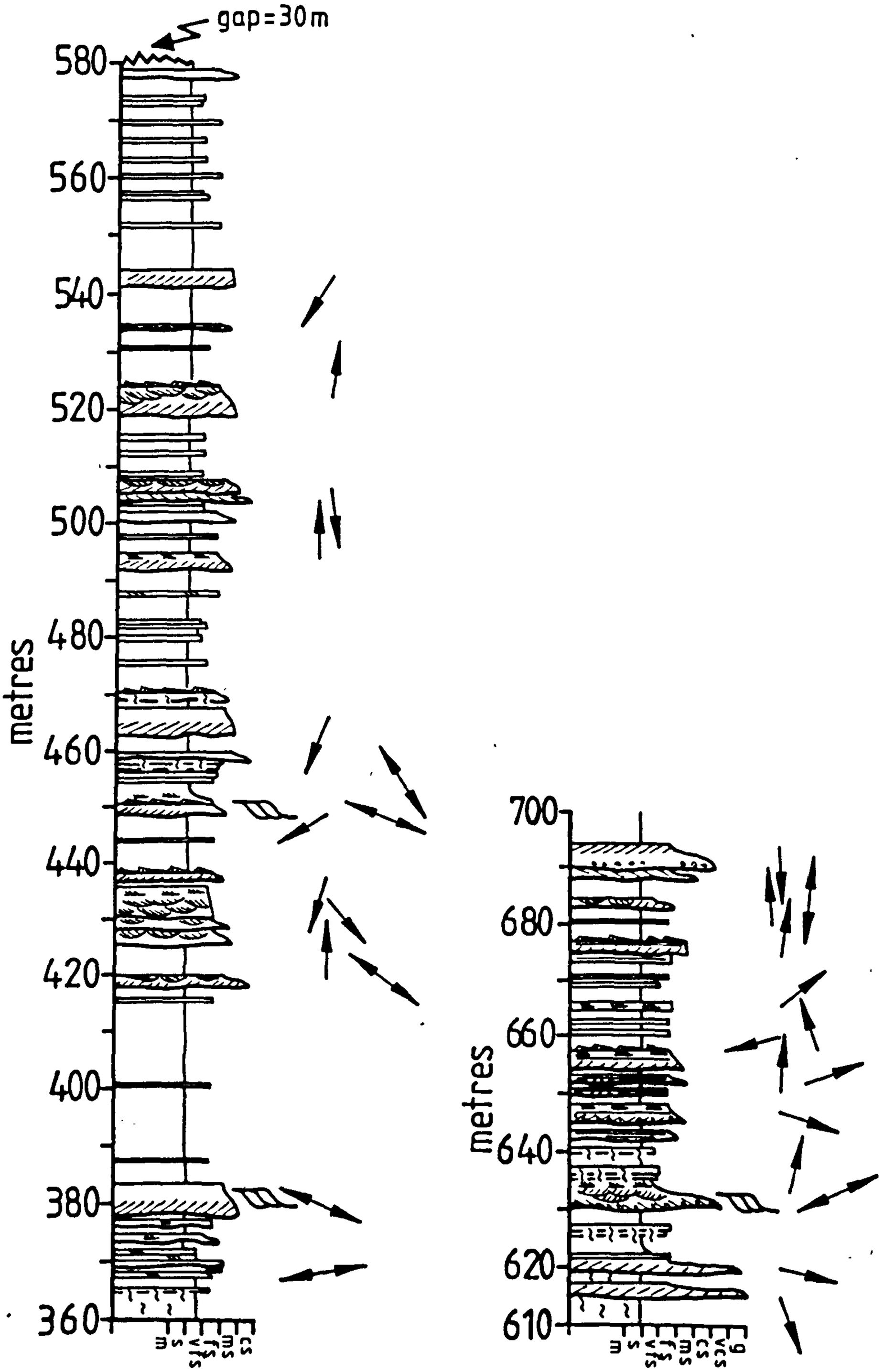

Fig. 4.6b. Petilla Member Sheet Sandstone Facies at Petilla: graphic log.

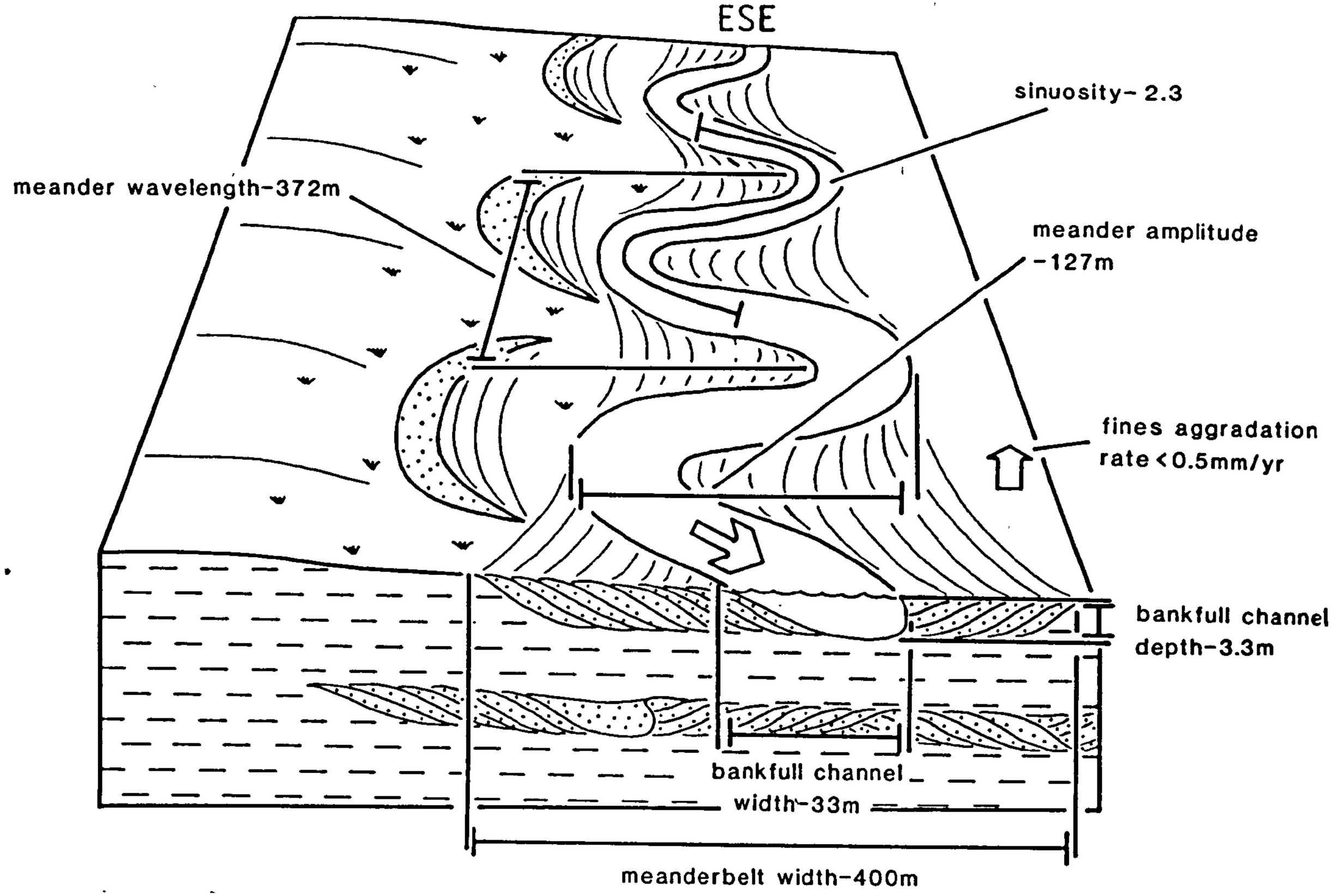

Fig. 4.7. Reconstruction of the palaeomorphologic parameters of the Sheet Sandstone Facies. Based on an idea for a diagram by Gardner (1985, fig. 9). Compare with the Ribbon Sandstone Facies palaeomorphology shown in Fig. 6.20.

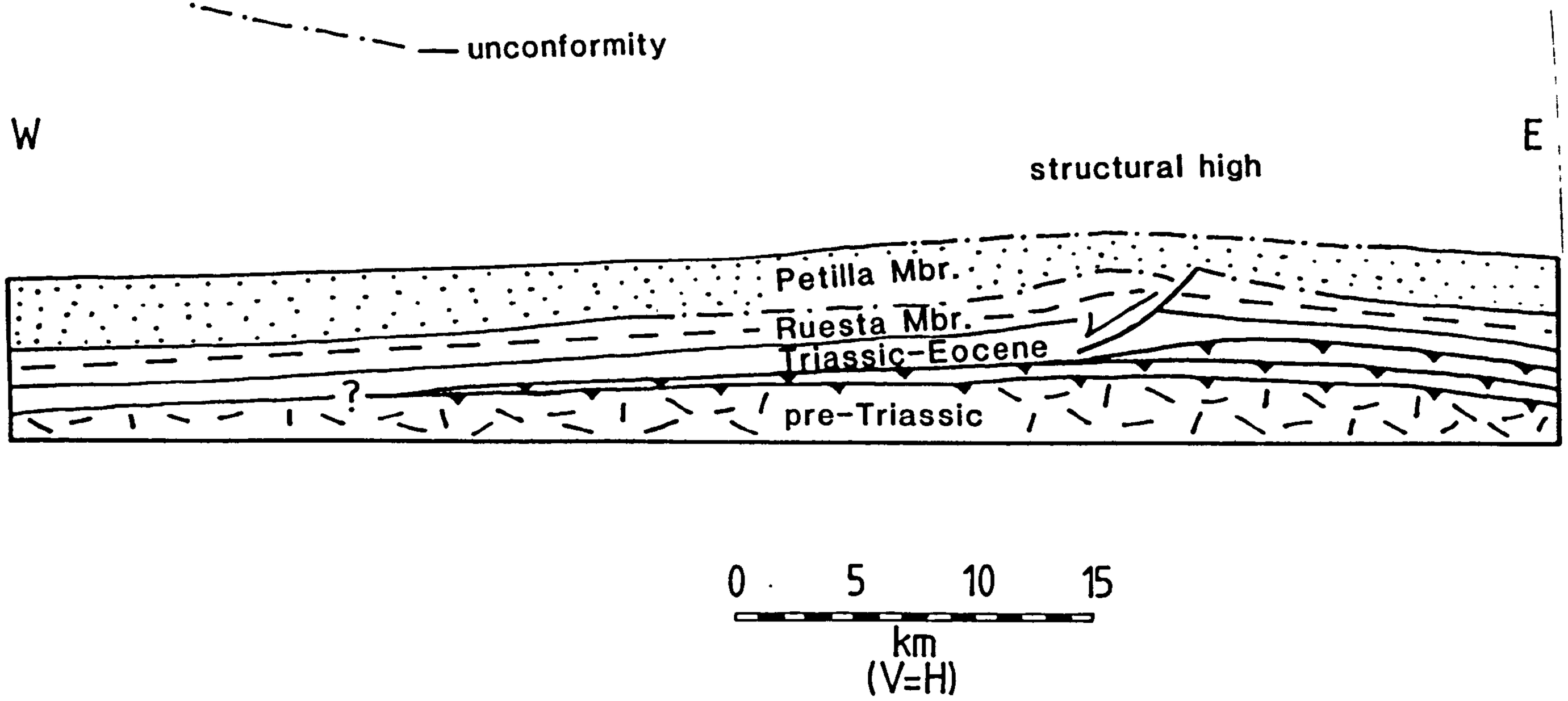

Fig. 4.8. Strike-parallel section through the study area along the line of section 2.6 shown in Fig. 2.1. The section depicts the shape in profile of the basin at the end of Petilla Member deposition.

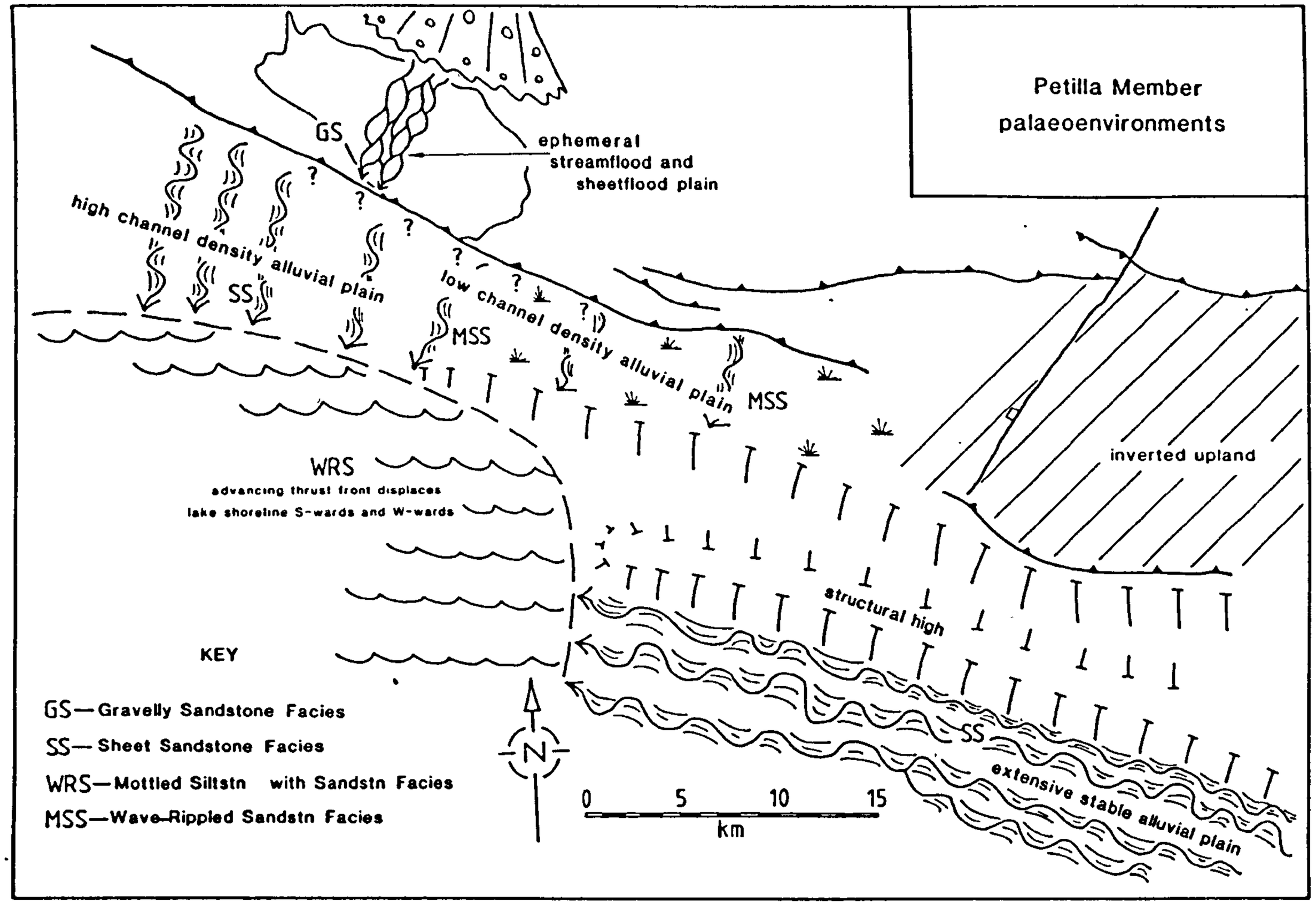

Fig. 4.9. Schematic palaeoenvironmental reconstruction of the study area during deposition of the Petilla Member.

Plate 4.1a. Gravelly Sandstone Facies at Alzorriz showing the sheet-like form of sand bodies.

Plate 4.1b. Composite sand volcano on the upper surface of a Gravelly Sandstone Facies sandstone at Alzorriz.

Plate 4.1c. Seven metre thick, four storey fluvial sand body in the Sheet Sandstone Facies of the Rio Arba valley. The base of the vertical sandstone is on the right.

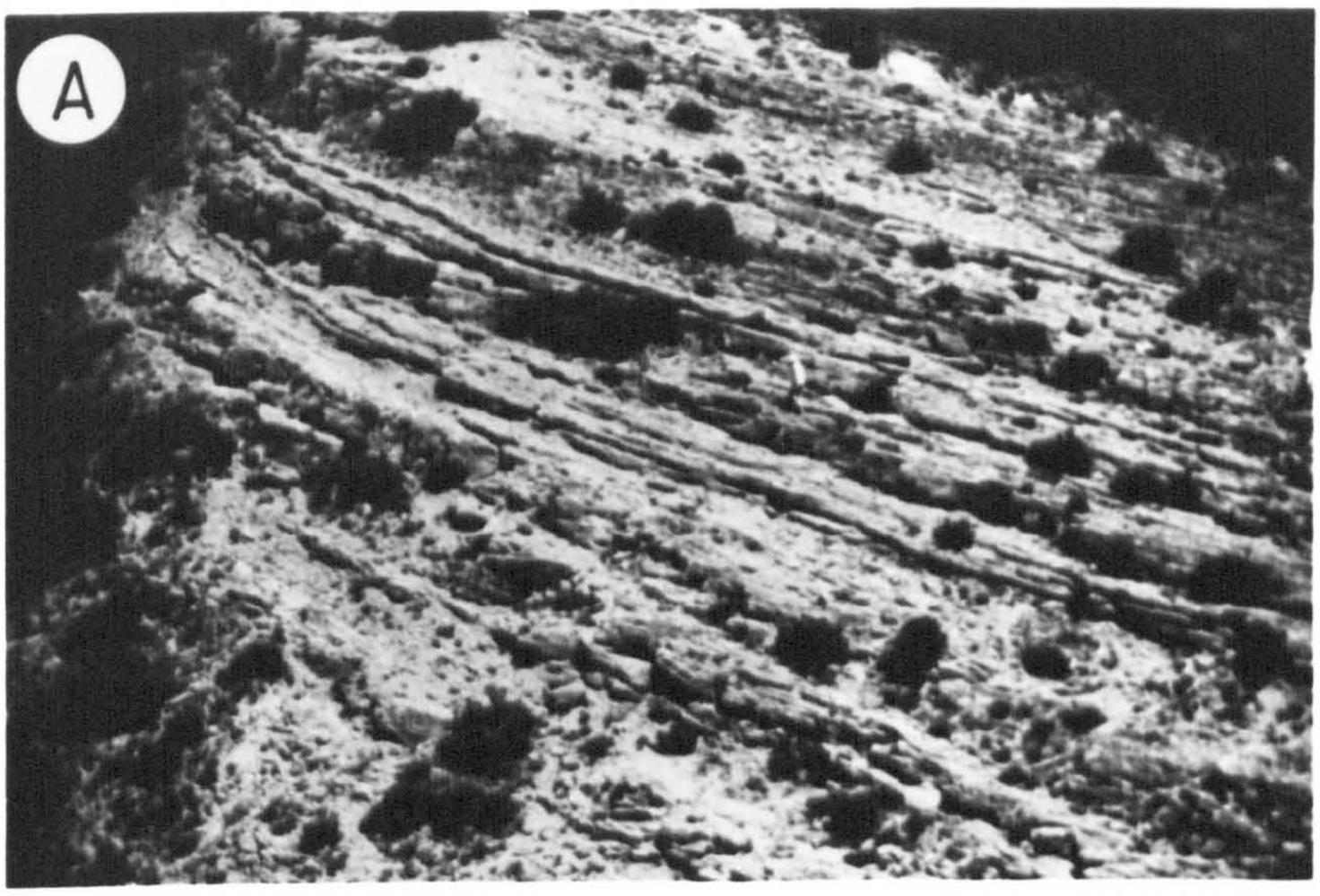
A


B

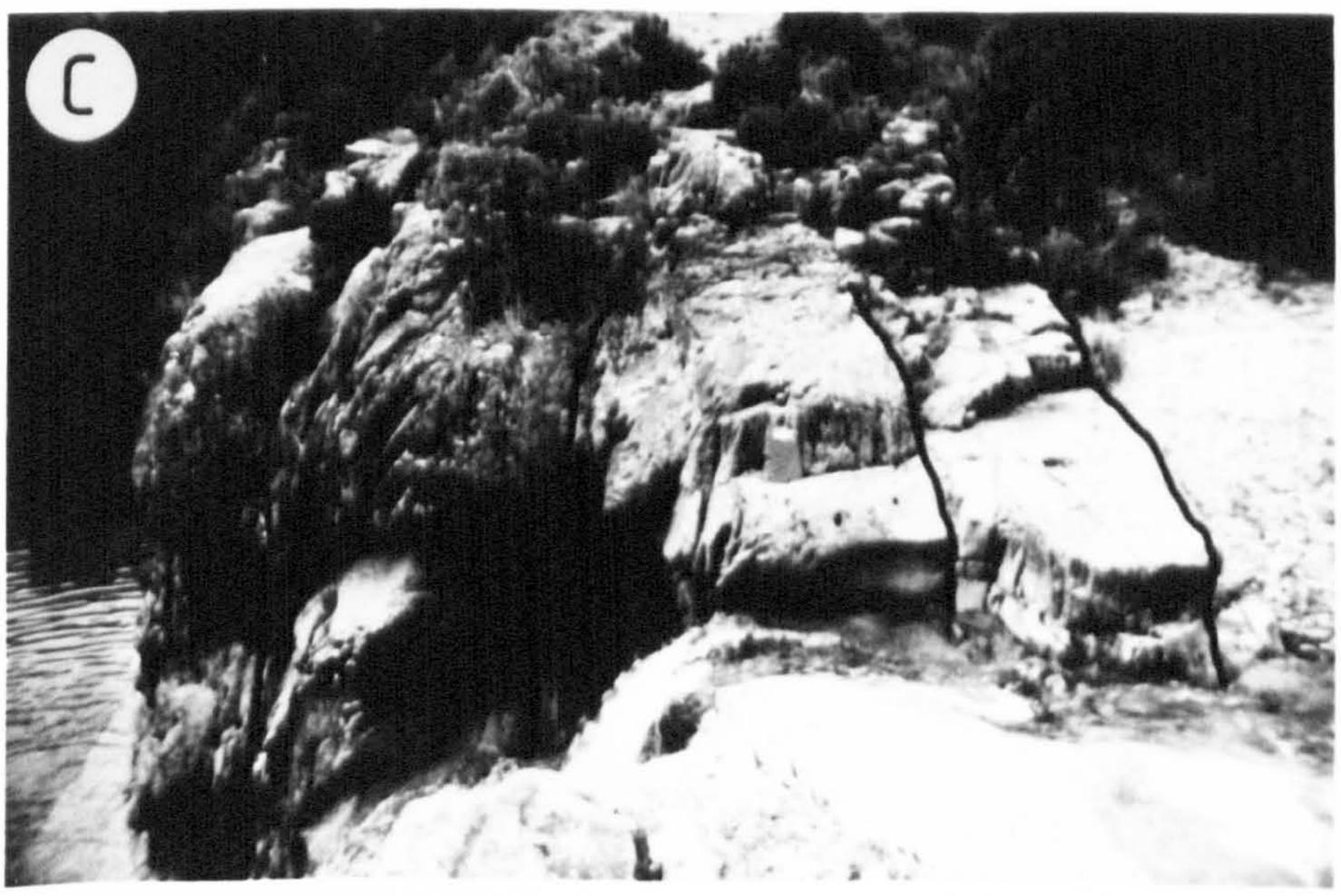
C

Plate 4.2 Photomosaic of the Sheet Sandstone Facies at Petilla. Note the lateral extent of the vertical sandstone bodies.

CHAPTER 5

BASIN EVOLUTION DURING DEPOSITION OF THE BERNUES FORMATION

The Chattian to Aquitanian (Puigdefabregas 1975) Bernues Formation comprises up to 2300m of conglomerate and sandstone that are well exposed along the southern flank of the Pena flexure and in the Olleta and Izaga sub-basins. Despite the subtle upward coarsening trend noted in the Petilla Member Sheet Sandstone Facies (Chapter 4), the appearance of the first thick-bedded conglomerate of the Bernues Formation is comparatively sudden and marks the base of the formation. Along the length of the Pena flexure, this lithofacies transition may be considered a convenient geologic divide between the West Jaca thrust top basin to the north, and the Ebro basin.

The generally coarse grain size of the sediments within the formation attests to their deposition during a climactic episode of tectonic activity. The onset of Bernues Formation deposition signified additional development of the Pena flexure duplex with, most importantly, emergence of the Pena flexure backthrust at the depositional surface. By analysing facies characteristics, palaeocurrents and the provenance of the Bernues Formation, particularly its conglomerates, this chapter shall record the evolution of the study area during its tectonic climax at the end of the Oligocene.

5.1 GENERAL DESCRIPTION OF ALLUVIAL FAN AND FLUVIAL FACIES

5.1.1 Pena flexure

The six most accessible outcrops of the Bernues Formation along the Pena flexure are located at, from east to west, the Rio Arba valley, the Sos-Uncastillo road, Sos, Pena, Caseda and Gallipienzo. Six main facies are recognised in the above successions, termed Massive Conglomerate Facies, Conglomerate with Sandstone Facies, Gravelly Sandstone Facies, Current-Rippled Sandstone Facies, Mottled Siltstone with Sandstone Facies and the Sheet Sandstone Facies.

Near the Sierra de Santo Domingo in the valley of the Rio Arba, the formation comprises 630m of rapidly upward coarsening, clast-supported conglomerate. They are stacked in crudely stratified, erosively based wedges up to nine metres thick and are illustrated schematically in the facies log of Fig. 5.1. The lower 130m of the measured section displays typical features of the Conglomerate with Sandstone Facies and comprises the basal part of the formation in the Rio Arba. In this facies, beds of well imbricated, inversely-graded conglomerate are separated by finer-grained intervals that constitute

approximately 25% of the sequence. The inter-conglomerate, fine-grained suite is composed of thin-bedded, planar based, fine-grained sandstone and unmottled, massive siltstone. Occasional lenticular bodies of trough and planar cross-stratified, medium-grained sandstone are preserved within, and between, conglomerate beds.

The upper 120m of the Rio Arba facies log (Fig. 5.1) exhibits features typical of the Massive Conglomerate Facies. In these sequences, sandstone is volumetrically negligible and the succession is dominated by stacked sheets of well imbricated, clast-supported conglomerate with erosive bases (erosive reliefs between 15 and 80 cm). The conglomerate sheets have an average thickness of two metres and, occasionally, thin-bedded, cross-stratified sandstone is preserved beneath the erosive base of a conglomerate body. The bulk of the Bernues Formation in the Rio Arba valley comprises Massive Conglomerate Facies.

The peripheral fringes of the Rio Arba conglomerates are characterised by restricted exposures of Conglomerate with Sandstone Facies in which sheet-like, planar based beds of gravel interfinger with upper plane-bed and current ripple laminated, fine-grained sandstone. In two examples (eg. at 182m in the facies log of Fig. 5.1), unsorted, matrix-supported beds of pebble- to large boulder-grade (clast diameters up to 90 cm; see Plate 5.1b) conglomerate have been recognised. These planar, non erosively based beds of unsorted conglomerate are up to 180 cm thick and mainly comprise clasts of Campodarbe Formation molasse sandstone.

The conglomerate dominated Bernues Formation succession to the southwest of Petilla, that forms a watershed on the road between Sos and Uncastillo, also comprises Massive Conglomerate Facies. Here, conglomerate forms thick, erosively based beds of massive, upward coarsening and upward fining, gravel- to boulder-grade material. Sandstone and finer-grained intervals in the Sos-Uncastillo outcrop constitute roughly 20% of the 30m thick succession.

Figure 5.2 is a measured section through the conglomeratic succession at the abandoned Navarrese guard settlement of Pena. In terms of the ratio of conglomerate to finer-grained sediment, the sequence at Pena is transitional between the Massive Conglomerate Facies, typified by the bulk of the Rio Arba succession, and the Conglomerate with Sandstone Facies that comprises the basal part of the Rio Arba sequence. The conglomerate at Pena occurs as multistorey bodies of amalgamated conglomerate sheets, each one bounded by an erosive base displaying between 10 and 90 cm of erosive relief. These multistorey conglomerate bodies are up to twelve metres thick and are separated by

sandstone intervals that comprise 25% of the Pena sequence. Inter-conglomerate sandstone comprises thin-bedded, planar based, tabular sheets of burrowed, fine-grained sandstone up to 35 cm thick, with local concordantly-filled scours (cf. Singh 1972, figs. 2 and 3) and occasional thin, gravelly horizons. These tabular sheets are dominated by upper plane-bed lamination and current-rippled upper parts. The local scours, up to 350 cm wide and 60 cm deep, truncate underlying sandstone and are filled by medium-bedded (up to 40 cm thick) trough and planar cross-stratified, medium-grained sandstone with occasional reactivation surfaces. A profile through typical inter-conglomerate, fine-grained sandstone at Pena is illustrated in Fig. 5.3.

The four facies logs of Fig. 5.4 present a measured 435m thick section through the Bernues Formation exposed at Gallipienzo. A classic upward coarsening sequence is evident. The lower 80m, and 200-320m intervals of the succession comprise Current-Rippled Sandstone Facies and are characterised by single storey, erosively based, channelised bodies of medium-grained sandstone separated by thick packages of stacked, tabular, fine-grained sandstone beds and subordinate siltstone. The erosively based sand bodies have moderate to high erosive reliefs of between 20 and 200 cm, and in seven examples, their internal structure is dominated by lateral accretion surfaces. The lateral accretion surfaces are well-defined by thin-bedded, fine-grained sandstone and they are commonly truncated by overlying thin-bedded, planar-based, fine-grained sandstone. The sand bodies are between one and four metres thick and have width to depth ratios greater than fifteen. Internally, they commonly display a subtle upward fining from planar tabular cross-stratified, medium-grained sandstone to current ripple laminated, fine-grained sandstone. Packages of planar based, fine-grained sandstone that occur between the erosively based sand bodies are pervasively burrowed and dominated by upper plane-bed and current ripple lamination with occasional wave-rippled upper surfaces. Subordinate, pale brown siltstone intervals in the Current-Rippled Sandstone Facies are generally massive and unmottled.

The 85-200m interval of the Gallipienzo sequence is occupied by sediments that exhibit features typical of the Mottled Siltstone with Sandstone Facies, previously described here from the Campodarbe Formation in Chapters 3 and 4. At Gallipienzo, the facies is dominated by massive siltstone with subordinate, planar based, fine-grained sandstone beds and occasional erosively based, medium to fine-grained sandstone units up to one metre thick. As in the Aibar sequence described in Chapter 4, the Mottled Siltstone with Sandstone Facies at Gallipienzo contains common gypsum veins parallel to bedding and up to six

centimetres thick. However, it differs by showing little or no sign of colour mottling or even the most incipient palaeosol development.

The upper 140m of the Gallipienzo sequence is characteristic of the Conglomerate with Sandstone Facies. Conglomerate constitutes 26% of the facies and forms single and multistorey, wedge shaped beds of inversely graded conglomerate bodies defined by erosive bases. Conglomerate bases vary from being abrupt, erosive surfaces with up to two metres of relief, to gravel lined, low relief erosive bases that interfinger intricately with the fine-grained sandstone into which they scour. Bedding surfaces within conglomerate bodies generally display a crudely to well developed clast imbrication. Thick, multistorey conglomerates, such as those at 395m and 420m in Fig. 5.4, exhibit well defined, internal erosion surfaces that bound individual storeys. Each storey is inversely graded and occasionally contains planar tabular cross-stratified gravel in the thickest parts of a conglomerate storey.

The volumetrically dominant, finer-grained intervals of the Conglomerate with Sandstone Facies at Gallipienzo display many of the typical characteristics of the Current-Rippled Sandstone Facies. Like at Pena, they are dominated by fine-grained sandstone that forms planar based, laterally persistent, tabular units between 5 and 40 cm thick. The tabular, fine-grained sandstone is intensely burrowed and contains common pink and white mottling of rootlets. Internally, the thin beds are constructed from upper plane-bed to current ripple laminated sandstone. However, local scours erode up to 90 cm into underlying fine-grained sandstone beds and are discordantly- and concordantly-filled by thicker-bedded, fine-grained sadnstone with planar cross-lamination and occasional lateral accretion surfaces. Exquisite exposure conditions beneath the shelter of some of the larger conglomerate bodies enables the detailed morphology of cosets of planar tabular cross-stratification and climbing ripple lamination to be observed. Complex second and third order (Allen 1983) erosion surfaces define bundles of colour mottled, fine-grained sandstone with abundant internal reactivation surfaces.

Two kilometres to the south of Gallipienzo, a small cliff beside the Rio Aragon exposes Bernues Formation Conglomerate with Sandstone Facies. Massive conglomerate comprises 22% of the sequence in which it forms single storey, sheet-like units up to 260 cm thick, with crudely defined inverse grading and low relief erosive bases that, in parts, interfinger with sandstone. The conglomerate bodies are separated by thin-bedded, planar based, fine-grained sandstone with upper plane-bed and current ripple lamination. Abundant local scours are filled with thicker-bedded fine- to medium-grained sandstone that displays planar cross-stratification and reactivation surfaces.

The Bernues Formation as exposed along the southern flank of the Pena flexure is thus dominated by conglomerate-sandstone sequences. However, at two localities, sandstone-siltstone sequences that characterise the finer-grained 'gaps' between the coarser conglomeratic sequences were measured. A 295m thick facies log through rocks exposed along the road south of Sos is presented in Fig. 5.5. The bulk of the succession has characteristics transitional between the Current-Rippled Sandstone Facies and Mottled Siltstone with Sandstone Facies. The lower 200m is characterised by increasingly thinner packages (ranging from one to sixteen metres thick) of stacked, planar based, fine-grained sandstone, tabular units with burrowed bases, upper plane-bed to current ripple lamination, and occasional thicker, trough cross-stratified units with wave-rippled upper surfaces. Local scours within the fine-grained sandstone packages are up to 250 cm wide and 50 cm deep, and are commonly filled by concordantly draped, thicker-bedded, fine-grained sandstone with planar tabular cross-stratification and rare reactivation surfaces. Finer-grained intervals of mottled siltstone with rootlets separate the fine-grained sandstone packages.

Above the 20m thick exposure gap at 210m, the remaining 70m of the sequence displays features typical of the Gravelly Sandstone Facies described from the Izaga sub-basin in Chapter 4. The sequence contains several erosively based, upward fining, single and multistorey sandstone bodies. They are up to 300 cm thick, with width to depth ratios greater than twenty, and are constructed from internally scoured, planar and trough cross-stratified gravel to medium-grained sandstone. Beneath the sand bodies' erosive bases (with reliefs of up to 120 cm) small, isolated (ie. unstratified) calcrete nodules, up to 3 cm diameter, are common. The erosively-based sandstones are separated by packages of thin-bedded, internally-scoured, fine-grained sandstone up to ten metres thick, with wave-rippled upper surfaces, and subordinate colour mottled siltstone intervals.

A unique feature of the Gravelly Sandstone Facies to the south of Sos is a large, sandstone-filled, ribbon-type (Friend *et al.* 1979) palaeochannel, approximately 15m wide and 3-4m deep, that occurs at 252m in Fig. 5.5 (also see Plate 5.1a). This sand body has a high relief erosive base of up to three metres, well defined, laterally thinning wings (Friend *et al.* 1979), and is filled with thin-bedded, tabular, fine-grained sandstone beds up to 20 cm thick. The fill ranges from thicker-bedded, trough cross-stratified, coarse-grained sandstone at the base to upper plane-bed and current ripple laminated, fine-grained sandstone toward the top of the sand body. Pink and grey colour mottled rootlets and burrows are abundant throughout the fill.

A second measured section through finer-grained sediments deposited between major conglomeratic sequences of the Pena flexure Bernues Formation is presented from south of Caseda in Fig. 5.6. This 240m thick sequence is dominated by Mottled Siltstone with Sandstone Facies, with an interval of Gravelly Sandstone Facies between 100 and 130m. The former facies is characterised by upward thinning packages of thin-bedded, planar based, tabular, fine-grained sandstone with undulating, wave-rippled upper surfaces and concordantly-draped local scours. The basal units of these fine-grained sandstone packages commonly comprise a thicker (up to one metre), low relief, erosively based sequence of planar cross-stratified medium- to fine-grained sandstone that grades into 10cm thick fine-grained sandstone sheets which display upper plane-bed to current ripple lamination.

The 30m thick sequence of Gravelly Sandstone Facies in the central part of the Caseda facies log (Fig. 5.6) is dominated by single and multistorey, erosively-based units of gravel to planar cross-stratified very coarse-grained sandstone. These gravel bodies are separated by current ripple laminated, fine-grained sandstone tabular beds with local scours. Like the sandstone-siltstone sequence to the south of Sos, the sequence south of Caseda contains pervasively colour mottled siltstone intervals.

5.1.2 Olleta sub-basin

The most completely exposed section through the Bernues Formation of the Olleta sub-basin is located along the road south of Olleta, on the southern limb of the Olleta syncline. An 85m thick measured section (Fig. 5.7) displays characteristic features of the Current-Rippled Sandstone Facies. The sequence is dominated by sandstone that occurs as erosively-based (variable relief of between 10 and 100 cm), upward fining units up to 270 cm thick, and, as packages of stacked, tabular, fine-grained sandstone beds with upper plane-bed to current ripple lamination. The single storey, erosively based sand bodies have width to depth ratios of between five and thirty, and are filled with planar tabular and trough cross-stratified gravel to medium-grained sandstone, with small internal scours. In a single example, lateral accretion surfaces, displaying abundant internal reactivation surfaces, form the margin of a 170 cm thick sandstone. Volumetrically-subordinate, colour mottled siltstone forms the finer-grained intervals in the Current-Rippled Sandstone Facies south of Olleta.

5.1.3 Izaba sub-basin

A measured section through the Conglomerate with Sandstone Facies that crops out in a stream gully to the northwest of Celigueta, in the eastern part

of the Izaga sub-basin, is presented in the facies log of Fig. 5.8. Fifty three percent of the sequence comprises well imbricated, single to multi-storey, massive conglomerate bodies that become progressively thicker toward the top of the 56m thick succession. The conglomerates are laterally persistent, sheet-like units and are commonly inversely graded with gravel lined bases that, although erosive, are commonly concordant with underlying sandstone. Toward the top of the sequence, internal erosion surfaces within conglomerate bodies overlie thin, lenticular units of cross-stratified, fine-grained sandstone. The inter-conglomerate, sandstone dominated intervals are similar in character to those described from the Conglomerate with Sandstone Facies of Gallipienzo and Pena. Sandstone occurs as planar based, laterally persistent, tabular beds with burrowed bases and an upward transition from upper plane-bed to current ripple lamination. Abundant local scours are concordantly-filled with cross-stratified, medium to fine-grained sandstone containing reactivation surfaces. Thin wedges of cross-stratified and massive gravel up to 50 cm thick are occasionally developed within sandstone intervals, especially beneath large conglomerate bodies.

5.2 PALAEOCURRRENTS

Except for the stations at Sos, Caseda and Olleta, the eight palaeocurrent rose diagrams shown in Fig. 5.9 are based on data derived from large populations of clast imbrication measurements. Where possible, the method of Rust (1972) was followed. In this study, about fifty measurements of maximum projection (AB) planes of disc shaped pebbles were recorded from each sample site. In Conglomerate with Sandstone Facies, such as at Gallipienzo, sample sites were located within individual conglomerate bodies in a sequence. In Massive Conglomerate Facies, such as in the Rio Arba succession, sample sites were located at roughly equally spaced intervals through the conglomerate sequence. The palaeocurrent measurements for stations at Sos, Caseda and Olleta are based mainly on the orientations of channel margins and erosive scours.

One would expect alluvial fans sourced from a major, linear mountainfront, such as the Pena flexure, to disperse roughly perpendicularly to its strike (eg. the alluvial fans on each side of Death Valley, California, as documented by Hooke 1972; also see the strike-normal dispersion of the Izaga alluvial fan system as illustrated in Figs. 4.4, 5.9 and 6.2). The anomalously 'diverted' dispersion of the fans shown in rose diagrams from the stations at Sos-Uncastillo, Sos, Pena and Caseda provides evidence for the possibility of a

hidden structural influence, such as a small, extensional rift roughly 15-20 km wide, striking transversely to the trend of the Pena flexure. Significant thickening of the Bernues Formation in the area between Sos and Gallipienzo, from a mean regional thickness of 1100m, to 2300m (Fig. 2.9), additionally suggests the presence of a blind rift beneath the Caseda area (see Hancock & Bevan (1987) for more examples of foreland extensional structures striking transversely to thrust fronts).

5.3 CLAST PROVENANCE

Depositional source and relative clast transport distance may be assessed by systematically examining changes in clast size, roundness and lithology both within, and between, conglomerate sequences. The above three parameters, recorded from the five main conglomerate successions of the Bernues Formation in the study area, are summarised in Fig. 5.10. Sampling was carried out by marking the ten largest clasts of the same lithotype (reworked Campodarbe Formation molasse sandstone) in a randomly chosen $1m^2$ area and recording the dimensions of their principal axes and roundness (using the chart of Krumbein, 1941, plate 1). The lithologies of up to fifty clasts in each $1m^2$ area were also determined. The maximum clast size (MCS) stated in Fig. 5.10 represents the mean dimension of the longest (A) axes and the roundness values also represent means of all the clasts measured at each station.

It may be seen that there are no significant trends in clast size, roundness or lithology between conglomerate sequences within the study area. However, the measured sections in the Rio Arba valley and at Gallipienzo and Izaga exhibit upward fining followed by upward coarsening, upward coarsening followed by upward fining and upward coarsening, respectively. Roundness indices vary between 0.71 and 0.84, corresponding with the sub-rounded to rounded categories of Powers (1953). All of the conglomerate sequences in the study area are, without exception, dominated by reworked or 'cannibalised' Campodarbe Formation sandstone clasts that constitute between 65 and 95% of clast lithology assemblages. A similar predominance of cannibalised, locally derived molasse clasts has beenreported from the Eocene alluvial fans studied by Atkinson (1983) in the Graus basin of the central South Pyrenees. In the West Jaca basin, the next most abundant clast lithology is pale grey, alveolined and nummulitic limestone of the mid Eocene Ager and Guara Formations. They comprise betweeen 5 and 20% of the conglomerate clast lithotypes. Clasts of mid Eocene Hecho Formation wacke sandstone and granitoid lithologies from the Axial Zone of the Pyrenees constitute up to 15% of clast assemblages.

5.4 DEPOSITIONAL ENVIRONMENTS

Several independent features of the Pena flexure and Izaga sub-basin conglomeratic sequences, and their closely related sandstone and siltstone dominated sequences, record deposition on semi-arid alluvial fans:

(1) radial dispersion from a point source (Fig. 5.9);
(2) highly 'compressed' downflow changes in grain size and sedimentary structures (Galloway 1985) contrasting to the more gradual downflow changes that characterise 'humid' alluvial fans (eg. Boothroyd & Nummedal 1978);
(3) well defined areal relationships with major structures, with lithosomes banked up against their sediment sources (cf. Wells 1984); and
(4) restricted areal extent of lithosomes (3-14 km^2 along the Pena flexure), as contrasting to the larger areas of humid alluvial outwashes (Boothroyd & Nummedal 1978; Ethridge 1985).

From descriptions of sheetflood deposits on semi-arid alluvial fans of the southwestern USA by Bull (1972), the following features of Bernues Formation conglomerates are collectively considered here to be diagnostic of their deposition by sheetfloods.

(1) Sheet-like bed geometry with width to depth ratios generally greater than fifteen. Where substantial erosive scours on the bases of otherwise sheet-like units are present (eg. Plate 5.2a), Blair (1987) has suggested that they reflect sheetflood turbulence, possibly due to confinement of the flow in a sinuous fanhead canyon before its emergence onto the alluvial fan surface.
(2) Well sorted, clast-supported, imbricated conglomerate (cf. Rust 1978) with a lack of high relief (>30 cm) sedimentary structures that would indicate relatively deep water, rather than shallow, sheet-like floods.

The observation that most semi-arid alluvial fans display a down-fan decrease in mass flow deposition (and a corresponding increase in hydraulic depositional processes) and grain size has led numerous authors to recognise proximal to distal sub-environments in alluvial fan systems (eg. McGowen & Groat 1971; Bull 1972; Spearing 1975; Rust 1981). In the conglomeratic Bernues Formation succession exposed in the Rio Arba valley, a similar distinction is proposed, the typical components of which are illustrated in Plates 5.2a-5.2d. Massive Conglomerate Facies (Plate 5.2b; also represented between 170 and 290m in the facies log of Fig. 5.1) are typical deposits of the proximal fanhead environment. These sequences are dominated by coarse, stacked sheetflood

units with an absence of sandstone and the presence of rare mass flow deposits (eg. Plate 5.1b). The planar, non-erosive base of the one metre thick mass flow unit shown in Plate 5.1b, and the dominance of boulder sized clasts up to 90 cm diameter with a subordinate sandstone matrix, suggests that it conforms with the 'surging' debris flow of Nemec & Steel (1984, fig. 15) in which deposition was by non-cohesive mass flow processes.

Since mass flow deposition is a common process in the proximal regions of semi-arid alluvial fans, it is appropriate to question why, although present, mass flow deposits are so rare in the proximal Massive Conglomerate Facies. According to Bull (1977), debris flows are promoted by steep slopes, lack of vegetation, ephemeral water supply and a source providing debris with a muddy matrix. The following two observations provide some explanation for the paucity of debris flows preserved in the Massive Conglomerate Facies.

(1) The lack of mud in the cannibalised Campodarbe Formation sediment source for Bernues Formation alluvial fans would have limited debris flows to cohesionless mass flow processes.
(2) From descriptions of modern alluvial fans, substantial levees are commonly built by cohesionless debris flows in proximal fan regions (eg. Rust & Koster 1984, fig. 9; Blair 1987, fig. 7). Thus, the preservation potential of such deposits could be exceptionally low due to the high chance of levees being breached and reworked during the waning flow stages of alluvial fan depositional events.

Plate 5.2c, also from the Rio Arba sequence, illustrates typical mid fan deposits in which small gravel-filled channels interfinger with lenticular and wedge shaped units of cross-stratified sandstone. A similar facies has been described by McGowen & Groat (1971, fig. 16) from the Cambrian Van Horn Sandstone of west Texas. They interpret the alternating conglomerate-sandstone sequence as resulting from widening of the proximal fanhead canyon, with a consequent decrease of flow depth, stream competence and stream gradient, and the subsequent development of a braided stream system. The cross-stratified sandstone therefore represents bars that were deposited during episodes of decreased discharge and/or waning flow.

In the southern part of the Bernues Formation alluvial fan system exposed in the Rio Arba valley, common, erosively based, gravel-filled channels, such as that shown in Plate 5.2d, occur within a sandstone dominant sequence (also see the 230-295m interval and 80-130m interval of the Sos and Caseda facies logs in Figs. 5.5 and 5.6, respectively). Such a sequence is interpreted here as the product of distal alluvial fan deposition in which 'goosefoot'-like

(cf. Allen *et al.* 1983) gravel bedload channels traversed sandy profan aprons. Thus, in summary, the conglomeratic succession along the eastern part of the Pena flexure is interpreted as the depositional product of a relatively large (14 km^2), semi-arid, alluvial fan system that displays a well defined distinction between its proximal, mid fan and distal facies.

Despite exhibiting features typical of alluvial fan deposition, Conglomerate with Sandstone Facies exposed along the western part of the Pena flexure, and in the Izaga sub-basin, reveal the following important contrasts to the succession in the Rio Arba valley.

(1) A smaller percentage of the sequences comprise conglomerate (26% compared with 90% in the Rio Arba), with a corresponding increase in the proportion of sandstone and siltstone.
(2) A less well defined distinction between proximal and distal alluvial fan sub-environments.

Along the Pena flexure, these differences are interpreted largely in terms of variations in the tectonic controls on sedimentation (Section 5.5). Bernues Formation alluvial fan deposits of the western Pena flexure and Izaga sub-basin are typified by the upper part of the Gallipienzo sequence (shown in the facies log of Fig. 5.4) in which multistorey conglomerate bodies are separated by suites of stacked, tabular, fine-grained sandstone (also shown in Fig. 5.3). Although the conglomerate bodies are dominated by phenomena indicative of their deposition by sheetfloods, the occasional presence of cross-stratified conglomerate storeys suggests that streamflood deposition was a more important process than it was in the alluvial fans that produced Massive Conglomerate Facies.

The inter-conglomerate body sequences of stacked, tabular, fine-grained sandstone display many of the characteristics of the Current-Rippled Sandstone Facies that occurs, for example, in the Gallipienzo succession beneath the lowest conglomerate (see Figs. 5.3 and 5.4 and Plate 5.2a for detail). These sequences contain abundant evidence of ephemeral deposition by sandy sheetfloods, including common upper plane-bed lamination, waning flow sedimentary structures and rootlets (cf. Tunbridge, 1981). Similar sediments described by Heward (1978a; Interlobe Association, p.469) are interpreted by him as interlobe deposits that accumulated rapidly in the intervals between, and/or lateral to, conglomerate lobe depositional events. The Conglomerate with Sandstone Facies is thus interpreted as the product of sheetflood and rare streamflood deposition on relatively small (3 km^2) alluvial fans containing interlobe areas of sandstone dominated, sheetflood sedimentation.

Additionally, the following two marginal alluvial fan sub-environments are recognised.

(1) In the 0-85m and 200-260m intervals of the Gallipienzo sequence (Fig. 5.4), for example, erosively based, upward fining sand bodies occur within Current-Rippled Sandstone Facies. These represent the deposits of moderately sinuous (1.3-1.8) streams, up to 20m wide and 150 cm deep, with mean width to depth ratios of 12.5 (derived from equations presented by Allen 1965; Khan 1971; Ingles & Grant 1975; see Section 4.2.4 for elaboration), that drained south-southwestward across the profan sheetflood plain. The sandy profan aprons experienced relatively low rates of sedimentation compared with alluvial fan surfaces. This was mainly due to most sediment having been deposited on the fan surface, and hence, the profan aprons were reached only by relatively sediment bare streams and sheetfloods. This process generated Current-Rippled **Sandstone** Facies sequences that, significantly, display no signs of embryonic palaeosol development (cf. Boyd 1983, p.180).

(2) Colour mottled, gypsiferous, siltstone dominated sequences of Mottled Siltstone with Sandstone Facies are interpreted as having been deposited in the most starved parts of the deposystem. They record low rates of sedimentation in depositional 'shadows' located between neighbouring alluvial fan systems (eg. the 85-200m interval of the Gallipienzo sequence in Fig. 5.4 and much of the inter-fan Sos and Caseda sequences shown in Figs. 5.5 and 5.6, respectively). The presence of gypsum veins and colour mottling in such sequences reflect relatively long periods of emergence and drying (cf. Bown & Kraus 1981; Allen *et al.* 1983) with consequent palaeosol development.

In the alluvial fan related successions of the Bernues Formation, the following scales of sequence development (applying Heward's (1978b, p.671) definition of 'sequence') are recognised.

(1) On the scale of centimetres to tens of centimetres. For example, common inverse grading above the gravel lined, erosive bases of individual conglomerate storeys is interpreted as being due to very rapid sedimentation on the rise of an individual flood event (Allen *et al.* 1983).

(2) On the scale of metres to tens of metres, Heward (1978) has highlighted some of the problems involved with interpreting sequences that occur on this scale (eg. see Table 1 of Heward 1978) since they may record short to moderate durations of intrinsic alluvial fan behaviour (eg. climatically

induced fanhead entrenchment, lobe switching and abandonment; see Heward 1978b) and/or extrinsic (eg. tectonic) processes taking place in the basin as a whole. Thus, the progressive upward coarsening of the multistorey conglomerate body between 15 and 27m in the Pena facies log (Fig. 5.2) is interpreted here as recording a short to moderate duration of alluvial fan behaviour, such as progradation by a process of fanhead entrenchment and lobe spreading (cf. Blair 1987). However, does the cyclic arrangement of multistorey conglomerate bodies at Gallipienzo reflect the discontinuous nature of the build up and subsequent liberation of debris in the feeder canyon (see fig. 2 of Heward 1978b), or, do the cycles record discontinuous thrust-loading and uplift along the basin margin (cf. Atkinson 1983)?

(3) Sequences on the scale of tens of metres to hundreds of metres (mega sequences) appear to provide some insight into longer term alluvial fan behaviour (Heward 1978b). Thus, the patterns of upward coarsening, upward fining and clast roundness trends displayed by alluvial fan sequences between 30 and 600m thick (**Fig.** 5.10) reflect the influence that thrust movements had on sedimentation during Bernues Formation times.

Although not recognised previously as a common basin margin setting (eg. see Heward 1978, fig. 4), alluvial fans in thrust belts commonly show evidence of having shed from an advancing fall line formed by an emergent thrust tip (eg. the Izaga sub-basin). In such settings, upward coarsening due purely to progradational alluvial fan construction will be enhanced by the tectonic encroachment of the fan apex upon an arbitrary fixed point. Along the Pena flexure, the tectonic setting of alluvial fans is more unusual because they formed in the hangingwall of a 'passively underthrust' backthrust (see Chapter 2). The special features of Pena flexure alluvial fan deposition are described in Section 5.5 but a simple example of the control that the backthrust had on sedimentation is provided by comparing the successions at Gallipienzo and two kilometres to the south of Gallipienzo. Both sequences are dominated by conglomerate bodies of the Conglomerate with Sandstone Facies which, at Gallipienzo, are multistorey and, to the south, are single storey. This transition from multistorey to single storey conglomerates is interpreted here as reflecting a southward increase in the rate of subsidence, further from the influence of the active backthrust tip.

5.5 ALLUVIAL FANS, GROWTH FOLDING AND TECTONICS ALONG THE PENA FLEXURE

Emergence of the Pena flexure backthrust at the start of Bernues formation deposition created a major topographic ridge that formed the northern margin of the Ebro basin in the study area. The development of this emergent backthrust induced the southward dispersion of several alluvial fans in the hangingwall of the backthrust. The accumulation of Bernues Formation alluvial fan conglomerate may be correlated with this tectonic climax in the evolution of the Pena flexure for the following reasons.

(1) Semi-arid alluvial fans require a faulted mountainfront to induce and sustain substantial liberation and deposition of conglomeratic detritus (Heward 1978a; Rust & Koster 1984). Thus, the stratigraphically lowest appearance of significant quantities of conglomerate at the base of the Bernues Formation successions along the Pena flexure records the emergence of the backthrust.

(2) Figures 5.11 and 5.12 illustrate that there is a major progressive offlap unconformity (Riba 1976a) throughout the Petilla Member to Uncastillo Formation sediment pile, to the south of the Pena flexure backthrust. Though considerably less complex than the unconformities and growth folding described from the eastern Ebro basin by Riba (1976a) and Anadon *et al.* (1986), the Pena flexure progressive unconformity reflects a comparable uplift history. The progressive offlap of the Pena flexure indicates a relatively simple tectonic history of accelerated uplift and rotation of the depositional surface from Petilla Member to Uncastillo Formation times. The most rapid period of uplift may be deduced by considering the rates of change of dip through the sedimentary succession. In the Rio Arba valley, for example, a 18° change of dip (from 89 to 71°) accompanies 2300m of thickness of the Petilla Member. However, a 56° dip change (from 71 to 15°) accompanies only 630m of the Bernues Formation. These relationships suggest that the rate of uplift and land surface rotation was at its peak during deposition of the Bernues Formation. This uplift and rotation is interpreted here as a response to underthrusting of, and consequent displacement on, the listric shaped backthrust of the Pena flexure passive-roof duplex (sée Chapter 2).

Balanced sections through the Pena flexure (Figs. 2.3 and 2.4) also reveal a westward reduction in the amount of displacement on the Pena flexure backthrust, from approximately 2500m at Sos to 1000m near Gallipienzo. This variation in thrust displacement is reflected in the following changes in the style of Bernues Formation alluvial fans along the Pena flexure.

(1) A systematic westward decrease in the percentage of conglomerate in alluvial fan sequences, from greater than 95% in the Rio Arba to less than 25% at Gallipienzo.
(2) A decrease in alluvial fan area, from about 14 km^2 in the Rio Arba valley to 3 km^2 at Gallipienzo, reflecting a reduced drainage basin area and/or a reduced quantity of conglomeratic detritus.

There are three possible explanations for the westward decrease in the proportion of conglomerate in Pena flexure alluvial fan sequences.

(1) Massive Conglomerate Facies, such as those exposed in the Rio Arba, are interpreted here as proximal, semi-arid alluvial fan deposits. The Conglomerate with Sandstone Facies, as best exemplified at Gallipienzo, conforms with the distal alluvial fan model of Rust (1981) from the Carboniferous Cannes de Roche Formation of eastern Canada. It may be that the westward decrease in alluvial fan proximality, as implied by the westward decreasing percentage of conglomerate, is a result of erosion of the proximal facies of the alluvial fan sequences in the west. However, this hypothesis contradicts the observation of decreased backthrust displacement toward the west which, if anything, would be expected to maximise the preservation of sequences in the western part of the Pena flexure.
(2) In sympathy with the westward decrease in backthrust displacement, there would have been a relative increase in subsidence and preservation potential toward the west. Thus, greater quantities of sandstone and siltstone in alluvial fans would be deposited and preserved in the tectonically less active depositional environment of the western Pena flexure.
(3) Conglomerate with Sandstone Facies represents the deposits of alluvial fans with less available conglomeratic detritus in their drainage basins compared with those of the Massive Conglomerate Facies. It is therefore not surprising that, the alluvial fans which were active along the western part of the Pena flexure deposited Conglomerate with Sandstone Facies sequences because smaller displacements on the backthrust in the west would have liberated smaller volumes of coarse-grained sediment.

Furthermore, the area of Bernues Formation alluvial fans also decreases toward the west along the Pena flexure. From studies of alluvial fans in the semi-arid regions of the southwestern USA, it has been demonstrated that, other factors being equal, alluvial fan area approximates to drainage basin

area (eg. Bull 1962; Bluck 1964; Denny 1965; Hooke 1968; Hooke 1972). Thus, to a large extent, the decrease in alluvial fan area along the Pena flexure, from 14 km^2 in the east to 3 km^2 in the west, reflects correspondingly smaller drainage basin areas. However, Rockwell *et al.* (1985) cast doubt on this generalisation by demonstrating that, through a mechanism of tectonically enhanced fanhead entrenchment (cf. Bull 1964; Hunt & Mabey 1966; Denny 1967; Williams 1970; Heward 1978b), deposition along tectonically youthful mountain-fronts (such as the Pena flexure during Bernues Formation times) may result in 'oversized' alluvial fans with areas up to six times that of their drainage basins.

In a similar process to the growth of alluvial fans on the western margin of Death Valley (Hooke 1972), oversized alluvial fans along the Pena flexure would have been emphasised by the forelandward tilting of the depositional basin floor above the southward dipping listric backthrust. Thus, it seems that the Pena flexure alluvial fans' drainage basins comprised small, Campodarbe Formation molasse dominated hinterlands, structurally defined by the syndepositionally active Pena flexure backthrust.

5.6 BASIN CONFIGURATION

A possible, generalised palaeoenvironmental reconstruction of the semi-arid study area during Bernues Formation deposition is illustrated in Fig. 5.13. Southward and westward propagation of the thrust front from its Petilla Member position produced an expanded area of topographically inverted upland that occupied the central part of the study area. Hence, the bulk of the study area was characterised by a laterally dispersing pattern of generally coarse, conglomeratic sedimentation around the margins of a central, uplifted 'core'. Continued displacement along the Pena flexure backthrust, in particular, provided a Campodarbe Formation molasse dominated sediment source that sustained semi-arid alluvial fan deposition throughout most of Bernues Formation times.

Siltstone and sandstone alluvial fan related sequences accumulated in the following two main settings.

(1) Interfan areas sandwiched between neighbouring alluvial fans that behaved as depositional 'shadows' characterised by low rates of sedimentation with consequent palaeosol development.

(2) Sandy, profan aprons affected by sandy and silty, gravel-bare streams and sheetfloods. Significantly, these sequences display no signs of embryonic palaeosol development.

Immediately forelandward of the western half of the Pena flexure, the development of a transversely striking, 15 to 20 km wide, blind rift is defined by a substantially thicker Bernues Formation sequence in the area of the proposed rift and a 'diversion' of alluvial fan dispersion toward the axis of the rift. External to the Pena flexure, definition of the Olleta sub-basin became pronounced by Bernues Formation times, mainly due to the strong pull of palaeocurrents toward its synclinal depocentre. The Izaga sub-basin escaped the topographic inversion of the main West Jaca basin and remained as an isolated depocentre until Uncastillo Formation times.

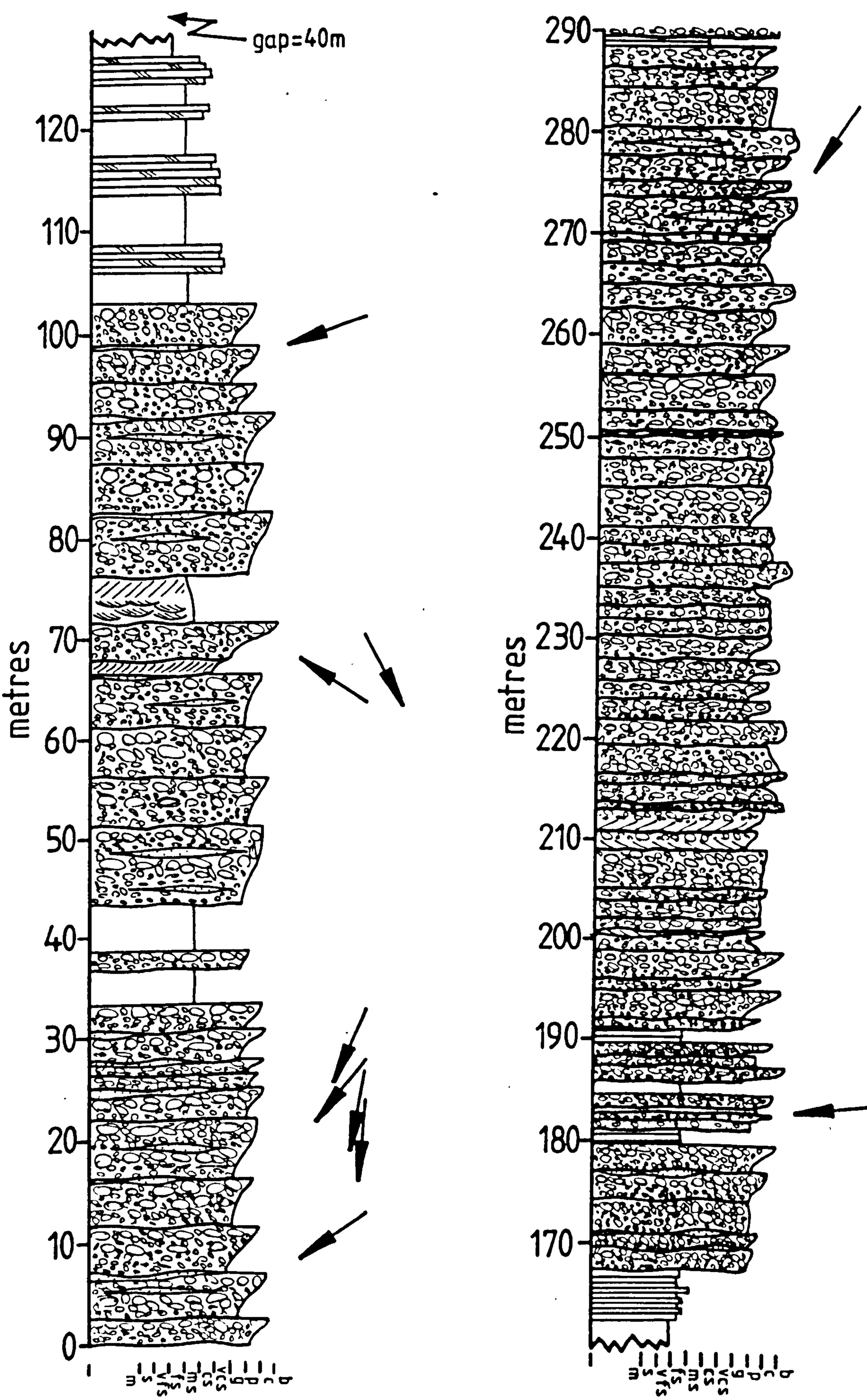

Fig. 5.1. Bernues Formation Conglomerate with Sandstone Facies (0-170m) and Massive Conglomerate Facies (170-290m) in the Rio Arba valley: graphic log.

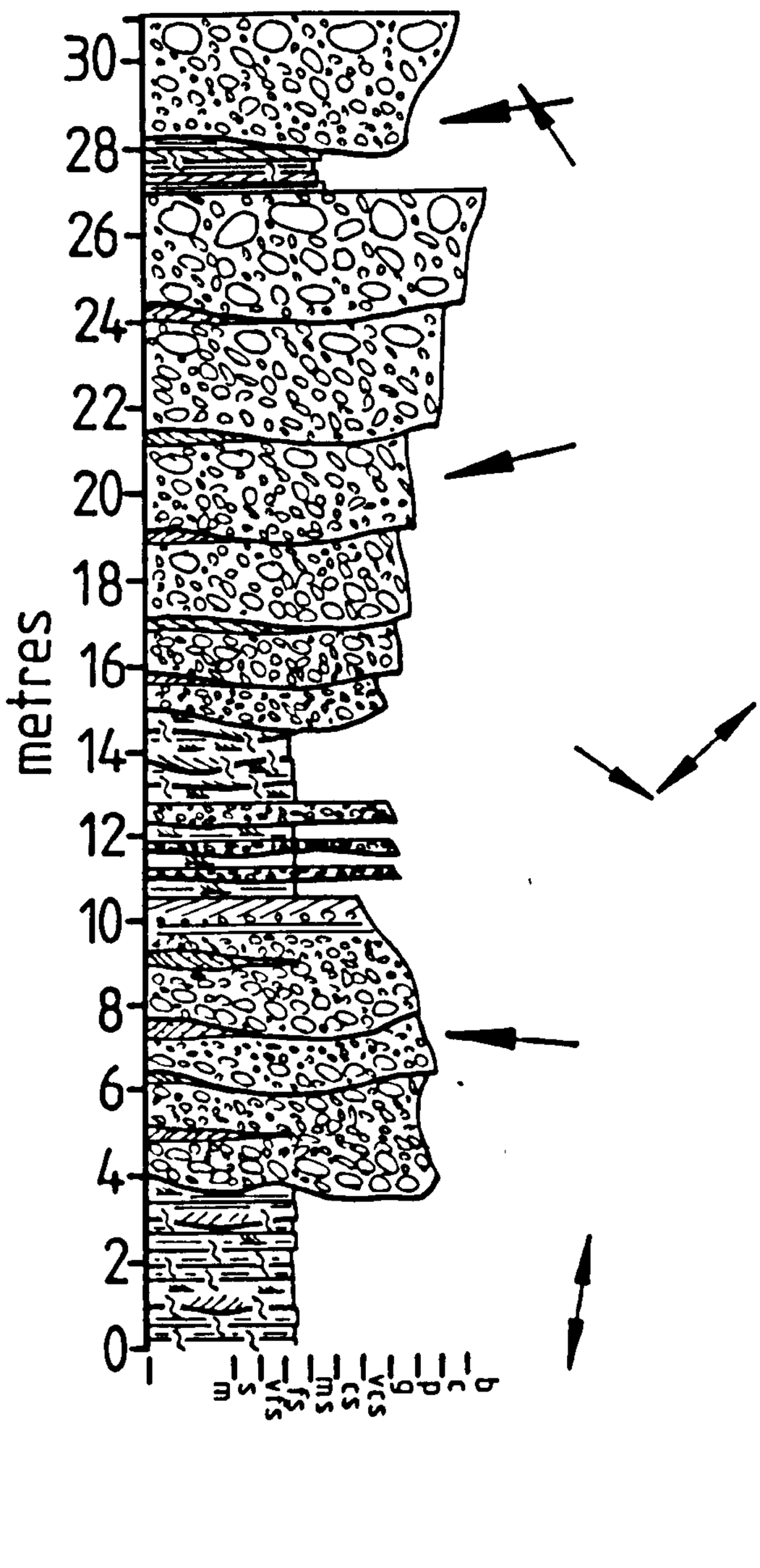

Fig. 5.2. Bernues Formation Conglomerate with Sandstone Facies at Pena: graphic log.

Fig. 5.3. Photomosaic and interpretive line drawing of fine-grained sandstone, erosively overlain by a conglomerate body (15-27m in the log of Fig. 5.2) in the Conglomerate with Sandstone Facies at Pena.

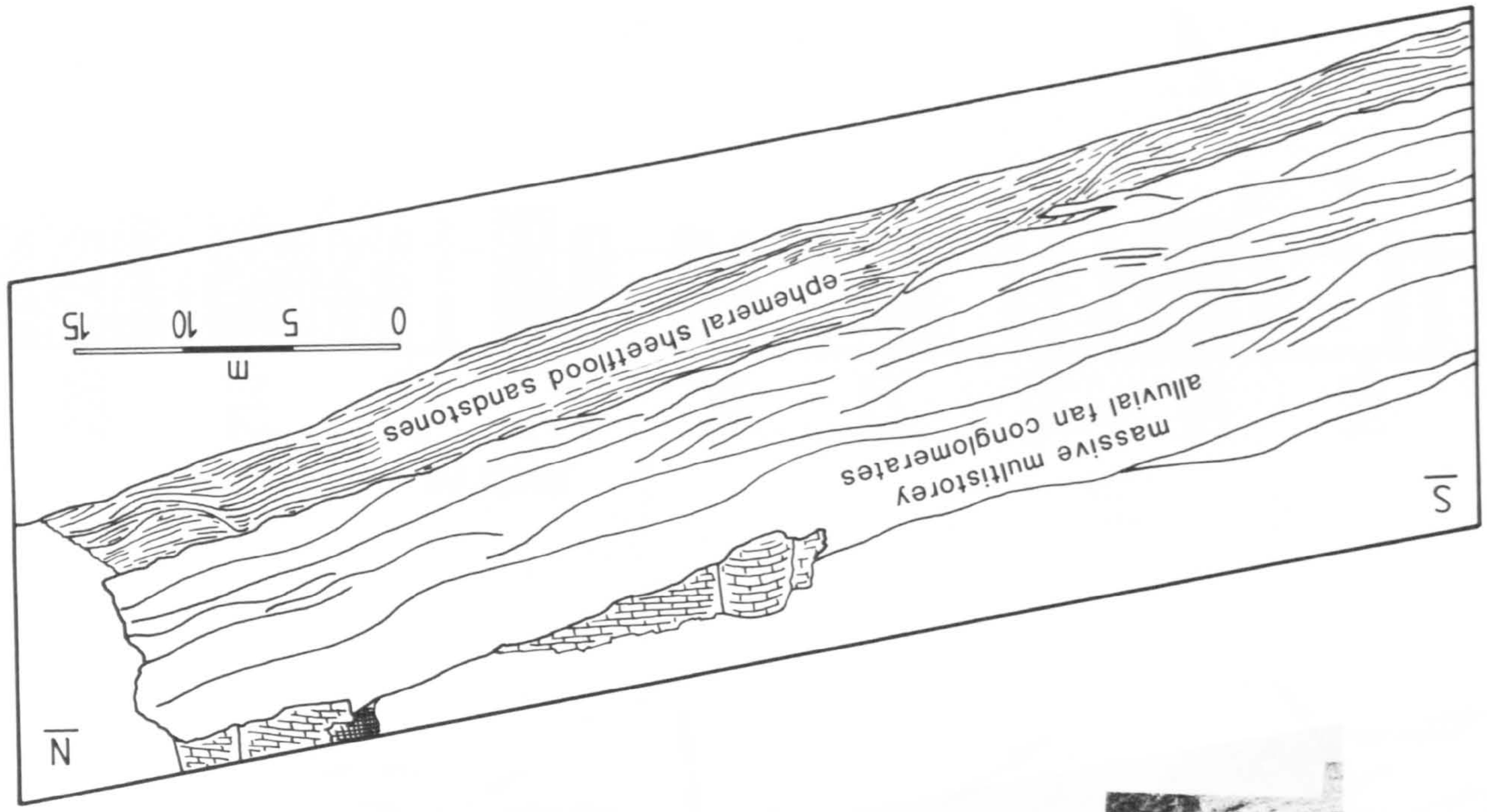
massive multistorey
alluvial fan conglomerates
ephemeral sheetflood sandstones
0 5 10 15
m
S
N

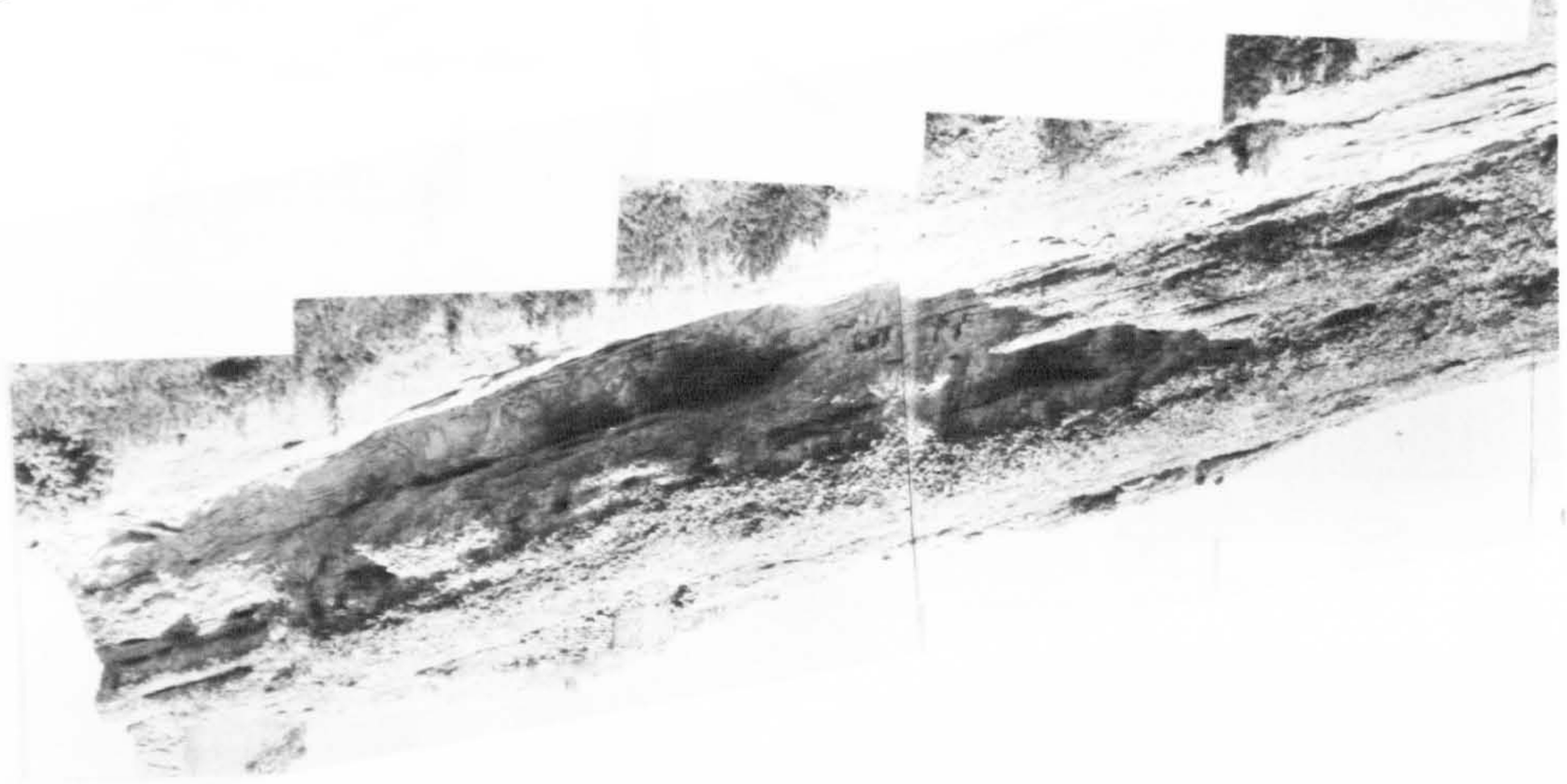

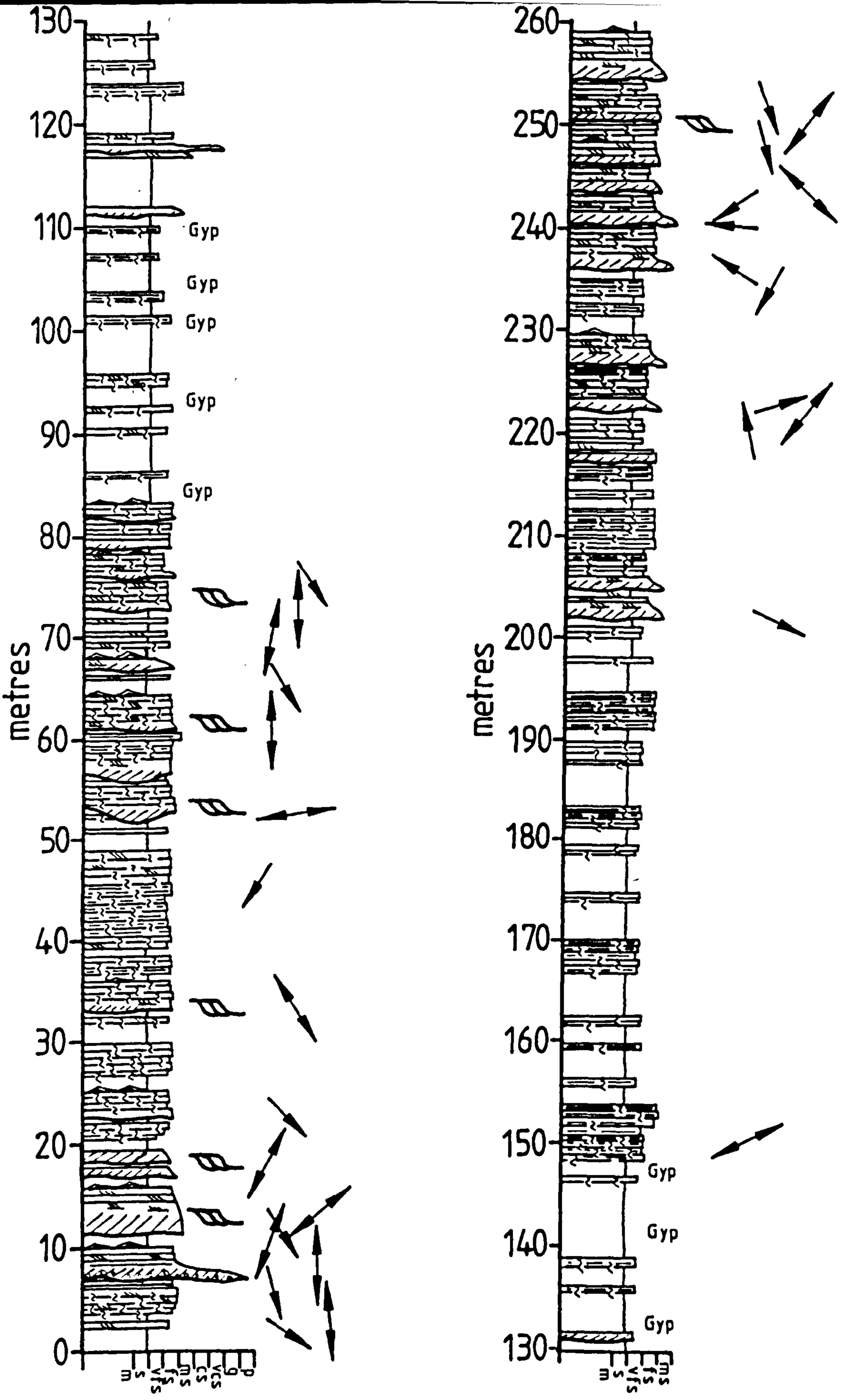

Fig. 5.4a. Bernues Formation Current-Rippled Sandstone Facies (0-85m, 200-260m) and Mottled Siltstone with Sandstone Facies (85-200m) at Gallipienzo: graphic log.

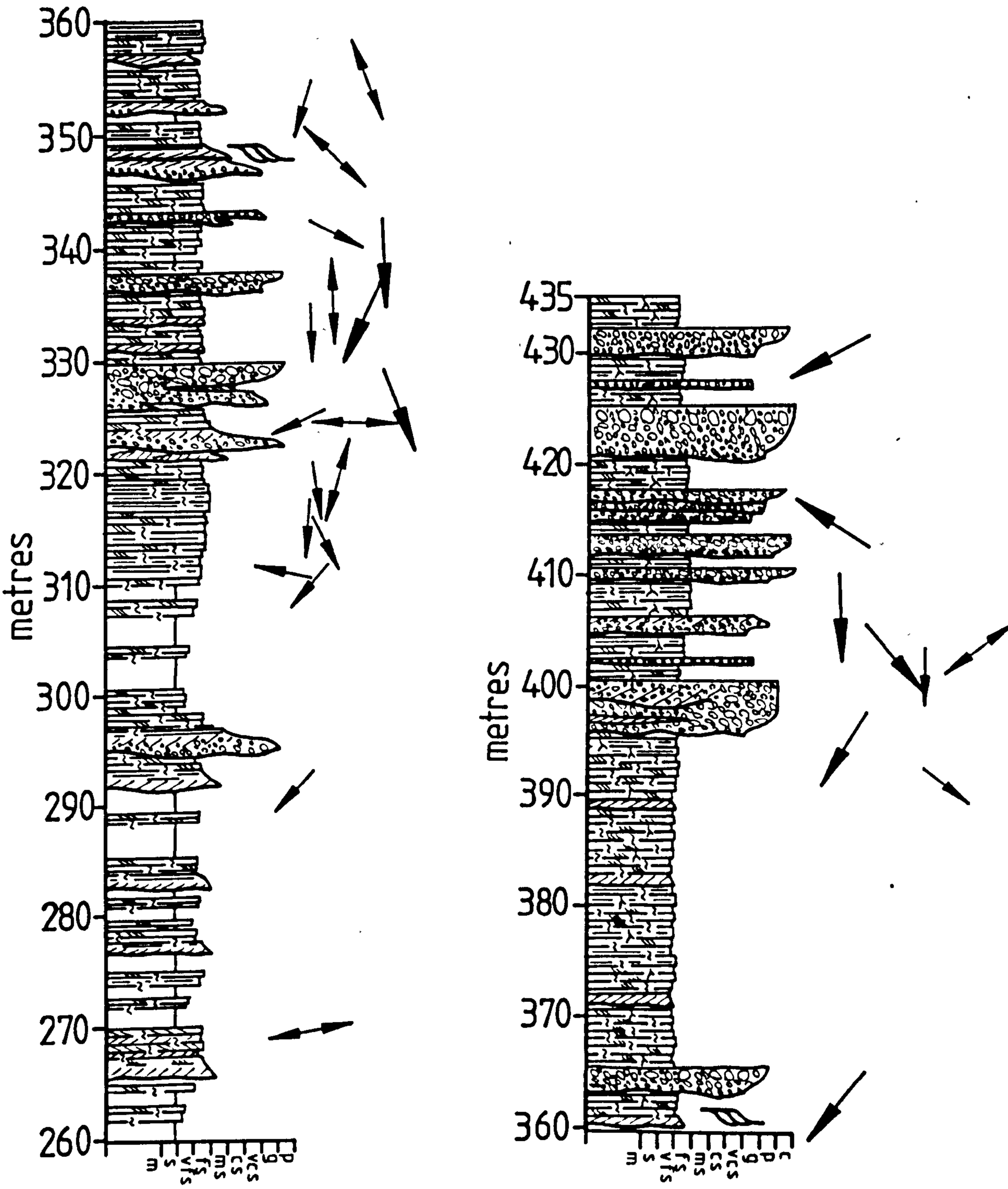

Fig. 5.4b. Bernues Formation Mottled Siltstone with Sandstone Facies (260-310m) and Conglomerate with Sandstone Facies (310-435m) at Gallipienzo: graphic log.

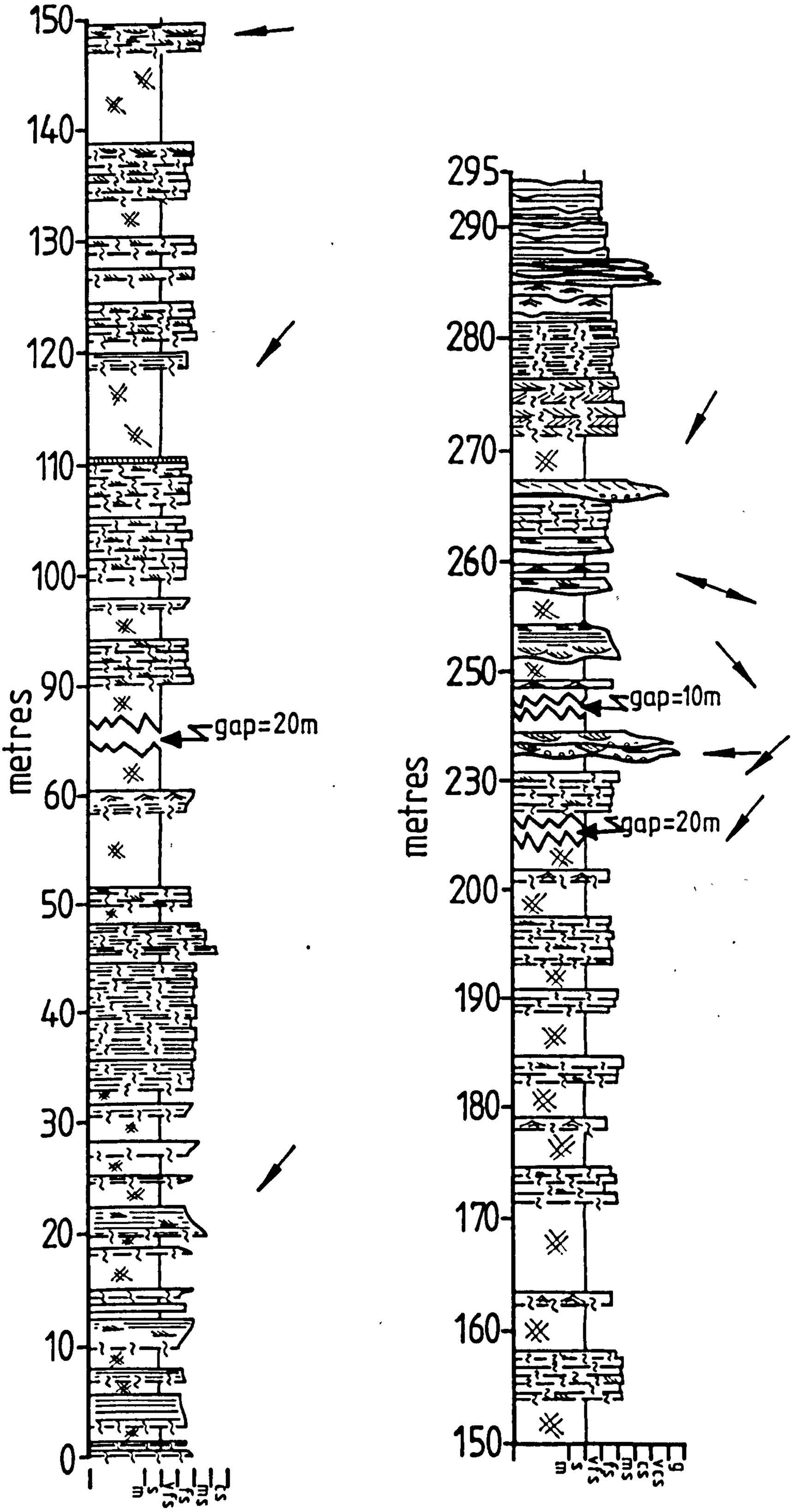

Fig. 5.5. Bernues Formation Mottled Siltstone with Sandstone Facies at Sos: graphic log.

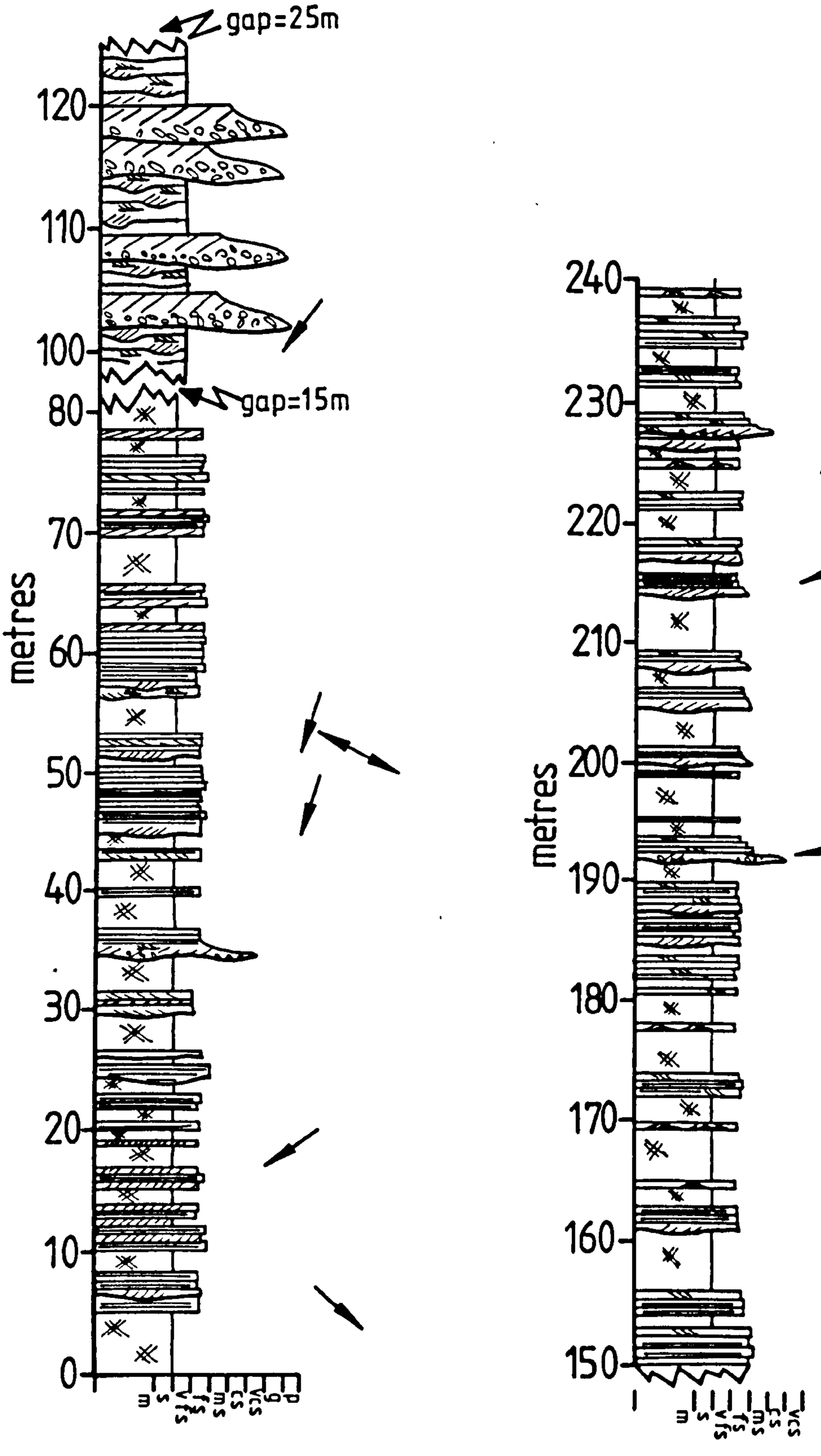

Fig: 5.6. Bernues Formation Mottled Siltstone with Sandstone Facies (0-80m, 150-240m) and Gravelly Sandstone Facies (100-130m) at Caseda: graphic log.

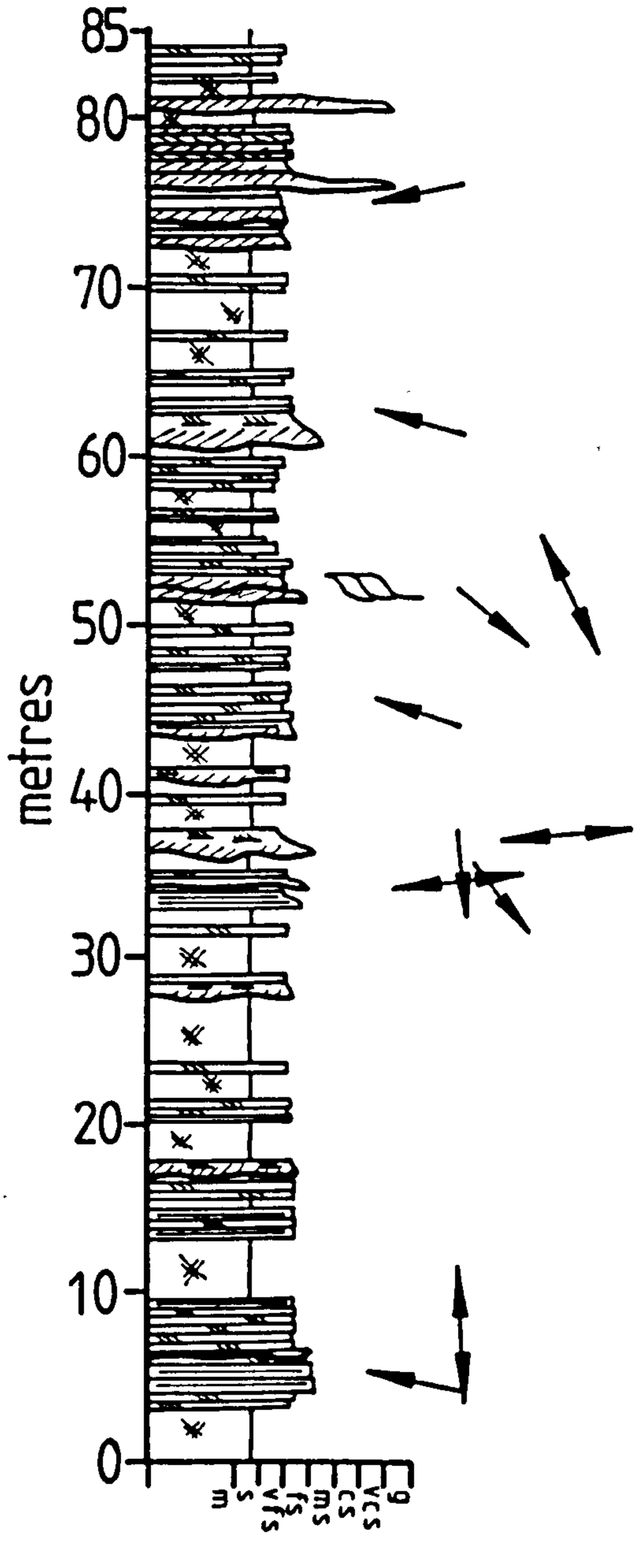

Fig. 5.7. Bernues Formation Mottled Siltstone with Sandstone Facies south of Olleta, Olleta sub-basin: graphic log.

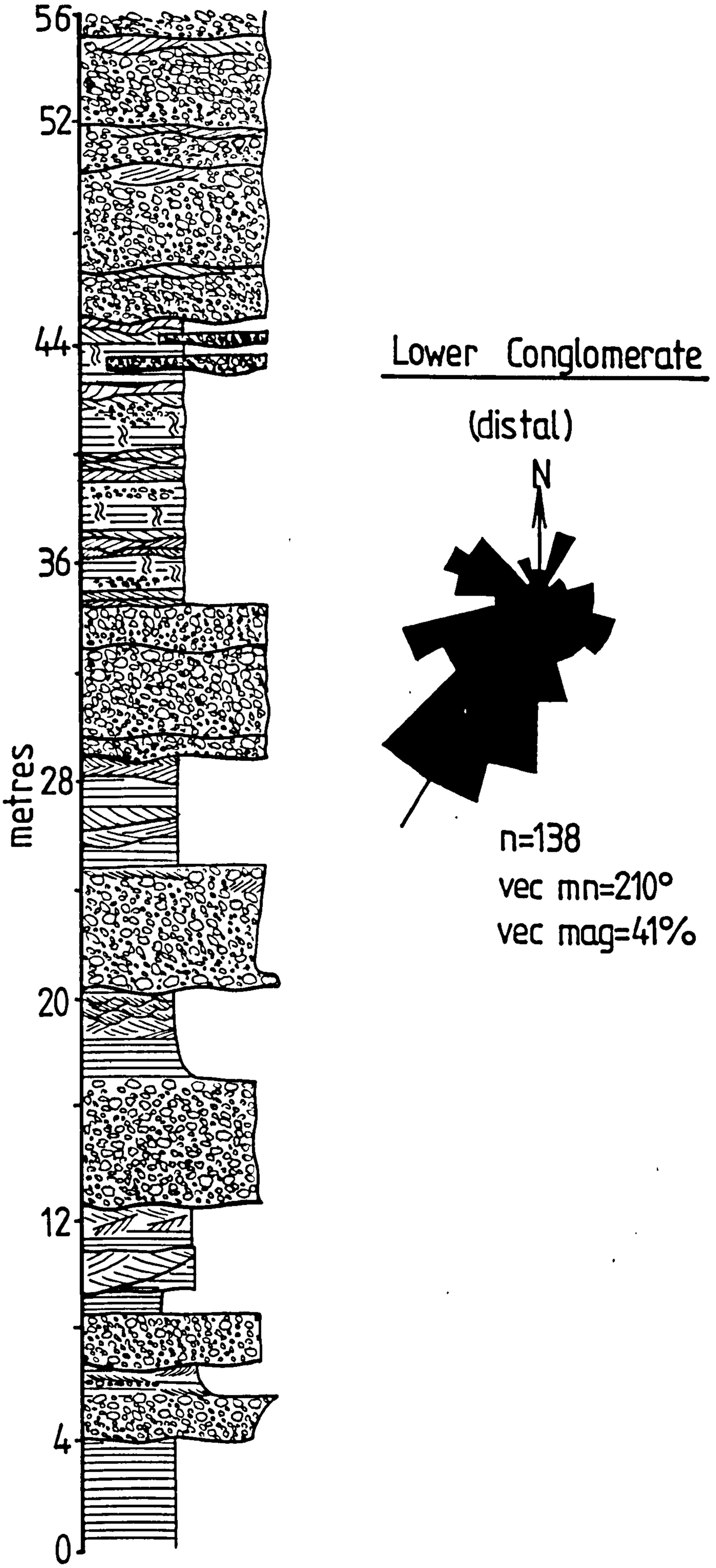

Lower Conglomerate

(distal)

n=138

vec mn=210°

vec mag=41%

Fig. 5.8. Bernues Formation Conglomerate with Sandstone Facies at Celigueta, Izaga sub-basin: graphic log and palaeocurrent rose diagram. Compare the dispersion of palaeocurrents displayed by the rose diagram with the more proximal Massive Conglomerate Facies of the Izaga sub-basin shown in Fig. 6.1.

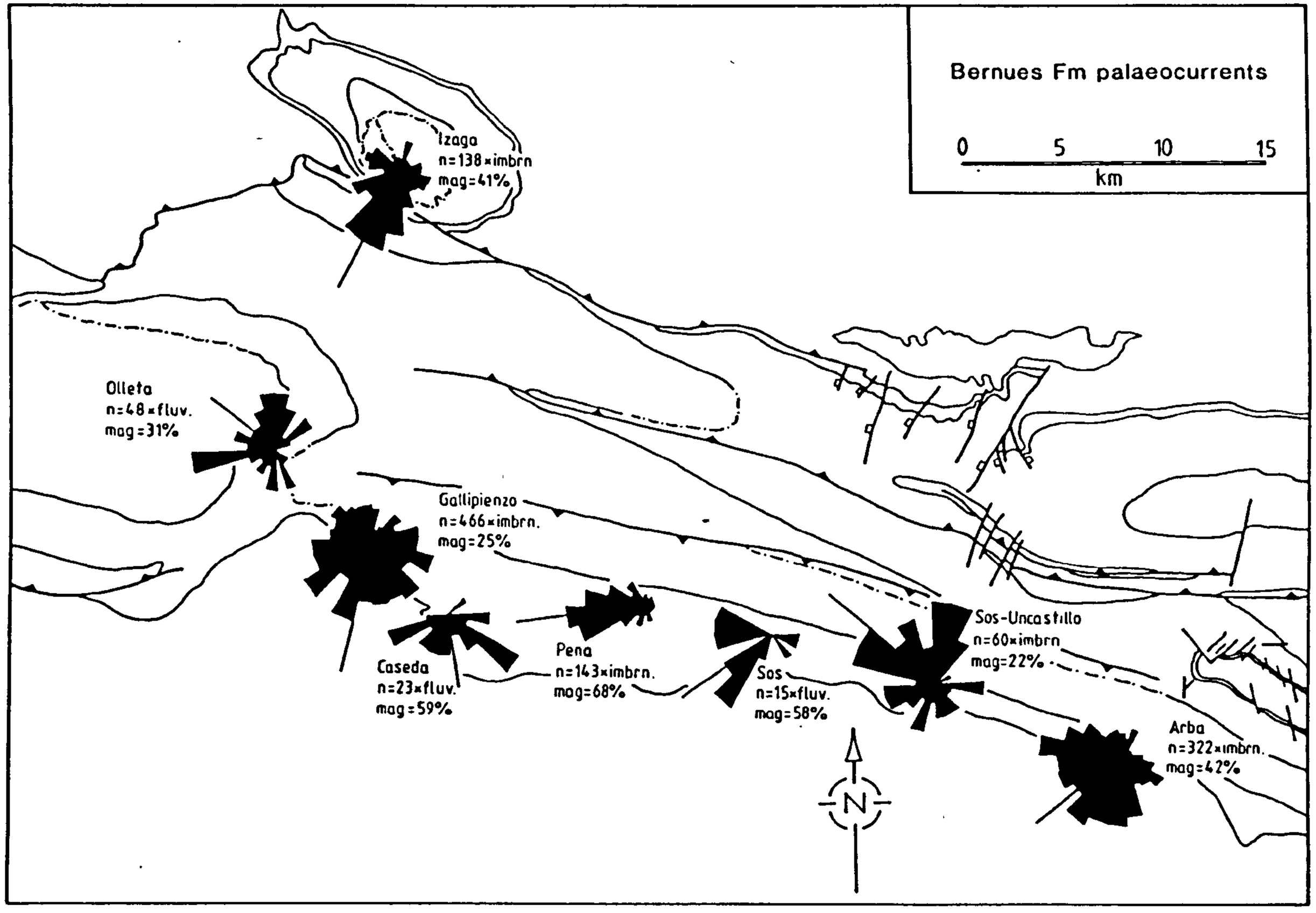

Fig. 5.9. Palaeocurrent rose diagrams depicting Bernues Formation dispersion directions in the study area. Structural symbols and lithostratigraphic contacts as in Fig. 1.3.

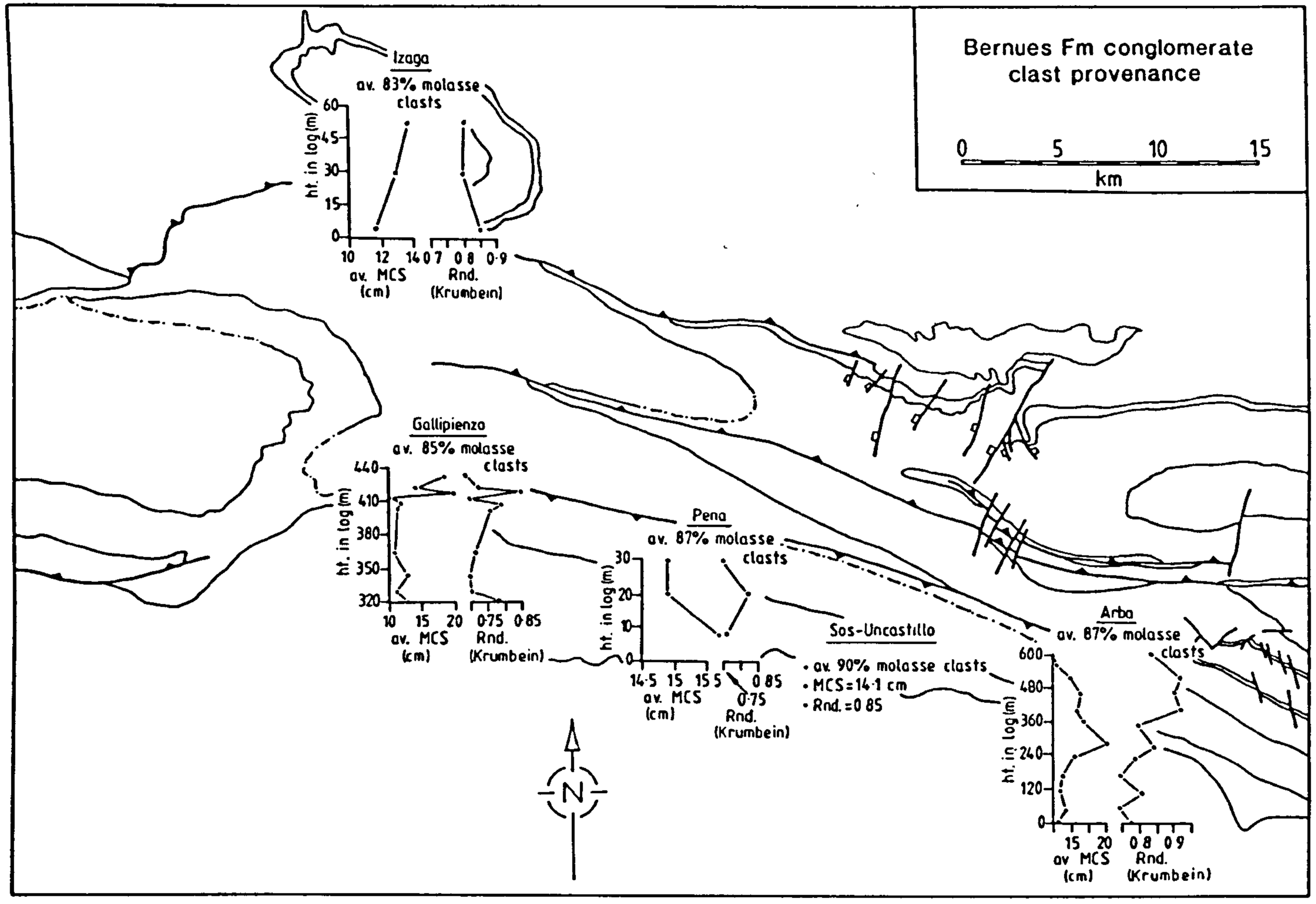

Fig. 5.10. Maximum clast size (MCS) and roundness (Rnd.) of reworked molasse clasts, and clast lithological assemblages from five Bernues Formation conglomerate sequences. Structural symbols and lithostratigraphic contacts as in Fig. 1.3.

Fig. 5.11. Photograph and interpretive line drawing of a view south-eastward from Gallipienzo through the Pena flexure. Note the progressive offlap unconformity in the Petilla Member to Uncastillo Formation succession.

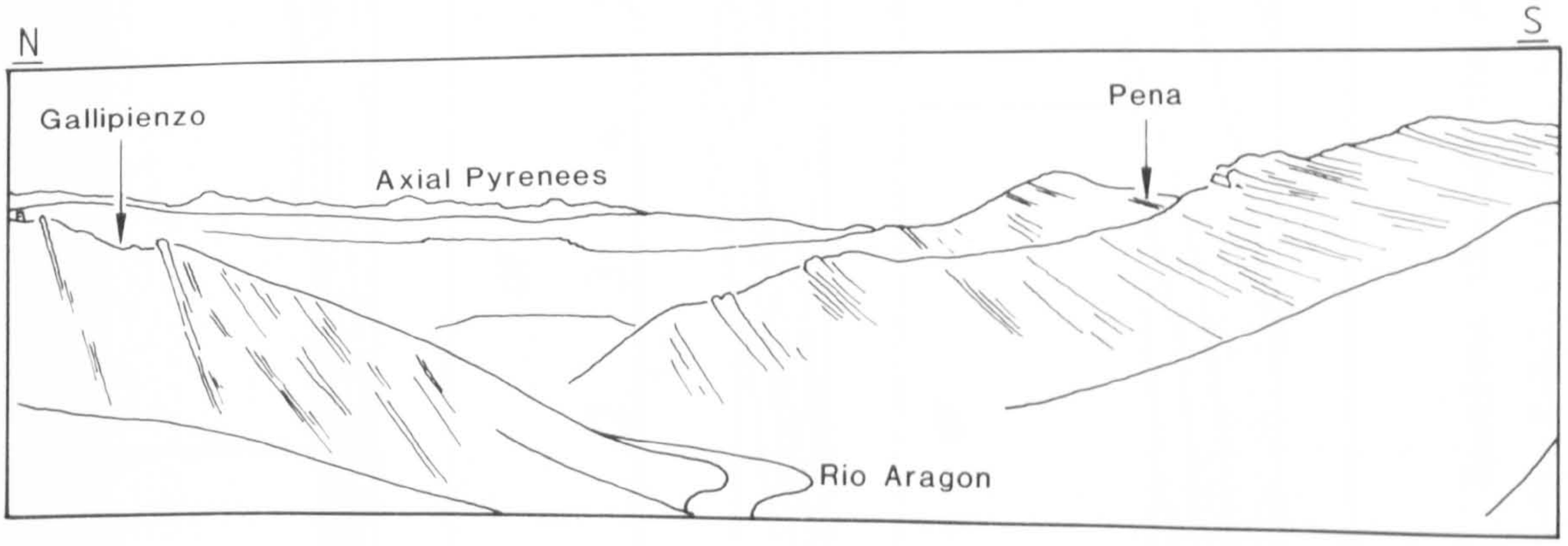
N
S
Gallipienzo
Axial Pyrenees
Pena
Rio Aragon

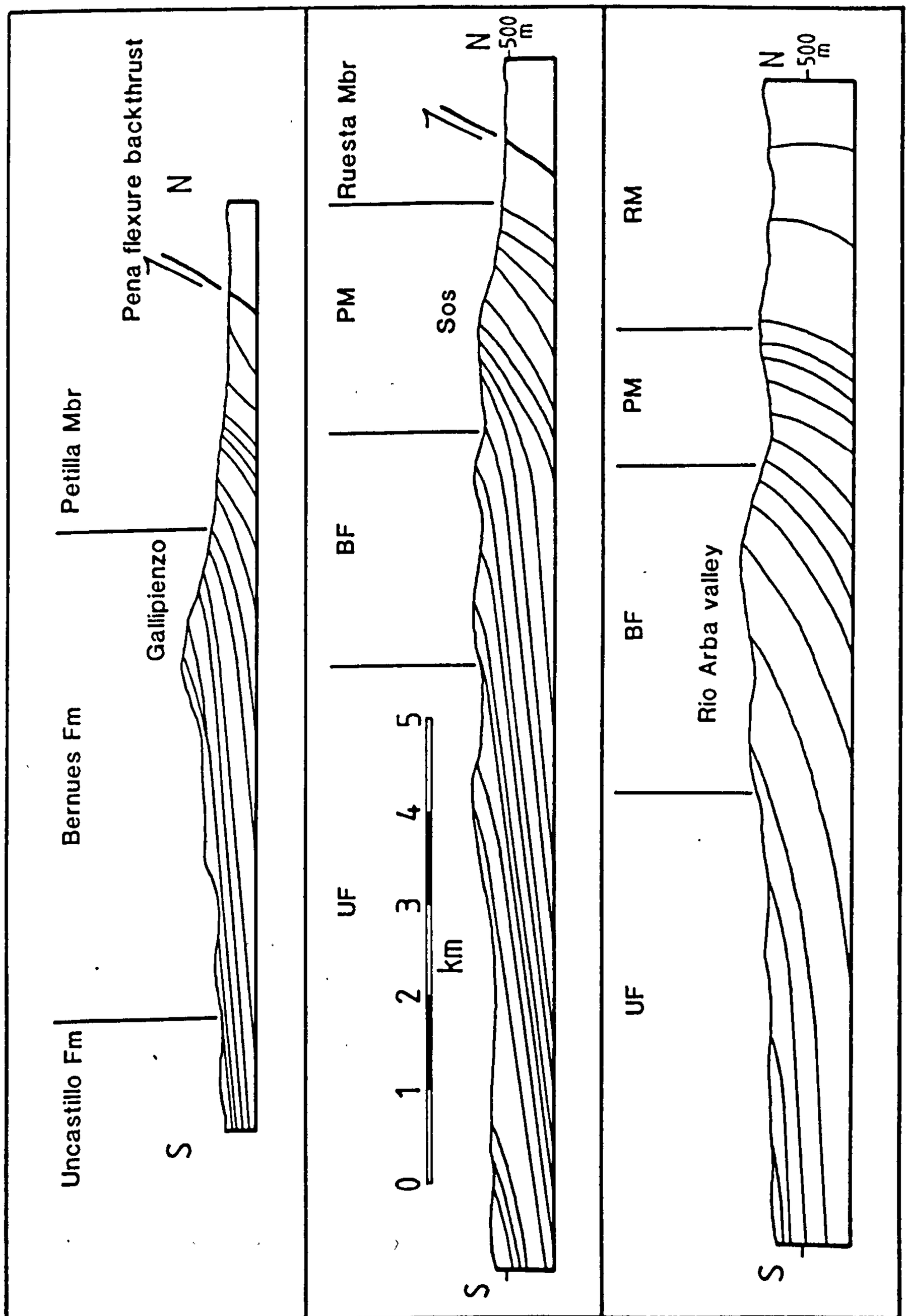

Fig. 5.12. Sections through the Pena flexure 'growth monocline', along the lines of Figs. 2.2-2.4 (shown in Fig. 2.1), depicting detailed stratigraphic geometry.

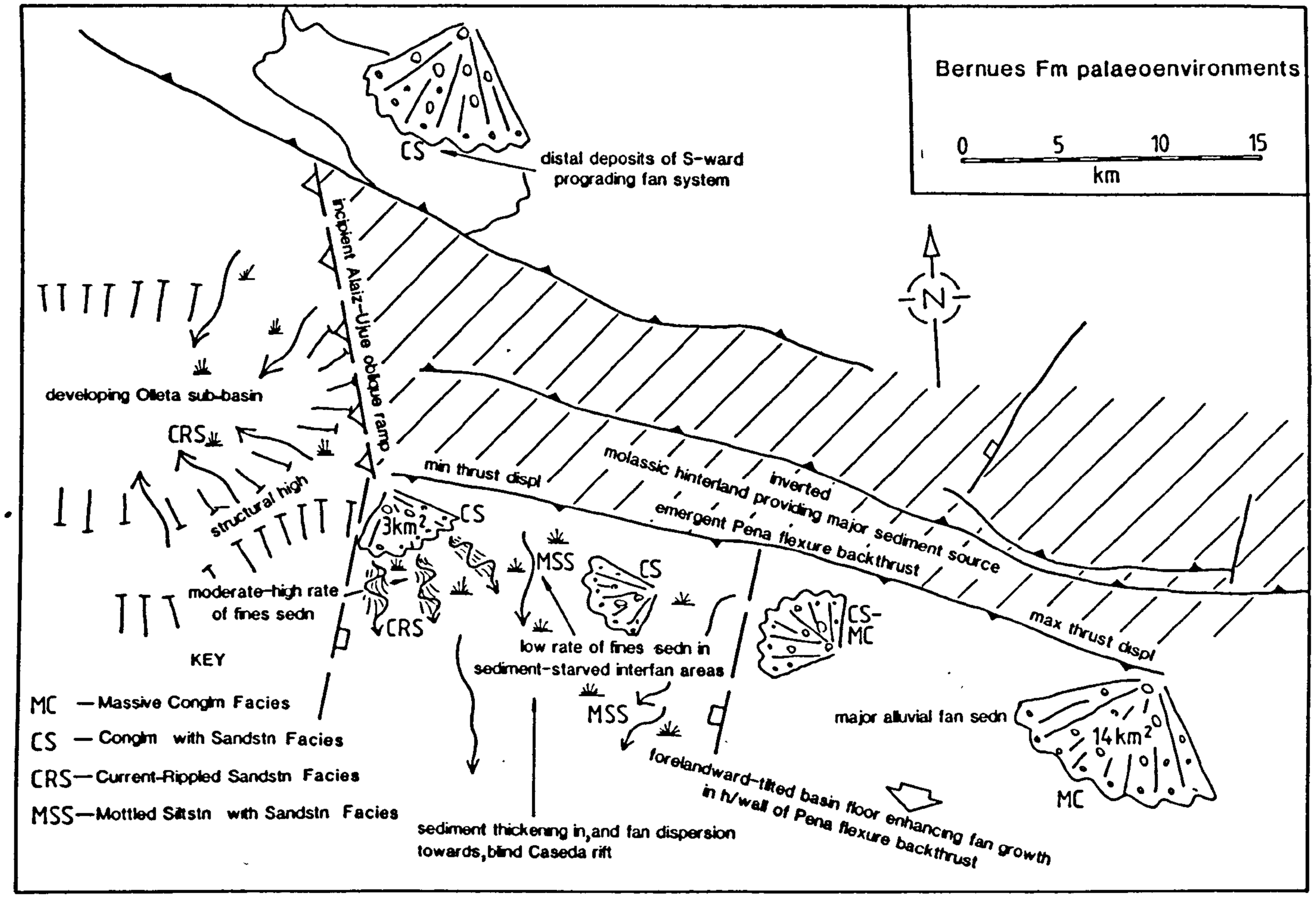

Fig. 5.13. Schematic palaeoenvironmental reconstruction of the study area during deposition of the Bernues Formation.

Plate 5.1a. Fine-grained sandstone-filled, ribbon palaeochannel at 252m in the interfan sequence shown in Fig. 5.5.

Plate 5.1b. Blocks of unsorted debris flow conglomerate containing cobble to large boulder sized clasts in Massive Conglomerate Facies of the Rio Arba valley.

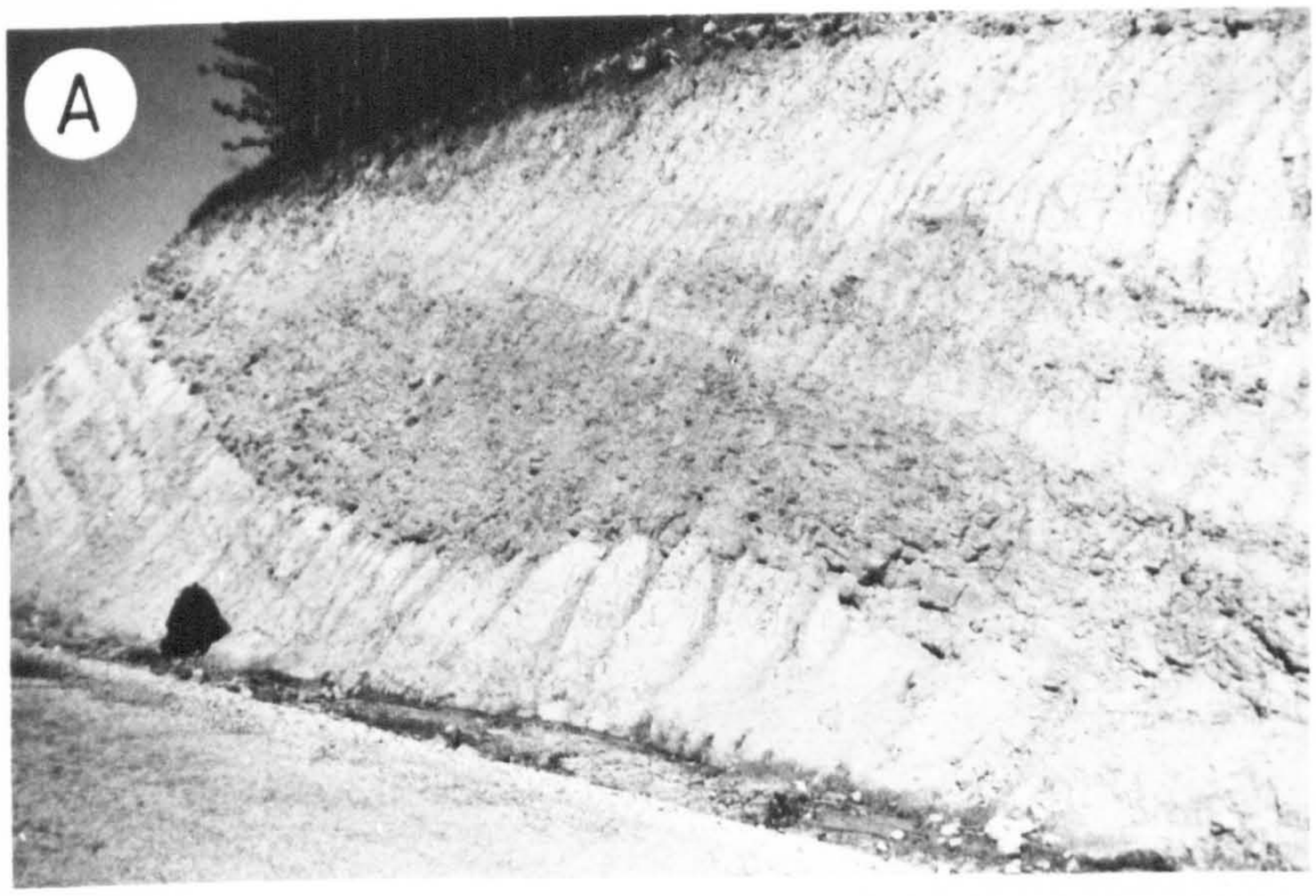
A


B

Plate 5.2a. Conglomerate with Sandstone Facies at Gallipienzo displaying up to two metres of erosive relief at the base of a conglomerate body overlying thin-bedded, fine-grained sandstone.

Plate 5.2d. Erosively based, gravel-filled channels in a sandstone dominated Conglomerate with Sandstone Facies sequence at the southern end of the Rio Arba valley Bernues Formation outcrop.

Plate 5.2b. Massive Conglomerate Facies in the Rio Arba valley with thin, fine-grained sandstone separating stacked, massive, conglomerate bodies.

Plate 5.2c. Erosively based, gravel-filled channels interfingering with wedge shaped units of cross-stratified sandstone in Massive Conglomerate Facies of the Rio Arba valley.


C


A


D

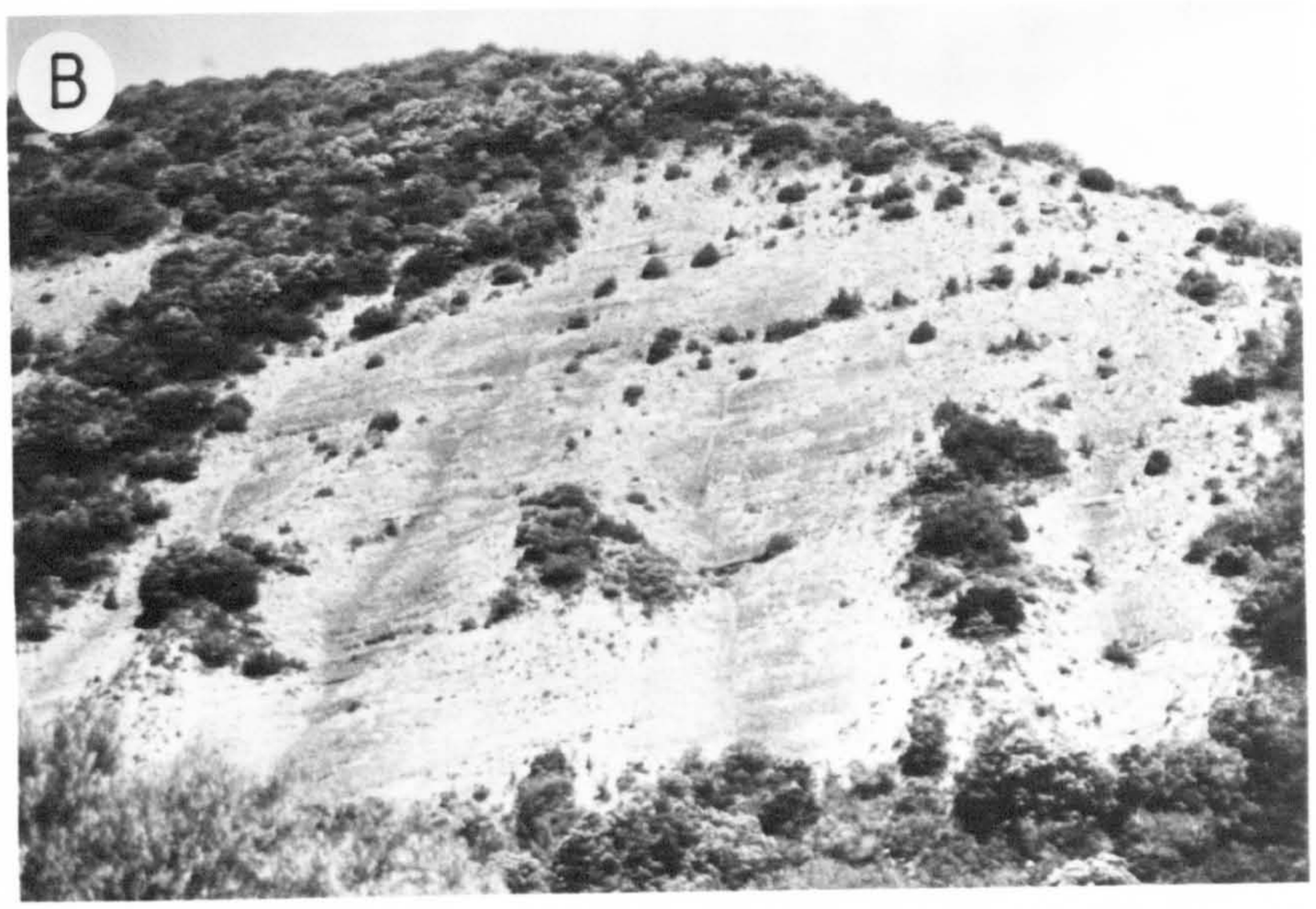
B

CHAPTER 6

BASIN EVOLUTION DURING DEPOSITION OF THE UNCASTILLO FORMATION

Sand- and gravel-rich sediments of the Aquitanian to Burdigalian Uncastillo Formation are exposed extensively in gently dipping to flat lying successions around the peripheral parts of the study area. In Chapter 5 it was established that the regional tectonic climax occurred during deposition of the Bernues Formation when the limit of maximum thrust displacement was reached. Uncastillo Formation times therefore represented a period of post-climactic adjustment to the newly imposed basin configuration. This comprised a central, topographically inverted zone, and peripheral depocentres in the Izaga, Olleta and Ujue sub-basins and along the northern margin of the Ebro basin.

By means of a general analysis of facies characteristics, alluvial architecture, fluvial palaeomorphology and provenance it is here proposed to demonstrate the post-deformation climax evolution of the West Jaca basin. In particular, detailed facies evaluation of the superbly exposed fluvial sequences of the Uncastillo Formation, and comparison of them with those of the Petilla Member, may shed some light on how ancient river systems responded to local and regional tectonic activity.

6.1 IZAGA SUB-BASIN ALLUVIAL FAN SEDIMENTATION

6.1.1 General facies description

The facies log shown in Fig. 6.1 represents a 48m section through the Uncastillo Formation succession in the Izaga sub-basin that rests with angular unconformity on the underlying Bernues Formation. The Uncastillo Formation occupies the upper 350m of the total Izaga sub-basin Oligo-Miocene succession and comprises Massive Conglomerate Facies, comparable to similar sequences described from the Bernues Formation of the Rio Arba valley (Chapter 5). The Izaga sequence consists of stacked, erosively based units (between 50 and 400 cm thick) of moderately well sorted, clast-supported, massive and occasionally cross-stratified conglomerate. Internally, individual conglomerate bodies are commonly inversely graded. Sandstone is volumetrically negligible in the Izaga sequence but, where present, occurs as laterally impersistent, lenticular wisps of upper plane-bed and current ripple laminated fine-grained sandstone, erosively truncated by an overlying conglomerate unit.

6.1.2 Palaeocurrents

Figure 6.2 shows seven palaeocurrent rose diagrams derived from the measurement of Uncastillo Formation successions in the study area. Dispersion directions indicated by the Izaga station rose diagram are derived from recording the orientations of the AB planes of imbricated, reworked molasse, conglomerate pebbles. The Izaga rose diagram reveals that the mean direction of dispersion in the Izaga sub-basin conglomeratic sequence remained remarkably constant between Bernues and Uncastillo Formation deposition (toward 210° and 212°, respectively).

6.1.3 Clast provenance

The proportion of reworked Campodarbe Formation molasse clasts in the Izaga conglomerate sequence remained constant between Bernues and Uncastillo Formation deposition at 80% molasse and 20% Palaeocene Ager and Guara Formation limestone. Mean maximum size of molasse clasts (MCS) increased from 12.9 cm in the Bernues Formation to 15.1 cm in the Uncastillo Formation. In sympathy with such an upward coarsening trend, roundness decreased from 0.81 to 0.73 (using the scale of Krumbein, 1941).

6.1.4 Depositional environments

The Massive Conglomerate Facies of the Izaga sub-basin is interpreted in the same way as similar Bernues Formation sequences exposed in the Rio Arba valley (see Chapter 5), as the product of deposition on the proximal parts of a semi-arid alluvial fan. The dominance of sheet-like units of moderately sorted, clast-supported conglomerate with an absence of cut banks and minimal evidence of bar formation suggests that deposition was mainly from sheetfloods (Bull 1972). Common inverse grading within individual sheetflood units (see Fig. 6.1) may record very rapid sedimentation on rising flood events (cf. Allen *et al.* 1983).

It is likely that the Uncastillo Formation conglomerate sequence represents proximal deposits of the same alluvial fan system that formed the distal fan conglomerates of the Bernues Formation in the Izaga sub-basin. The following reasons are advanced for this interpretation.

(1) There is a consistency of dispersion directions between the sequences and a systematic decrease in palaeocurrent variance (see Figs. 5.8 and 6.1).
(2) There is a systematic upward coarsening (from a maximum molasse clast size of 11.5 to 15.1 cm) and a corresponding decrease in roundness (from 0.85 to 0.73) between the sequences.

(3) There is a similarity in clast assemblages, suggesting that each sequence was sourced from a common drainage basin.

The above three relationships are consistent with there having been an increase in alluval fan proximality between Bernues and Uncastillo Formation deposition. In Fig. 6.3, a model is presented to explain this relatively sudden increase. The model shows how the angular unconformity that separates the two sequences probably records an episode of land surface tilting and subsequent erosion related to the forelandward advance of the thrust defined fall line, from which the Izaga alluvial fan system was shed.

6.2 OLLETA SUB-BASIN ALLUVIAL FAN AND FLUVIAL SEDIMENTATION

6.2.1 General facies description

Three facies are recognised in Uncastillo Formation sequences located near Artariain, Olleta, and along the Olleta-Pueyo and Artariain-Barasoain roads. These are, respectively, the Sheet Sandstone Facies, Conglomerate with Sandstone Facies and Ribbon Sandstone Facies.

The Sheet Sandstone Facies (Fig. 6.4) are most completely exposed near the village of Artariain where the sequence comprises prominently weathered, erosively based beds of upward fining sandstone between one and seven metres thick, and with width to thickness ratios of between 10 and 150. These laterally extensive sand bodies constitute 37% of the measured sequence and between them occur suites of red and grey mottled massive siltstone and subordinate packages of stacked, tabular, burrowed, fine-grained sandstone. The packages of sandstone comprise thin-bedded units that are dominated by upper plane-bed and current ripple lamination.

In vertical section, the detailed morphology of the erosively based sandstone bodies consists of a base, that displays up to 120 cm of relief, overlain by between one and three storeys separated by third order (Allen, 1983) erosion surfaces. However, single storey sand bodies are most common and are mainly constructed from planar tabular cross-stratified lower parts that pass upward into trough cross-stratification and upper plane-bed lamination, commonly with an interference rippled upper surface. Where present, multi-storey sand bodies in the sequence commonly contain a single storey that is constructed from medium- to fine-grained sandstone lateral accretion surfaces (eg. Fig. 6.5). Preservation of the full vertical extent of a set of lateral accretion surfaces is inhibited by the erosive base of an overlying sandstone storey.

A rare lateral profile through a Sheet Sandstone Facies sand body is illustrated in Fig. 6.6 which shows that they consist of multilaterally arranged, third order erosion surfaces that define internal scours up to 15m wide and 150 cm deep. At Artariain, a roughly 100 x 100m natural pavement, exposing the upper surface of the sand body shown in Figs. 6.5 and 6.6, displays an undulating ridge and trough topography with up to 120 cm relief between troughs and ridges. The ridge crests are broadly curviplanar in plan view but appear to have no uniform orientation. It is proposed that these remarkable hummocks represent the shallow creek bed topography preserved by a combination of 'flashy' flood scouring and post-flood draping by fine sediment (L.T. Middleton: personal communication in 1987).

Correlated facies logs through a Conglomerate with Sandstone Facies sequence exposed to the north of the village of Olleta are illustrated in Fig. 6.7. Sheet-like conglomerate units, with erosive bases that display between 20 and 200 cm of relief, constitute between 35 and 48% of the Olleta sequences. They are separated by intervals of planar and erosively based sandstone and colour mottled siltstone. The clast-supported conglomerate bodies are between 50 and 550 cm thick and are commonly ill sorted to inversely graded. In general terms, they display a simpler internal structure than similar Bernues Formation conglomerate sequences. Olleta conglomerate bodies are dominated by massive conglomerate with few discernible internal erosion surfaces (ie. they are generally of single storey construction), however, immediately above the bases of some units occur planar cross-stratified conglomerates.

The finer-grained, inter-conglomerate intervals are characterised by colour mottled siltstone with packages of thin-bedded, planar based fine-grained sandstone and occasional erosively based, multistorey sandstone bodies. These sand bodies are up to 22m wide and have low width to thickness ratios of less than fifteen, suggesting that they are of ribbon type geometry (Friend *et al.* 1979). The ribbons have high relief, curviplanar erosive bases, which incise up to 250 cm into underlying siltstone, and are internally constructed from trough cross-stratified and subordinate current ripple laminated medium- to fine-grained sandstone. Significantly, in several examples the erosive bases of incoming conglomerate units occupy scours that mimic exactly the scour relief of an underlying, abandoned sandstone body.

The third main lithofacies recognised in the Uncastillo Formation of the Olleta sub-basin is the Ribbon Sandstone Facies whose typical deposits are illustrated in the composite photomosaics and interpretive line drawings of

Figs. 6.8 and 6.9. Vertically restricted exposures are characterised by single to multistorey and/or multilateral ribbon sand bodies with high relief erosive bases (50-200 cm incision) and width to thickness ratios of between 4.8 and 14.3. Individual sandstone storeys commonly fine upward from coarse- to fine-grained sandstone and they display well defined lateral accretion surfaces (eg. Fig. 6.8). In the example of a ribbon sand body illustrated in Fig. 6.9, lateral accretion surfaces occur as several simple, curviplanar surfaces that define the margin of an obliquely accreting channel migrating laterally and vertically, in an analogous way to climbing ripple lamination (Reineck & Singh 1980).

In addition to lateral accretion surfaces, the ribbon sandstone bodies display planar tabular and trough cross-stratification that alternates with thin intervals of upper plane-bed lamination. Scour base lags of intraformational mudstone and siltstone clasts commonly occupy the lowest parts of many of the sand bodies.

The siltstone dominated fines sequence between the ribbon sandstones is most notable for the total lack of colour mottling. Sand bodies are generally poorly interconnected due to their encasement in the pale brown siltstone with subordinate packages of planar based, thin-bedded sandstone up to 60 cm thick. Immediately beneath the erosive bases of sand bodies, and the proximal parts of their laterally equivalent 'wings' (Friend *et al.* 1979), sequences comprising gently dipping (5-10°), intensively burrowed and heterolithic (on a scale of centimetres) fine-grained sandstone and siltstone are common. These are laterally impersistent intervals up to three metres thick that mainly display current ripple lamination, where not obliterated by the bioturbation.

6.2.2 Palaeocurrents

The three rose diagrams that indicate dispersion directions in the Uncastillo Formation of the Olleta sub-basin (Fig. 6.2) are derived chiefly from measurement of the orientations of erosive channel margins and lateral accretion surfaces (Artariain and western Olleta, Fig. 6.2) and the AB planes of imbricated conglomerate clasts (Olleta, Fig. 6.2). The diagrams emphasise the fact that by Uncastillo Formation times, the Olleta sub-basin was a hydrologically isolated depocentre with a 'strong 'pull' of drainage toward its synclinal axis.

6.2.3 Fluvial palaeomorphology and clast provenance

The vertically restricted Conglomerate with Sandstone Facies of the Olleta sub-basin separates two fluvial lithofacies whose palaeomorphology and sandstone body geometry contrast strongly. Applying the equations of Allen

(1965), Cotter (1971), Khan (1971) and Leeder (1973) (see Section 4.2.4 for methodology), a mean palaeochannel width to depth ratio of 9.8 was calculated for Sheet Sandstone Facies sand bodies. This ratio compares with a mean value of 9.6 derived from sand bodies in the Ribbon Sandstone Facies. Thus, using the empirically derived palaeosinuosity equation of Schumm (1963), sinuosities of stream channels that deposited the two facies were calculated as being roughly equal at 1.89 and 1.9, respectively.

However, as a later section will demonstrate, there exists substantial evidence to suggest that these sinuosity values are not comparable because special conditions prevailed during deposition of the Ribbon Sandstone Facies that influenced the width to depth ratio of its channels, thus producing an exaggerated sinuosity value.

Provenance data for the Conglomerate with Sandstone Facies sequence exposed at Olleta is presented in Fig. 6.7. Measurement of the dimensions of reworked, Campodarbe Formation molasse clasts shows that the sequence coarsens upward, though there is no corresponding decrease in roundness as might be expected from a proximality increase implied by such upward coarsening. Significantly, of all the conglomerate sequences in the study area, the Olleta conglomerates display the most varied clast assemblage, being dominated by Campodarbe Formation clasts (75%), but with 17% igneous and metamorphic clasts from the Axial Zone and 8% Palaeocene limestone clasts.

6.2.4 Depositional environments

The Sheet Sandstone and Ribbon Sandstone Facies exhibit numerous features that are diagnostic of their deposition in fluvial environments.

(1) They comprise erosive margins that define the bases of sandstone-filled palaeochannels.
(2) There is a dominance of planar tabular and trough cross-stratification, and upper plane-bed lamination in the construction of the sand bodies. Such structures are typical within-channel bedforms and are indicative of deposition by migrating sand waves, sinuous crested dunes and high energy shallow water floods, respectively (Reineck & Singh 1980).
(3) They display abundant incipient to well developed lateral accretion surfaces representing lateral accretion of channel margin point bars (Allen 1963).
(4) A well developed, colour mottled (in the Sheet Sandstone Facies) fines sequence, typical of deposition in a floodbasin environment experiencing periodic wetting and drying (Bown & Kraus 1981), occurs between sand bodies.

Evidence for a degree of ephemerality is provided by the widespread occurrence of upper plane-bed lamination (cf. Tunbridge 1981) in the sand bodies and mud clast lined erosive scour lags (cf. Rust 1984). However, although only a relatively short period separated deposition of the two facies, during which time the Olleta sub-basin experienced no significant change in climate, vegetation or source lithology, the obvious contrast in alluvial architecture of the sheet and ribbon sand bodies suggests a rapid and major change in the regional tectonic regime.

Allen (1978) and Bridge & Leeder (1979) have simulated the controls on alluvial stratigraphy, or architecture, using computers to model the interactions between avulsion frequency, channel dimensions, channel zone of influence and subsidence rate. Where channel dimensions and avulsion frequency are fixed at a constant rate, then subsidence rate acts as the dominant control on determining whether sheet or ribbon type sand bodies develop. However, Blakey & Gubitosa (1984) have pointed out that the development of sheets or ribbons can be a function of whether the avulsion frequency to rate of subsidence ratio is high or low, respectively. It is suggested here that the Sheet Sandstone Facies was deposited by moderate to high sinuosity channels traversing an areally extensive and relatively low relief floodbasin in (cf. Section 4.2.5) experiencing slow subsidence. The rapidly subsiding floodbasin characteristic of Ribbon Sandstone Facies deposition, however, was areally restricted in extent, a factor that may largely be attributed to the entrenchment of palaeochannels and development of small palaeovalleys (see Section 6.3.4).

The Conglomerate with Sandstone Facies exposed at Olleta (Fig. 6.7) is interpreted as the product of an environment similar to that which deposited the conglomeratic Bernues Formation exposed at Gallipienzo (Chapter 5). Like at Gallipienzo, the Olleta sequence comprises alternating erosively based sand bodies, sheet type, thin-bedded sandstone, and erosively based, moderately sorted, massive conglomerate bodies, comparable to the lower member of the Carboniferous Cannes de Roche Formation described from Quebec by Rust (1981). Such a sequence was deposited on the distal parts of an alluvial fan, in the zone where the conglomeratic fan surface interfingers with a fluvial channel- and sheetflood-dominated profan, sandy apron. It is likely that the presence of albeit limited amounts of cross-stratified conglomerate records deposition by streamflood, as well as sheetflood processes, at the alluvial fan toe where a braided stream system developed (cf. McGowen & Groat 1971, fig. 30). The southward increase in thickness of the inter-conglomerate sandstone suites suggests a fairly high rate of subsidence and aggradation that increased southward, toward the centre of the sub-basin.

6.3 SOUTHERN PENA FLEXURE FLUVIAL SEDIMENTATION

6.3.1 General facies description

Along the length of the Pena flexure and northwestern Ebro basin margin, from the Ujue sub-basin to the Rio Arba valley and beyond, fan shaped conglomerate bodies of the Bernues Formation pass southward and stratigraphically upward into a facies characterised by sandstone bodies that display a mean width to depth ratio of less than fifteen. These ribbon sand bodies (Friend *et al.* 1979) form the Ribbon Sandstone Facies and are most prominently exposed on hillsides and in roadcuts near Ujue (Figs. 6.10 and 6.11), the Canal de las Bardenas (Fig. 6.12), Uncastillo (Figs. 6.13-6.17) and the Rio Arba valley (Figs. 6.18 and 6.19, Plate 6.1).

Laterally impersistent, lenticular sand bodies comprise between 27 and 50% of Ribbon Sandstone Facies sequences and form units up to 85m wide and 9m thick, with width to depth ratios of between four and twelve. The ribbons most commonly occur as uninterconnected, multistorey bodies with up to six vertically and laterally arranged storeys (eg. Fig. 6.15) defined by third order internal erosion surfaces. The sand bodies have smooth (eg. Fig. 6.15) to undulating (eg. Plate 6.1) erosive bases, with between 50 and 400 cm of erosive relief, and they commonly display well developed sandstone wings (eg. Fig. 6.18) that are laterally persistent for up to 100m from the sand body to which they are attached.

Of the twelve large, erosively based sandstones measured and profiled along the southern Pena flexure, nine of them display incipiently (eg. Figs. 6.11, 6.12 and 6.15) to well developed (eg. Fig. 6.16) lateral accretion surfaces along part of the sand body margin. The lateral accretion surfaces mainly indicate restricted lateral 'combing' distances of a few metres (and, more importantly, of only a fraction of preserved channel width), however, the example illustrated in Fig. 6.16 exhibits extensively developed lateral accretion surfaces that indicate a lateral combing distance of about 60m. Examination of the detailed morphology of the lateral accretion units shown in Fig. 6.16 reveals the abundance of internal reactivation surfaces, siltstone wedges, oversteepened surfaces and, in one part, a small slump or collapse zone. A second example of the type of obliquely migrating lateral accretion surfaces illustrated from the Olleta sub-basin in Fig. 6.9 is also shown from near Uncastillo in Fig. 6.17. Here, simple, curviplanar surfaces define the depositional margins of an obliquely accreting channel with an 'angle of climb' of approximately 30-35°.

In the eastern part of the study area, near Uncastillo and Luesia, the ribbon sand bodies are generally constructed from planar tabular cross-stratified and upper plane-bed laminated, weakly upward fining medium- to fine-grained sandstone, with subordinate current ripple lamination. However, Ribbon Sandstone Facies in the central and western parts of the southern Pena Flexure comprises erosively based bodies that are commonly filled with siltstone and thin-bedded, planar based fine-grained sandstone containing current ripple lamination and intensive bioturbation (eg. Figs. 6.11 and 6.12). Desiccation cracks and intraformational siltstone clasts commonly occur along the erosive bases of ribbon sandstone bodies across the study area.

The sandstones are generally encased in a fines sequence dominated by massive, unmottled, pale brown siltstone and packages of stacked, planar based, thin-bedded and burrowed fine-grained sandstone. No evidence of even the most embryonic calcrete development or pedogenesis has been observed in the fines sequence. Restricted intervals of heterolithic (on a scale of centimetres), siltstone and fine-grained sandstone, up to three metres thick, are preserved beneath some sand bodies and the near-channel parts of their sandstone wings (eg. Fig. 6.18). These sequences dip gently away from sand bodies at angles of up to 10° and contain thin-bedded, planar based sandstone dominated by current ripple lamination and common bioturbation.

6.3.2 Palaeocurrents

In Fig. 6.2, palaoecurrent directions displayed by the Ujue, Canal de las Bardenas, Uncastillo and Arba diagrams are mainly inferred from measurement of erosive sand body margins and lateral accretion surfaces. The rose diagrams from Uncastillo and the Rio Arba preliminarily confirm, at least in this study area, the more extensive results of Hirst & Nichols (1986) who recognised two alluvial distribution systems along the northern margin of the western Ebro basin. These systems had their apices located at structural lows along the topographic break between the Exterior Sierras and the Ebro basin. The westernmost of the two radial distributory systems, the Luna System (Nichols 1987), had its apex in the valley of the Rio Arba, and hence, palaeocurrents would have spread radially from that point. The Ujue and Canal de las Bardenas palaeocurrent data suggests the presence of another radial alluvial system, the Ujue System, with an apex located at the northern margin of the Ujue sub-basin.

6.3.3 Fluvial palaeomorphology

The gentle dip of the rocks of the early Miocene Ribbon Sandstone Facies implies that the palaeomorphological characteristics of channels that

formed the sand bodies may often be observed directly in the field. This contrasts with exposure conditions of, say, the Petilla Member Sheet Sandstone Facies where, because they are now vertical, the recognition and recording of channel features is less straightforward.

Although sand bodies of the Ribbon Sandstone Facies are variable in their dimensions, the palaeomorphologic characteristics of a typical ribbon sandstone are summarised in Fig. 6.20. The sinuosity value of 1.14 presented in this diagram is derived from equations given by Langbein & Leopold (1966) and Miall (1976) (see Section 4.2.4) which relate mean changes in palaeocurrent azimuths between superjacent sand bodies in a sequence, to channel sinuosity. Otherwise, the channel, meander loop and meanderbelt dimensions are derived directly from field observations. The data presented in Fig. 6.20 shows that Ribbon Sandstone Facies palaeochannels were characterised by a low width to depth ratio and sinuosity, and that they drained across floodplains experiencing rapid to very rapid rates of overbank fines aggradation.

Confidence in the values presented in Fig. 6.20, particularly sinuosity, may be gained from inspecting similar, low width to depth ratio, ribbon type sand bodies, also of early Miocene age, deposited in an analogous setting in the central part of the Ebro basin. For example, flat lying sandstone bodies near Caspe in Huesca, are preferentially weathered from their surrounding overbank material so that they now form upstanding, curvilinear ridges that reflect the morphology of the Miocene palaeochannel directly. Individual sandstones in the Caspe 'ribbon fields' (Riba *et al.* 1967; Williams 1975; Friend *et al.* 1986) are up to 300m in length, along which they display mild sinuosities of 1.2 or less.

6.3.4 Depositional environments and the tectonic significance of the ribbon sandstone bodies

Within the Ribbon Sandstone Facies the following features provide evidence for its deposition in a floodbasin traversed by fluvial channels.

(1) Laterally impersistent sandstone and siltstone filled lenticular bodies with erosive bases and many typical within-channel bedforms.

(2) Incipiently to extensively developed lateral accretion surfaces at the margins of sand bodies are common.

(3) Preservation of near-channel, heterolithic sandstone-siltstone sequences that conform with descriptions of modern and ancient levee deposits by Singh (1972), Allen *et al.* (1983) and Farrell (1987) (eg. Fig. 6.18).

Therefore the Petilla Member to Uncastillo Formation evolution of the Pena flexure was sedimentologically dominated by two episodes of fluvial deposition, punctuated by a relatively short interval of alluvial fan deposition. However, despite the close temporal and spatial proximity of the Petilla Member and Uncastillo Formation, they display a striking contrast in alluvial architecture and sand body geometry that cannot be explained in terms of a major change in climate, bank composition or other autocyclic factors. The main sedimentological features considered here to be of regional significance in interpreting the controls on Ribbon Sandstone Facies deposition include the following observations.

(1) There are sandstone bodies encased in fines that display width to depth ratios of less than fifteen.
(2) Lateral accretion surfaces are of limited extent thus implying a restricted width of meanderbelt influence.
(3) Concave-upward cut-and-fill erosion surfaces dominate the internal structure of the sand bodies.
(4) Preservation of levee deposits (eg. Fig. 6.18) and the total absence of incipient palaeosol-related mottling or calcrete development in the overbank sequence are especially noteworthy.
(5) Some spectacularly extensive sandstone wings are preserved (eg. Fig. 6.18).
(6) Palaeovalleys preserve up to six vertically stacked ribbon sandstone bodies (eg. Fig. 6.19) encased in overbank fines.
(7) Two examples of obliquely migrating or 'climbing' lateral accretion surfaces (eg. Figs. 6.9 and 6.17) are preserved. Friend *et al.* (1981, fig. 4.38) have described similar oblique accretion surfaces from Campodarbe Formation fluvial sediments in the eastern part of the Jaca basin. They interpreted this arrangement as reflecting a transition between meandering (laterally accreting) streams and braided (vertically accreting) streams.

The above seven distinctive attributes of the Ribbon Sandstone Facies are recognised as being unique in the study area. They combine to provide substantial evidence for the importance of vertical accretion in both the overbank and within-channel fluvial sub-environments of the Ribbon Sandstone Facies. It could be argued that, on their own, observations such as restricted width to depth ratios, restricted lateral accretion surface development and the preservation of palaeovalleys (representing areas of high channel

nucleation) imply that the ribbon sand bodies could equally have been deposited by vertically incising (as opposed to vertically aggrading) streams. However, the abundance of cut-and-fill structures, preservation of near-channel levees, sandstone wings and obliquely migrating lateral accretion surfaces, and the lack of evidence for palaeosols, all indicate deposition in an environment characterised by a high sediment preservation potential. If the Ribbon Sandstone Facies were deposited at a time of falling base level, and hence strong downcutting of streams, sediment preservation would have been low to negligible, particularly in the overbank sub-environment. It is therefore proposed here that a rising base level, or high rate of basin floor subsidence, controlled the architecture of the Ribbon Sandstone Facies through a mechanism of maximising sediment preservation potential.

Deposition was dominated by low to moderate sinuosity sandy stream systems that drained radially southward (Fig. 6.2) from apices located along the newly created topographic front represented by the Pena flexure (cf. Hirst & Nichols 1986). In conjunction with the relatively low width to depth ratio, and hence the restricted floodplain extent, characteristic of tectonically youthful mountainfront valleys (as would have characterised the south flank of the Pena flexure) (Rockwell *et al.* 1986), the high rate of floodbasin aggradation led rapidly to channel entrenchment and stunted meanderbelt development.

Applying the method of Collinson (1978), meanderbelt width of the ribbon sand bodies was compared with the potential width that meanderbelts could theoretically have attained. The results confirm that for even the most extensively developed point bar units (eg. Fig. 6.16), there is a large and significant discrepancy between actual and potential maximum meanderbelt widths. It is reported here that restricted meanderbelt widths in Ribbon Sandstone Facies palaeochannels provides strong evidence for the influence of a major external control hindering meander development.

It is also likely that a high floodplain aggradation rate, with consequent channel entrenchment and suppressed meanderbelt development, led to a higher than average avulsion frequency as a result of hydrological metastability, particularly during flood. Allen (1965) and Leeder (1975) have noted a widespread increase in the amount of overbank deposition toward channel margins, a phenomenon implying that exceptionally high rates of overbank deposition may have typified those parts of the floodplain immediately adjacent to channels. This process would have enhanced channel instability by maximising the height difference between active channel segments and surrounding parts of the floodplain, and thus increasing bank strength.

Considering the limited floodplain extent and likely floodplain topography, which comprised a series of small valleys and interfluves, it is perhaps not surprising that, following avulsion, channels frequently relocated on sites vertically coincident with an underlying, abandoned channel segment (eg. Fig. 6.19). This mechanism established palaeovalleys in which the degree of sandstone body interconnectedness depends on the amount of floodbasin aggradation during the time that lapsed between a site's abandonment and reoccupation by a succeeding channel. It may be that this limit on the number of floodbasin sites available for relocation following avulsion explains the relatively large size of Ribbon Sandstone Facies palaeochannels (compare width and depth values shown in Figs. 4.7 and 6.20). A typical active channel during Uncastillo Formation times had a mean cross sectional area of 200m^2, although maximum cross-sectional areas are closer to 750 m^2.

Among the factors that may influence channel dimensions are position in the fluvial hierarchy (Friend 1978), seasonality and ephemerality of flow (Friend *et al.* 1986; Miall 1976), residence interval between avulsions (Allen 1978; Bridge & Leeder 1979), load type (Schumm 1960) climate (Shepherd 1978) and tectonics. It is considered here that an increase in ephemerality and a change in tectonic conditions (mainly an increased subsidence rate) are responsible for the greater channel size in Ribbon Sandstone Facies palaeochannels. Despite being difficult to diagnose unequivocally, ephemeral flow is indicated by the following observations.

(1) Upper plane-bed lamination and waning flow sedimentary structures (cf. Tunbridge 1981) are present in many of the multi stage fills of the sand bodies.
(2) Abundant reactivation surfaces, such as illustrated in the lateral accretion surfaces of Fig. 6.16, suggest rapid, 'flashy' fluctuations in flow.
(3) There exist sandstone bodies, such as that illustrated in Plate 6.1, in which irregularly distributed patches of incipient lateral accretion surfaces overlie an undulating, erosive base. This architecture is interpreted by Friend *et al.* (1981, fig. 4.39) as recording a history of successively alternating episodes of stable, lateral channel accretion with ephemeral, flood-induced scouring.

Leopold *et al.* (1964) stated that for 75% of the time, discharge fills a channel to less than one third of its bankfull depth. Thus, if ephemeral flow was an important process during deposition of the Ribbon Sandstone Facies

then, in combination with enhanced entrenchment and levee construction, it is conceivable that these channels were usually filled to a level that was only a fraction of their preserved bankfull depth. it is therefore likely that the greater size of Ribbon Sandstone Facies Sand bodies does not necessarily reflect a greater than average discharge.

In summary, the Ribbon Sandstone Facies is interpreted as the product of a distinctly aggradational episode of fluvial sedimentation, with strong vertical accretion induced mainly by rapid subsidence. Similar aggradational sequences have recently been described, in which lateral stability and vertical accretion were induced by climate (eg. Shepherd 1978), volcanism (eg. Smith 1987), autocyclic processes (eg. Behrensmeyer & Tauxe 1982) and tectonics (eg. Nami & Leeder 1978; Behrensmeyer & Tauxe 1982; Kraus & Middleton 1987; Shuster & Steidtmann 1987).

6.4 BASIN CONFIGURATION

The cessation of major thrust displacement in the study area led to the waning of alluvial fan deposition and gave way to an episode of sandy fluvial deposition and denudation of the recently created tectonic landscape. However, the recent structural activity during Bernues Formation times imposed a significantly greater rate of basin subsidence and a steeper depositional slope on the peripheral depocentres in the Izaga and Olleta sub-basins, and along the southern Pena flexure.

A schematic palaeoenvironmental model of the study area during Uncastillo Formation deposition is presented in Fig. 6.21. It depicts an accelerated basin subsidence rate and steeper depositional slope exerting a profound influence on stream and floodplain morphology and regional patterns of fluvial dispersion. The map (Fig. 6.21) shows that the Olleta sub-basin and southern flank of the Pena flexure were characterised by radial, distributary, fluvial systems comprising minor apexal alluvial fans and sandy ephemeral streams that issued from apices located at structurally controlled low points along the length of the Pena flexure and the Alaiz-Ujue oblique ramp. These low sinuosity streams drained rapidly aggrading floodplains of limited aereal extent and, in the Ebro basin, formed part of much larger terminal fan systems (cf. Mukerji 1976; Parkash *et al.* 1983) that terminated up to 60 km downstream in large, central basin lake complexes (Friend 1978; Hirst & Nichols 1986).

The Izaga sub-basin remained as an isolated centre of increasingly proximal, southward dispersing alluvial fan deposition throughout Uncastillo Formation times. Continued alluvial fan sedimentation in the Izaga sub-basin

reflects reversion of the forelandward propagating thrust system toward the hinterland as orogenic stresses declined, and hence, reactivation of closer, pre-existing thrusts became mechanically favourable (cf. Morley 1987). A similar process of hinterland reversion is recorded by the early Miocene reactivation of the Sierra de Alaiz thrust which swung approximately 45° in an anticlockwise rotation, about a pivot point at its eastern end (Fig. 6.21).

The latest emergent thrust in the study area, and possibly the latest in the entire southern Pyrenees, developed to the south of Tafalla where it emplaced Petilla Member and Bernues Formation siltstone and gypsum onto Uncastillo Formation sandstone.

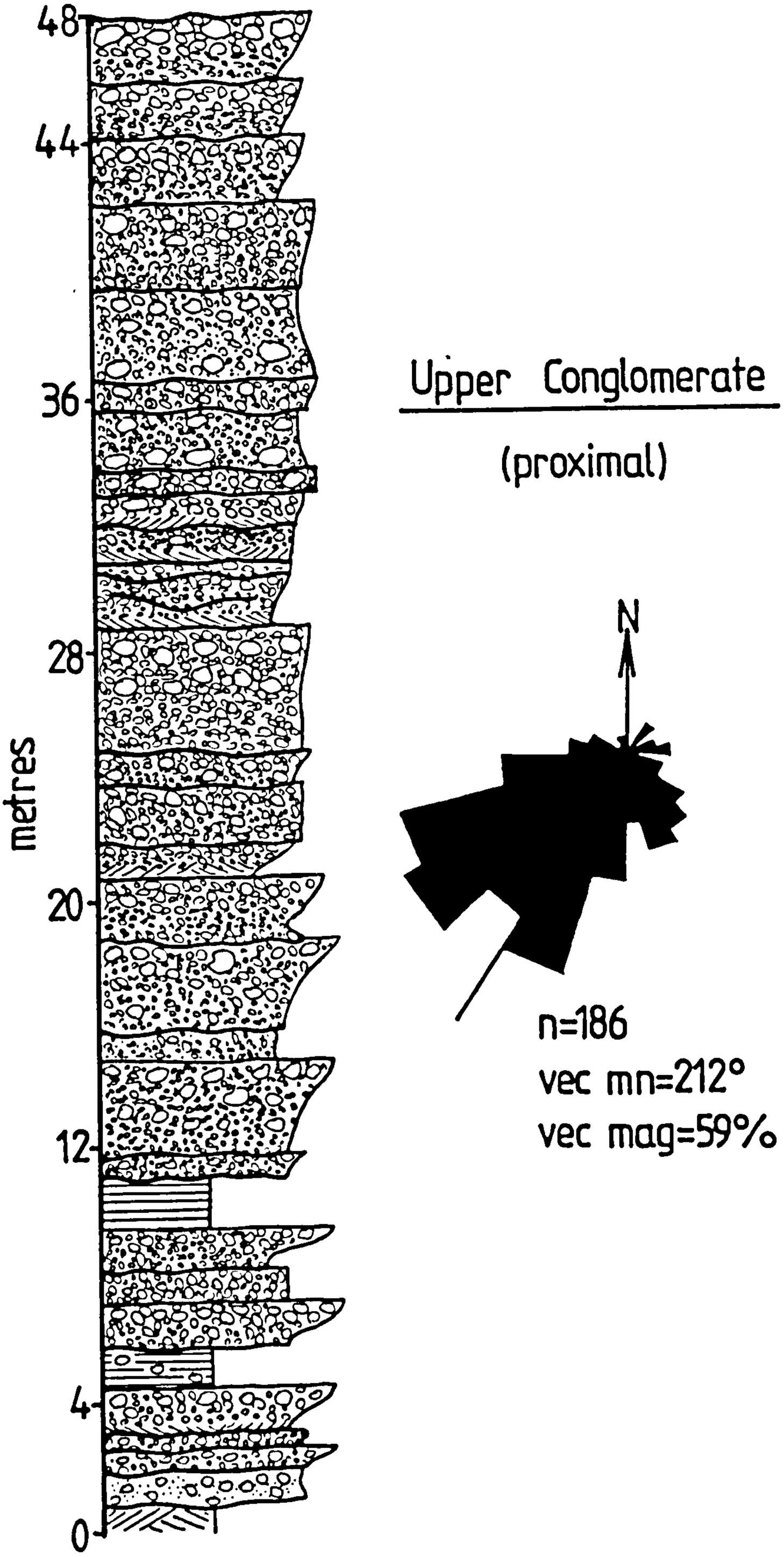

Fig. 6.1. Uncastillo Formation Massive Conglomerate Facies in the Izaga sub-basin: graphic log and palaeocurrent rose diagram. Compare the dispersion of palaeocurrents displayed by the rose diagram with the more distal Conglomerate with Sandstone Facies of the Izaga sub-basin shown in Fig. 5.8.

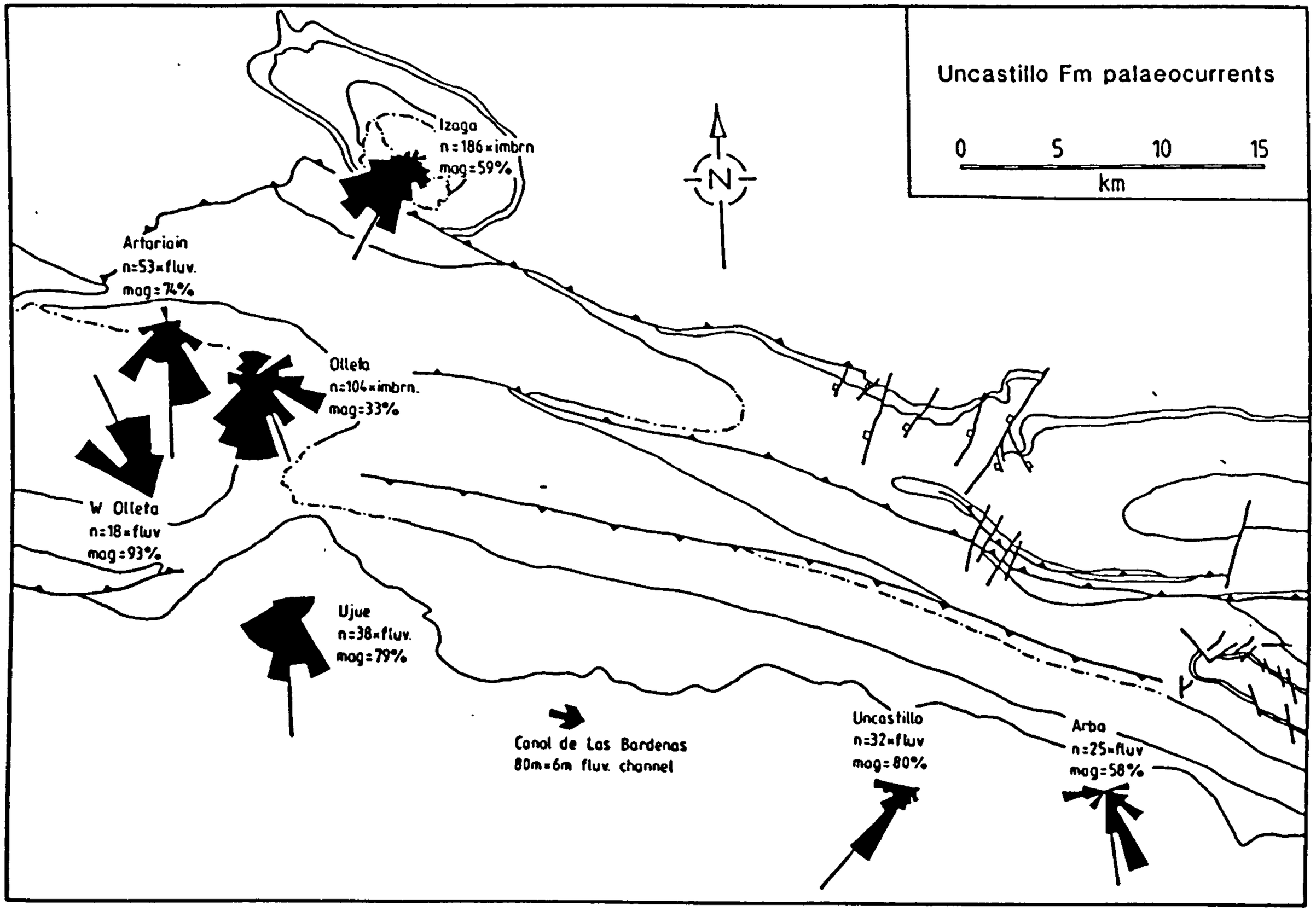

Fig. 6.2. Palaeocurrent rose diagrams depicting Uncastillo Formation dispersion directions in the study area. Structural symbols and lithostratigraphic contacts as in Fig. 1.3.

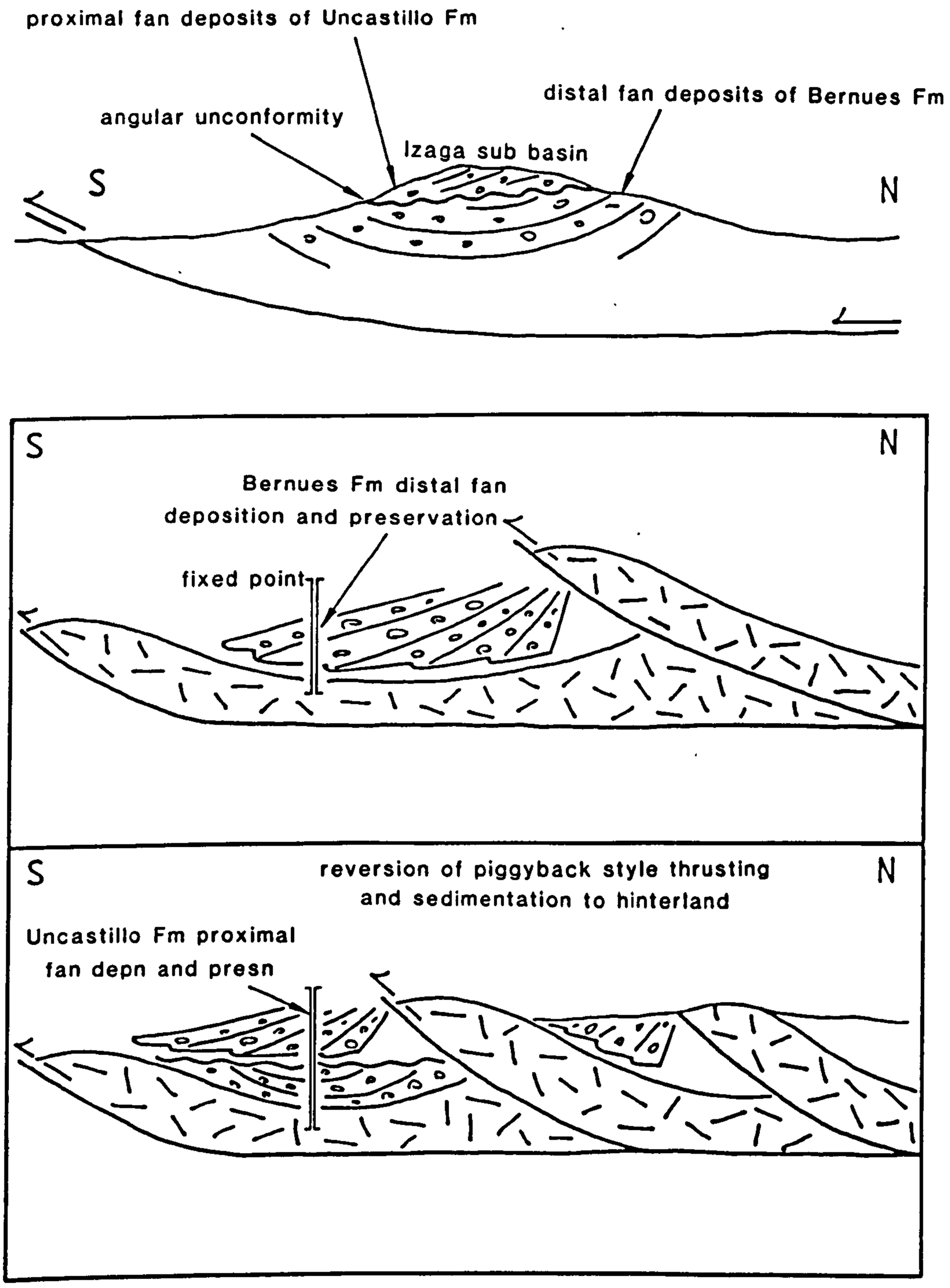

Fig. 6.3. Model to explain the sudden jump in proximality recorded by the Izaga sub-basin alluvial fan system between deposition of the Bernues and Uncastillo Formations. Stipple depicts pre-Bernues Formation stratigraphy.

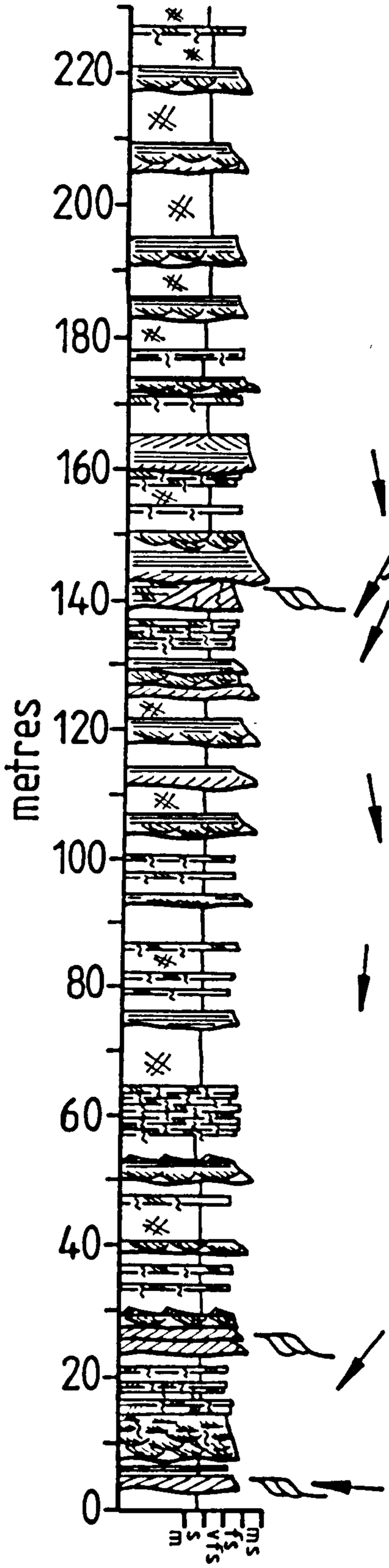

Fig. 6.4. Uncastillo Formation Sheet Sandstone Facies at Artariain, Olleta sub-basin: graphic log.

Fig. 6.5. Photomosaic and interpretive line drawing of fine-grained sandstone lateral accretion surfaces beneath a seven metre thick sand body (143m in Fig. 6.4) at Artariain, Olleta sub-basin.

Fig. 6.8. Photomosaic and interpretive line drawing of a flat lying two storey palaeochannel in Ribbon Sandstone Facies five kilometres west of Artariain, Olleta sub-basin. The lower storey displays well developed lateral accretion surfaces.


SSE
palaeocurrent vec mn=203°
NNW
0 1 2 3 4 5
metres

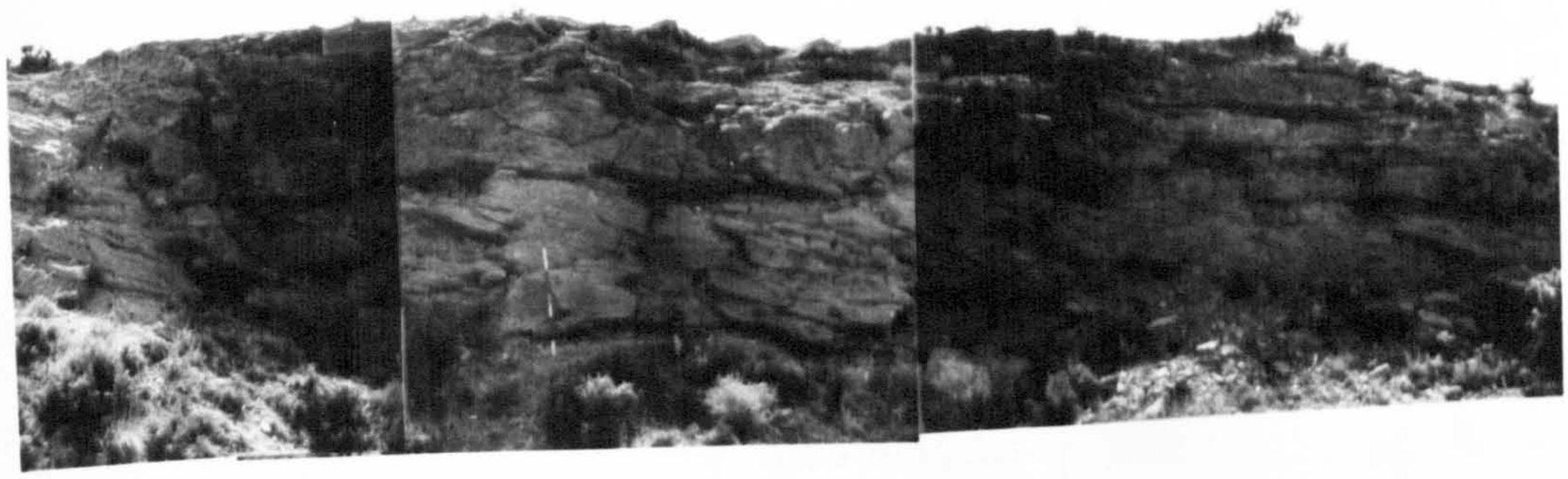
NE
palaeocurrent vec mn=190°
palaeochannel width:depth=9·2
SW
0 5 10
metres

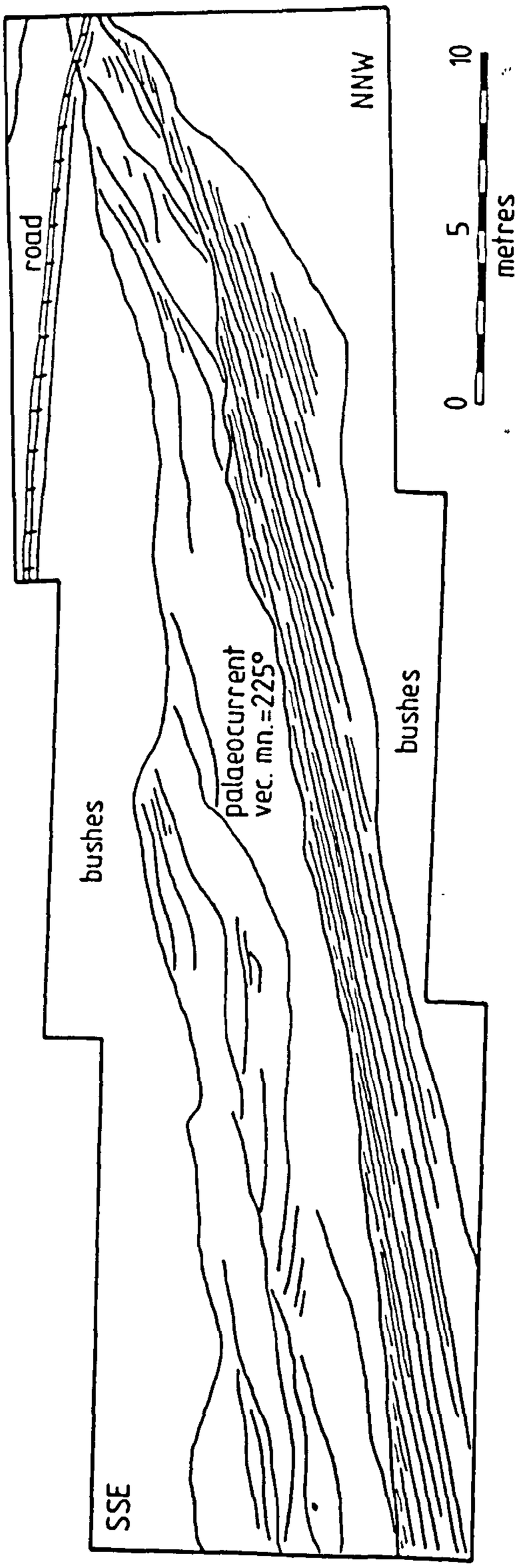

Fig. 6.6. Interpretive line drawing traced from a photograph showing a lateral profile through a Sheet Sandstone Facies sand body (143-150m in Fig. 6.4) at Artariain, Olleta sub-basin.

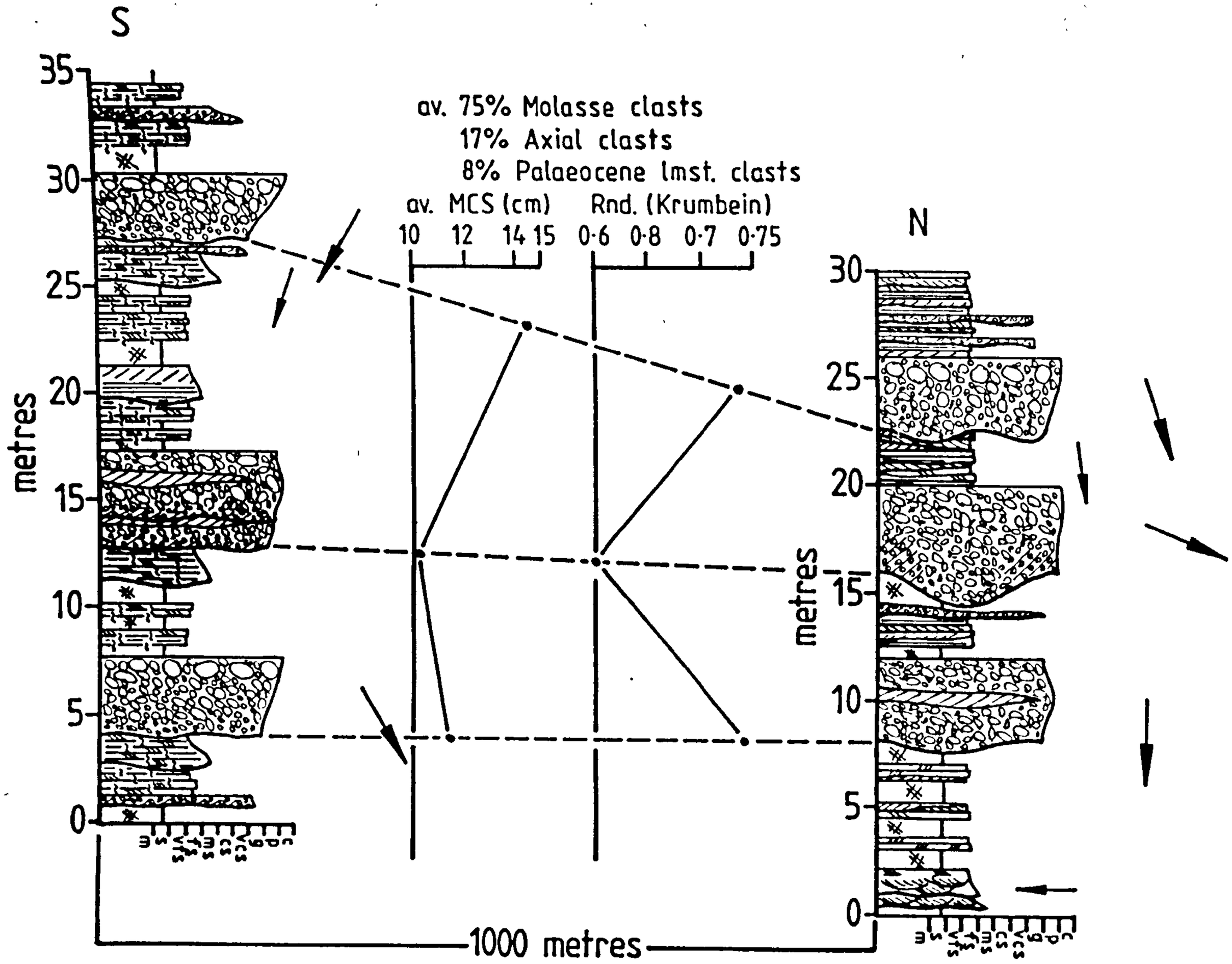

Fig. 6.7. Uncastillo Formation Conglomerate with Sandstone Facies at Olleta, Olleta sub-basin: correlated graphic logs. Also shown are data for maximum clast size (MCS) and roundness (rnd.) of reworked molasse clasts through the sequence, and the conglomerate clast lithological assemblage.

Fig. 6.9. Photomosaic and interpretive line drawing of a flat lying palaeo-channel in Ribbon Sandstone Facies at Maqurriain, Olleta sub-basin. Note the well developed, planar asymptotic cross-stratification climbing up 'obliquely accreting' lateral accretion surfaces.

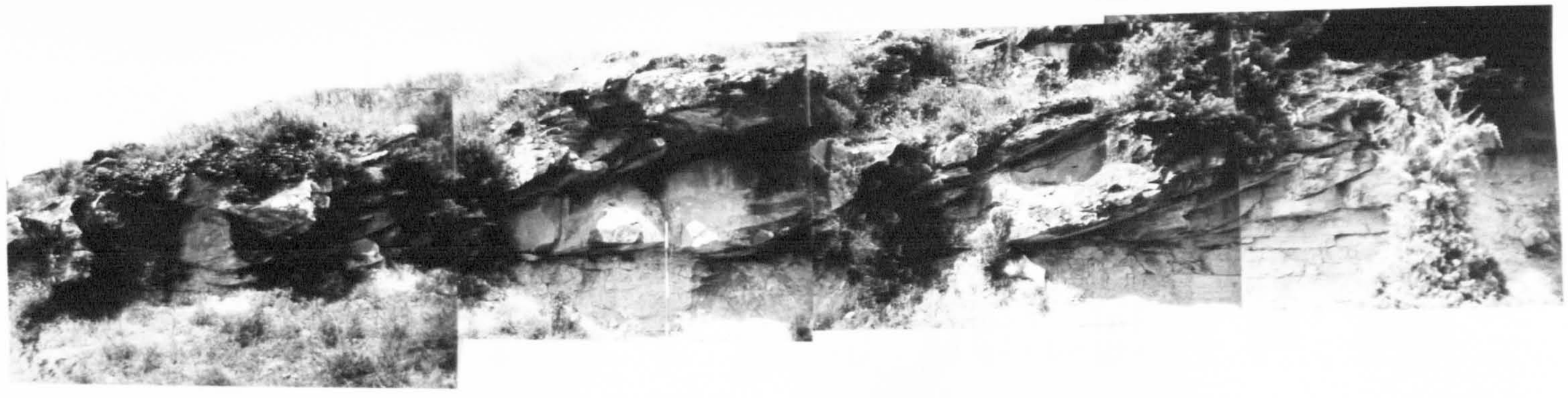

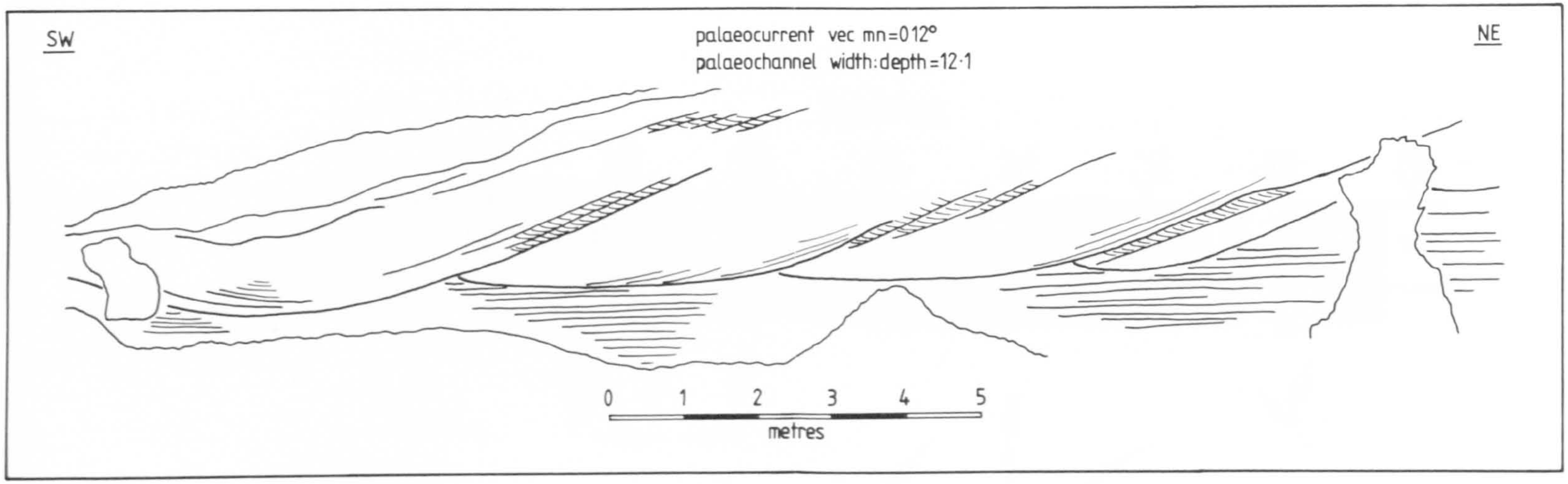
SW
palaeocurrent vec mn=012°
palaeochannel width:depth=12·1
NE
0 1 2 3 4 5
metres

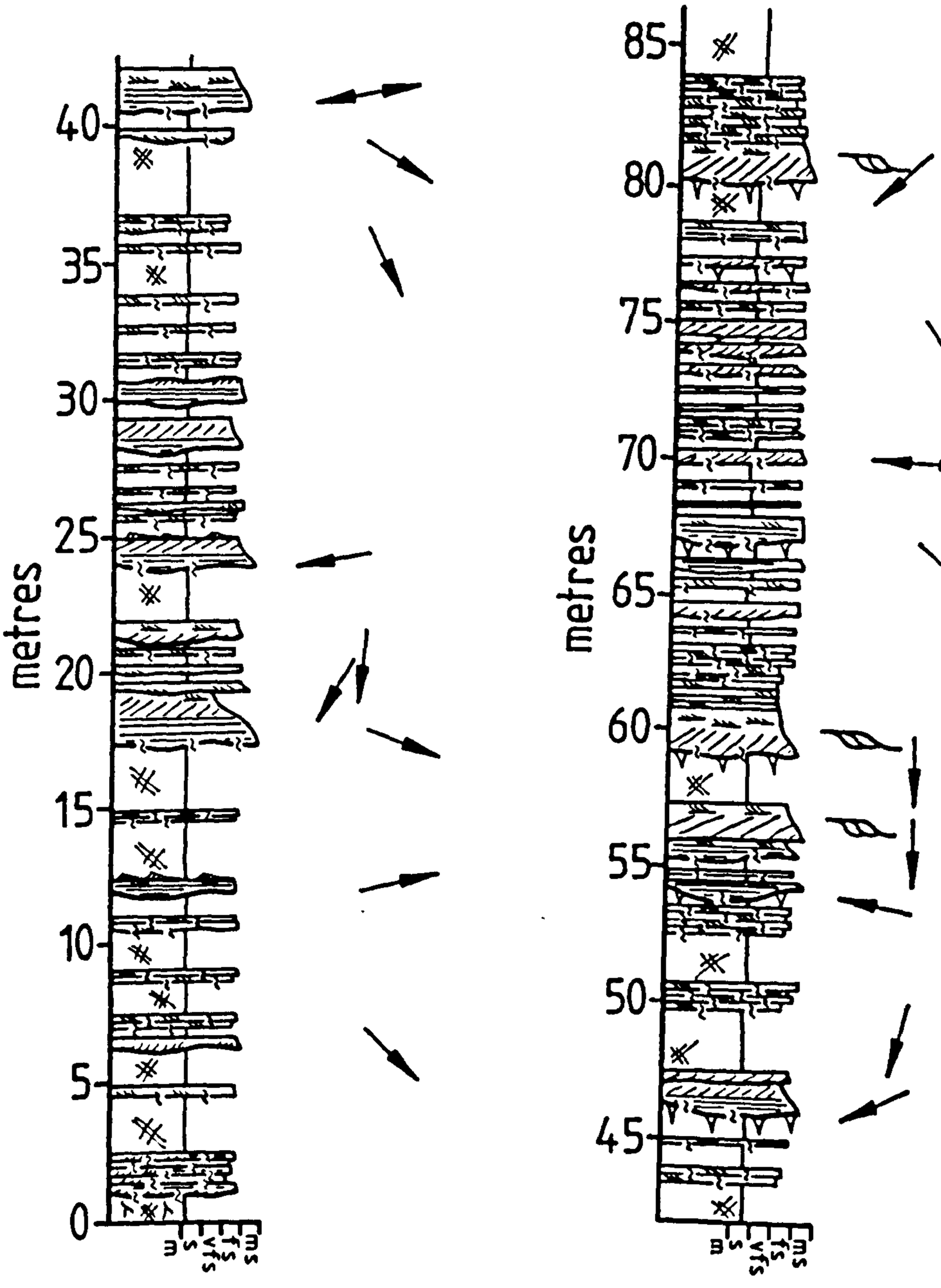

Fig. 6.10. Uncastillo Formation Ribbon Sandstone Facies ten kilometres south of Ujue, Ujue sub-basin: graphic log.

Plate 6.1. Photomosaic of a flat lying palaeochannel in the Ribbon Sandstone Facies of the Rio Arba valley. Note the highly irregular erosive base and poorly developed lateral accretion surfaces. Northeast is to the left; scale bar is five metres.

Fig. 6.11. Photomosaic and interpretive line drawing of a flat lying, fine-grained sandstone- and siltstone-filled palaeochannel in Ribbon Sandstone Facies ten kilometres south of Ujue, Ujue sub-basin (80-82m in Fig. 6.10). Note the poorly developed lateral accretion surfaces at the channel margins.

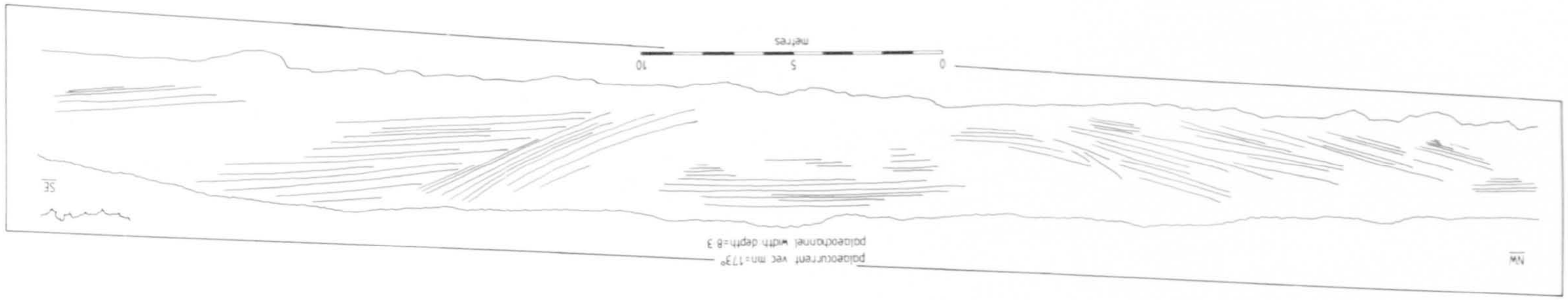
NW
SE
palaeocurrent vec mn:173°
palaeochannel width:depth=8:3
0
5
10
metres

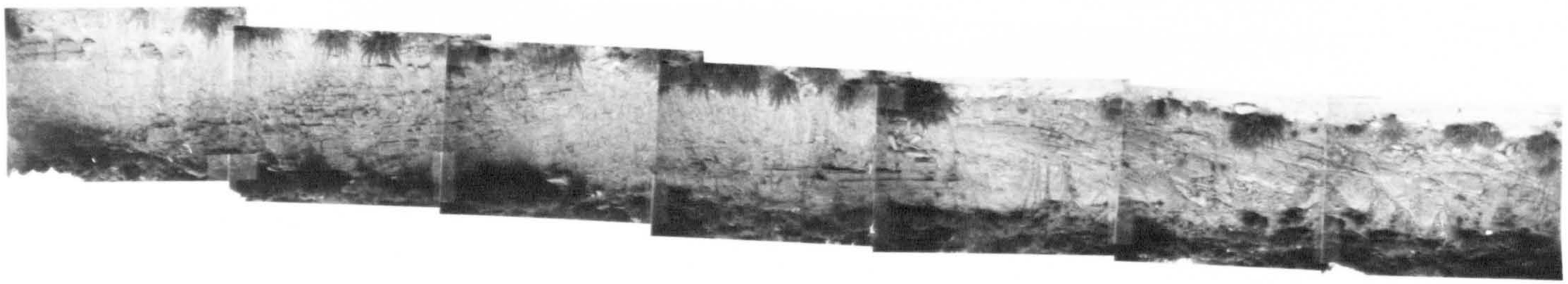

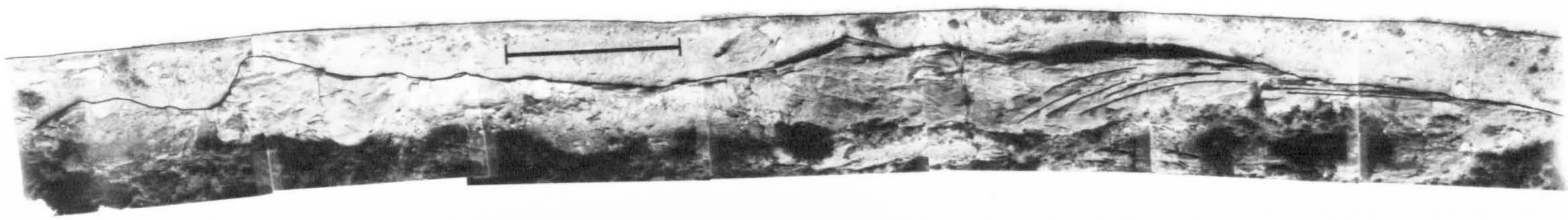

Fig. 6.12. Photomosaic and interpretive line drawing of a flat lying, fine grained sandstone- and siltstone-filled palaeochannel in Ribbon Sandstone Facies exposed beside the Canal de las Bardenas, nine kilometres south of Caseda. Note the large size of the channel and its poorly developed lateral accretion surfaces.

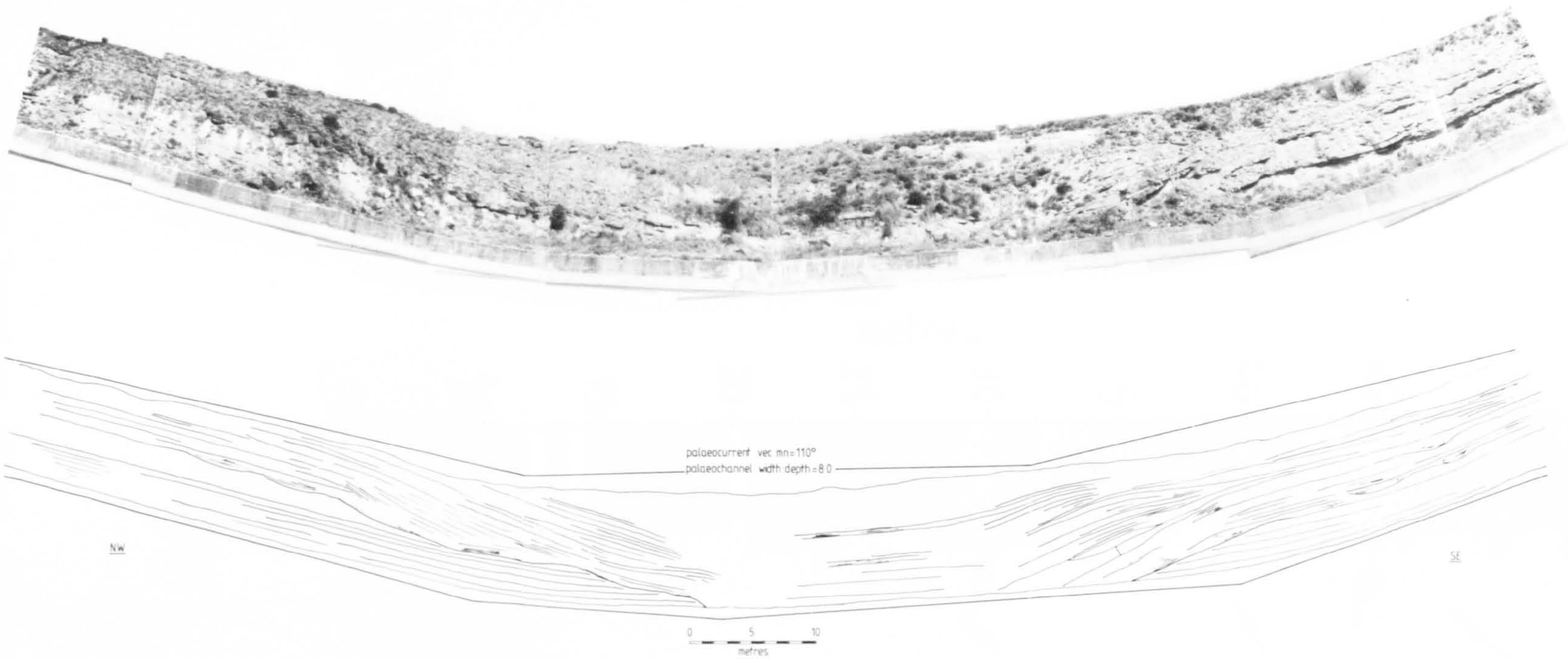
palaeocurrent vec mn=110°
palaeochannel width depth=8 0
NW
SE
0
5
10
metres

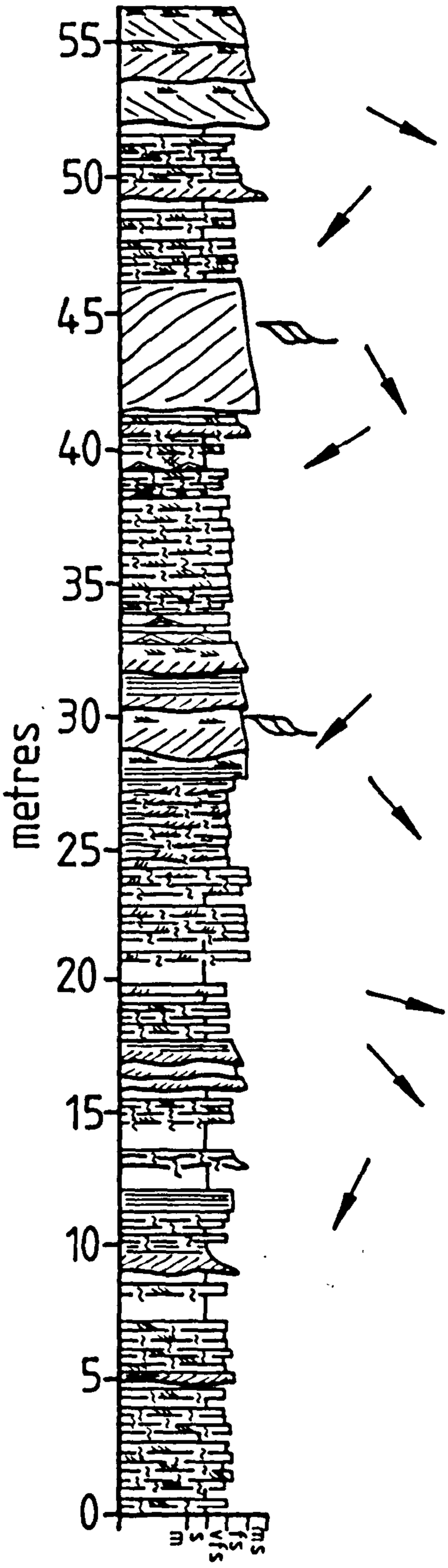

Fig. 6.13. Uncastillo Formation Ribbon Sandstone Facies at Uncastillo: graphic log.

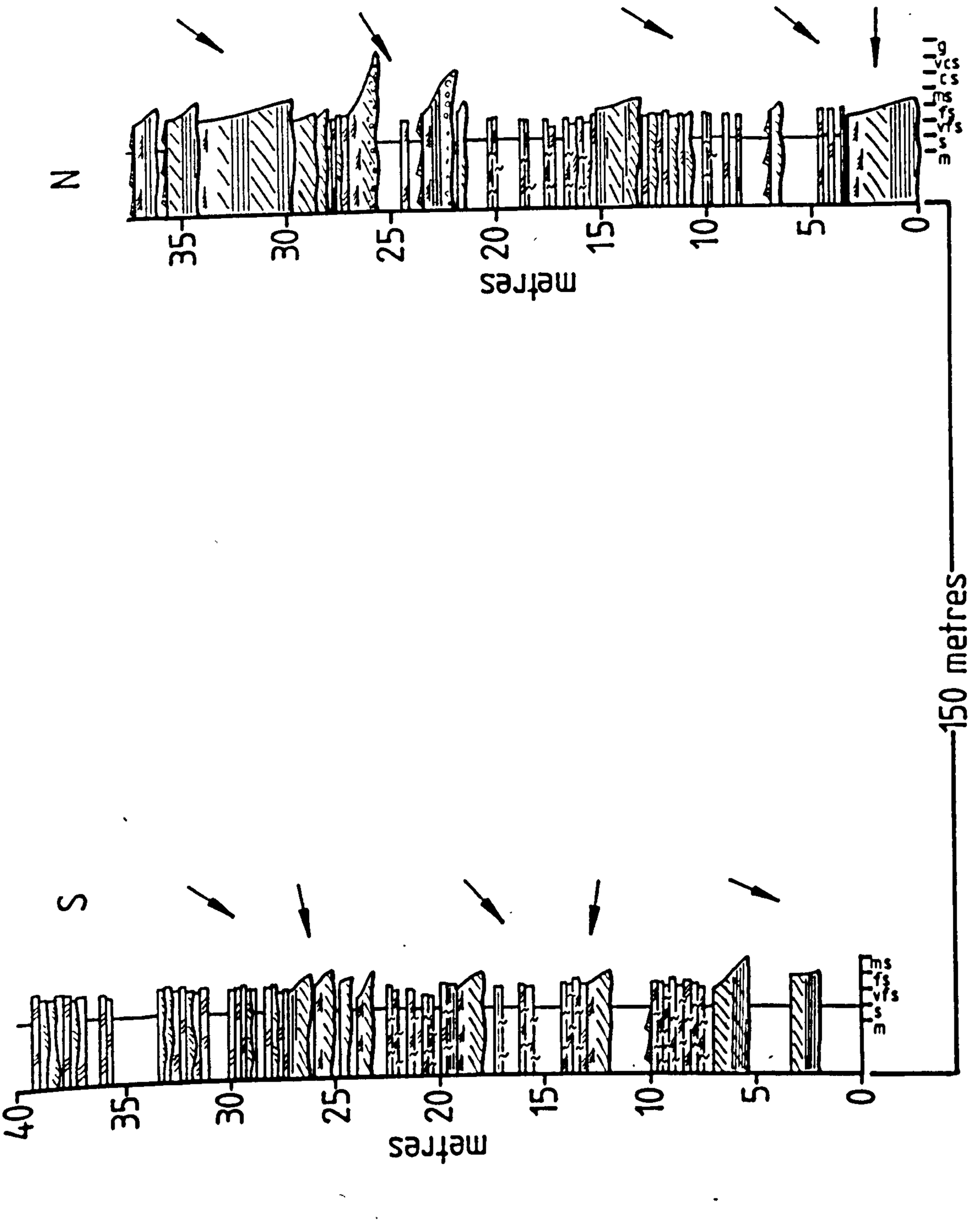

Fig. 6.14. Uncastillo Formation at Uncastillo: cor-related graphic logs.

Fig. 6.15. Photomosaic and interpretive line drawing of a flat lying, multi-storey palaeochannel in Ribbon Sandstone Facies at Uncastillo. Note the preservation of clearly defined depositional and erosive margins, with poorly developed lateral accretion surfaces on the depositional margins.

Fig. 6.17. Photomosaic and interpretive line drawing of a flat lying palaeochannel in Ribbon Sandstone Facies five kilometres north of Uncastillo. Note the well developed 'oblique accretion' surfaces, similar to those illustrated in Fig. 6.9.

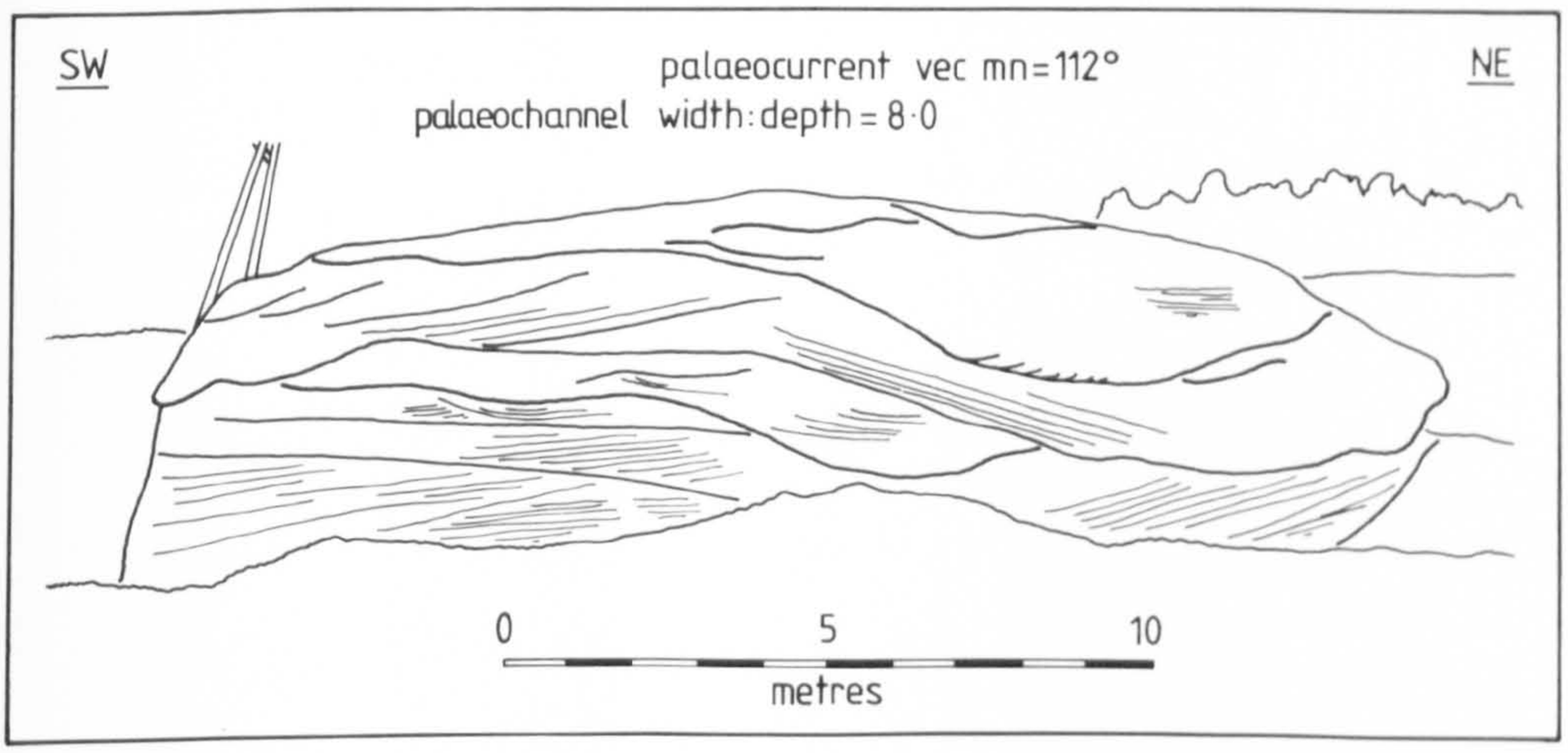
SW
palaeocurrent vec mn=112°
palaeochannel width:depth = 8·0
NE
0
5
10
metres

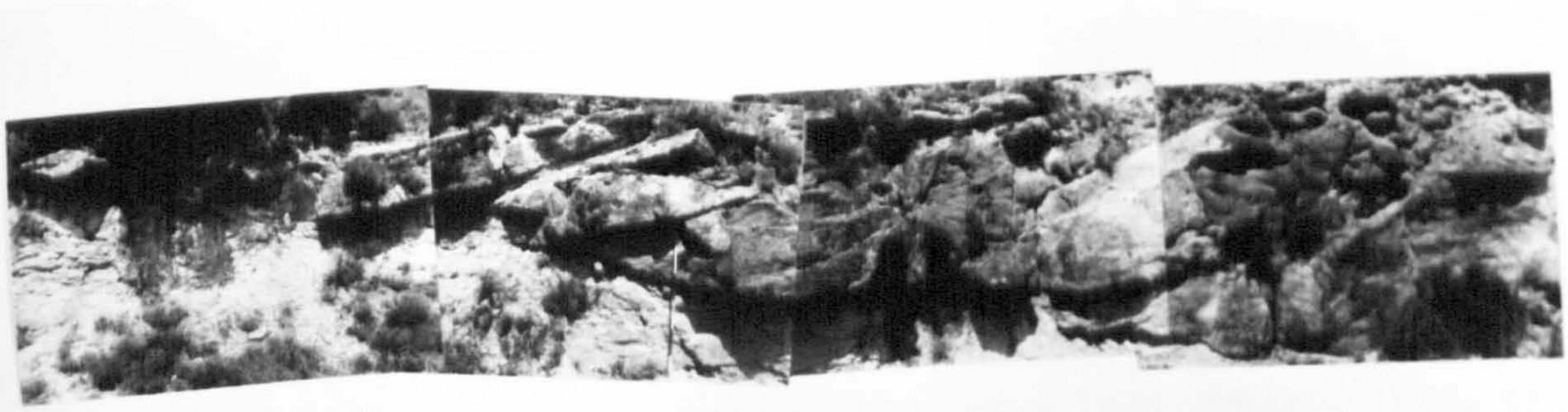

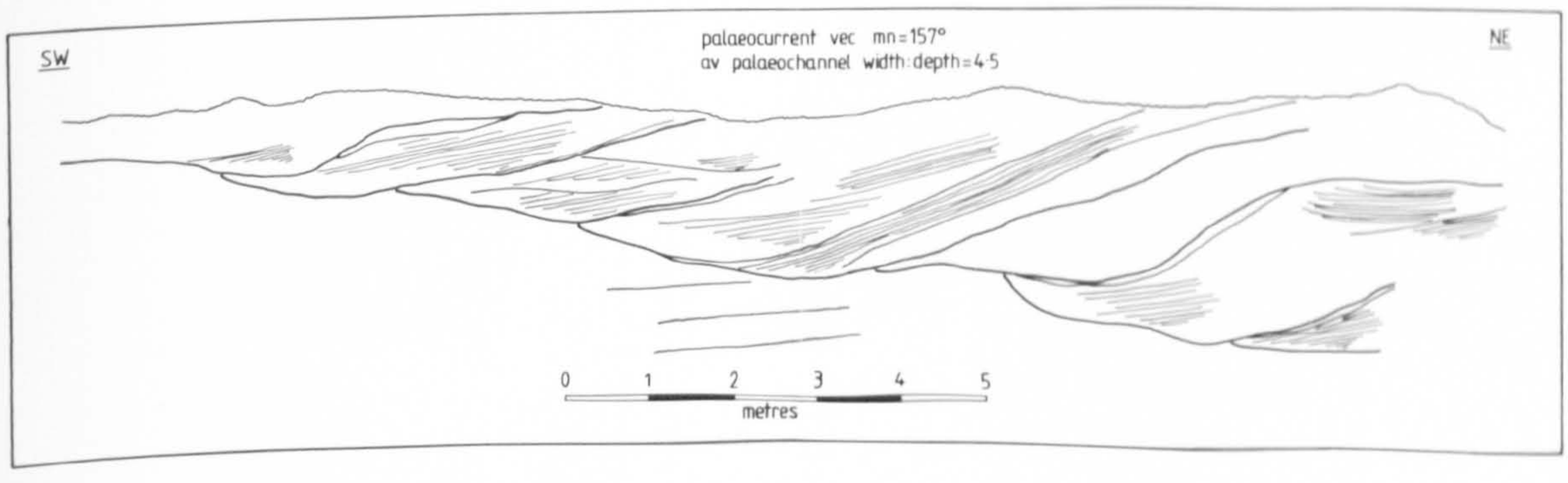
SW
palaeocurrent vec mn=157°
av palaeochannel width:depth=4·5
NE
0
1
2
3
4
5
metres

Fig. 6.16. Photomosaic and interpretive line drawing of a flat lying palaeochannel in Ribbon Sandstone Facies at Uncastillo. Note the well developed lateral accretion surfaces migrating from right to left and a thicker-bedded, channel fill sequence on the left.

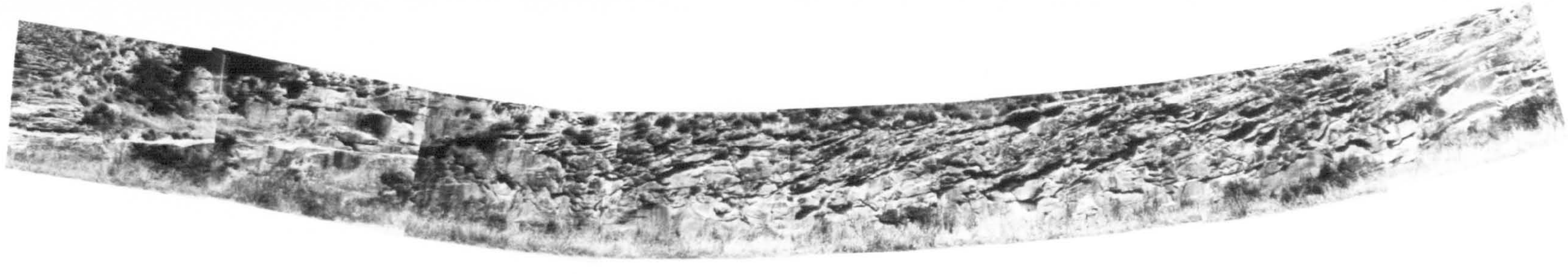

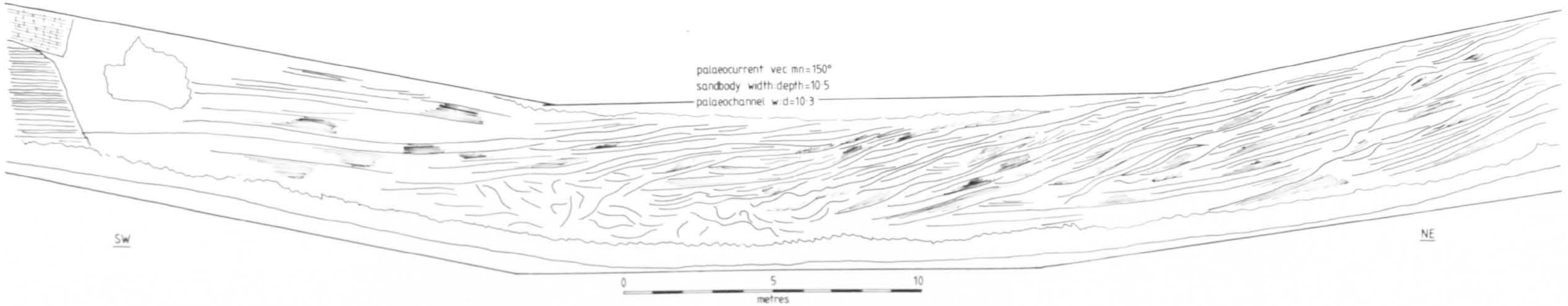
palaeocurrent vec mn=150°
sandbody width:depth=10:5
palaeochannel w:d=10:3
SW
NE
0
5
10
metres

Fig. 6.18. Photograph and interpretive line drawing of a flat lying, multi-storey palaeochannel in Ribbon Sandstone Facies exposed beside the Rio Arba. Note the well developed sandstone wings, that extend laterally for 150m, and the heterolithic levee deposits, beneath the near-channel parts of the wings, that dip gently away from the palaeochannel axis.

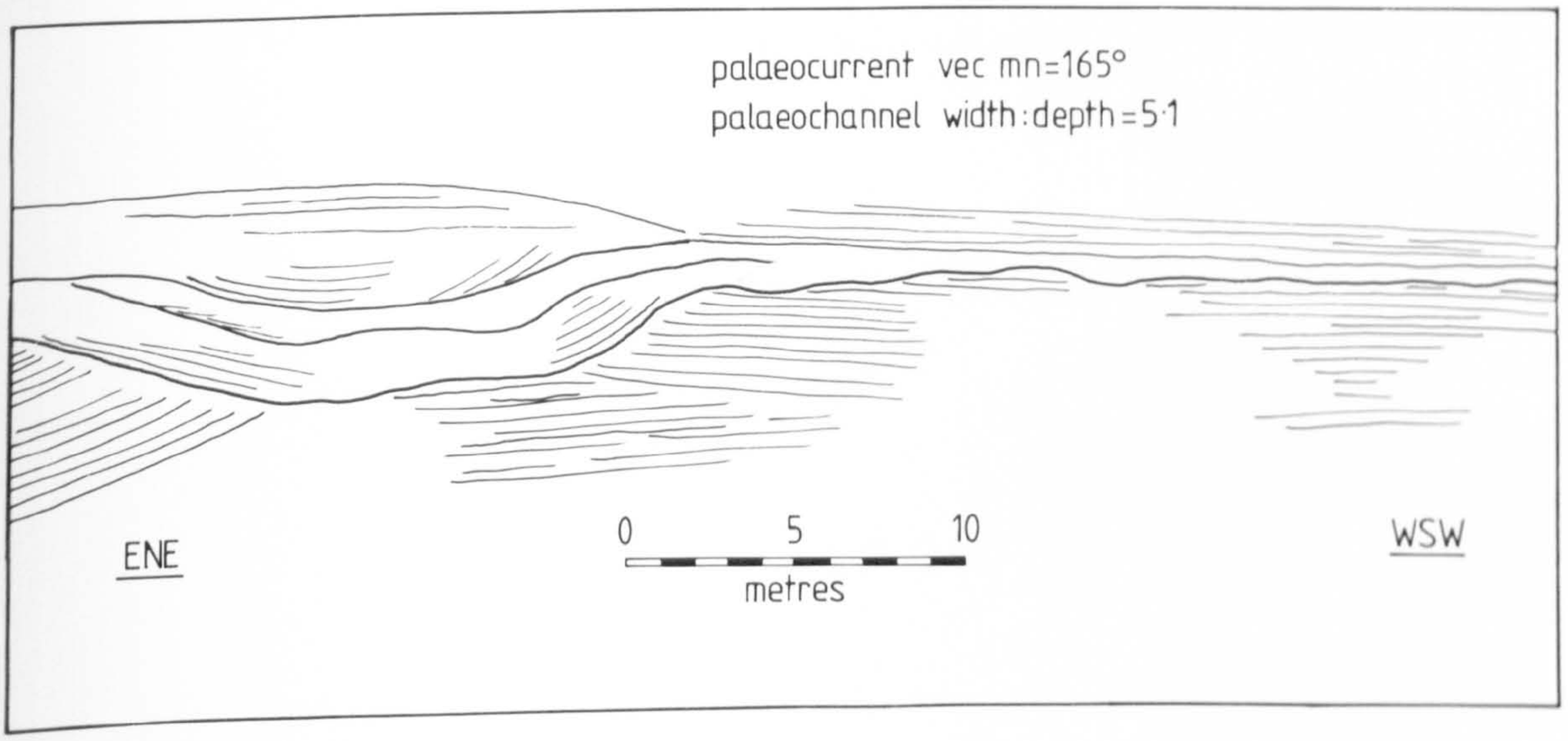
palaeocurrent vec mn=165°
palaeochannel width:depth=5·1
ENE
0
5
10
metres
WSW

Fig. 6.19. Photograph and interpretive line drawing of a flat lying sequence of six, stacked sand bodies exposed beside the Rio Arba in a Ribbon Sandstone Facies palaeovalley.

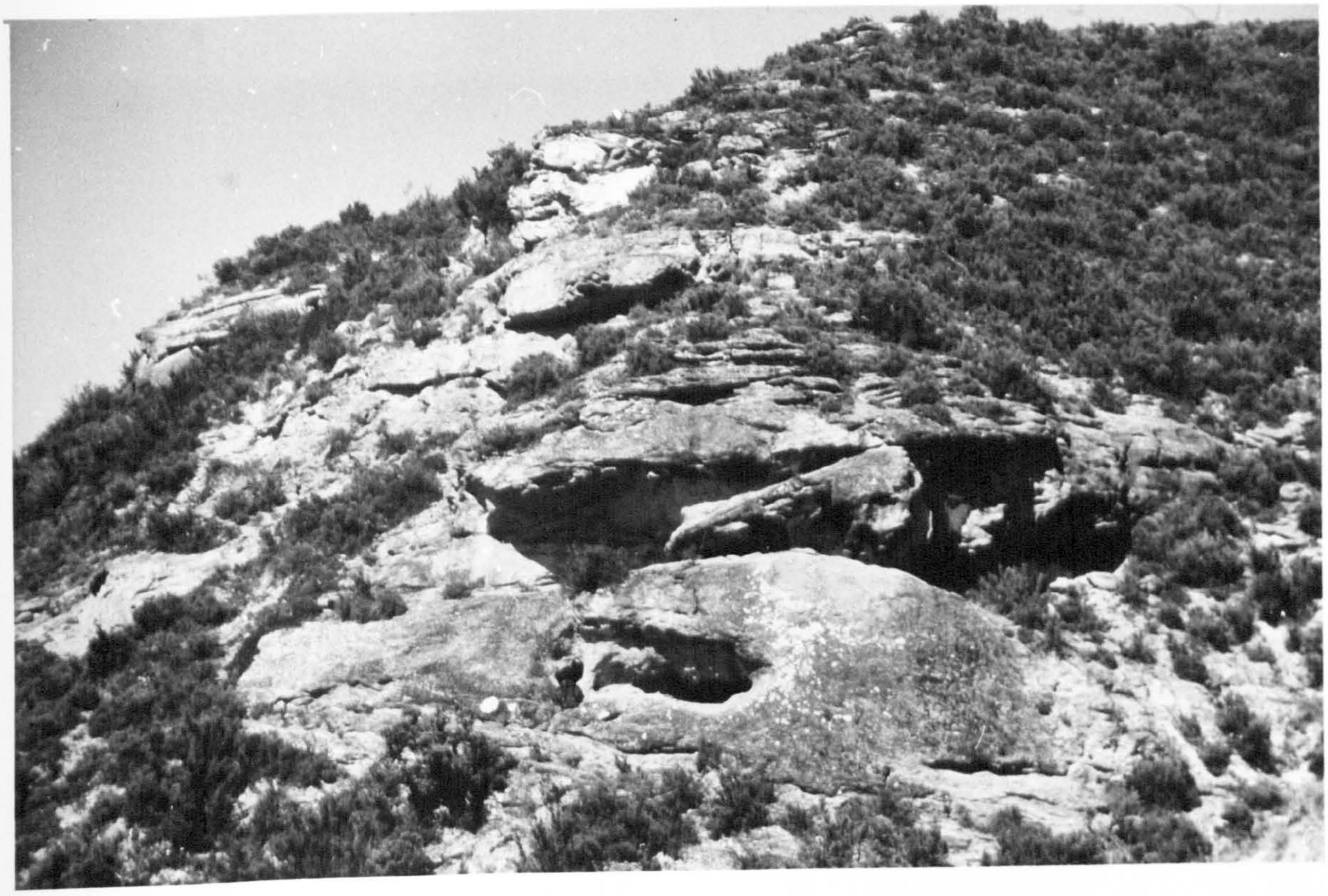

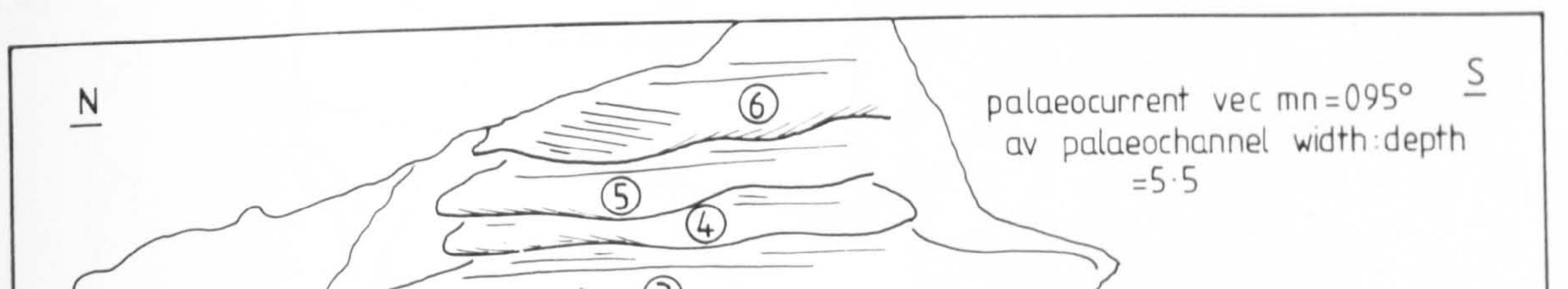
N
S
palaeocurrent vec mn=095°
av palaeochannel width:depth
=5·5
6
5
4
3
2
1
0
5
10
metres

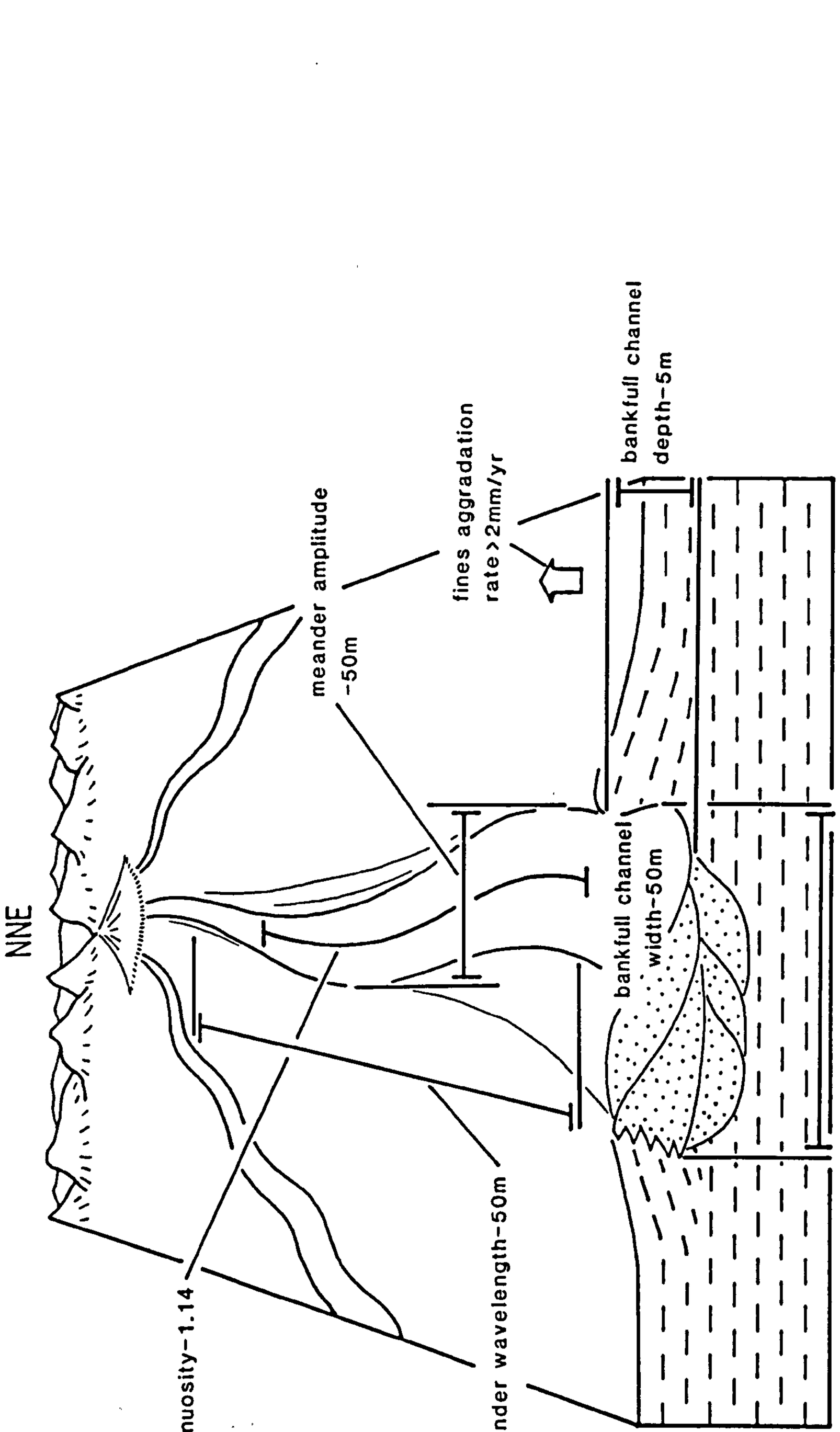

Fig. 6.20. Reconstruction of the palaeomorphologic parameters of the Ribbon Sandstone Facies. Based on an idea for a diagram by Gardner (1985, fig. 9). Compare with the Sheet Sandstone Facies palaeomorphology shown in Fig. 4.7.

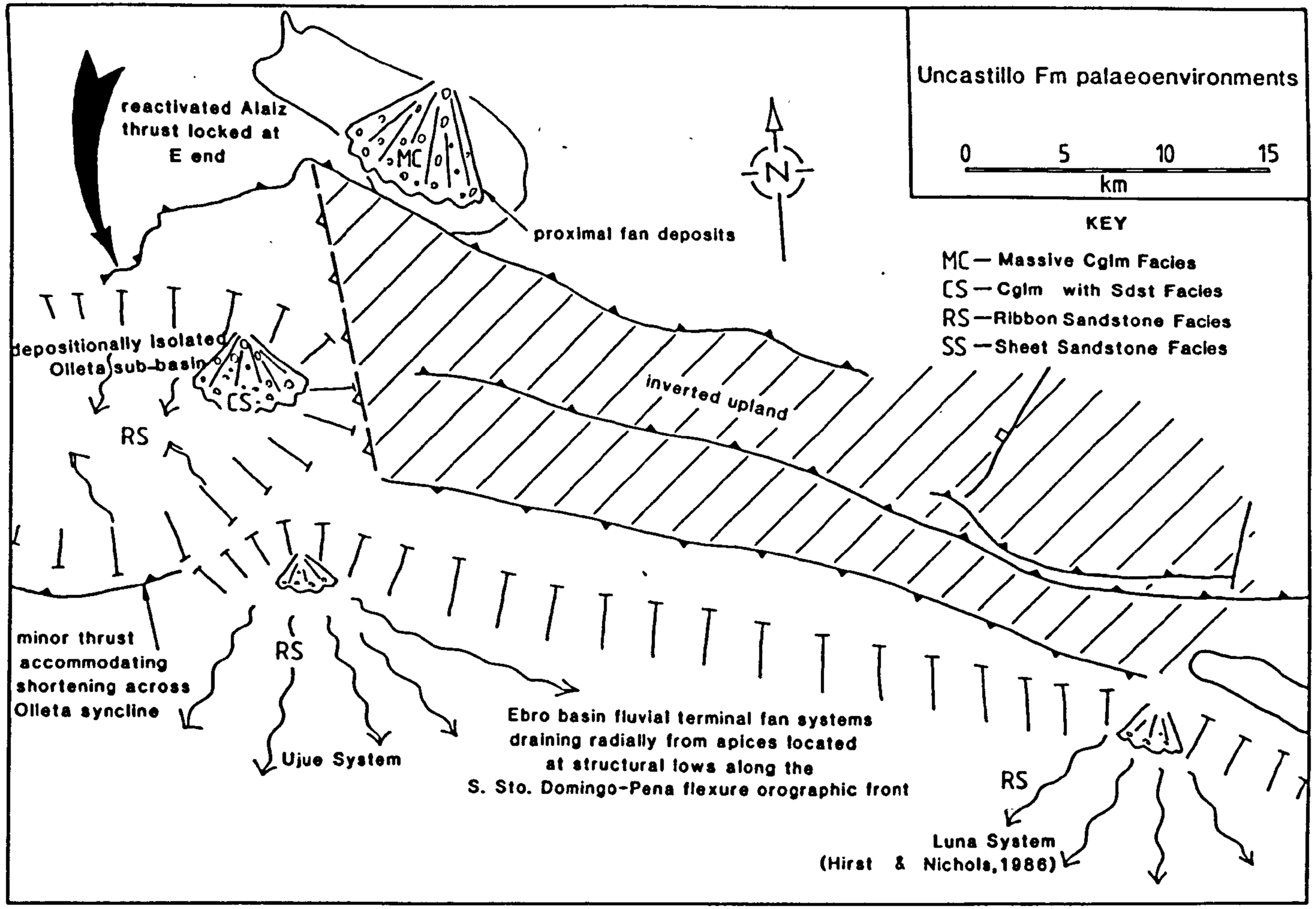

Fig. 6.21. Schematic palaeoenvironmental reconstruction of the study area during deposition of the Uncastillo Formation.

CHAPTER 7

MESOFRACTURES OF THE WEST JACA BASIN AND NORTHWESTERN EBRO BASIN

7.1 PURPOSE AND SCOPE

The aim of this chapter is to analyse mesofracture systems in the rocks of the study area in order to infer from them regionally significant compression and extension directions. Use of the prefix 'meso-' follows that of Turner & Weiss (1963) who employed it to describe structures that range in size from less than a centimetre to a few metres, and that are observable in a single, continuous exposure. In this study, the overwhelming majority (>85%) of mesofractures are joints. The definition of 'joint' used here follows that of Hancock (1985): "A barren, closed fracture on which there is no measurable slip or dilation at the scale of observation".

An initial stimulus for investigating the joints was provided by Hancock's (1985) report that there are abundant joints and rare mesofaults in the central part of the Jaca basin, to the east of the study area. His assemblages collectively indicate that the dominant bulk strain regime at the time of jointing involved layer-parallel elongation normal to fold hinge lines. In the West Jaca basin, joints are also very abundant but associated mesofaults are rare despite the presence of major thrusts (see Chapter 2). The two principal objectives of investigating joints in the West Jaca basin were:

(1) to determine the stress history of the study area which lies south of, and external to, the regional cleavage front exposed in the Sierra de Orba; and

(2) to investigate any systematic relationship between 'domains' of joint assemblages and thrust system geometry. For example, in areas of limited exposure could mesofracture analysis be useful for determining the location of thrusts?

7.2 CONVENTIONS AND METHODOLOGY

A comprehensive review of the principles of inferring stress trajectories from mesofractures is presented by Hancock (1985). To summarise, three classes of fracture are recognised, extension, hybrid-shear and shear fractures, each with its own distinctive range of conjugate shear angles (2θ) about the maximum principal stress axis (σ_1): The classes and subclasses of fractures together with stress conditions during their formation are summarised in Fig. 7.1. The orientations of the principal stresses may be deter-

mined knowing that, at the time of failure, an extension fracture is initiated perpendicular to σ_3 and in the principal stress plane containing σ_1 and σ_2, and that conjugate hybrid and shear fractures enclose an acute bisector parallel to σ_1.

Approximately one hundred fracture sampling sites (here called stations) were studied. Because the degree of exposure is relatively good, stations could be roughly uniformly spaced throughout the study area. The volume of rock surveyed at each station was generally less than 10000 m^3 and within each station the dips of beds are uniform. The principal fracture types other than joints are veins, mainly concentrated in the Ruesta fault zone, and mesofaults which, although rare, occur locally but not selectively with respect to tectonic setting. At each station the following attributes of joints and joint networks were recorded.

(1) Three-dimensional orientations.
(2) Genetic class, that is, whether the joint is an extension, hybrid-shear or shear fracture.
(3) Order of joint development as determined from abutting and cutting relationships.
(4) Joint system architecture, as defined by Hancock (1985).

Each station was analysed separately on lower hemisphere, equal area diagrams on which cyclographic traces of mean fracture sets and bedding were plotted. From the mean orientations of sets, the orientations of the principal stresses were determined using the principles outlined above. The assignment of joints to sets and genetic classes was carried out using criteria discussed by Hancock (1985). The relative age relationship between adjacent joints was determined mainly using the axiom that a younger joint abuts an older one. Where joints cross-cut each other it is often not possible to be certain about which one is the older. In such settings, experience indicates that it is usually the 'strongest' joints (ie. those joints which have the longest traces on bedding planes, and which are most dilated and widely spaced) that prove to be the oldest. However, where bedding plane trace lengths and spacings of joints exceed the extent of an outcrop, these parameters may be difficult to assess.

Lower hemisphere, equal area diagrams of mean joint sets at each station, classified according to genetic class and age, are superimposed on maps of the West Jaca basin in Figs. 7.2, 7.3 and 7.4.

7.3 MESOFRACTURE ANATOMY OF THE LERDA RAMP ANTICLINE

Before interpreting regional patterns of fracture development shown in Figs. 7.2-7.4, it is important to analyse the distribution of mesofractures in a well exposed, strike-normal section through the Lerda ramp anticline (Fig. 7.5) for the following reasons.

(1) To identify any 'within-fold' trends in fracture development. These may be used as a control to distinguish tectonically significant regional patterns of mesofractures from local patterns reflecting local strains generated during folding.
(2) To assess the timing of fracturing relative to folding.

In Fig. 7.5, it is shown that the Lerda ramp anticline is dominated by systematic joints, veins and mesofaults in *ac* (Plate 7.1a), using the fabric axis notation of Turner & Weiss (1963) and Hancock (1985, fig. 17). These fractures reflect lateral extension parallel to strike and are interpreted as having formed before folding because they are abutted by non-systematic radial cracks (Plate 71.b) which clearly formed during folding. Evidence for there having been flexural slip during folding is provided by fibre sheets containing a dip-parallel lineation (Plate 7.1c) on bedding planes in the same flexure that contains the syn-folding radial cracks.

About 200 m to the south of the fold core, and approximately 80m stratigraphically above it, the dominant systematic joints are in *bc*. They indicate that at this level the principal extension direction was oriented N-S, parallel to dip direction. The distribution of systematic fracture sets in the Lerda ramp anticline therefore suggests that the principal direction of elongation switches through 90°, from being strike-parallel in the fold core to being dip-parallel in the envelope of the fold. This relationship may be interpreted as reflecting the location of a neutral surface, above which there was hinge-normal stretching and below which there was hinge-normal contraction.

The reported close relationship between mesofracture geometry and position within a fold highlights the need to base tectonically significant interpretations on only regional scale mesofracture patterns.

7.4 MESOFRACTURE DOMAINS

The following three mesofracture domains are identified on the basis of which set or conjugate system of fractures contains the oldest structures (Fig. 7.6).

(1) HANGINGWALL DOMAIN. This domain coincides with the hangingwall rocks of thrusts and contains single sets of E-W striking extension fractures and conjugate-shear or hybrid-shear fractues enclosing an E-W oriented acute bisector. Hangingwall domains comprise the majority of the study area.

(2) FOOTWALL DOMAIN. In areally restricted domains up to three kilometres in advance of thrust traces, strike-parallel joints are consistently superimposed on an older system of N-S striking mesofractures.

(3) LATERAL RAMP DOMAIN. The third domain coincides with the location of the Ruesta fault zone and is expressed by a discrete zone of conjugate-shear and extension veins and joints whose acute bisectors or bedding plane traces, respectively, strike north-northeast, that is, parallel to the strike of the Ruesta fault zone.

A key feature in identifying the domains was the recognition of which set contains the oldest fractures at each station. Readily interpreted examples of fractues at stations from which the above conclusions were drawn are shown in Plates 7.1a, 7.1b, 7.2a and 7.2b. Their interpretation does not pose a problem because at the illustrated stations the fracture pattern comprises either single sets or conjugate sets. However, in the examples shown in Plates 7.2c and 7.2d, a careful assessment of abutting and cutting relationships is critical to recognising different generations of joints and thus determining the oldest set or system.

As an example of the reasoning, employed, Plate 7.2c depicts the upper surface of a vertical 'wall' of E-W striking sandstone at Petilla. Three main sets of systematic joints belonging to two systems are present in the sandstone. Firstly, a system of conjugate *hko* (Hancock 1985) hybrid-shear joints with an acute bisector parallel to the *a* fabric axis and, an E-W striking set of *bc* extension joints. Inspection of Plate 7.2c reveals that the *bc* joints consistently abut the *hko* conjugate hybrid-shear joints. Thus, in this instance the station was assigned to the Footwall Domain characterised by older strike-normal joints.

A second example of the methodology is shown in Plate 7.2d which illustrates the upper surface of a vertical bed of sandstone striking E-W. The bedding plane displays a complex pattern of systematic and non-systematic E-W and N-S striking extension joints and curviplanar fractures interpreted as curving from extension into shear joints. Although at this station the E-W striking joints are the most closely spaced and pervasive, some of them abut the wider-spaced, more dilated and longer, N-S striking joints. Thus, this station illustrates a typical Footwall Domain assemblage with strike-parallel extension joints abutting or cutting older strike-normal joints.

7.5 THRUST TECTONIC CONTROLS ON THE DISTRIBUTION OF MESOFRACTURE DOMAINS AND EXTENSION DIRECTIONS

From the mesofracture assemblages that characterise the three domains, the following directions of extension are inferred.

(1) N-S elongation parallel to the regional thrust transport direction is the oldest extensional direction to be recorded in Hangingwall Domains.
(2) E-W elongation perpendicular to thrust transport direction occurred first in Footwall Domains.
(3) Lateral Ramp domains comprise fractures that developed when the direction of elongation was locally parallel to the dip of an underlying lateral ramp.

Figures 7.7 and 7.8 illustrate possible mechanisms for generating these extensional stresses during thrusting. In Fig. 7.7a, extension parallel to thrust transport in the thrust belt is shown as being related to internal strains that could arise during contractional folding. Extension normal to fold hinges could have occured during folding above a neutral surface, as for example in the Lerda ramp anticline (Fig. 7.5). An alternative explanation for the abundance of *bc* extension joints in the central part of the Jaca basin was proposed by Hancock (1985) who interpreted them as products of growth folding when older, lower layers on fold limbs will be more stretched. In Fig 7.7a, growth folding is illustrated as having been related to deformation above the tips of blind thrusts and/or diapirism of Keuper rocks. Whether fractures of Hangingwall Domains formed during post-depositional, contractional folding or during growth folding, both interpretations assume that the fractures reflect stresses active during the closing stages of folding. Two observations support this assumption.

(1) Mesofractures are symmetrically arranged with respect to folds in the West Jaca basin.
(2) Despite their symmetry with respect to fold geometry, bedding is not, off-set across the majority of fractures. If all fractures formed before fold amplification they would have been reactivated to form small faults (Hancock 1985). To illustrate the ease with which former joints may be reactivated by small amounts of simple shear, consider the offsets of bedding shown by the gently dipping sequence in Plate 7.3a. The absence of reactivated E-W striking extension joints in the study area suggests that they formed at a late stage in the folding process.

Explanations for the development of fractures characterising the Footwall and Lateral Ramp Domains are provided in Fig. 7.8. A simplified cross section through a thrust sheet parallel to its strike (Fig. 7.8) shows that there is a displacement gradient which increases from zero at each lateral tip to a maximum in the central part of the thrust. Such a displacement gradient also implies a loading gradient in the footwall of the thrust sheet that could be accommodated by strike-parallel elongation, manifested by strike-normal extension fractures. This model of strike-normal elongation in the immediate footwall of a thrust also implies that the fractures formed before detachment of the Footwall Domain and subsequent thin skin folding. This conclusion is consistent with the observation that, in the Lerda ramp anticline, *ac* extension joints in the Footwall Domain were formed before folding.

From inspection of Fig. 7.8, it may also be appreciated that the displacement gradient between the lateral tips and central part of a thrust is also transmitted to the hangingwall of a thrust. In the Ruesta fault zone, this strike-parallel elongation is largely accommodated by a series of hangingwall collapse faults downthrowing westward, toward the lateral tip of the underlying thrust sheet (see Chapter 3). Additionally, between the collapse faults, strike-parallel elongation was accommodated by the development of north-northeast striking shear and extension joints.

At this point it is appropriate to consider why the buried Alaiz-Ujue oblique ramp (Fig. 7.6) is not defined by a mesofracture assemblage typical of a Lateral Ramp Domain. The oblique ramp trends subparallel to thrust transport direction and hence some sign of there having been ramp-parallel extension might be anticipated in the mesofracture assemblage. However, as demonstrated in Chapter 2, the Alaiz-Ujue ramp is a relatively complex structural divide, to the west of which there was reactivation (eg. the Sierra de Alaiz thrust) and a 45° anticlockwise rotation of structural trends.

At Artariain, a large, gently dipping bedding plane pavement, immediately west of the Alaiz-Ujue oblique ramp, records some aspects of these structural complexities. The station is dominated by an oldest set of extension joints with a mean strike of 055°, a direction subparallel to the present strike of the Sierra de Alaiz thrust. However, close examination of this set of extension fractures reveals that some of them behaved as small, sinistral, strike-slip faults. This interpretation of their character is partly based on 50 x 100 cm 'pop-up' (rhomb horst) that occurs at a 'restraining bend' in a fracture zone in which there is a left-handed stepping of fracture segments (Plate 7.3b). Additionally, inspection of millimetre wide limonitic seams, whose

orientations and architecture mimic those of the neighbouring, larger mesofractures, reveals that the seams striking parallel to the 055° set of extension joints are commonly arranged in an en-echelon pattern compatible with there having been sinistral shear. These observations suggest that the joints at Artariain were initiated before reactivation of the Sierra de Alaiz thrust, but that they too were affected by the phase of late Oligocene or early Miocene reactivation.

Thus, summarising, mesofractures in the West Jaca basin are interpreted as products of extensional stresses that were generated during thrusting and thin skin deformation. However, there remains the need to account for the abundant and widespread extension joints striking E-W, parallel to the Pyrenean orogen, immediately south of the mountain front in the Ebro basin. These structures are equally as pervasive as those to the north of the mountain front, but are formed in flat lying and relatively undeformed rocks (eg. Plate 7.2b). Figure 7.7b and c illustrates the following mechanisms by which N-S, orogen-normal extensional stresses could have developed in the northwest Ebro basin.

(1) Above a passive-roof duplex (see Chapter 2) the overriding wedge of Ebro basin rocks could have experienced N-S stretching generated by underthrusting of the hinterland rocks in the duplex (Fig. 7.7b).

(2) Figure 7.7c illustrates a model whereby N-S extension is related to the flexing of a foreland basin. The simultaneous character of sedimentation and subsidence at many foreland basin margins means that flexure induced stretching could be transmitted through a foreland basin sequence from the earliest stages of thrust load induced subsidence.

Because orogen-parallel extension joints occur up to 25 km south of the mountainfront and along that part of the Ebro basin margin not underlain by a passive-roof duplex, the model preferred here is that of late, flexure induced stretching.

7.6 EXTENSION IN THRUST-FOLD BELTS: CONCLUSIONS

(1) The distribution of mesofracture domains reflects thrust system geometry. In the West Jaca basin three domains are recognised: Footwall Domains, containing older joints striking normally to the regional trend of thrusts and folds indicating that elongation was perpendicular to thrust transport direction; Hangingwall Domains, containing older joints striking subparallel to the regional trend of thrusts and folds indicating that elongation was parallel to thrust transport direction; and Lateral Ramp Domains, con-

taining older joints striking subparallel to the trend of underlying lateral ramps indicating that elongation was locally parallel to the dip of an underlying lateral ramp.

(2) The overprinting of separate mesofracture systems reflects thrust system evolution.

(3) Large areas of the South Pyrenean thrust-fold belt and adjacent undeformed foreland basin were elongated parallel to thrust transport direction.

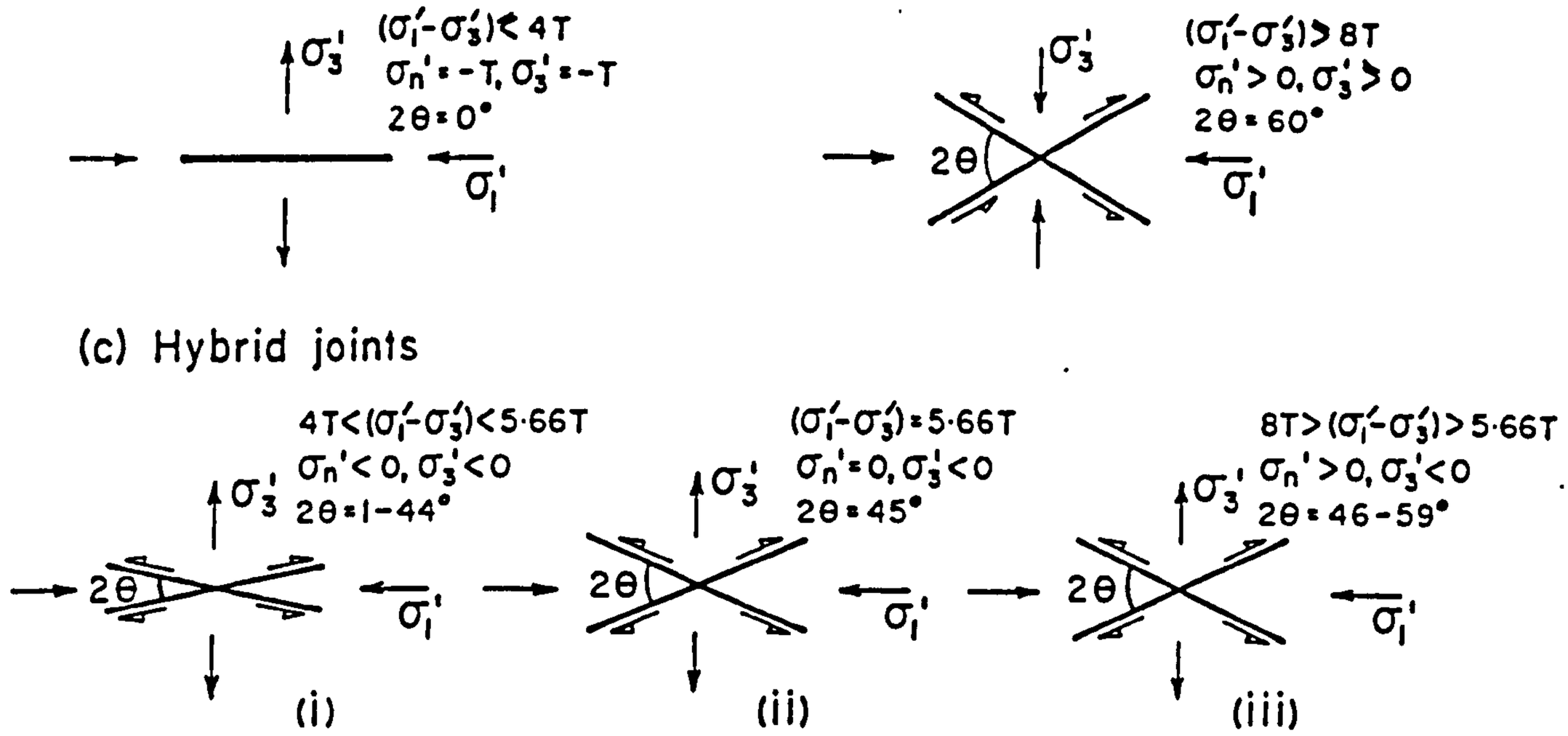

Fig. 7.1. Stress conditions during the formation of (a) extension fractures, (b) shear fractures, and (c) three subclasses of hybrid-shear fractures assuming that a composite failure envelope of the type shown in (d) is appropriate to describe failure conditions. (e) Cartoon of an imaginary fracture spectrum comprising coaxial extension, hybrid and shear fractures shown at 10° intervals in a continuum of directions intersecting at a common point. 2θ - conjugate shear angle; σ_1', σ_2', σ_3' - maximum, intermediate and minimum effective principal stresses; σ_n' - effective stress normal to a failure plane; $(\sigma_1'-\sigma_3')$-differential stress; T - tensile strength. From Hancock (1986, fig. 1).

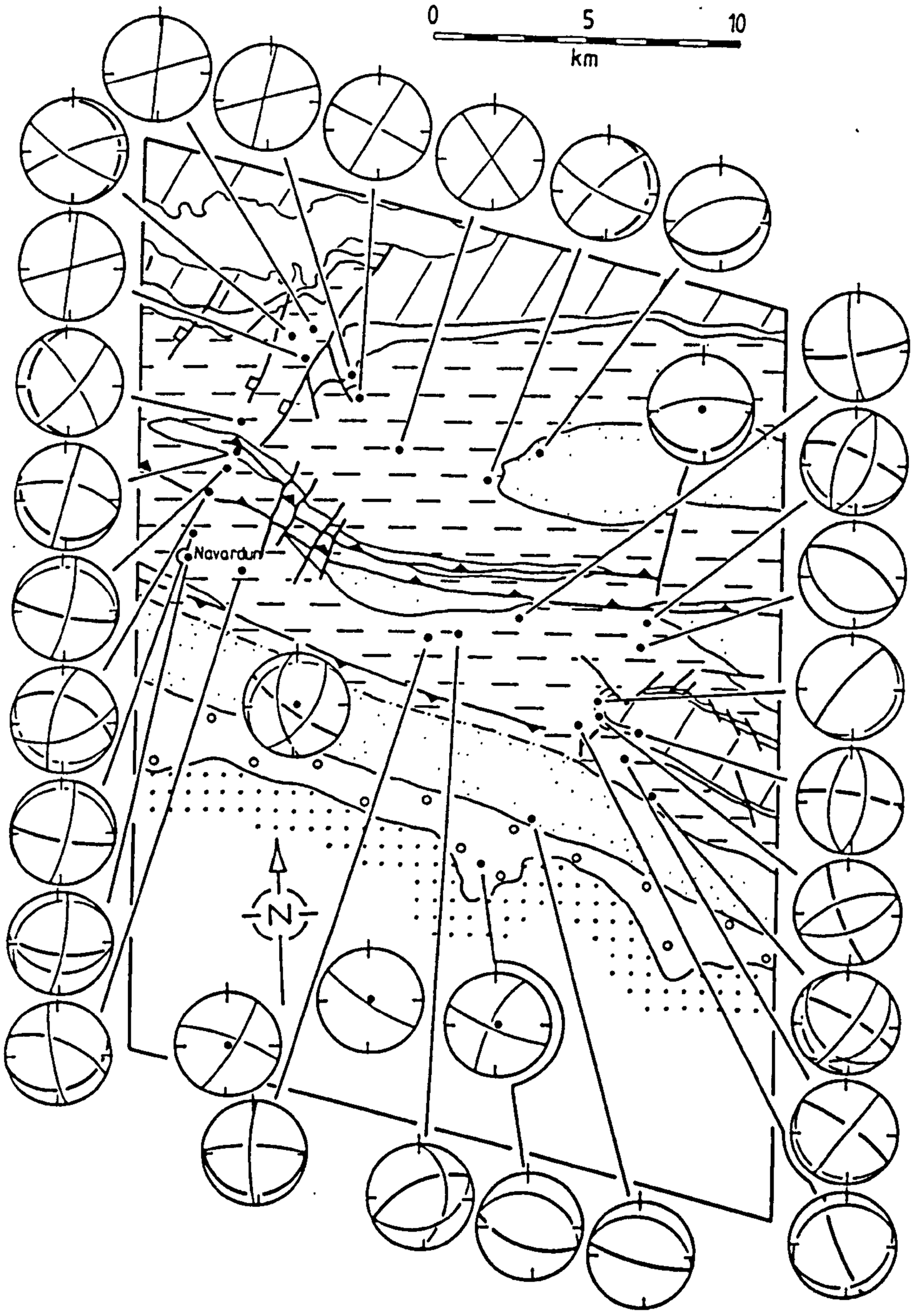

Fig. 7.2. Lower hemisphere, equal area diagrams showing the orientations of fractures and bedding at joint stations (locations represented by solid dots) in the eastern part of the study area. Where regional dip is detectable, bedding is depicted by a heavy, interrupted great circle. Younger joints are depicted by a great circle, broken where it intersects that of an older joint set. Great circles of conjugate joints are shown crossing each other. The names of stations discussed in the text are indicated. Geological framework and ornament as in Fig. 1.3.

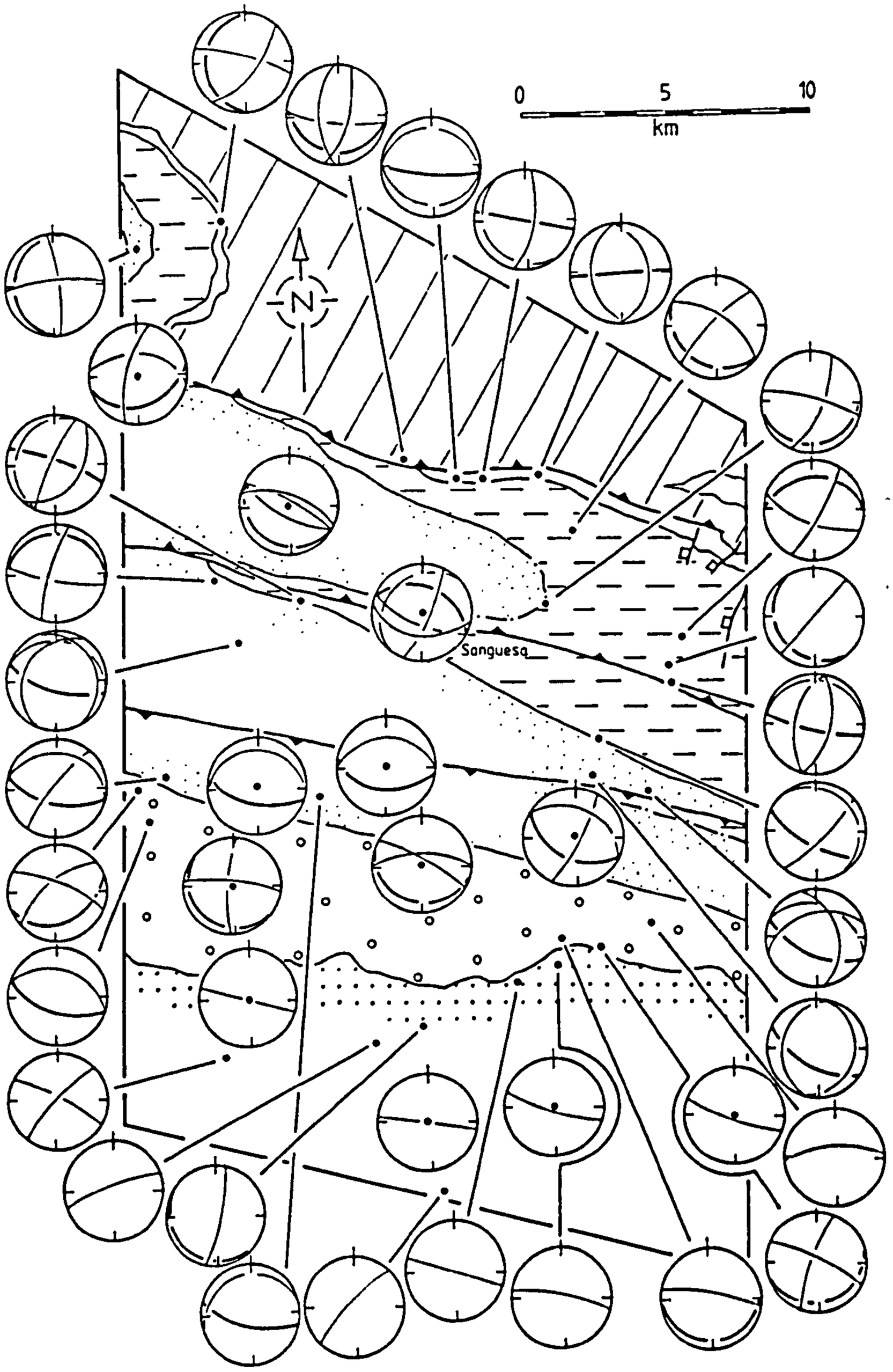

Fig. 7.3. Lower hemisphere, equal area diagrams showing the orientations of fractures and bedding at joint stations in the central part of the study area. Notations and conventions as in Fig. 7.2. Geological framework and ornament as in Fig. 1.3.

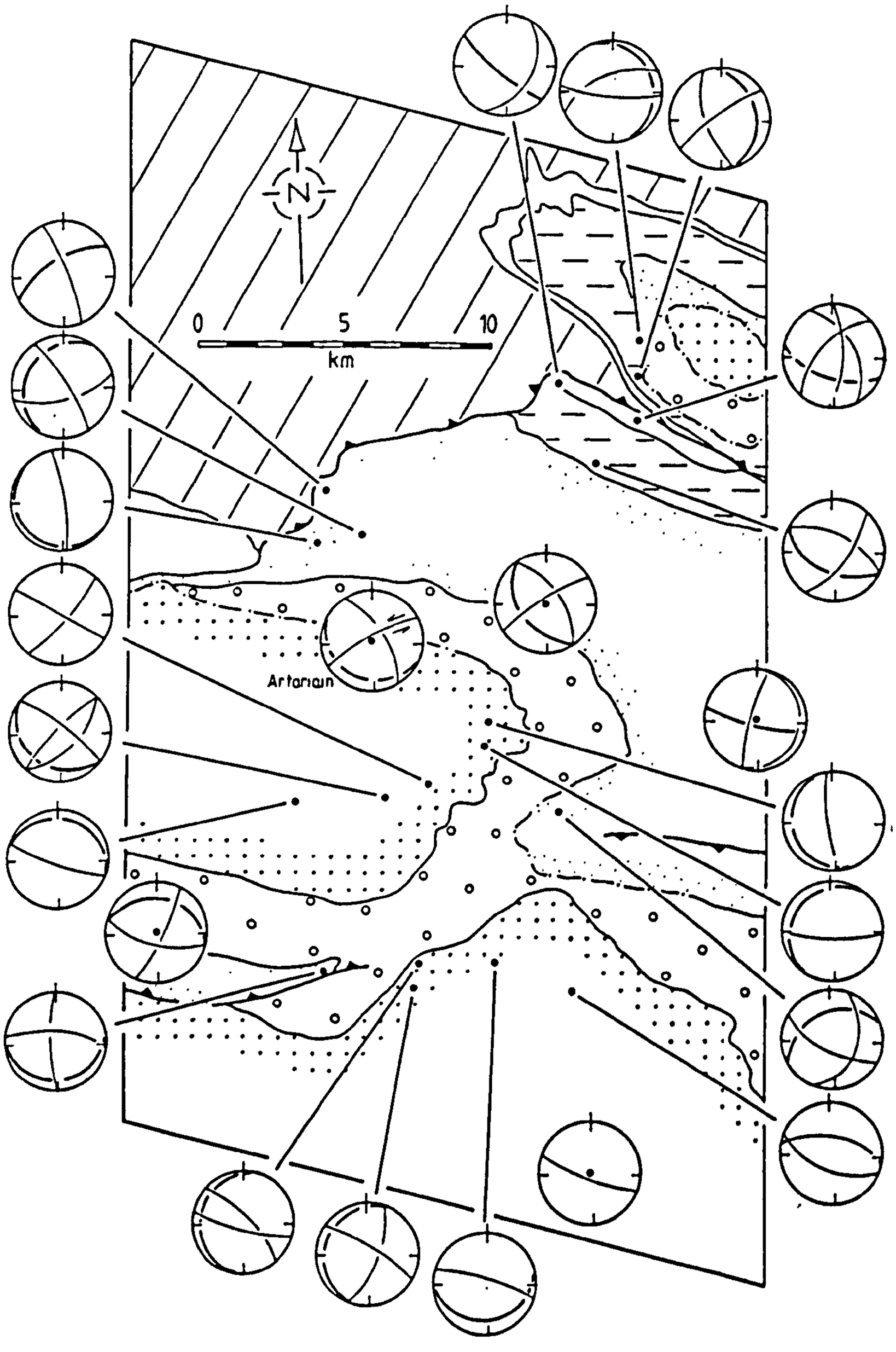

Fig. 7.4. Lower hemisphere, equal area diagrams showing the orientations of fractures and bedding at joint stations in the western part of the study area. Notations and conventions as in Fig. 7.2. Geological framework and ornament as in Fig. 1.3.

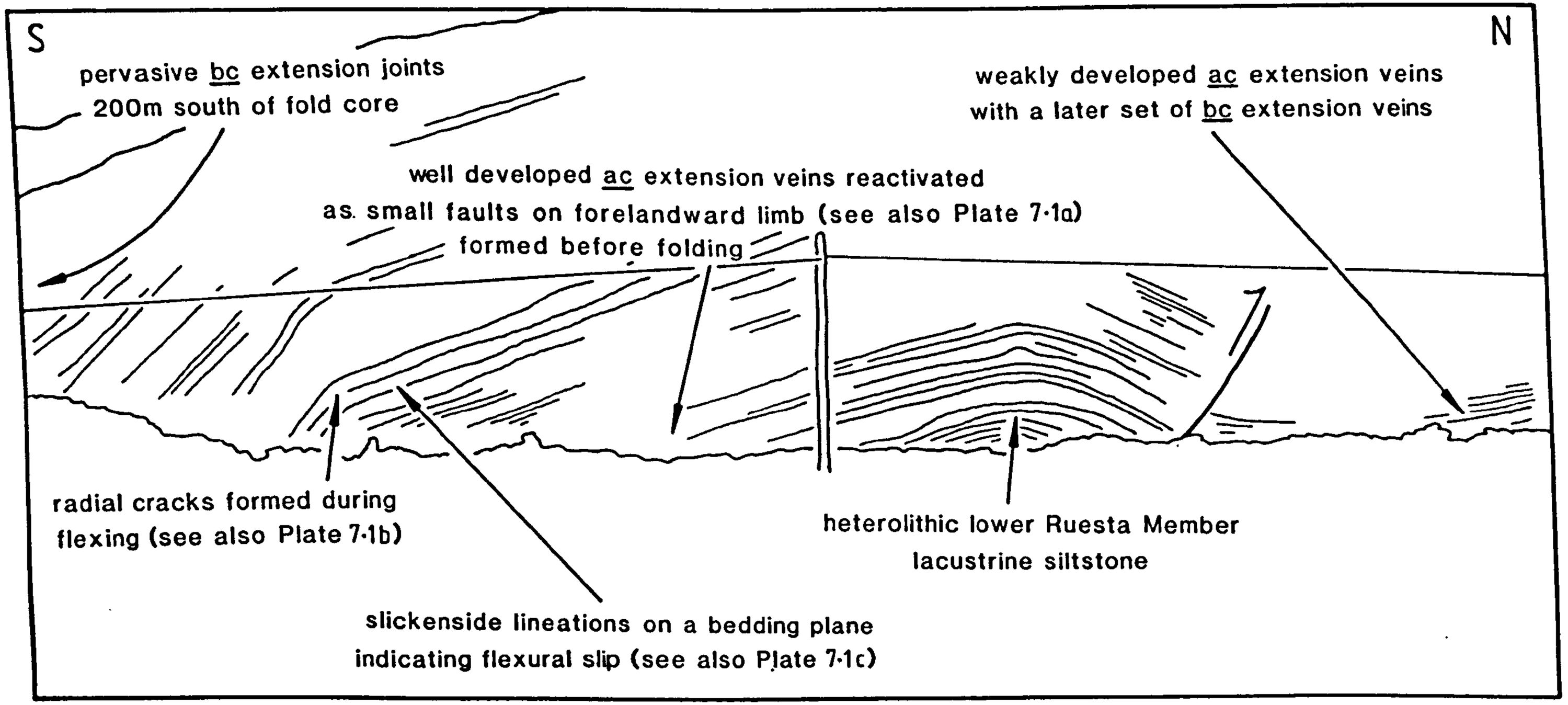

Fig. 7.5. Fracture geometries within the Lerda ramp anticline; the profile is drawn from the photomosaic in Fig. 2.8.

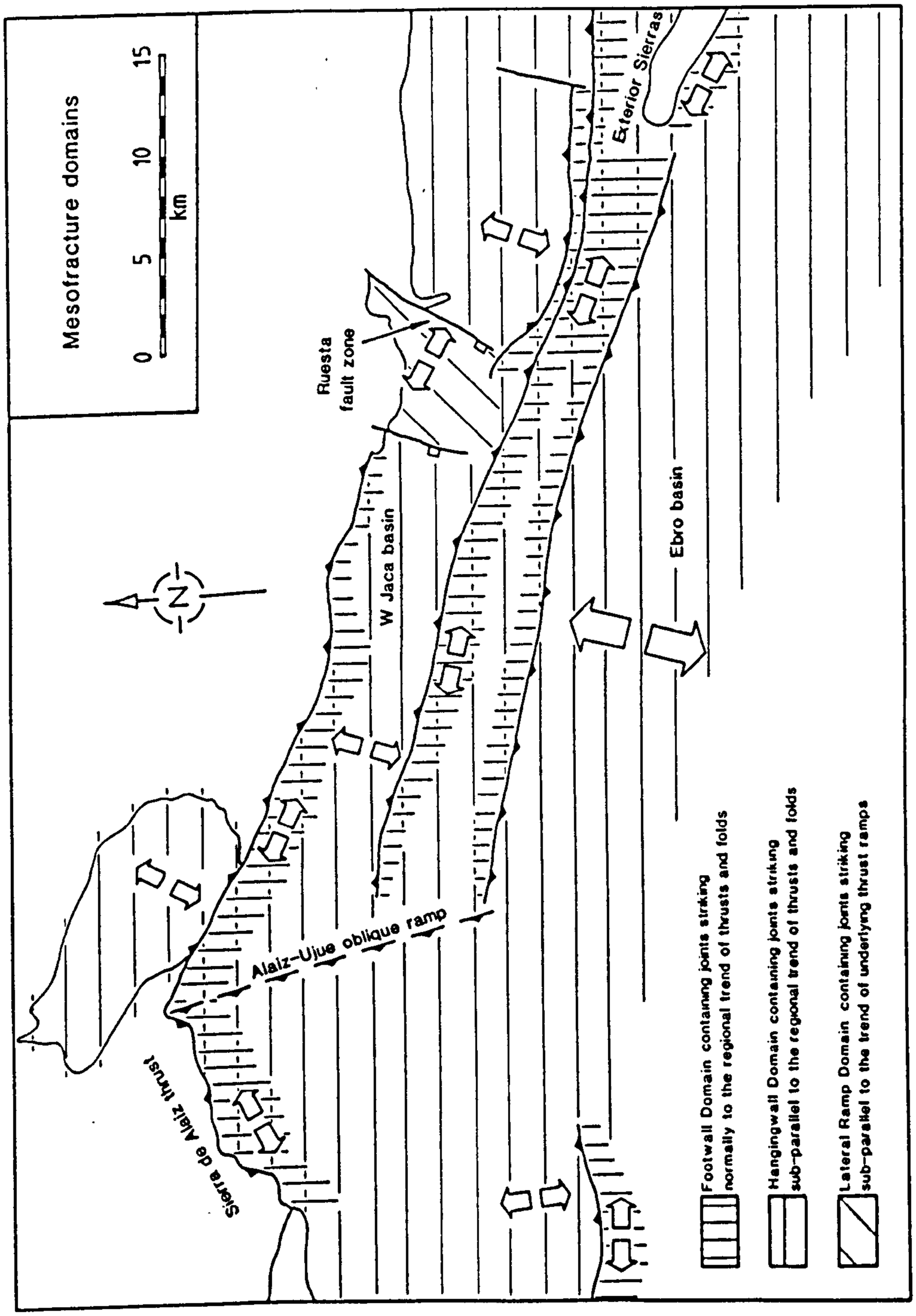

Fig. 7.6. Mesofracture domains and their relationship with thrust system geometry in the West Jaca basin. General geology as outlined in Fig. 1.3.

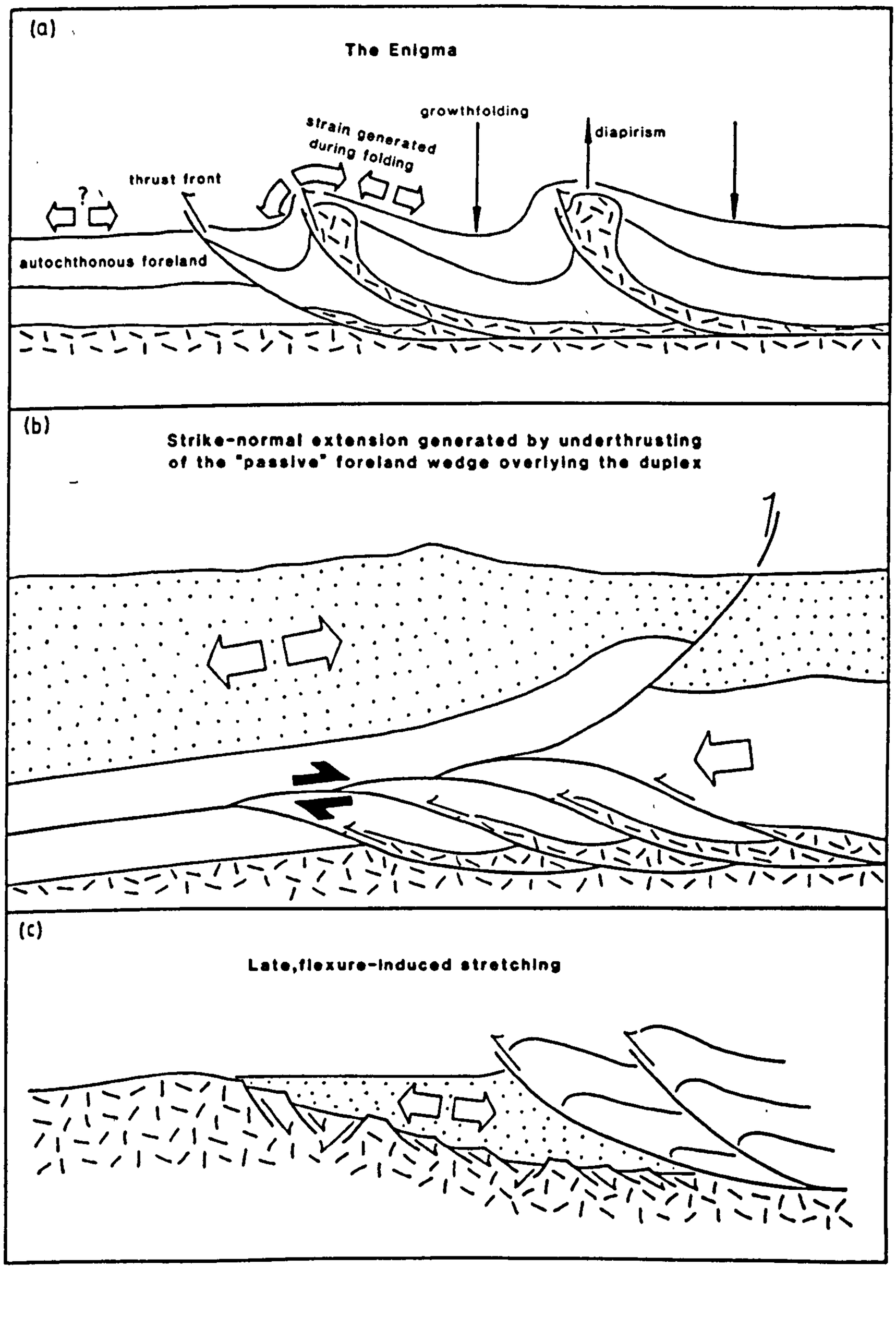

Fig. 7.7. Schematic N-S sections illustrating possible origins of extensional strain in the South Pyrenean orogen (a) and its foreland (b and c). (c) is modified from Dewey *et al.* (1986, fig. 4B). See text for details.

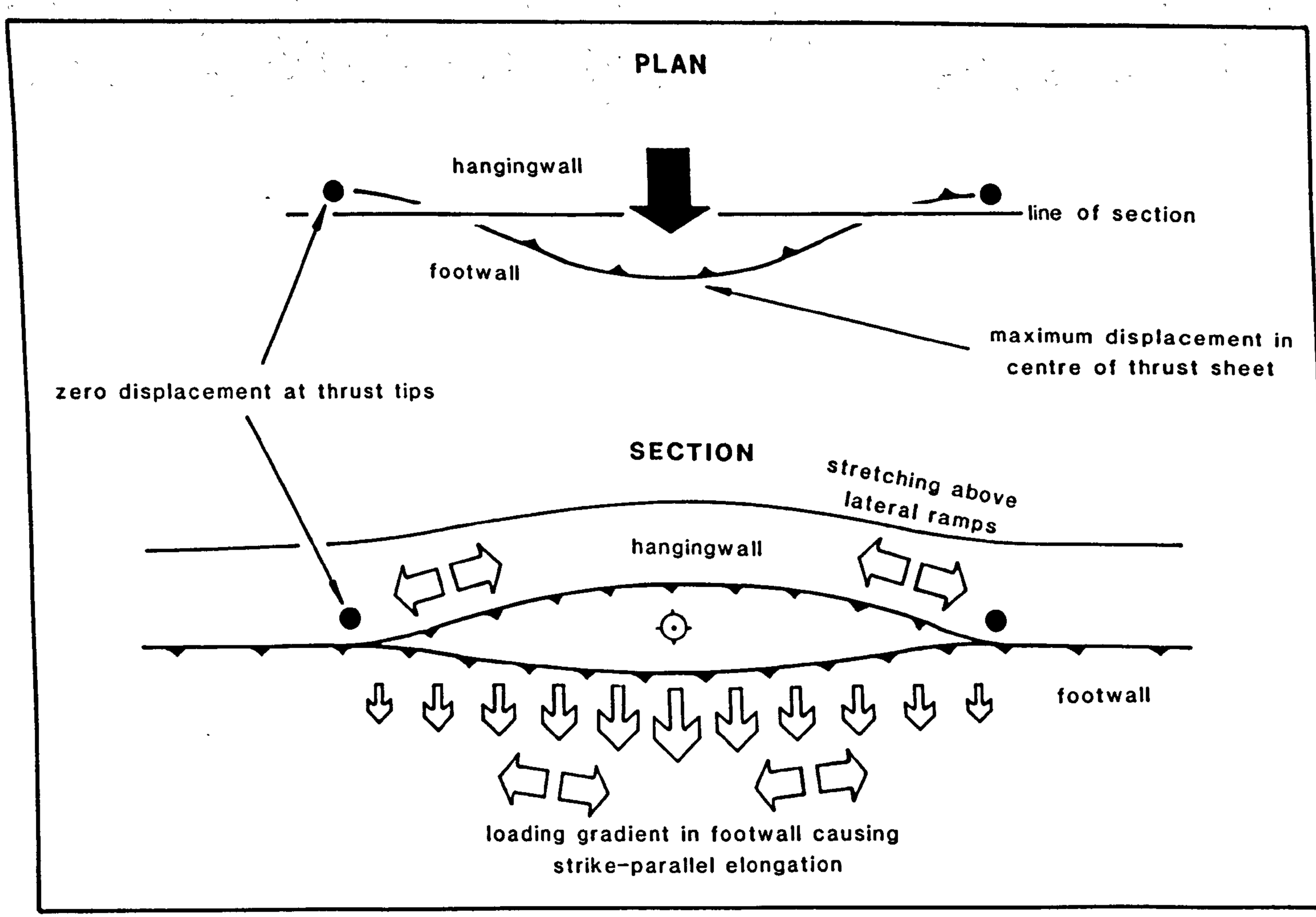

Fig. 7.8. Likely mechanisms for producing strike-parallel elongation in the footwall of a thrust and in the hangingwall above its lateral ramps. It should be noted that the width in plan of the Footwall Domain will be largely determined by the steepness of the thrust surface. Steeper thrusts will impose less of a load on the footwall and thus the width of the resultant Footwall Domain of strike-parallel extension will be less.

Plate 7.1a. *ac* extension veins reactivated as small faults on the forelandward limb of the Lerda ramp anticline.

Plate 7.1c. Dip-parallel fibre lineations on a bedding plane in the Lerda ramp anticline.

Plate 7.1b. Syn-folding radial cracks in a tight flexure on the forelandward limb of the Lerda ramp anticline. The cracks clearly abut *ac* extension fractures similar to those shown in Plate 7.1a.

Plate 7.1d. Closely-spaced, pervasive *bc* extension joints in steeply dipping sandstone near Caseda. Note the presence of short, non-systematic, cross-joints that consistently abut the *bc* joints.


A

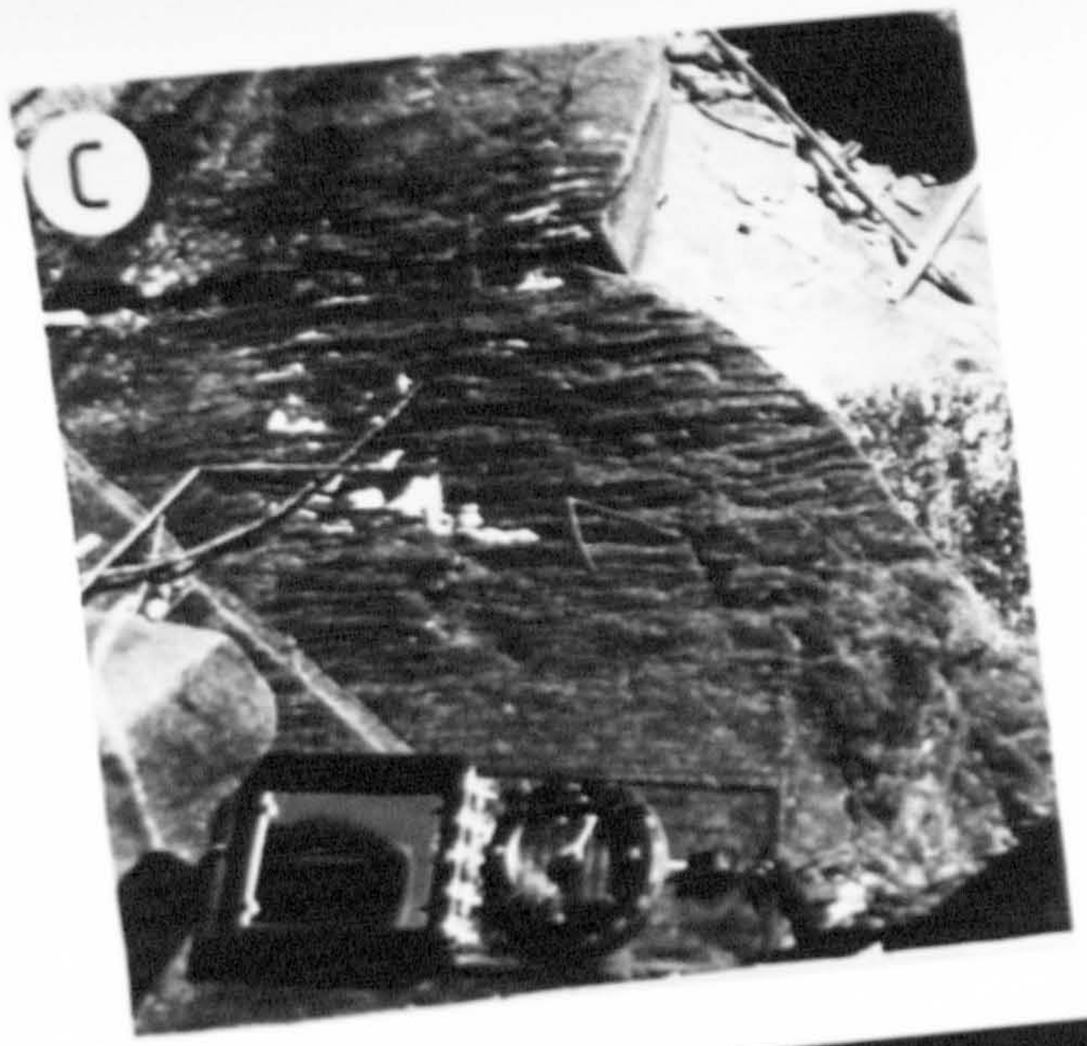
C


B


D

Plate 7.2a. Conjugate shear joints with roughly E-W oriented intersects in flat lying rocks of the northwest Ebro basin at Ujue.

Plate 7.2c. Complex pattern of joint traces exposed on the upper surface of a vertical, E-W striking sandstone at Petilla. See text for discussion.

Plate 7.2b. Much dilated, well developed extension joints, striking parallel to the long axis of the Pyrenean orogen, in a flat lying, five metre thick fluvial sandstone at Huesca. View east along the northern margin of the Ebro basin.

Plate 7.2d. Two superimposed generations of joints exposed on the upper surface of a vertical, E-W striking sandstone, two kilometres south of the Sierra de Santo Domingo. See text for discussion.


C


A


D

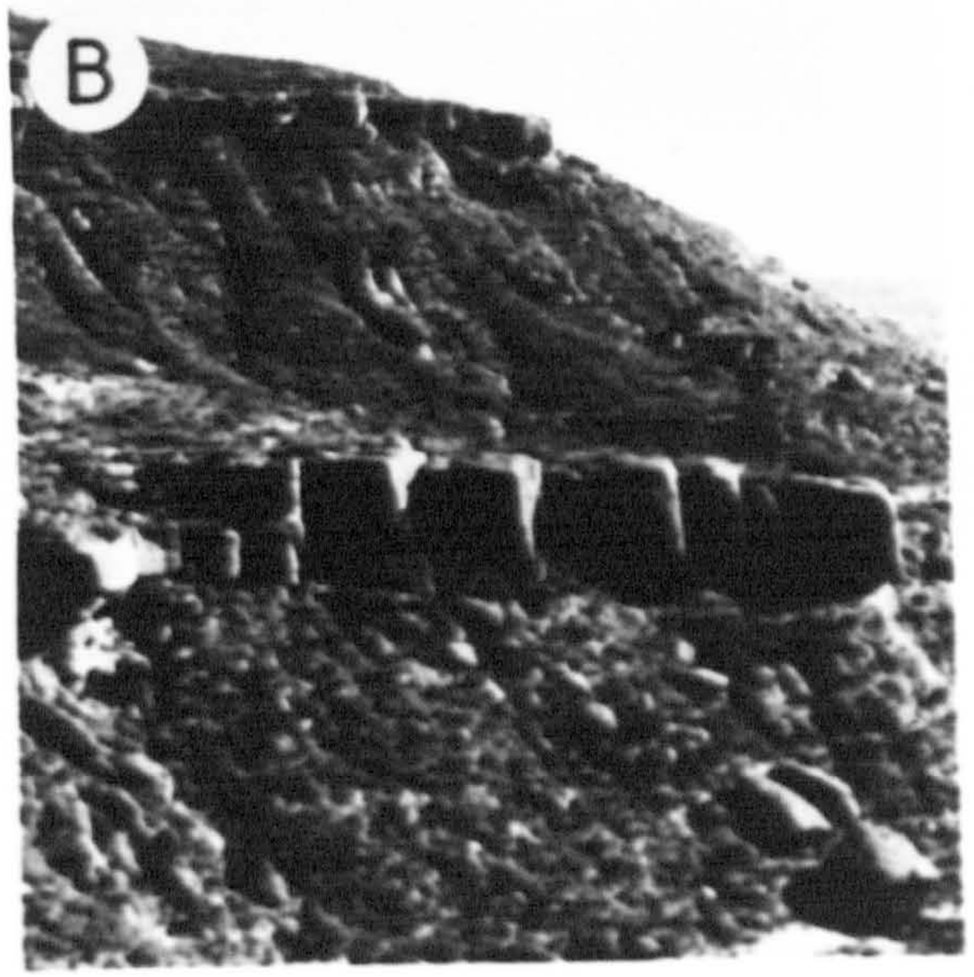
B

Plate 7.3a. A gently south dipping sandstone containing E-W striking former extension joints reactivated to form small normal faults. See text for discussion.

Plate 7.3b. A 'pop-up' at the step between a pair of joint traces, reactivated during later events, at Artariain. See text for discussion.

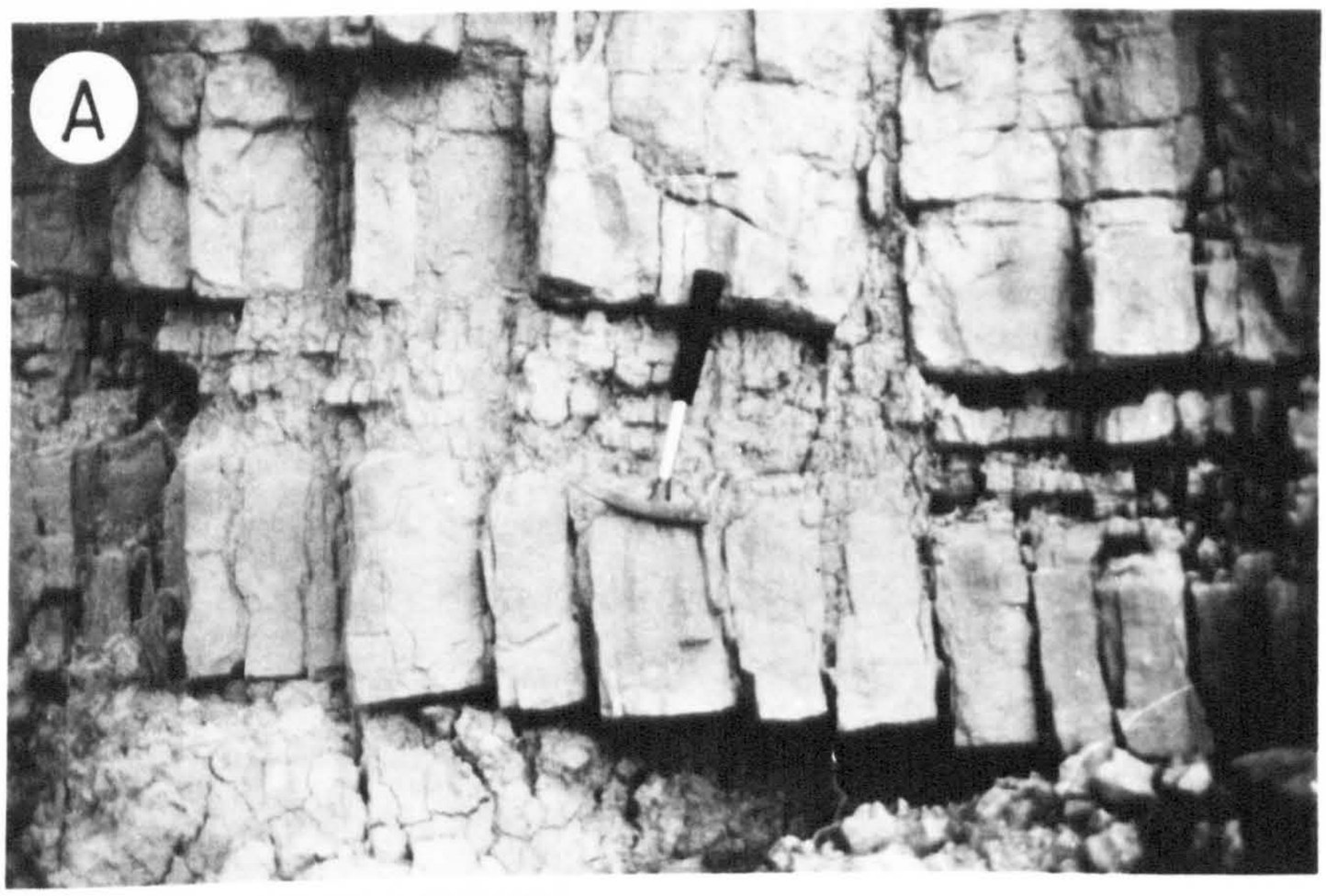
A


B

CHAPTER 8

DISCUSSION AND CONCLUSIONS

8.1 EVOLUTION OF THE WEST JACA BASIN: ITS REGIONAL SIGNIFICANCE AND SOME GENERAL IMPLICATIONS FOR THRUST-TOP BASINS

The following summary of the tectonic and stratigraphic evolution of the West Jaca thrust-top basin serves to highlight the regional implications of this study and, in addition, it focuses on aspects of general applicability.

Tectonically induced elevation of the study area above sea level in the earliest Oligocene produced a rapid transition from marine to continental deposition. During this episode, the study area was a relatively low lying, tectonically inactive foreland region, located immediately south of a major topograhic range (now the Sierras de Orba, Leyre and Alaiz) trending sub-parallel to the long axis of the Pyrenean orogen. The range was underlain by thrusted Mesozoic and early Palaeogene limestone and marl and it defined the South Pyrenean mountainfront.

Roughly uniform subsidence imposed by thrust stacking during the early Oligocene, and, consequent loading of the foreland margin led to the formation of the West Jaca molasse basin. At first, the study area was dominated by a relatively simple deposystem comprising extensive lakes that reflect high subsidence and a generally low clastic influx. Sequences whose variable sand and mud composition was controlled by water depth, distance from the shoreline and clastic influx, accumulated in the lakes.

However, in the northeast of the study area, early propagation of the Pyrenean thrust front into the basin elevated it and generated a locally derived clastic influx. This represents the oldest expression of thrusting in the West Jaca basin and led to an upward coarsening sequence recording lake regression and the incoming of a fluvial system. A lateral ramp at the western end of the Ruesta thrust caused E-W elongation in the hangingwall of the thrust sheet and the development of a N-S trending zone of normal faults, the Ruesta fault zone. The normal faults of the Ruesta fault zone downthrow toward the west and, on the western side of the main normal fault, a local onlap unconformity records the evolution of a hangingwall rollover anticline. Development of the strike-normal Ruesta fault zone during the early Oligocene complicated the distribution of sedimentary facies and caused an interfering drainage pattern to develop. For example, a fluvial system active during the evolution of the Ruesta fault zone drained roughly southward, that is, axially with respect to the local trend of the fault zone, but laterally with respect to the regional trend of the Pyrenean orogen.

Further southward and westward propagation of the Pyrenean thrust system during the mid Oligocene, as recorded by localised unconformities younger than the early Oligocene and forelandward of the Ruesta thrust, imposed two main changes on the study area. Firstly, there was a significantly greater clastic influx, and secondly, steeper and more consistently defined basin floor gradients were created. From this time onward, deposition in the main part of the study area took place in a basin that was demonstrably detached from the pre-Triassic basement by a thrust fault, that is, it was from then on a thrust-top basin.

The encroachment of the locus of thrusting from the north and east meant that the lake (or lakes) which dominated the early Oligocene environment retreated toward the southwest corner of the study area. Lakes were succeeded by alluvial deposystems that, along the northern margin of the basin flowed laterally southward, and, to the south of the growing mountainfront (the embryonic Pena Flexure), flowed westward, that is, axially. These contrasting drainage patterns reflect various degrees of proximality to active thrusting, and hence, the steepest depositional slopes. For example, lateral drainage at the basin margin was a response to major thrusting and loading along the Leyre-Alaiz thrust, less than ten kilometres to the north. However, more than twenty kilometres to the south, the axial fluvial system reflects along-strike variations in uplift and subsidence; in this case, a thrusted sediment source that was located perhaps one hundred kilometres further east. Thus, the evolution of the linked thrust system as it propagated into the West Jaca basin began to be recorded by division of the main basin into sub-basins. By the mid Oligocene there were two sub-basins, containing a laterally draining fluvial system to the north and an axially-draining fluvial system to the south.

The tectonic climax of deformation in the study area was during the late Oligocene when the frequency of thrust emergence, the rate of thrust displacement and basin floor subsidence, and the clastic influx to the basin increased dramatically. These changes were largely brought about by the development of the Pena flexure passive-roof duplex with the emergence of a northward verging backthrust at the depositional surface. Sustained displacement on the backthrust provided a constant supply of conglomeratic sediment that was deposited in several sub-basins by alluvial fans dispersing from apices located at structurally controlled topographic lows. The late Oligocene configuration of the basin was thus dominated by a central area of upland that had experienced a tectonically induced transition from subsidence and net

sedimentation, to uplift and net erosion. This topographic inversion was accompanied by deposition in structurally defined sub-basins by laterally dispersing alluvial fans.

The early Miocene was a period of post-tectonic adjustment of the basin deposystems to the newly imposed basin configuration. Denudation of the tectonic landscape caused large volumes of relatively locally derived sand and silt to be liberated. Cessation of movement on the Pena flexure backthrust meant that the passive-roof duplex was fully developed, having achieved up to 45% N-S shortening. Its formation imposed rapid subsidence on the neighbouring basins. The combination of high clastic influx and rapid subsidence is recorded in the high rates of sand and silt aggradation that were characteristic of the radial fluvial systems draining from apices again defined by structural low points. It is likely that denudation of the N-facing scarp formed by the Pena flexure backthrust meant that more distal, sand-carrying drainage systems to the north could breach the barrier separating the topographically inverted upland from the depositional sub-basins. This may explain the source of the relatively sudden sand influx in the early Miocene.

During the early Miocene, geometric evolution of the regional thrust system was complete and hence there was maximum definition of up to four hydrologically isolated sub-basins in the study area. Despite the waning of additional thrust propagation from the beginning of the Miocene, orogenic stresses still required some form of structural response. An example of such a response is the Miocene reactivation of the Sierra de Alaiz thrust which originally defined the western end of the early Oligocene mountainfront. During the Miocene, however, declining late orogenic contraction reactivated the pre-existing Sierra de Alaiz thrust instead of developing a new and more forelandward thrust. An analogous process of hinterland reactivation has also been recognised in the southern Norwegian Caledonides by Morley (1987) who attributes the cause as the ever increasing distance between orogenic sutures and foreland thrust tips. Where orogenic contraction is minimal, such as in the western part of the study area during the early Miocene, it may be mechanically more favourable to reactivate a pre-existing structure than to advance the thrust front still further.

Interpretations of depositional environment and tectonic setting for the ten clastic sedimentary facies recognised in the West Jaca basin are summarised in Table 8.1. The summary evolution of the basin also highlights several attributes that are considered here as being characteristic of thrust-top basins in general.

(1) Thrust-top basins form in regions of thin skin thrusting that tend to characterise the margins of collisional orogens. For example, in the southern Pyrenees the depth to detachment decreases forelandward from about twenty kilometres in the Axial Zone to three kilometres at the northern margin of the Ebro foreland basin (Deramond *et al.* 1984).

(2) Because of the relatively limited depth to detachment beneath thrust-top basins and the fact that while sediment is accumulating they are sites of orogenic contraction, movement of a basin over a buried ramp-flat tectonic topography will be expressed at the surface. For example, sequences showing characteristics of growthfolds record an actively-deforming depositional surface. Localised unconformities reflect local ramp-related tilting and erosion.

(3) Backthrusting is likely to be a common process in the structural evolution of a thrust-top basin. Such thrusts are interpreted here as forming at orogen margins during the waning stages of thrust propagation, and, below a critical depth to detachment (which would vary according to the angle of initiation of the backthrust, the gliding quality of the detachment horizon and the density of the hangingwall rocks). Along such margins, the relative thinness of the deforming cover means that the overburden resisting the formation of an incipient backthrust is small and underthrusting is therefore mechanically easy. In the West Jaca basin, the Pena flexure reflects an underlying passive-roof duplex which evolved by 'passive' underthrusting of the overlying Ebro basin foreland wedge.

(4) As a thrust-top basin develops it becomes increasingly divided into hydrologically-isolated sub-basins due to the geometric evolution of the underlying thrust system. In the West Jaca basin, a process that operated at the same time as compartmentalisation was the topographic inversion of the more hinterlandward compartments as imbricate stacking, during a piggyback sequence of thrusting, increased the thickness of the uppermost crust.

(5) The sedimentological development of a thrust-top basin-fill reflects thrust system evolution. For example, deposystems in a thrust-top basin commonly display evidence of having dispersed from an advancing fall line formed by an emergent thrust. This increase in proximality may result in a switch from axial to lateral drainage (eg. compare the Sheet and Ribbon Sandstone Facies of the Pena flexure), tectonically enhanced upward-coarsening (eg. the Ruesta Member to Bernues Formation sequences of the Pena flexure and Izaga sub-basin) and a reduction in palaeocurrent variance

(eg. the decreasing variance of the Petilla Member to Uncastillo Formation palaeocurrent rose diagrams of the Izaga sub-basin).

8.2 ALLUVIAL RESPONSE TO THRUST TECTONICS: THE EVOLUTION OF THE PENA FLEXURE

The block diagrams of Fig. 8.2 depict the structural and sedimentological evolution of the Pena flexure passive-roof duplex from the mid Oligocene, through the late Oligocene, to the early Miocene. The Pena flexure is the most forelandward major thrust culmination to have developed in the Southwest Pyrenees and is considered here to have locally defined the mountainfront. The trace of the synformal bend at the foot of the monoclinal flexure provides a convenient boundary line separating the thrust-fold belt to the north from the undeformed, autochthonous Ebro foreland basin. The trace of the synform is roughly coincident with the outcrop of the contact between the Petilla Member and the Bernues Formation along the southern flank of the flexure.

The following changes brought about by the development of the flexure are here considered to be characteristic of the evolution of mountainfronts in general.

(1) Flexing imposes a steeper gradient on neighbouring depositional basins, causing a rapid transition from axial drainage to lateral drainage.
(2) Major subsurface imbrication of thrusts (accommodating up to 45% N-S shortening beneath the Pena flexure) imposes a significant load on the neighbouring basin margin. Such crustal loading causes increasingly rapid subsidence, largely expressed by exceptionally high rates of sediment aggradation and preservation.
(3) Thrust emergence and subsequent displacement (late Oligocene in the study area) causes an increased clastic influx recorded by greater volumes of coarse sediment from the time of emergence onward.

Much of Chapters 4 to 6 dealt with the response of individual Jaca and Ebro basin deposystems to the development of the Pena flexure. This section concentrates on the general implicatons of Pena flexure evolution and, in particular, the tectonic controls on variations in alluvial stratigraphy displayed so strikingly by fluvial sequences such as the Sheet Sandstone Facies and the Ribbon Sandstone Facies.

Table 8.2 is a summary of the palaeoenvironmental and sedimentary sequence characteristics of the Sheet and Ribbon Sandstone Facies. The following contrasting parameters are considered here to be most significant: sand body width; sand body width to thickness ratio; the extent to which lateral accret-

ion surfaces are developed; sand body sedimentary structures; and, palaeocurrent vector magnitudes. From the viewpoint of hydrocarbon entrapment, and assuming similar petrophysical properties and burial conditions, a randomly chosen section through a Sheet Sandstone Facies sand body yields a potential reservoir with a mean cross sectional area of roughly 8000 m^2. This value contrasts with a mean 120 m^2 cross sectional area through a randomly chosen Ribbon Sandstone Facies sand body.

Because the two facies are separated by only 1000m of relatively rapidly deposited alluvial fan conglomerate, it may be assumed that there was no significant change in climate or bank composition between their deposition. The single palaeoenvironmental parameter which is considered here to be the most critical in explaining the sequence contrasts is the quadrupling of overbank fines aggradation rate between Sheet and Ribbon Sandstone Facies deposition. As argued in Chaper 6, the increase in overbank sedimentation following Pena flexure development led to relatively rapid channel entrenchment and consequent stunted meanderbelt development. The lateral restriction in the zone of channel influence is reflected in small meander wavelengths and amplitudes, and immature, undeveloped meanderbelts during deposition of the Ribbon Sandstone Facies. This contrasts to mature, fully developed meanderbelts that characterised the unentrenched, and thus, laterally unrestricted Sheet Sandstone Facies' environment.

A similar transtion from 'pre-tectonic', dominantly laterally accreting facies, to 'post-tectonic', dominantly vertically accreting facies may be observed in the pre- and post-conglomerate, fluvial sandstone sequences of the Uncastillo Formation in the Olleta sub-basin (Chapter 6). The above case study of the Sheet and Ribbon Sandstone Facies highlights the importance of external tectonic processes in controlling foreland basin facies evolution. In the West Jaca basin, the volume of fluvial sandstone bodies does not reflect the magnitude of the river systems that formed them.

8.3 CONCLUSIONS

(1) Thrust-top basins form and fill while being carried piggyback on active thrust sheets. Commonly, they develop where an advancing thrust front propagates into a neighbouring foreland basin, thus detaching its proximal margin from a sub-thrust basement.

(2) Thrust-top basins are special among sedimentary basins in that they experience orogenic contraction during sedimentation. Evidence for contemporaneous shortening and filling during their evolution includes localised

unconformities and growthfolds. Such phenomena record an actively deforming depositional surface experiencing folding, tilting and erosion as the basin moved over a relatively near surface, ramp-flat tectonic topography.

(3) During **their** Palaeogene to early Neogene evolution, the South Pyrenean thrust-top basins in general, and the West Jaca basin in particular, display substantial evidence of having been affected by a thrust front that propagated both southward, toward the foreland, and westward, parallel to the axis of the orogen. For example, along the length of the South Pyrenees, a highly diachronous marine regression sequence and a diachronous series of discrete alluvial fan conglomerate sequences mark the arrival time of the thrust front as it propagated westward, in a series of punctuated displacement events. In the West Jaca basin, the axially migrating deformation front is reflected in lateral (E-W) variations in the amount of N-S shortening and the depth to detachment.

(4) Paradoxically, the most rapid rate of subsidence in the southern Pyrenees occured in the Olleta sub-basin, at the western limit of the axially propagating thrust front, where orogenic contraction and crustal loading was probably at a minimum. The contradiction between expectation and actuality suggests that a 'basement' duplex beneath the South Pyrenees (Camara & Klinowitz 1985) exerted a major influence on basin development. It is proposed here that subsidence in the South Pyrenean basins was initiated by the basement duplex but that, in any one part of the region, subsidence was halted by topographic inversion associated with the arrival of the westward propagating 'cover' thrust system.

(5) At the foreland margin of the West Jaca thrust-top basin, the synformal trace of the Pena flexure may be used to define the Southwest Pyrenean mountainfront. The Pena flexure is interpreted as being underlain by a passive-roof duplex; an increasingly widely recognised category of mountainfront structure that is expressed by an emergent backthrust. In the South Pyrenees, backthrusts are common only at the orogen margin where the relatively shallow depth to detachment (<3 km) provides minimal resistance to underthrusting, and hence, allows a backthrust to emerge at the synorogenic surface.

(6) Three characteristic mesofracture domains are recognised in the West Jaca basin: Footwall Domains, containing older jointsstriking normally to the regional trend of thrusts and folds indicating that elongation was perpendicular to thrust transport direction; Hangingwall Domains, containing

older joints striking sub-parallel to the regional trend of thrusts and folds indicating that elongation was parallel to thrust transport direction; and Lateral Ramp Domains, containing older joints striking sub-parallel to the trend of the underlying lateral ramps indicating that elongation was locally parallel to the dip of an underlying lateral ramp. The distribution of the domains reflects thrust system geometry. The overprinting of separate mesofracture systems within domains reflects thrust system evolution.

(7) The stratigraphic and sedimentological development of thrust-top basin fills, especially their increasing compartmentalisation into hydrologically isolated sub-basins, is closely related to the evolution of the underlying thrust system. For example, analysis of the Ruesta fault zone, a region of strike-normal extension faults that express a buried lateral ramp, reveals how the laterally oriented fault zone locally controlled facies evolution, dispersion patterns and sand body interconnectedness.

(8) The importance of tectonic processes in controlling thrust-top basin facies development means that the dimensions of a deposystem are not necessarily proportional to the dimensions of its final depositional 'product'. For example, the 'pre-tectonic' Sheet Sandstone Facies environment produced laterally persistent, high volume sand bodies deposited by lateral accretion on slowly subsiding, areally extensive, alluvial plains. However, the 'post-tectonic' Ribbon Sandstone Facies comprises laterally confined, relatively low volume sand bodies deposited by vertical accretion on rapidly subsiding, areally restricted, alluvial plains.

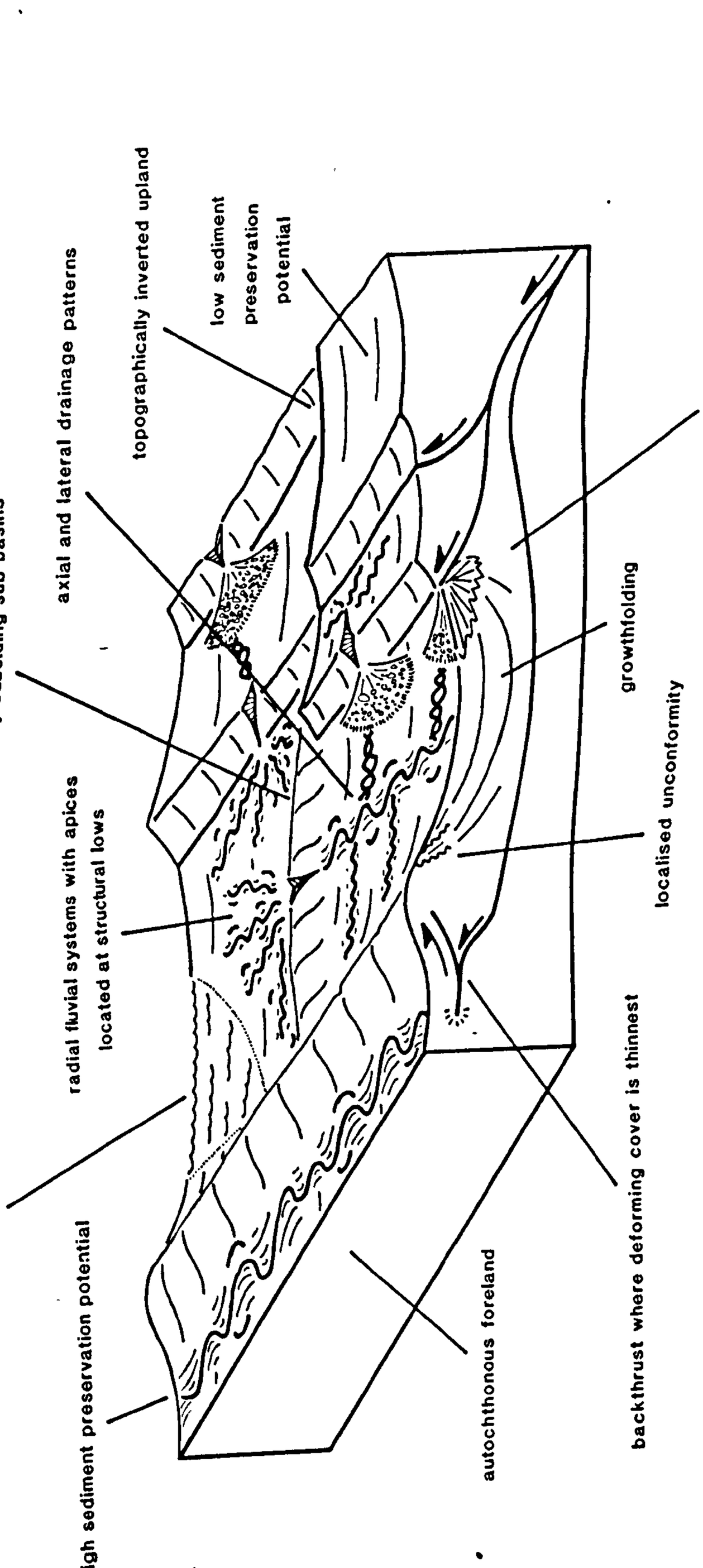

Fig. 8.1. Schematic block diagram summarising the typical tectonic, stratigraphic and sedimentological features of thrust-top basins.

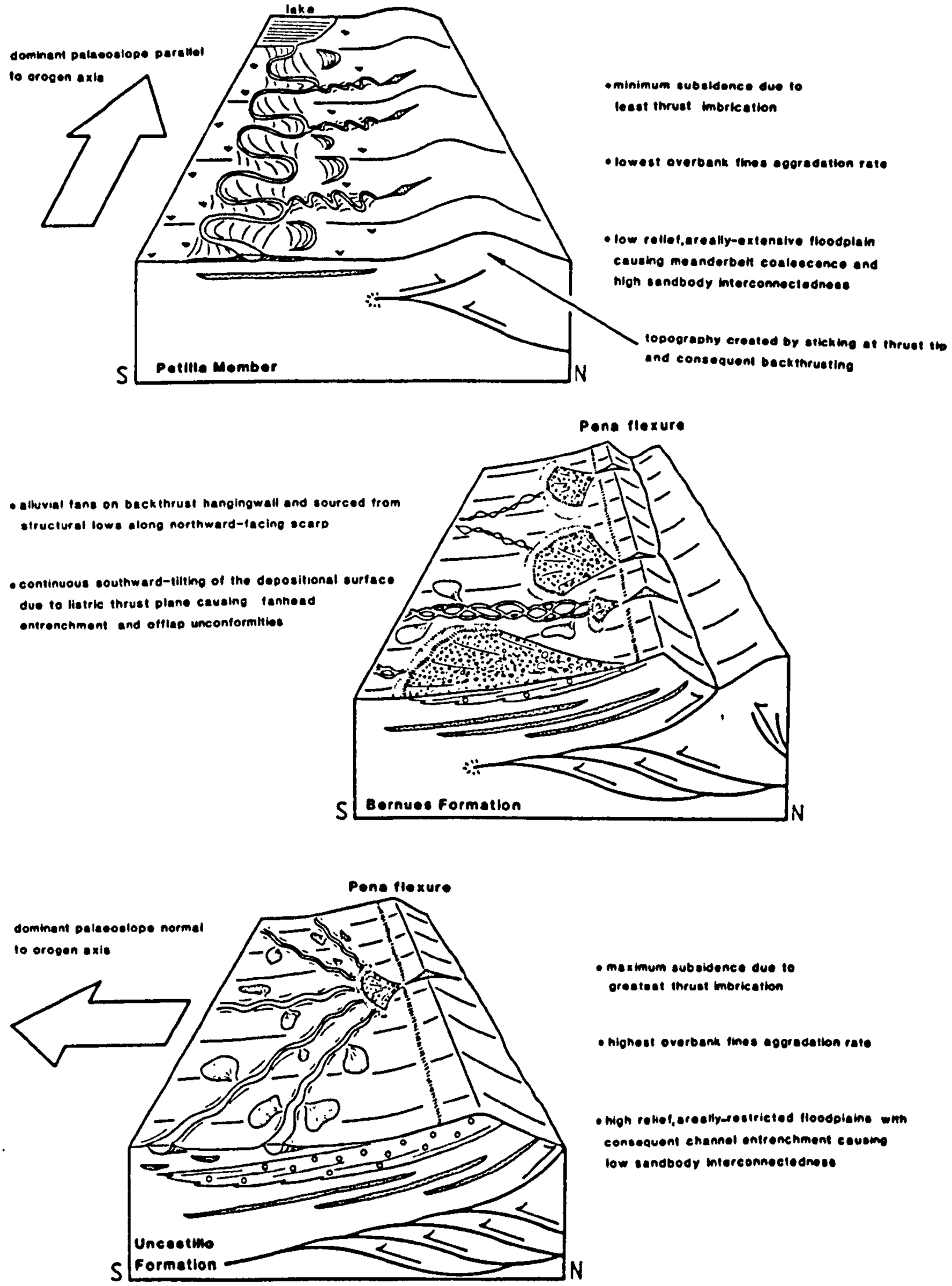

Fig. 8.2. Block diagrams illustrating the evolving geomorphology and depositional environments of the Pena flexure mountainfront during the mid Oligocene to early Miocene. The sequence of passive-roof duplex development is based on the computer simulated sequential evolution of the Alberta syncline triangle zone by Charlesworth & Gagnon (1985, fig. 2).

Table 8.1. Depositional environments, tectonic settings and potential reservoir volumes of the ten clastic lithofacies recognised in the West Jaca thrust-top basin.

Facies and abbreviation	Depositional environment	Tectonic setting	Sand body volume, lateral extent and interconnectedness
Massive Conglomerate (MC)	alluvial fan head		low
Conglomerate with Sandstone (CS)	alluvial fan toe	increasingly proximal	low
Gravelly Sandstone (GS)	profan ephemeral braidplain	with respect to fault-	moderate
Current-Rippled Sandstone (CRS)	sandy sheetflood plain	defined basin margin	moderate
Mottled Siltstone with Sandstone (MSS)	mud dominant alluvial plain	also characteristic of sediment starved interfan areas	low
Ribbon Sandstone (RS)	low sinuosity fluvial	relatively rapidly subsiding (and aggrading) post-tectonic climax	high
Sheet Sandstone (SS)	high sinuosity fluvial	relatively slowly subsiding (and aggrading) pre-tectonic climax	very high
Multistorey Sand Body (MSB)	fluviolacustrine mouthbar and fluvial	transitional low to high clastic influx generated by initial tectonic activity	high
Wave-Rippled Sandstone (WRS)	nearshore marginal lacustrine	topographically lowest parts of the basin occupied by a shallow lake during relative tectonic inactivity	moderate
Massive Grey Mudstone (MGM)	offshore lacustrine	deeper, longer lived and more extensive lake located in areas of sustained rapid subsidence	low

Table 8.2. Palaeoenvironmental and sequence characterístics of the Sheet Sandstone Facies and Ribbon Sandstone Facies. Unbracketed and bracketed figures refer to mean values and ranges, respectively.

	Parameter	Sheet Sandstone Facies	Ribbon Sandstone Facies
PALAEOENVIRONMENTAL CHARACTERISTICS	bankfull channel width	33 (12-55)	40 (6-80)
	bankfull channel depth	3.3 (22-5.5)	5 (1-8)
	width:depth	10 (8-20)	8 (5-12)
	sinuosity	2.3 (1.6-2.6)	1.14 (1.1-1.7)
	meanderbelt width	400 (300-600)	50 (6-85)
	meanderbelt amplitude	127 (80-200)	50
	meander wavelength	372 (240-600)	50
	overbank fines aggradation rate	$\leqslant$0.5 mm yr.$^{-1}$	$\geqslant$2 mm yr.$^{-1}$
	depositional environment	perennial, sand dominated axial systems with areally extensive alluvial plains	ephemeral, sand dominated, radial lateral systems with laterally restricted alluvial plains
SEQUENCE CHARACTERISTICS	sand body width	1500 (300-6000)	24 (6-85)
	sand body thickness	5.3 (1.5-13)	5 (1.2-9)
	mean sand body cross sectional area	8000m^2	120m^2
	width:thickness	300 (100-800)	9.4 (4.8-14.3)
	% channel sandstone in sequence	32% (20-42%)	34% (27-50%)
	sand body structure	mean 2(0-4) channel storeys; commonly multilateral	mean 3(0-6) channel storeys; rarely multilateral
	lateral accretion surfaces	common and developed to full potential	common but not developed to full potential
	sand body sedimentary structures	well defined upward fining; much evidence of lateral accretion	poorly defined upward fining; much evidence of vertical accretion
	sand body erosive relief	0.4 (0.1-2)	1.5 (0.5-4)
	overbanks	mottled siltstone and sandstone with rare calcrete nodules	generally unmottled siltstone and sandstone
	palaeocurrent vector magnitudes	15% (13-17%)	77% (58-93%)

Footnote: all dimensions in metres

REFERENCES

ALLEN, J.R.L. 1963. The classification of cross-stratified units with notes on their origin. *Sedimentology*, *2*, 93-114.

ALLEN, J.R.L. 1965. A review of the origins and characteristics of Recent alluvial sediments. *Sedimentology*, *5*, 89-191.

ALLEN, J.R.L. 1966. On bedforms and palaeocurrents. *Sedimentology*, *6*, 153-190.

ALLEN, J.R.L. 1968. *Current Ripples*. North-Holland, Amsterdam.

ALLEN, J.R.L. 1970. Studies in fluviatile sedimentation: A comparison of fining-upwards cyclothems with special reference to coarse-member composition and interpretation. *Journal of Sedimentary Petrology*, *40*, 298-323.

ALLEN, J.R.L. 1978. Studies in fluviatile sedimentation: an exploratory quantitative model for the architecture of avulsion-controlled alluvial suites. *Sedimentary Geology*, *21*, 129-147.

ALLEN, J.R.L. 1983. Studies in fluviatile sedimentation: Bars, bar-complexes and sandstone sheets (Low sinuosity braided streams) in the Brownstones (L. Devonian), Welsh Borders. *Sedimentary Geology*, *33*, 237-293.

ALLEN, J.R.L. & BANKS, C.M. 1972. An interpretation and analysis of recumbent-folded, deformed cross-bedding. *Sedimentology*, *19*, 257-268.

ALLEN, P.A. 1981a. Wave-generated structures in the Devonian lacustrine sediments of south-east Shetland and ancient wave conditions. *Sedimentology*, *28*, 369-381.

ALLEN, P.A. 1981b. Devonian lake margin environments and processes, SE Shetland. *Journal of the Geological Society of London*, *138*, 1-14.

ALLEN, P.A., CABRERA, L., COLOMBO, F. & MATTER, A. 1983. Variations in fluvial style on the Eocene-Oligocene alluvial fan of the Scala Dei Group SE Ebro basin, Spain. *Journal of the Geological Society*, *140*, 133-146.

ALLEN, P.A. & MATTER, A. 1982. Oligocene meandering stream sedimentation in the eastern Ebro basin, Spain. *Eclogae Geologie Helvetica*, *75*, 33-49.

ANADON, P., CABRERA, L., COLOMBO, M., MARZO, M. & RIBA., O. 1986. Syntectonic intraformational unconformities in alluvial fan deposits, eastern Ebro basin margin (NE Spain). *In*: ALLEN, P.A. & HOMEWOOD, P. (Eds.), *Foreland Basins*, International Association of Sedimentologists Special Publication, *8*, 259-271.

ATKINSON, C.D. 1983. *Comparative sequences of ancient fluviatile deposits in the Tertiary South Pyrenean basin, Northern Spain*. PhD Thesis, University of Wales.

BAGNOLD., R.A. 1946. Motion of waves in shallow water: Interactions of waves and sandy bottoms. *Proceedings of the Royal Society of London, A187,* 1-15.

BALLY, A.W., BERNOULLI, D., DAVIS, G.A. & MONTADERT, A. 1981. Listric Normal Faults. *Oceanologica Acta, 4th Proceedings 26th International Geological Congress; Geology* of *Continental Margins Symposium.* Paris, 87-101.

BANKS, C.J. & WARBURTON, J. 1986. 'Passive-roof' duplex geometry in the frontal structures of the Kirthar and Sulaiman mountain belts, Pakistan. *Journal of Structural Geology, 8,* 229-237.

BEADLE, L.C. 1974. *The Inland Waters of Tropical Africa.* Longman, London.

BEAUMONT, C. 1978. The evolution of sedimentary basins on a visco-elastic lithosphere: theory and examples. *Geophysical Journal of the Royal Astronomical Society, 55,* 471-479.

BEAUMONT, C. 1981. Foreland basins. *Geophysical Journal of the Royal Astronomical Society, 65,* 291-329.

BEHRENSMEYER, A.K. & TAUXE, L. 1982. Isochronous fluvial systems in Miocene deposits of Northern Pakistan. *Sedimentology, 29,* 331-353.

BENNETT, R.H. 1977. Pore-water pressure measurements: Mississippi delta submarine sediments. *Marine Geotechnic, 2,* 177-189.

BERNOULLI, D. 1964. Sur Geologie des Monte Generoso (Lombardische Alpen). *Beitr. Geologie Karte Schweiz, 118,* 134-149.

BERTRAND, M. 1897. Structure des Alpes francaises et recurrence de certains facies sedimentaires. *Vle. International Geologique Congress (Zurich),* 161-177.

BLAIR, T.C. 1987. Sedimentary processes, vertical stratification sequences, and geomorphology of the Roaring River alluvial fan, Rocky Mountain National Park, Colorado. *Journal of Sedimentary Petrology, 87,* 1-18.

BLAKEY, R.C. & GUBITOSA, R. 1984. Controls of sandstone body geometry and architecture in the Chinle Formation (Upper Triassic), Colorado Plateau. *Sedimentary Geology, 38,* 51-86.

BLUCK, B.J. 1964. Sedimentation of an alluvial fan in southern Nevada. *Journal of Sedimentary Petrology, 34,* 395-400.

BLUCK, B.J. 1971. Sedimentation in the meandering River Endrick. *Scottish Journal of Geology, 7;* 93-138.

BLUCK, B.J. 1974. Structure and directional properties of some valley sandur deposits of Southern Iceland. *Sedimentology, 21,* 533-554.

BLUCK, B.J. & KELLING, G. 1963. Channels from the Upper Carboniferous Coal Measures of South Wales. *Sedimentology, 2,* 29-53.

BOILLOT, G. 1984. Some remarks on the continental margins in the Aquitaine and French Pyrenees. *Geological Magazine, 121*, 407-412.

BOMBOLAKIS, E.G. 1986. Thrust-fault mechanics and origin of a frontal ramp. *Journal of Structural Geology, 8*, 281-290.

BOOTHROYD, J.C. & NUMMEDAL, D. 1978. Proglacial braided outwash: a model for humid alluvial fan deposits. *In*: MIALL, A.D. (Ed.), *Fluvial Sedimentology*, Canadian Society of Petroleum Geologists Memoir, *5*, 641-669.

BOUMA, A.H. 1962. *Sedimentology of some Flysch Deposits: A graphic approach to facies interpretation.* Elsevier, Amsterdam, 168 pp.

BOWN, T.M. & KRAUS, M.J. 1981. Lower Eocene alluvial palaeosols (Willwood Formation, northwest Wyoming, USA) and their significance for palaeoecology, palaeoclimatology and basin analysis. *Palaeogeography, Palaeoclimatology and Palaeoecology, 34*, 1-30.

BOYD, J.D. 1983. *Sedimentology of the Lower Dingle Group, Southern Dingle Peninsula, S.W. Ireland.* PhD Thesis, University of Bristol.

BOYER, S.E. & ELLIOTT, D. 1982. Thrust systems. *Bulletin of the American Association of Petroleum Geologists, 66*, 1196-1230.

BRIDGE, J.S. 1985. Paleochannel patterns inferred from alluvial deposits: a critical evaluation. *Journal of Sedimentary Petrology, 55*, 579-689.

BRIDGE, J.S. & DIEMER, J.A. 1983. Quantitative interpretation of an evolving ancient river system. *Sedimentology, 30*, 599-623.

BRIDGE, J.S. & LEEDER, M.R. 1979. A simulation model of alluvial stratigraphy. *Sedimentology, 26*, 617-644.

BULL, W.B. 1962. Relations of alluvial fan size and slope to drainage-basin size and lithology in western Fresno County, California. *US Geological Survey Professional Paper, 450-B*, 51-53.

BULL, W.B. 1964. History and causes of channel trenching in western Fresno County, California. *American Journal of Science, 262*, 249-258.

BULL, W.B. 1972. Recognition of alluvial fan deposits in the stratigraphic record. *In*: RIGBY, J.K. & HAMBLIN, W.K. (Eds.), *Recognition of Ancient Sedimentary Environments.* Society of Economic Paleontologists and Mineralogists Special Publication *16*, 63-84.

BUTLER, R.W.H. 1982a. The terminology of structures in thrust belts. *Journal of Structural Geology, 4*, 239-245.

BUTLER, R.W.H. 1982b. Hangingwall strain: a function of duplex shape and footwall topography. *Tectonophysics, 88*, 235-244.

CADISCH, J., EUGSTER, H. & WENK, E. 1968. *Erläuterungen Blatt Scuol-Schuls-Tarasp Schw. Geol. Kommission*, Kummerly and Frey, A.G., Bern.

CAMARA, P. & KLIMOWITZ, J. 1985. Interpretation geodiminica de la sentiente centro-occidental surpirenaica, (Cuencas de Jaca-Tremp). *Estudios geologico, 41*, 391-404.

CANT, D.J. & WALKER, R.G. 1978. Fluvial processes and facies sequences in the sandy braided South Saskatchewan River, Canada. *Sedimentology, 25*, 625-649.

CAREY, S.W. 1958. The tectonic approach to continental drift. *In*: CAREY, S.W. (Ed.). *Continental Drift*, University of Tasmania, Hobart, 177.

CASATI, P. & GAETANI, M. 1968. Lacune nel Triassico Superiore nel Giurassico del Canto Alto-Monte di nese (Prealpi Bergamasche). *Bolletin Societe Geologico Italia, 87*, 719-731.

CASTIELLA, J., SOLÉ, J. & DEL VALLE, J. 1978. Cartografia geologica a partir de la investigacion geologica de Navarra a escala 1:25000. *Diputacion Foral de Navarra, Pamplona*.

CHARLESWORTH, H.A.K. & GAGNON, L.G. 1985. Intercutaneous wedges, the triangle zone and structural thickening of the Minheer Coal Seam at Coal Valley in the Rocky Mountain Foothills of central Alberta. *Bulletin of Canadian Petroleum Geology, 33*, 22-30.

CHOUKROUNE, P. 1976. Structure et evolution tectonique de la zone nord-Pyreneene. Memoires Societe Geologique de France, 127, 1-116.

CHOUKROUNE, P., LE PICHON, X., SEGURET, M. & SIBUET, J.C. 1973. Bay of Biscay and Pyrenees. *Earth and Planetary Science Letters, 18*, 109-118.

CHOUKROUNE, P. & MATTAUER, M. 1978. Tectonique de plaques et Pyrenees: sur le fonctionnement de la faille transformante nord-pyreneene; comparisons avec des modeles actuels. *Bulletin Societe Geologique de France, 20*, 689-700.

CHOUKROUNE, P. & SEGURET, M. 1973. Tectonics of the Pyrenees, role of gravity and compression. *In*: DE JONG, K.H. & SCHOLLEN, R. (Eds.), *Gravity and Tectonics*, Wiley, New York, 113-133.

COLLINSON, J.D. 1978. Vertical sequence and sand body shape in alluvial sequences. *In*: MIALL, A.D. (Ed.), *Fluvial Sedimentology*, Canadian Society of Petroleum Geologists Memoir, *5*, 577-587.

COLLINSON, J.D. & THOMSON, D. 1982. *Sedimentary Structures*. George, Allen and Unwin, 194 pp.

COOPER, M.A. & MARSHALL, J.D. 1981. ORIENT: A computer program for the resolution and rotation of paleocurrent data. *Computers & Geosciences, 7*, 153-165.

COOPER, M.A. & TRAYNER, P.M. 1986. Thrust-surface geometry: implications for thrust belt evolution and section-balancing techniques. *Journal of Structural Geology, 8*, 305-312.

COTTER, E. 1971. Paleoflow characteristis of a late Cretaceous river in Utah from analysis of sedimentary structures in the Ferron Sandstone. *Journal of Sedimentary Petrology, 41,* 129-138.

CRUSAFONT, M. & PONS, J.M. 1969. Nuevos datos sobre el Aquitaniense del Norte de la provincia de Huesca: *Acta Geelogica Hispanica, 4,* 124-125.

DAHLSTROM, C.D.A. 1969. Balanced cross sections. *Canadian Journal of Earth Sciences, 6,* 743-757.

DAVISON, I. 1986. Listric normal fault profiles: calculation using bed-length balance and fault displacement. *Journal of Structural Geology, 8,* 209-210.

DEL VALLE, A. 1929. Investigacion de sales potasicas en Navarra. *Bolletin Instituto Geologico y Minero de Espana, 51,* 89-107.

DEL VALLE, A. 1932. Descubrimiento de la cuenca potasica de Navarra. *Notas y comunicaciones Instituo Geologico y Minero de Espana, 4,* 3-21.

DENNY, C.S. 1967. Fans and pediments. *American Journal of Science, 265,* 81-105.

DEPAPE, G. 1950. Sur une flore d'age Oligocene de Cervera (Catalogne). *C.r. Seances Academie Sciences Paris, 230.*

DERAMOND, J. 1979. *Mecanisme de deformation et mise en place des nappes; exemple de la nappe de Gavarnie (Pyrenees centrales).* Thesis, University of Toulouse.

DERAMOND, J., FISCHER, M., HOSSACK, J., LABAUME, P., SEGURET, M., SOULA, J-C., VIALLARD, P. & WILLIAMS, G.D. 1984. Field Guide of Conference Trip to the Pyrenees. *Chavauchement et deformation conference, Toulouse,* 1-28.

DE SITTER, L.U. 1964. *Structural Geology.* McGraw Hill, London, Second Edition.

DEWEY, J.F., HEMPTON, M.R., KIDD, W.S.F., SAROGLU, F. & SENGOR, A.M.C. 1986. Shortening of continental lithosphere: the neotectonics of Eastern Anatolia - a young collision zone. *In*: COWARD, M.P. & RIES, A.C. (Eds.), *Collison Tectonics.* Geological Society Special Publication, *19,* 3-36.

DONALDSON, A.C. 1969. Paleostream analysis. *In*: DONALDSON, A.C. (Ed.), *Some Appalachian coals and carbonates: Models of ancient shallow-water deposition.* Pre-convention guidebook, Geological Society of America, 265-277.

VAN EDEN, J.G. 1970. A reconnaissance of deltaic environment in the Middle Eocene of the South-Central Pyrenees, Spain. *Geologie und Mijnbouw, 49,* 145-157.

ELLIOTT, T. 1974. Interdistributary bay sequences and their genesis. *Sedimentology, 21,* 611-622.

ELLIOTT, T. 1976. The morphology, magnitude and regime of a Carboniferous fluvial-distributary channel. *Journal of Sedimentary Petrology*, 46, 70-76.

ELTER, P. & SCHWAB, S. 1959. Nota illustrativa della carta geologica all' 1:50000 della regione Carro-Zeri-Pontrenoli. *Bolletin Societe Geólogico Italia, 78*, 157-177.

ELTER, P. & TREVISAN, L. 1973. Olistostromes in the tectonic evolution of the northern Apennines. *In*: DE JONG, K.A. & SCHOLTEN, R. (Eds.), *Gravity and Tectonics*, Wiley, London, 175-188.

ETHRIDGE, F.G. 1985. Modern alluvial fans and fan-deltas. *In*: *Recognition of Fluvial Depositional Systems and their Resource Potential*. Society of Economic Palaeontologists and Mineralogists Short Course Lecture Notes, *19*, 101-127.

ETHRIDGE, F.G. & SCHUMM, S.A. 1978. Reconstructing palaeochannel morphologic and flow characteristics: methodology, limitations and assessment. *In*: MIALL, A.D. (Ed.), *Fluvial Sedimentology*, Canadian Society of Petroleum Geologists Memoir, *5*, 703-723.

FARRELL, K.M. 1987. Sedimentology and facies architecture of overbank deposits of the Mississippi River, False River Region, Louisiana. *In*: ETHRIDGE, F.G., FLORES, R.M. & HARVEY, M.D. (Eds.), *Recent Developments in Fluvial Sedi- mentology*. Society of Economic Paleontologists and Mineralogists Special Publication, *39*, 111-121.

FARRELL, S.G. 1984. A dislocation model applied to slump structures, Ainsa basin, South Central Pyrenees. *Journal of Structural Geology, 6*, 727-736.

FARRELL, S.G., WILLIAMS, G.D. & ATKINSON, C.D. 1987. Constraints on the age of movement of the Montsech and Cotiella Thrusts, South central Pyrenees, Spain. *Journal of the Geological Society, London, 144*, 907-914.

FISK, H.N. 1947. Fine-grained alluvial deposits and their effects on Mississippi River activity. *Mississippi River Communications*, Vicksburg, Mississippi, 82pp.

FLICHE, P. 1906. Nota sobre algunos vegetales terciarios de Cataluna. *Memoire Suisse Palaeontologique, 90*, 70pp.

FLORES, G. 1956. Lettera al presidente della Societa geologica Italiana. *Bolletin Societa Geologica della Italiana, 75*, 220-222.

FOUCH, T.D. & DEAN, W.E. 1982. Lacustrine and associated clastic depositional environments. *In*: SCHOLLER, P.A. & SPEARING, D. (Eds.), *Sandstone Depositional Environments*. American Association of Petroleum Geologists Memoir *31*, 87-114.

FRIEND, P.F. 1978. Distinctive features of some ancient river systems. *In*: MIALL, A.D. (Ed.), *Fluvial Sedimentology*, Canadian Society of Petroleum Geologists Memoir, *5*, 531-543.

FRIEND, P.F., HIRST, J.P.P. & NICHOLS, G.J. 1986. Sandstone-body structure and river processes in the Ebro basin of Aragon, Spain. *Cuadernos de Geologica: Fluvial Sedimentation in Spain*, Madrid.

FRIEND, P.F., MARZO, M., NIJMAN, W. & PUIGDEFABREGAS, C. 1981. Fluvial sedimentology in the Tertiary South Pyrenean and Ebro Basins, Spain. *In*: ELLIOTT, T. (Ed.), *Field Guides to Modern and Ancient Fluvial Systems in Britain and Spain*. University of Keele, 4.1-4.50.

FRIEND, P.F., SLATER, M.J. & WILLIAMS,, R.C. 1979. Vertical and lateral building of river sandstone bodies, Ebro basin, Spain. *Journal of the Geological Society, London, 136*, 39-46.

GALLOWAY, W.E. 1981. Depositional architecture of Cenozoic Gulf coastal plain fluvial systems. *Society of Economic Paleontologists and Mineralogists Special Publication, 31*, 127-155.

GALLOWAY, W.E. 1985. Modern alluvial fans and fan-deltas. *In*: *Recognition of Fluvial Depositional Systems and their Resource Potential*. Society of Economic Palaeontologists and Mineralogists Short Course Lecture Notes, *19*, 127-145.

GARDNER, T.W. 1985. Paleohydrology and paleomorphology of a Carboniferous, meandering fluvial sandstone. *Journal of Sedimentary Petrology, 53*, 99-1005.

GIBBS, A.D. 1983. Balanced cross-section construction from seismic sections in areas of extensional tectonics. *Journal of Structural Geology, 5*, 153-160.

GIBBS, A.D. 1984. Structural evolution of extensional basin margins. *Journal of the Geological Society of London, 141*, 609-620.

GIBBS, A.D. 1987. Development of extension and mixed-mode sedimentary basins. *In*: COWARD, M.P., DEWEY, J.F. & HANCOCK, P.L. (Eds.), *Continental Extensional Tectonics*. Geological Society Special Publication, *28*, 19-33.

GRIMAUD, S., BOILLOT, G., COLETTE, B., MAUFFRET, A., MILES, P.R. & ROBERTS, D.B. 1983. Western extension of the Iberian-European plate boundary during the early Cenozoic (Pyrenean) convergence: a new model. *Marine Geology, 45*, 63-77.

HAMBLIN, W.K. 1965. Origin of 'reverse drag' on the down-thrown side of normal faults. *Bulletin of the Geological Society of America, 76*, 1145-1164.

HANCOCK, P.L. 1985. Brittle microtectonics: principles and practice. *Journal of Structural Geology, 7*, 437-457.

HANCOCK, P.L. 1986. Joint spectra. *In*: NESBITT, R.W. & NICHOL, I. (Eds.), *Geology in the real world - the Kingsley Dunham volume.* The Institution of Mining and Metallurgy.

HANCOCK, P.L. & BEVAN, T.G. 1987. Brittle modes of foreland extension. *In*: COWARD, M.P., DEWEY, J.F. & HANCOCK, P.L. (Eds.) *Continental Extensional Tectonics.* Geological Society Special Publication, *28*, 127-137.

HARLAND, W.B., COX, A.V., LEWELLYN, P.G., PICKTON, C.A.G., SMITH, A.G. & WALTERS, R.A. 1982. *A Geologic Time Scale*, Cambridge Earth Sciences Series, Cambridge University Press, Cambridge.

HARMS, J.C. & FAHNESTOCK, R.R. 1965. Stratification, bedforms, and flow phenomena (with an example from the Rio Grande). *In*: MIDDLETON, G.V. (Ed.), *Primary Sedimentary Structures and Their Hydrodynamic Interpretation.* Society of Economic Paleontologists and Mineralogists Special Publication, *12*, 84-115.

HEWARD, A.P. 1978. Alluvial fan and lacustrine sediments from the Stephanian A and B (La Magdalena, Cinera-Matallana and Sabero) coalfields, northern Spain. *Sedimentology*, 25, 451-488.

HEWARD, A.P. 1978. Alluvial fan sequence and megasequence models with examples from Westphalian D-Stephanian B Coalfields, northern Spain. *In*: MIALL, A.D. (Ed.), *Fluvial Sedimentology*, Canadian Society of Petroleum Geologists Memoir, *5*, 669-703.

HIRST, J.P.P. & NICHOLS, G.J. 1986. Thrust tectonic controls on Miocene alluvial distribution patterns, southern Pyrenees. *In*: ALLEN, P.A. & HOMEWOOD, P. (Eds.), *Foreland Basins.* International Association of Sedimentologists Special Publication, *8*, 153-164.

HOBBS, B.E., MEANS, W.D. & WILLIAMS, P.F. 1976. *An Outline of Structural Geology*, Wiley International.

HOOKE, R.L.B. 1968. Steady-state relationships on arid-region alluvial fans in closed basins. *American Journal of Science, 266*, 609-629.

HOOKE, R. L. B. 1972. Geomorphic evidence for late Wisconsin and Holocene tectonic deformation, Death Valley, California. *Geological Society of America Bulletin, 83*, 2073-2098.

HOSSACK, S.R. 1979. The use of balanced cross-sections in the calculation of orogenic contraction: a review. *Journal of the Geological Society of London, 136*, 705-711.

HUBBERT, M.K. & RUBEY, W.W. 1959. Role of fluid pressure in mechanics of overthrust faulting. *Geological Society of America Bulletin, 70*, 115-206.

HUNT, C.B. & MABEY, D.R. 1966. Stratigraphy and structure, Death Valley, California. *US Geological Survey Professional Paper, 494-A*, 162pp.

HYNE, N.J., COOPER, W.A. & DICKEY, P.A. 1979. Stratigraphy of inter-montane, lacustrine delta, Catatumbo River, Lake Maracaibo, Venezuela. *Bulletin of the American Association of Petroleum Geologists, 63*, 2042-2057.

INGLES, O.H. & GRANT, K. 1975. The effect of compaction on various properties of coarse-grained sediments. *In*: CHILINGARIAN, G.V. & WOLF, K.H. (Eds.), *Compaction of coarse-grained sediments*. Elsevier, New York, 293-348.

INSTITUTO GEOLOGICO Y MINERO DE ESPANA. 1950a, 1950b, 1954, 1959. Mapa geologico de Espana. Explicacion de las hojas *174, 207, 208* & *175. Madrid.*

INSTITUTO GEOLOGICO Y MINERO DE ESPANA. 1974, 1976, 1978a, 1978b. Mapa geologico de Espana. *Servicio de Publicaciones Ministerio de Industria y Energia*, Hojas *141, 142, 175* & *207.*

JACKSON, R.G. II. 1976. Depositional model of point bars in the lower Wabash River. *Journal of Sedimentary Petrology, 46*, 579-594.

JACKSON, R.G. II. 1978. Preliminary evaluation of lithofacies models for meandering alluvial streams. *In*: MIALL, A.D. (Ed.), *Fluvial Sedimentology Canadian Society of Petroleum Geologists Memoir, 5*, 543-577.

JOHNS, D.R., MUTTI, E., ROSELL, J. & SEGURET, M. 1981. Origin of a thick redeposited carbonate bed in Eocene turbidites of the Hecho Group, South-central Pyrenees, Spain. *Geology, 9*, 161-164.

JONES, P.B. 1982. Oil and gas beneath east-dipping underthrust faults in the Alberta foothills. *In*: POWERS, R.B. (Ed.), *Geological Studies of the Cordillean Thrust Belt.* Rocky Mountain Association of Petroleum Geologists, *1*, 61-74.

KARNER, G.D. 1985. *Continental tectonics - a quantiative view of the thermal and mechanical properties of the continental lithosphere in compressional and extensional stress regimes.* Centre National d'Etudes Spatiales, Summer School of Space Physics, Toulouse, France, 53pp.

KELLING, G. & WILLIAMS, B.P.J. 1966. Deformation structures of sedimentary origin in the Lower Limestone Shales (Basal Carboniferous) of South Pembrokeshire, Wales. *Journal of Sedimentary Petrology, 36*, 927-939.

KHAN, H.R. 1971. *Laboratory study of alluvial river morphology.* PhD thesis, Colorado State University.

KRAUS, M.J. & MIDDLETON, L.T. 1987. Contrasting architecture of two alluvial suites in different structural settings. *In*: ETHRIDGE, F.G., FLORES, R.M. & HARVEY, M.D. (Eds.), *Recent Developments in Fluvial Sedimentology.* Society of Economic Paleontologists and Mineralogists Special Publication, *39*, 253-263.

KRUMBEIN, W.C. 1941. Measurement and geological significance of shape and roundness of sedimentary particles. *Journal of Sedimentary Petrology, 11*, 64-72.

KUENEN, P.H. 1948. Slumping in the Carboniferous rocks of Pembrokeshire. *Geological Society of London Quarterly Journal, 104*, 365-385.

KUSZNIR, N. & KARNER, G.D. 1985. Dependence of the flexural rigidity of the continental lithosphere on rheology and temperature. *Nature, 316*, 138-142.

LABAUME, P., SEGURET, M. & SEYVE, C. 1985. Evolution of a turbiditic foreland basin and analogy with an accretionary prism: example from the Eocene south Pyrenean basin. *Tectonics, 4*, 661-685.

LANGBEIN, W.B. & LEOPOLD, L.B. 1966. River meanders - theory of minimum variance. *Professional Paper of the US Geological Survey, 422-H.*

LEEDER, M.R. 1973. Fluviatile fining-upwards cycles and the magnitude of palaeochannels. *Geologial Magazine, 110*, 265-276.

LEEDER, M.R. 1975. Pedogenic carbonates and flood sediment accretion rates: a quantitative model for arid-zone lithofacies. *Geological Magazine, 112*, 257-270.

LEEDER, M.R. 1978. A quantitative stratigraphic model for alluvium, with special reference to channel density and interconnectedness. *In*: MIALL, A.D. (Ed.), *Fluvial Sedimentology*, Canadian Society of Petroleum Geologists Memoir, *5*, 587-597.

LEEDER, M.R. & ALEXANDER, J. 1987. The origin and tectonic significance of asymmetrical meander-belts. *Sedimentology, 34*, 217-227.

LEEDER, M.R. & GAWTHORPE, R.L. 1987. Sedimentary models for extensional tilt-block/half-graben basins. *In*: COWARD, M.P., DEWEY, J.F. & HANCOCK, P.L. (Eds.) *Continental Extensional Tectonics.* Geological Society Special Publication, *28*, 139-152.

LEOPOLD, L.B. & WOLMAN, M.G. 1960. River meanders. *Geological Society of America Bulletin, 71*, 769-794.

LEOPOLD, L.B., WOLMAN, M.G. & MILLER, J.P. 1946. *Fluvial processes in geomorphology*, Freeman, San Francisco.

LE PICHON, X. BONNIN, J,. FRANCHETEAU, J. & SIBUET, J.C. 1971. Une hypothese d'evolution tectonique du Golfe de Gascogne. *In*: DEBYSER, J., LE PICHON, X. & MONTADERT, L. (Eds.). *Histoire Structural du Golfe de Gascogne.* Paris: Technip, *6.2*, 1-44.

LE PICHON, X., BONNIN, J. & SIBUET, J.C. 1970. La faille nord-Pyreneene: faille transformante liee a l'ouverture du Golfe de Gascogne. *Comptes Rendus Academie des Sciences, 271*, 1941-1944.

LEVEY, R.A. 1978. Bedform distribution and internal stratification of coarse-grained point bars, Upper Congaree River, S.C. *In*: MIALL, A.D. (Ed.), *Fluvial Sedimentology*, Canadian Society of Petroleum Geologists Memoir, *5*, 105-129.

LINK, M.H. & OSBORNE, R.H. 1978. Lacustrine facies in the Pliocene Ridge Basin Group, Ridge Basin, California. *In*: MATTER, A. & TUCKER, M. (Eds.), *Modern and Ancient Lake Sediments*, International Association of Sedimentologists Special Publication, *2*, 169-175.

MANGIN, J.P. 1960. Le nummulitique sud-Pyreneen a l'Ouest de l'Aragon. *Pirineos, 51*, 1-631.

MANGIN, J.P. 1962. Traces de pattes d'oiseau x et flute-casts associes dans un "facies flysch" du Tertaire pyreneen. *Sedimentology, 1*, 163-166.

MARGALEF, R. 1957. Los microfosiles delago Mioceno de la Cerdana como indicadores ecologicos. *Curs. Confs. Instituto Investigacion Geologica Lucas Mallada, 4*, 13-17.

MATTAUER, M. 1969. Sur la rotation de l'Espagne. *Earth and Planetary Science Letters, 7*, 87-89.

MATTAUER, M. & HENRY, S. 1971. The Pyrenees. *In*: SPENCER, A.M. (Ed.). *Mesozoic-Canozoic Orogenic Belts: Data for Orogenic Studies.* Geological Society of London, Special Publication, *4*, 3-23.

McCLAY, K.R. & PRICE, N.S. 1981. Thrust and Nappe Tectonics. *Special Publication of the Geological Society of London, 9.*

VAN DER MEULEN, S. 1982. Sedimentary facies and setting of Eocene point bar deposits, southern Pyrenees, Spain. *Geologie en Mijnbouw, 61.*, 217-228.

VAN DER MEULEN, S. 1986. Sedimentary stratigraphy of Eocene sheetflood deposits, Southern Pyrenees, Spain. *Geological Magazine, 123*, 167-183.

MEY, P.H.W., NAGTEGAAL, P.J.C., ROBERTI, K.J. & HARTEELT, J.J.A. 1968. Lithostratigraphic subdivision of post-Hercynian deposits in the South-Central Pyrenees, Spain. *Leidse Geologie Mededelingen, 41*, 221-228.

McGOWEN, J.H. & GARNER, L.E. 1970. Physiographic Features and stratification types of coarse-grained point bars: Modern and ancient examples. *Sedimentology, 14*, 77-111.

McGOWEN, J.H. & GROAT, C.G. 1971. *Van Horn Sandstone, west Texas: An alluvial fan model for mineral exploration.* Bureau of Economic Geology of the University of Texas, Report and Investigation, *72*, 57pp.

MIALL, A.D. 1974. Palaeocurrent analysis of alluvial sediments: discussion of directional variance and vector magnitude. *Journal of Sedimentary Petrology, 44*, 1174-1185.

MIALL, A.D. 1976. Palaeocurrent and palaeohydrologic analysis of some vertical profiles through a cretaceous braided stream deposit. *Sedimentology, 23*, 459-483.

MIALL, A.D. 1985. Architectural-element analysis: a new method of facies analysis applied to fluvial deposits. *In*: *Recognition of Fluvial Depositional Systems and their Resource Potential.* Society of Economic Palaeontologists and Mineralogists Short Course Lecture Notes, *19*, 33-83.

McKEE, E.D., CROSBY, E.J. & BERRYHILL, H.L. 1967. Flood deposits. Bijou Creek, Colorado, June 1965. *Journal of Sedimentary Petrology, 37*, 829-851.

MORLEY, C.K. 1986. A classification of thrust fronts. *Bulletin of the American Association of Petroleum Geologists, 70*, 12-25.

MORLEY, C.K. 1987. Lateral and vertical changes of deformation style in the Osen-Roa thrust sheet, Oslo region. *Journal of Structural Geology, 9*, 331-343.

MORTON, R.A. & DONALDSON, A.C. 1978. The Guadalupe River and delta of Texas - a modern analogue for some ancient fluvial-deltaic systems. *In*: MIALL, A.D. (Ed.), *Fluvial Sedimentology*, Canadian Society of Petroleum Geologists Memoir, *5*, 773-789.

MUKERJI, A.B. 1976. Terminal fans of inland streams in Sutlej-Yamuna Plain, India. *Zeis Geomorphologie, 20*, 190-204.

MUTTI, E. 1977. Distinctive thin-bedded turbidite facies and related depositional environments in the Hecho Group (South-central Pyrenees, Spain). *Sedimentology, 24*, 107-131.

MUTTI, E. 1985. The Hecho submarine fan system, South-central Pyrenees, Spain. *Geo Marine Letters, 38*, 14-34.

MUTTI, E. & JOHNS, D.R. 1979. The role of sedimentary by-passing in the genesis of fan fringe and basin-plain turbidites in the Hecho Group System (South-Central Pyrenees). *Memoir Societe Geologico Italia, 18*, 15-22.

NAMI, M. 1976. An exhumed meander-belt from Yorkshire, England. *Geological Magazine, 113*, 47-52.

NAMI, M. & LEEDER, M.R. 1978. Changing channel morphology and magnitude in the Scalby Formation (M. Jurassic) of Yorkshire, England. *In*: MIALL, A.D. (Ed.), *Fluvial Sedimentology*, Canadian Society of Petroleum Geologists Memoir, *5*, 431-441.

NAYLOR, M.A. 1981. Debris flow (olistostromes) and slumping on a distal passive continental margin: the Palombini limestone-shale sequence of the northern Apennines. *Sedimentology, 28*, 837-853.

NAYLOR, M.A. 1982. The Casanova complex of the Northern Apennines: a melange formed on a distal passive continental margin. *Journal of Structural Geology, 4*, 1-18.

NEMEC, W. & STEEL, R.J. 1984. Alluvial and coastal conglomerates: their significant features and some comments on gravelly mass-flow deposits *In*: KOSTER, E.H. & STEEL, R.J. (Eds.), *Sedimentology of Gravels and Conglomerates*. Canadian Society of Petroleum Geologists Memoir, *10*, 1-31.

NICHOLS, G.J. 1987. The structure and stratigraphy of the western External Sierras of the Pyrenees, Northern Spain. *Geological Journal*, *22*, 245-259.

NIJMAN, W. 1981. Fluvial sedimentology and basin architecture of the Eocene Montanana Group, South Pyrenean Tremp-Graus Basin. *In*: ELLIOTT, T. (Ed), *Field Guides to Modern and Ancient Fluvial Systems in Britain and Spain*, Proceedings International Fluvial Conference, Keele, 3-27.

NIJMAN, W.J. & NID, S.D. 1975. The Eocene Montanana delta. *In*: ROSELL, J. & PUIGDEFABREGAS, C. (Eds.), *Sedimentary Evolution of the Palaeogene South Pyrenean Basin*. Ninth Congress of Sedimentology Nice. Special Publication of the International Association of Sedimentologists.

NIJMAN, W. & PUIGDEFABREGAS, C. 1978. Coarse-grained point bar structure in a molasse type fluvial system, Eocene Castisent Sandstone Formation, South Pyrenean Basin. *In*: MIALL, A.D. (Ed.), *Fluvial Sedimentology*, Canadian Society of Petroleum Geologists Memoir, *5*, 487-511.

OLIVET, J.L., BONNIN, J. BEUZART, P. & AUZENDE, J.M. 1981. Cinematique de l'Atlantique nord et central. *Centre National pour l'Exploitation des Oceans Paris, 1-4.*

OLIVET, J.L., BONNIN, J., BEUZART, P. & AUZENDE, J.M. 1982. Cinematique des plaques et palaeogeographie, revue: *Bulletin Societe Geologique de France*, *7*, 875-892.

OOMKENS, E. 1970. Depositional sequences and sand distribution in the post-glacial Rhone delta complex. *In*: MORGAN, J.P. & SHAVER, R.H. (Eds.), *Deltaic Sedimentation Modern and Ancient*. Society of Economic Paleontologists and Mineralogists Special Pulication, *15*, 198-212.

ORI, G.G. & FRIEND, P.F. 1984. Sedimentary basins formed and carried piggy-back on active thrust sheets. *Geology*, *12*, 475-478.

PARISH, M. 1984. A structural interpretation of a section through the Gavarnie nappe and its implications for Pyrenean geology. *Journal of Structural Geology*, *6*, 247-296.

PARKASH, B., AWASTHI, A.K. & GOHAIN, K. 1983. Lithofacies of the Markanda terminal fan, Kurukshetra district, Haryana, India. *In*: COLLINSON, S.D. & LEWIN, J. (Eds.), *Modern and Ancient Fluvial Systems*, International Association of Sedimentologists Special Publication, *6*, 337-345.

PAVONI, N. 1964. Aktive Horizontalverschiebungszonen der Erdkruste. *Bulletin Ver. Schweiz, 31*, 54-78.

PICARD, M.D. & HIGH, L.R. 1972. Criteria for recognizing lacustrine rocks. *In*: RIGBY, J.K. & HAMBUN, W.K. (Eds.), *Recognition of Ancient Sedimentary Environments*. Society of Economic Paleontologists and Mineralogists, Special Publication, *16*, 108-146.

PINILLA, A. & RIBA, O. 1972. Estudio sedimentologico de la zona aragonesa de la cuenca terciaria del Valle del Ebro. *Bolletin Royales Societe Espana Historico Naturales, 70*, 97-106.

PLATT, J.P., COWARD, M.P., DERAMOND, J. & HOSSACK, J. 1986. Thrusting and Deformation. *Journal of Structural Geology Special Issue, 8*, Numbers 3/4.

PLINT, A.G. 1983. Sandy fluvial point-bar sediments from the Middle Eocene of Dorset, England. *In*: COLLINSON, J.D. & LEWIN, J. (Eds.), *Modern and Ancient Fluvial Systems*, International Association of Sedimentologists Special Publication, *6*, 355-369.

POWERS, M. 1953. Visual estimation of sphericity and angularity of sedimentary particles. *Journal of Sedimentary Petrology, 23*, 117-119.

PRICE, R.A. 1986. The southeastern Canadian Cordillera: thrust faulting, tectonic wedging, and delamination of the lithosphere. *Journal of Structural Geology 8*, 239-254.

PUIGDEFABREGAS, C. 1973. Miocene point bar deposits in the Ebro basin, northern Spain. *Sedimentology, 20*, 133-144.

PUIGDEFABREGAS, C. 1975. La sedimentacion molasica en la cuenca de Jaca. *Momografias del Instituto de Estudios Pirenaicas, 104*, 188pp.

PUIGDEFABREGAS, C., RUPKE, N.A. & SOLE SEDO, J. 1975. The sedimentary evolution of the Jaca basin. *In*: ROSELL, J. & PUIGDEFABREGAS, C. (Eds.) *The Sedimentary Evolution of the Palaeogene South Pyrenean Basin*. International Association of Sedimentologists, 9th International Congress, Nice.

PUIGDEFABREGAS, C. & SOLER, M. 1973. Estructura de las Sierras Exteriories Pirenaicas en el corte del rio Gallego (prov. de Huesca). *Pireneos, 109*, 5-15.

PUIGDEFABREGAS, C. & VAN VLIET, A. 1978. Meandering stream deposits from the Tertiary of the Southern Pyrenees. *In*: MIALL, A.D. (Ed.), *Fluvial Sedimentology*, Canadian Society of Petroleum Geologists Memoir, *5*, 469-487.

REINECK, H.E. & SINGH, I.B. 1980. *Depositional sedimentary environments - with reference to terrigenous clastics*. Springer-Verlag, New York, Second Edition.

RIBA, O. 1976a. Syntectonic unconformities of the Alto Cardener, Spanish Pyrenees: A genetic interpretation. *Sedimentary Geology, 15*, 213-233.

RIBA, O. 1976b Tectogenese et sedimentation: deux modeles de discordances syntectoniques pyreneennes. *Bulletin du Bureau de Recherches Geologiques et Minieres, 4*, 383-401.

RIBA, O., VILLENA, S. & QUIRANTES, F. 1967. Nota preliminar sobre la sedimentacion en paleocanales terciarios de la zona de Caspe-Chiprana (Provincia de Zaragoza). *Annales Edafolica Agrobiologica, 26*, 617-634.

RIDD, M.F. 1970. Mud volcanoes in New Zealand. *Bulletin of the American Association of Petroleum Geologists, 54*, 601-606.

RIDER, M.H. 1978. Growth faults in the Carboniferous of western Ireland. *Bulletin of the American Association of Petroleum Geologists, 62*, 2191-2213.

RIES, A.C. 1978. The opening of the Bay of Biscay - a review. *Earth Science Reviews, 14*, 35-63.

ROCKWELL, T.K., KELLER, E.A. & JOHNSON, D.L. 1985. Tectonic geomorphology of alluvial fans and mountain fronts near Ventura, California. *In*: MORISAWA, M. & HACK, J.T. (Eds.), *Tectonic Geomorphology*, Binghampton Press, 183-207.

RUPKE, N.A. 1976. Sedimentology of very thick calcarenite - marlstone beds in a flysch succession, southwestern Pyrenees. *Sedimentology, 23*, 43-65.

RUST, B.R. 1972. Pebble orientation in fluviatile sediments. *Journal of Sedimentary Petrology, 42*, 384-388.

RUST, B.R. 1981. Alluvial deposits and tectonic style: Devonian and Eastern Gaspe. *In*: MIALL, A.D. (Ed.), *Sedimentation and Tectonics in Alluvial Basins*, Geological Association of Canada Special Paper, *23*, 49-75.

RUST, B.R. 1984. Proximal braidplain deposits in the Middle Devonian Malbaie Formation of Eastern Gaspe, Quebec, Canada. *Sedimentology, 31*, 675-695.

RUST, B.R. & KOSTER, E.H. 1984. Coarse alluvial deposits. *In*: WALKER, R.G. (Ed.), *Facies Models*. Geoscience Canada Reprint Series 1, Second Edition, 53-71.

SCHUMM, S.A. 1960. The effect of sediment type on the shape and stratification of some modern fluvial deposits. *American Journal of Science, 258*, 177-184.

SCOTT, A.J., HOOVER, R.A. & McGOWEN, J.H. 1969. Effects of Hurricane 'Beulah' 1967 on Texas coastal lagoons and barriers. *UNESCO, Simposia Internacional Sobre Lagunas Costeras*, 221-236.

SCHUMM, S.A. 1963. A tentative classification of alluvial river channels. *US Geological Survey Circular, 477*, 10pp.

SEGURET, M. 1972. Etude tectonique des nappes et series decollees de la partie centrale du versant sud des Pyrenees. *In: Serie Geologique Structurale, 21*, Ustella, Montpellier, 155pp.

SEGURET, M. & DAIGMERES, M. 1986. Crustal-scale balanced cross sections of the Pyrenees. *Tectonophysics, 129*, 303-313.

SHEPHERD, R.G. 1978. Distinction of aggradational and degradational fluvial regimes in valley-fill alluvium, Topia Canyon, New Mexico. *In*: MIALL, A.D. (Ed.), *Fluvial Sedimentology*, Canadian Society of Petroleum Geologists Memoir, *5*, 277-287.

SHUSTER, M.W. & STEIDTMANN, J.R. 1987. Fluvial sandstone architecture and thrust-induced subsidence, northern Green River Basin. *In*: ETHRIDGE, F.G., FLORES, R.M. & HARVEY, M.D. (Eds.), *Recent Developments in Fluvial Sedimentology*. Society of Economic Paleontologists and Mineralogists Speical Publication, *39*,, 279-287.

SINGH, I.B. 1972. On the bedding in the natural levee and the point bar deposits of the Gornti River, Uttar Pradesh, India. *Sedimentary Geology, 7*, 309-317.

SMITH, G.A. 1987. Sedimentology of volcanism-induced aggradation in fluvial basins: examples from the Pacific Northwest USA. *In*: ETHRIDGE, F.G., FLORES, R.M. & HARVEY, M.D. (Eds.), *Recent Developmentes in Fluvial Sedimentology*, Society of Economic Paleontologists and Mineralogists Special Publication, *39*, 217-229.

SELZER, G. 1934. Geologie der Sudpyrenaische Sierren in Ober-aragonien. *Neues Jahrbruch Geologie, Palaeontologie und Mineralogie, 88*, 370-406.

SOLER, M. & PUIGDEFABREGAS, C. 1970. Lineas generales de la geologia del Alto Aragon Occidental. *Pirineos, 106*, 5-15.

SOLE-SUGRANES, L. 1979. Gravity and compressive nappes in the southern Pyrenees (Spain). *American Journal of Science, 278*, 609-637.

SORAUF, J.E. 1965. Flow rolls of Upper Devonian rocks of south-central New York State. *Journal of Sedimentary Petrology, 35*, 553-563.

SOUQUET, P. 1967. *Le Cretace superieur sud-pyrenen en Catalogne, Aragon et Navarre*. Thesis, Faculte de Science , Universite de Toulouse.

SPEARING, D.R. 1975. Summary Sheets of Sedimentary Deposits. *Geological Society of America, MC-8*.

STEEL, R.S. & AASHEIM, J.M. 1978. Alluvial sand deposition in a rapidly subsiding basin (Devonian, Norway). *In*: MIALL, A.D. (Ed.), *Fluvial Sedimentology*, Canadian Society of Petroleum Geologists Memoir, *5*, 385-413.

STEILA, D. 1976. *The Geography of Soils*. Prentice-Hall, New Jersey, 222pp.

WILLIAMS, P.F. 1969. Notes on some deformation structures of sedimentary origin in the Little Haven-Amroth coalfield, Pembrokeshire. *Geological magazine, 106*, 395-411.

WILLIAMS, P.F., COLLINS, A.R. & WILTSHIRE, R.G. 1969. Cleavage and penecontemporaneous deformation structures in sedimentary rocks. *Journal of Geology, 77*, 415-425.

WILLIAMS, R.C. 1975. *Fluvial deposits of Oligo-Miocene age in the southern Ebro basin, Spain.* PhD thesis, University of Cambridge.

WOODCOCK, N.H. 1976. Structural style in slump sheets: Ludlow Series, Powys, Wales. *Journal of the Geological Society of London, 132*, 399-415.

WOODCOCK, N.H. & FISCHER, M.W. 1986. Strike-slip duplexes. *Journal of Structural Geology, 8*, 725-735.